Geological Survey of Canada
Commission géologique du Canada

PAPER
ÉTUDE 88-1D

CURRENT RESEARCH PART D
INTERIOR PLAINS AND ARCTIC CANADA

RECHERCHES EN COURS PARTIE D
PLAINES INTÉRIEURES ET RÉGION ARCTIQUE DU CANADA

1988

Canada

NOTICE TO LIBRARIANS AND INDEXERS

The Geological Survey's Current Research series contains many reports comparable in scope and subject matter to those appearing in scientific journals and other serials. Most contributions to Current Research include an abstract and bibliographic citation. It is hoped that these will assist you in cataloguing and indexing these reports and that this will result in a still wider dissemination of the results of the Geological Survey's research activities.

AVIS AUX BIBLIOTHÉCAIRES ET PRÉPARATEURS D'INDEX

La série Recherches en cours de la Commission géologique paraît une fois par année; elle contient plusieurs rapports dont la portée et la nature sont comparables à ceux qui paraissent dans les revues scientifiques et autres périodiques. La plupart des articles publiés dans Recherches en cours sont accompagnés d'un résumé et d'une bibliographie, ce qui vous permettra, nous l'espérons, de cataloguer et d'indexer ces rapports, d'où une meilleure diffusion des résultats de recherche de la Commission géologique.

GEOLOGICAL SURVEY OF CANADA
PAPER 88-1D
COMMISSION GÉOLOGIQUE DU CANADA
ÉTUDE 88-1D

CURRENT RESEARCH PART D

INTERIOR PLAINS AND ARCTIC CANADA

RECHERCHES EN COURS PARTIE D

PLAINES INTÉRIEURES ET RÉGION ARCTIQUE DU CANADA

1988

Available in Canada through

authorized bookstore agents and other bookstores

or by mail from

Canadian Government Publishing Centre
Supply and Services Canada
Ottawa, Canada K1A 0S9

and from

Geological Survey of Canada offices:
601 Booth Street
Ottawa, Canada K1A 0E8
3303-33rd Street N.W
Calgary, Alberta T2L 2A7
100 West Pender Street
Vancouver, British Columbia V6B 1R8

A deposit copy of this publication is also available
for reference in public libraries across Canada

Cat. No. M44-88/1D	Canada:	$10.00
ISBN 0-660-53899-7	Other countries:	$12.00

Price subject to change without notice

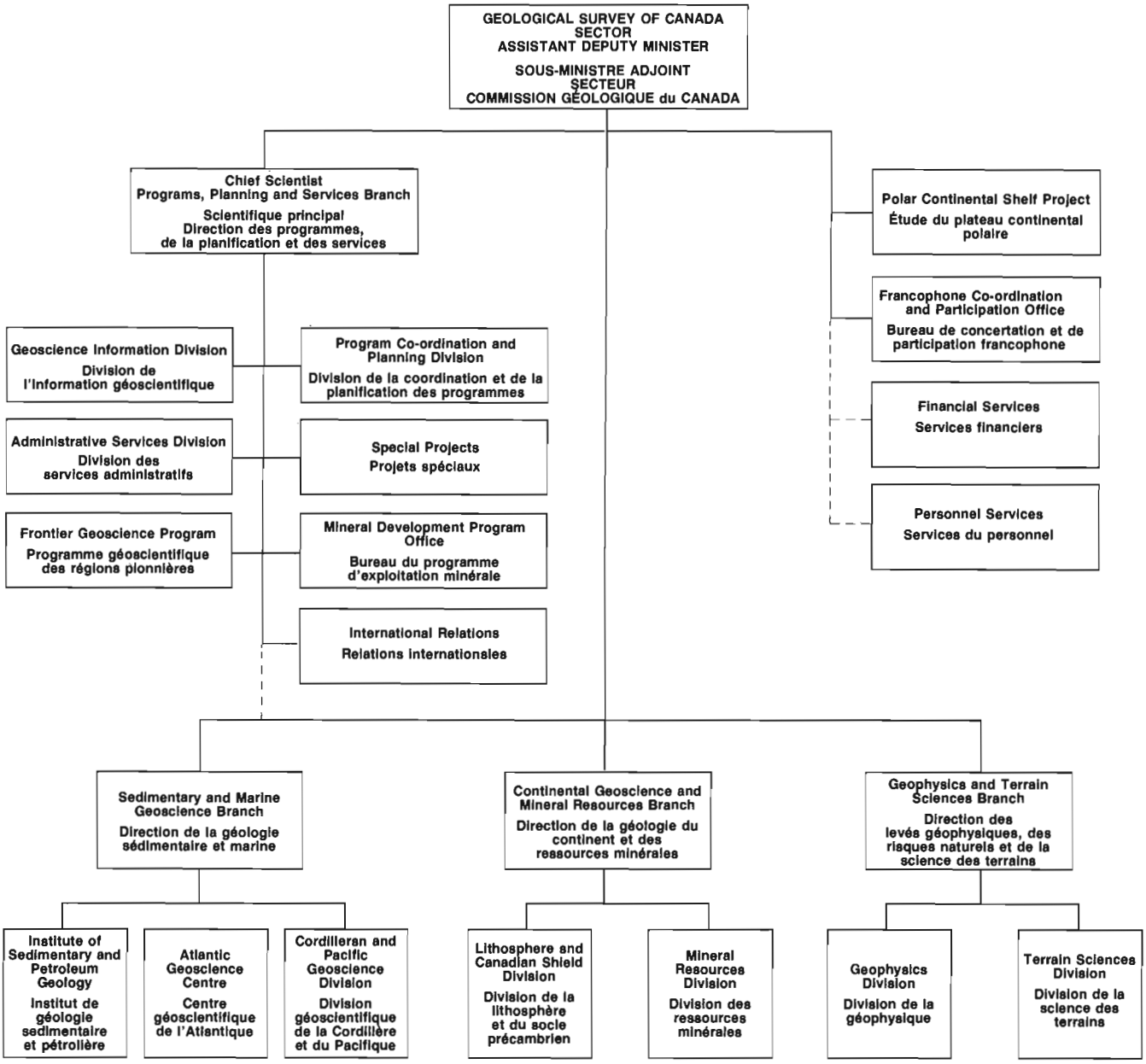
GEOLOGICAL SURVEY OF CANADA
SECTOR
ASSISTANT DEPUTY MINISTER
SOUS-MINISTRE ADJOINT
SECTEUR
COMMISSION GÉOLOGIQUE du CANADA
Chief Scientist
Programs, Planning and Services Branch
Scientifique principal
Direction des programmes,
de la planification et des services
Polar Continental Shelf Project
Étude du plateau continental polaire
Francophone Co-ordination and Participation Office
Bureau de concertation et de participation francophone
Financial Services
Services financiers
Personnel Services
Services du personnel
Geoscience Information Division
Division de l'information géoscientifique
Program Co-ordination and Planning Division
Division de la coordination et de la planification des programmes
Administrative Services Division
Division des services administratifs
Special Projects
Projets spéciaux
Frontier Geoscience Program
Programme géoscientifique des régions pionnières
Mineral Development Program Office
Bureau du programme d'exploitation minérale
International Relations
Relations internationales
Sedimentary and Marine Geoscience Branch
Direction de la géologie sédimentaire et marine
Continental Geoscience and Mineral Resources Branch
Direction de la géologie du continent et des ressources minérales
Geophysics and Terrain Sciences Branch
Direction des levés géophysiques, des risques naturels et de la science des terrains
Institute of Sedimentary and Petroleum Geology
Institut de géologie sedimentaire et pétrolière
Atlantic Geoscience Centre
Centre géoscientifique de l'Atlantique
Cordilleran and Pacific Geoscience Division
Division géoscientifique de la Cordillère et du Pacifique
Lithosphere and Canadian Shield Division
Division de la lithosphère et du socle précambrien
Mineral Resources Division
Division des ressources minérales
Geophysics Division
Division de la géophysique
Terrain Sciences Division
Division de la science des terrains

Separates

A limited number of separates of the papers that appear in this volume are available by direct request to the individual authors. The addresses of the Geological Survey of Canada offices follow:

601 Booth Street,
OTTAWA, Ontario
K1A 0E8

Institute of Sedimentary and Petroleum Geology,
3303-33rd Street N.W.,
CALGARY, Alberta
T2L 2A7

Cordilleran and Pacific Geoscience Division,
100 West Pender Street,
VANCOUVER, B.C.
V6B 1R8

Pacific Geoscience Centre
P.O. Box 6000,
9860 Saanich Road,
SIDNEY, B.C.
V8L 4B2

Atlantic Geoscience Centre,
Bedford Institute of Oceanography,
P.O. Box 1006,
DARTMOUTH, N.S.
B2Y 4A2

When no location accompanies an author's name in the title of a paper, the Ottawa address should be used.

Tirés à part

On peut obtenir un nombre limité de «tirés à part» des articles qui paraissent dans cette publication en s'adressant directement à chaque auteur. Les adresses des différents bureaux de la Commission géologique du Canada sont les suivantes:

601, rue Booth
OTTAWA, Ontario
K1A 0E8

Institut de géologie sédimentaire et pétrolière
3303-33rd St. N.W.,
CALGARY, Alberta
T2L 2A7

Division géoscientifique de la Cordillère
et du Pacifique
100 West Pender Street,
VANCOUVER, Colombie-Britannique
V6B 1R8

Centre géoscientifique du Pacifique
B.P. 6000,
9860 Saanich Road,
SIDNEY, Colombie-Britannique
V8L 4B2

Centre géoscientifique de l'Atlantique
Institut océanographique de Bedford
B.P. 1006,
DARTMOUTH, Nouvelle-Écosse
B2Y 4A2

Lorsque l'adresse de l'auteur ne figure pas sous le titre d'un document, on doit alors utiliser l'adresse d'Ottawa.

CONTENTS

INTRODUCTION

In 1987 the Geological Survey of Canada became a Sector within the Department of Energy, Mines and Resources, and was re-organized into the four Branches shown on the accompanying organizational chart. The primary role of the Survey, which was founded in 1842, continues to be to provide an overview of all facets of Canadian geology as a basis for national policy, for planning by government and industry, and for public information.

In order to provide interim results of its program a publication titled "Summary of Research" was initiated in 1963. The title was changed to "Current Research" in 1978 and the report was released three times a year (Part A, B and C). After 1982 Part C was no longer issued and Part B was discontinued in 1987 to encourage greater use of journal publication for short contributions.

Current Research, however, is the one series of GSC publications that gives the public a yearly overview of the range of the Geological Survey of Canada Sector activities. From time to time Current Research has been criticized for its size, as it was necessary for the user to buy a large volume to obtain a few pertinent papers. To introduce greater flexibility, this issue of Current Research is therefore available in six parts that can be purchased separately: four regional volumes, one volume of national and general programs, and a volume that contains abstracts of all the reports. The Parts are:

Part A: Abstracts/Résumés
Part B: Eastern and Atlantic Canada
Part C: Canadian Shield
Part D: Interior Plains and Arctic Canada
Part E: Cordillera and Pacific Margin
Part F: National and General Programs

Identification of the Parts by letters is for convenience only and may be subject to change. Each of Parts B to F includes a paginated Table of Contents for the volume: Table of Contents for the other Parts of this series will be found at the back of each volume.

En 1987 la Commission géologique est devenue un secteur à l'intérieur du ministère de l'Énergie, des Mines et des Ressources et a été réorganisée en quatre directions indiquées sur l'organigramme d'accompagnement. Organisme fondé en 1842, la Commission a comme rôle principal de procurer un cadre d'ensemble de toutes les facettes de la géologie du Canada comme base d'une politique nationale pour la planification du gouvernement et de l'industrie et pour informer le public en général.

Afin de fournir les résultats préliminaires de son programme de recherche une publication ayant titre « Summary of Research » est apparue en 1963. Une nouvelle publication, ayant les mêmes buts, est apparue en 1978 sous le titre « Recherches en cours »; cet ouvrage était diffusé trois fois par année (parties A, B et C). Après 1982 la partie C a été abandonnée et ce fut de même pour la partie B en 1987. L'arrêt de ces publications avait pour but d'adopter une nouvelle forme d'édition pour satisfaire davantage l'usager.

La publication « Recherches en cours » appartient à part entière à la série des publications de la CGC et apporte à chaque année une vue d'ensemble des activités de la Commission géologique maintenant au niveau de secteur. De temps à autre la publication « Recherches en cours » a été critiquée pour son fort volume, plusieurs ont constaté qu'il était nécessaire d'acheter un gros volume uniquement pour n'avoir accès qu'à un petit nombre d'articles. Maintenant, cette publication est disponible en six parties en vente séparément, ce qui procure une plus grande flexibilité pour l'usager. La publication est répartie comme suit: quatre volumes régionaux, un volume couvrant les programmes nationaux et généraux et un dernier contenant les résumés de tous les articles. On y trouve les parties suivantes:

Partie A: Abstracts/Résumés
Partie B: Est et région atlantique du Canada
Partie C: Bouclier canadien
Partie D: Plaines intérieures et région arctique du Canada
Partie E: Cordillère et marge du Pacifique
Partie F: Programmes nationaux et généraux

L'identification des parties par une lettre a été adoptée uniquement par commodité; on pourra éventuellement utiliser une autre façon. Les parties B à F possèdent une table des matières paginée; il est à noter qu'à chacune des parties de cette série on y trouvera à l'endos une table des matières indiquant le contenu des autres parties.

Devonian stratigraphy of northwestern Devon Island, District of Franklin

Eric C. Prosh[1], Katherine A. Lesack[2], and Ulrich Mayr
Institute of Sedimentary and Petroleum Geology, Calgary

Prosh, E.C., Lesack, K.A., and Mayr, U., Devonian stratigraphy of northwestern Devon Island, District of Franklin; in Current Research, Part D, Geological Survey of Canada, Paper 88-1D, p. 1-10, 1988.

Abstract

On northwestern Devon Island, 2 km of relatively tectonically undisturbed Devonian strata are preserved. Dolomitic and clastic sediments of the Goose Fiord, Sutherland River and Prince Alfred formations were deposited during a period of intermittent Early Devonian tectonism. A thin, unnamed formation, possibly referable to the Vendom Fiord Formation, and occurring uniformly beneath the Blue Fiord Formation, is recognized for the first time from this area.

A transition to quiescent, carbonate-shelf conditions is indicated by the Blue Fiord Formation, and in it a four-fold subdivision of alternating limestone and dolomite units can be recognized. The Bird Fiord Formation, also subdivisible into four units, records a transition to more nearshore and fluvial conditions. The Middle-to-Upper Devonian Arctic Clastic Wedge is represented by the nonmarine Strathcona Fiord, Hecla Bay, Fram and Hell Gate formations.

Résumé

Dans le nord-ouest de l'île Devon, sont conservées 2 km de strates dévoniennes relativement peu perturbées tectoniquement. Les sédiments dolomitiques et clastiques des formations de Goose Fiord, de Sutherland River et de Prince Alfred se sont déposés durant une période de tectonisme intermittent survenue au Dévonien inférieur. On a identifié pour la première fois dans cette région une formation non dénommée, qui est peut-être l'équivalent de la formation de Vendom Fiord, et constitue un niveau uniforme au-dessous de la formation de Blue Fiord.

Le passage à un milieu sédimentaire carbonaté calme apparu sur une plate-forme continentale, est indiqué par la formation de Blue Fiord; on peut subdiviser celle-ci en quatre unités alternées, calcaires et dolomitiques. La formation de Bird Fiord, qui se laisse aussi subdiviser en quatre unités, marque la transition vers une sédimentation de type plus littoral et fluviatile. Le prisme clastique arctique, d'âge dévonien moyen à supérieur, est représenté par les formations non marines de Strathcona Fiord, d'Hecla Bay, de Fram et de Hell Gate.

[1] Department of Geology, University of Western Ontario, London, Ontario, N6A 5B7.
[2] Department of Earth Sciences, University of Waterloo, Waterloo, Ontario, N2L 3G1.

INTRODUCTION

During the summers of 1986 and 1987, a detailed investigation of the Devonian strata of northwestern Devon Island (Fig. 1) was undertaken as part of an ongoing project to map Grinnell Peninsula and surrounding areas. A virtually complete, composite section ranging from the (Upper Silurian) Devon Island Formation to the (Upper Devonian) Hell Gate Formation has been compiled, preliminary results of which are presented herein. Detailed lithological and biostratigraphic analyses (conodonts and palynomorphs) are in progress, and the results of these analyses will be forthcoming.

Thirteen stratigraphic sections were measured in an area extending north from Colin Archer Peninsula, in the vicinity of Norfolk Inlet, to Cardigan Strait, where a gently northwesterly dipping sequence of Devonian strata, some 2 km in thickness, is well exposed. The results from measurement of two other sections from the Prince Alfred Bay area are also presented, and correlations between these fifteen sections and sections from other previously studied areas are suggested.

STRATIGRAPHY

Devon Island Formation (upper part)

The Devon Island Formation, originally defined by Thorsteinsson (1963), is a relatively thin sequence of dark coloured, silty dolomite and limestone and impure siltstone of late Ludlovian to early Lochkovian age. Its upper contact is markedly diachronous, ranging in age from early Lochkovian at its type locality (near Prince Alfred Bay), where it is overlain by the Sutherland River Formation, to early Pridolian near Muskox Fiord in southwestern Ellesmere Island (Thorsteinsson and Uyeno, 1980), where it is overlain by the Goose Fiord Formation.

A continuous, 48 m thick sequence of uppermost Devon Island strata is exposed in a creek section on the south side of Norfolk Inlet (Section 5, Fig. 1). The dominant lithology is a silty to fine sandy, brown-grey dolomite, medium to thin bedded, and commonly exhibiting horizontal Planolites-like burrows (Fig. 4b). Thin beds of wavy-laminated dolomite and intraformational pebble paraconglomerate occur subordinately. Minor brachiopods and crinoid ossicles also occur. The uppermost five or so metres become sandier, and pass gradationally, although rapidly, into light buff, sandy dolomites of the Goose Fiord Formation. At this locality, the Devon Island/Goose Fiord contact can be most usefully placed above the last occurrence of Planolites-type burrows. This contact is readily recognizable at a distance by the transition from dark- coloured, thin beds to lighter coloured Goose Fiord strata exhibiting a more thickly bedded outcrop appearance (Fig. 4a). It is noteworthy that while the Devon Island/Goose Fiord contact is gradational at Norfolk Inlet, and also at Muskox Fiord (Thorsteinsson and Uyeno, 1980, p. 18), it appears to be disconformable some 200 km to the east at Grise Fiord (Mayr, 1982).

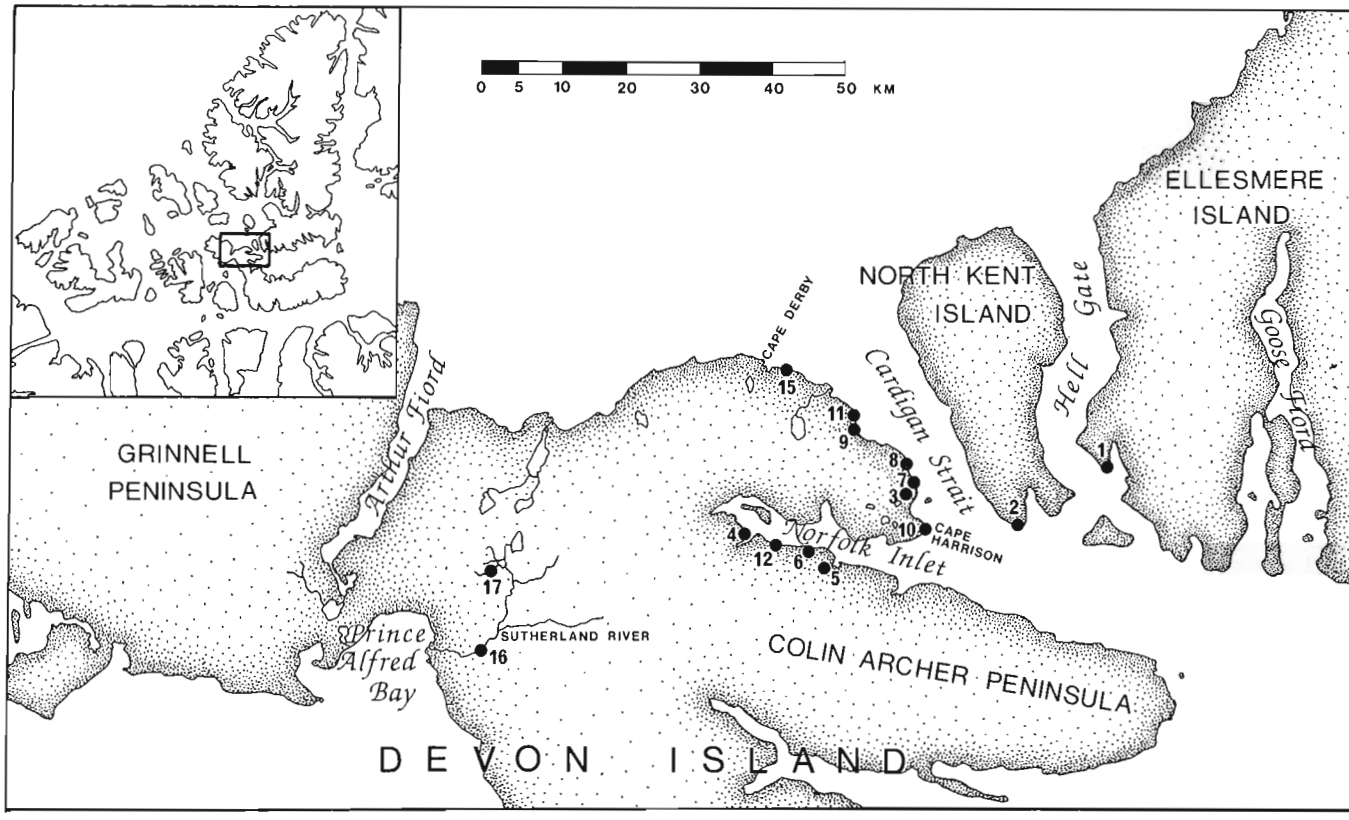

Figure 1. Index map of section locations, northwestern Devon Island and vicinity. Sections are consecutively numbered 1 through 12, and 15, 16, 17.

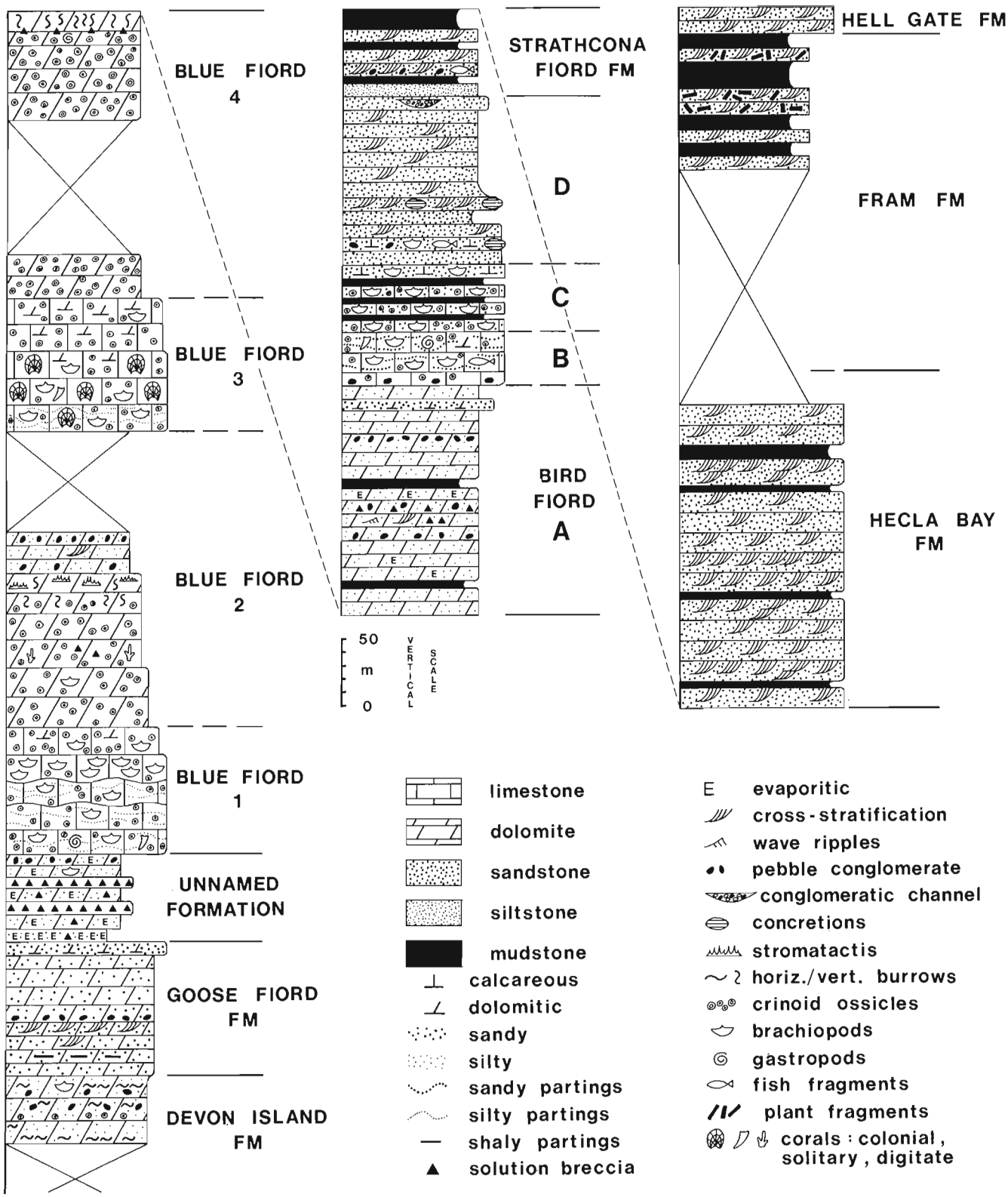

Figure 2. Composite stratigraphic section of Devonian formations in the Norfolk Inlet - Cardigan Strait area (composite of Sections 5, 6, 12, 10, 3, 7, 8, 9, 11 and 15, in ascending stratigraphic order).

Goose Fiord Formation — Sutherland River Formation

The Goose Fiord Formation was observed at Sections 1, 2, 5 and 6 (Fig. 1); it is most completely exposed at Section 5 (Fig. 4a). It is a resistant, cliff-forming unit, about 100 m thick throughout the Norfolk Inlet — Cardigan Strait area, and is composed chiefly of light buff to orange-buff, laminated to thin bedded, variably sandy dolomites and minor dolomitic sandstones. Thin (up to 1 m in thickness) beds of flat-pebble and ripclast conglomerate also occur, generally confined to the middle portion of the formation. A distinctive salmon pink sandstone consisting of coarse sand-sized, white quartz grains occurs near the top of the formation at Sections 1 and 5. The upper contact with the unnamed formation (see below) is in general poorly exposed, but where visible appears to be disconformable.

The Goose Fiord Formation thickens appreciably to the east, from approximately 100 m in the Cardigan Strait area, described here (Sections 1, 2, and 5), to roughly 300 m at Goose Fiord (Greiner, 1963), to 710 m at Grise Fiord (Mayr, 1982); from this, and its inferred temporal relationship with the underlying Devon Island Formation, it is evident that the Goose Fiord Formation was a westwardly prograding unit during Late Silurian through Early Devonian time. Prior to this investigation, the Goose Fiord Formation was not known from beyond southwestern Ellesmere Island.

The age of the Goose Fiord Formation is as yet poorly constrained, having yielded few diagnostic fossils, but near Muskox Fiord conodonts indicate an early Pridolian to possibly Early Devonian age span (Thorsteinsson and Uyeno, 1980). It is apparent, however, based on its relationship with the underlying, diachronous top of the Devon Island Formation, that the basal Goose Fiord becomes younger in a westerly direction, and is probably mostly Early Devonian in the vicinity of Norfolk Inlet.

The Goose Fiord Formation of southwestern Ellesmere Island and northwestern Devon Island is correlative with the upper Devon Island and Sutherland River formations of eastern Grinnell Peninsula (Fig. 3). The Goose Fiord and Sutherland River formations are best considered synonymous.

The Sutherland River Formation type section is located along the Sutherland River, and is described in Thorsteinsson (1963), Morrow and Kerr (1977), and Thorsteinsson and Uyeno (1980). This locality of the type section is shown as Section 16 on Figure 1. The contact of the type Sutherland River with the underlying Devon Island Formation does not outcrop, but is presumably conformable. The type section was examined during the summer of 1986 and consists, near the base of the Sutherland River Formation, of 12 m of light grey-brown, generally laminated, silty dolomite. Above an intervening 50 m covered interval, 50 m of light grey-brown,

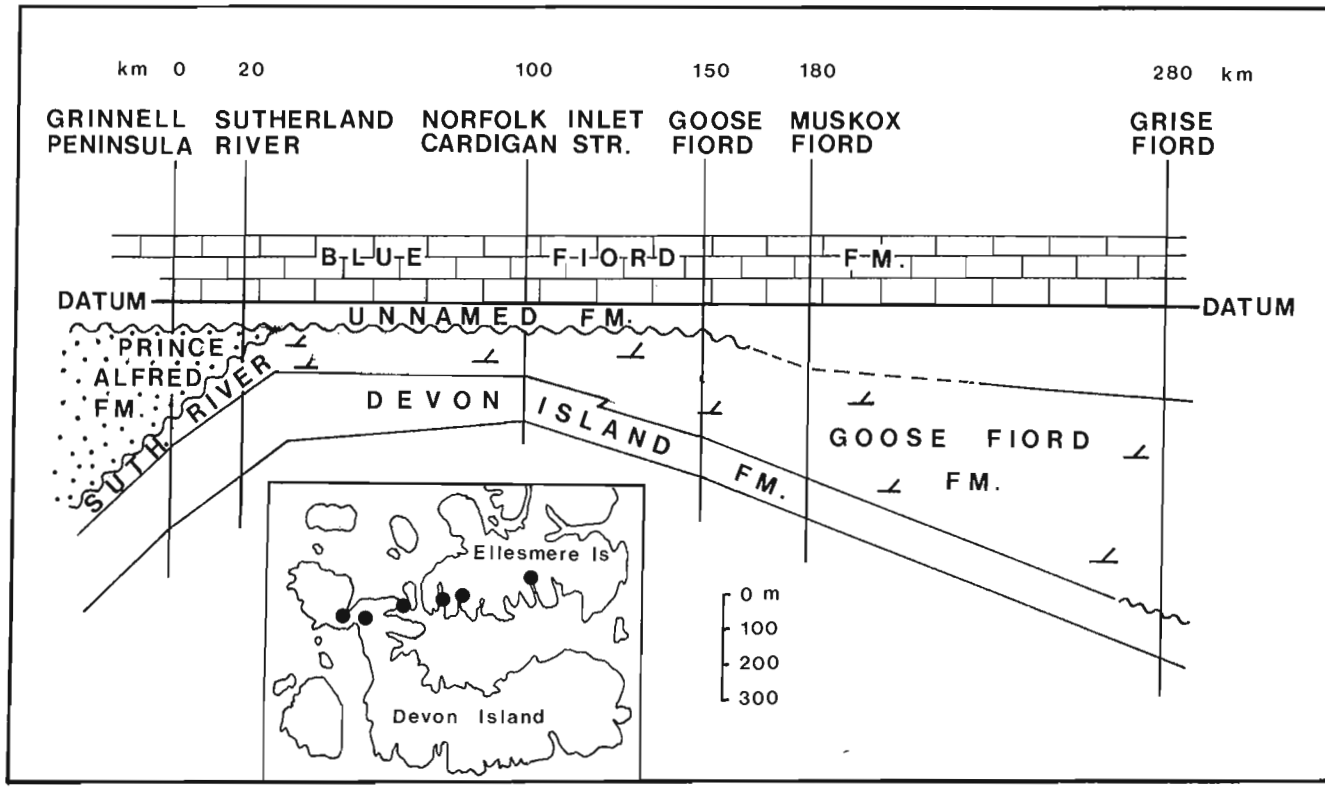

Figure 3. Inferred stratigraphic relationships of Lower Devonian formations, northwestern Devon Island and southwestern Ellesmere Island. Datum is the base of the Blue Fiord Formation, which approximates a time line. Sources are: Greiner, 1963 (Goose Fiord); Mayr, 1982 (Grise Fiord); McLaren, 1963 (Goose Fiord); Morrow and Kerr, 1977 (Grinnell Peninsula, Sutherland River); Thorsteinsson and Uyeno, 1980 (Sutherland River, Muskox Fiord); this report (Sutherland River, Norfolk Inlet - Cardigan Strait). The thickness of the Prince Alfred Formation at Grinnell Peninsula has been reinterpreted from Morrow and Kerr's (1977, their Section 8) original description.

laminated to very thin bedded, sparsely silty, fine crystalline dolomite are exposed; minor red and red-stained dolomite occur toward the top of this unit. The contact with the overlying Prince Alfred Formation is not exposed, but has been interpreted by Morrow and Kerr (1977) as a disconformity.

Prince Alfred Formation

The Prince Alfred Formation type section (Thorsteinsson, 1963; Morrow and Kerr, 1977; Thorsteinsson and Uyeno, 1980; Section 16 herein) is incompletely exposed, with some 48.5 m of outcrop visible. The lower 21 m are composed of beds of brown, variably dolomitic, fine grained sandstone, cream coloured, laminated, microcrystalline dolomite with small gypsum and halite casts, and intraformational conglomerate composed of angular dolomite pebbles in a very silty dolomite matrix. These same angular pebbles, clearly derived from the cream coloured dolomites, occur scattered throughout the sandstone, which also contains some grey-green mudchips. The remaining 27.5 m are composed of a generally massive, light grey-brown, fine grained sandstone with mudchips. Although Thorsteinsson and Uyeno (1980) estimated the thickness of the type Prince Alfred to be about 125 m, we believe it is more on the order of 60 to 65 m, allowing for some 60 m of the unnamed formation (see below) to intervene beneath the Blue Fiord (*non* Disappointment Bay) Formation.

Some 10 km to the north (and across the Grinnell Thrust), at Section 17 (Figs. 1, 4h), the uppermost 20 m of the Prince Alfred Formation are exposed beneath the unnamed formation. At this locality, the Prince Alfred is composed of grey to grey-brown, dolomitic sandstone that is locally crossbedded, and laminated, silty dolomite. Solution features are common. The upper contact with the unnamed formation is marked by a characteristic 2 m thick solution breccia, and is presumably disconformable.

The distribution of the Prince Alfred Formation is limited to southeastern Grinnell Peninsula and adjacent Devon Island, and it thickens and coarsens dramatically as the eastern limit of the Boothia Uplift is approached (Morrow and Kerr, 1977). The period of localized uplift recorded by the Prince Alfred Formation is probably represented to the east by an inferred hiatus between the Goose Fiord and unnamed formations (Fig. 3).

Unnamed formation

A recessive-weathering formation of remarkably uniform thickness overlies the Goose Fiord Formation in the Norfolk Inlet — Cardigan Strait area (Sections 1, 2 and 6, Fig. 1), and the Prince Alfred Formation near Grinnell Peninsula (Section 17). This thin unit, roughly 60 m in thickness, is composed of: grey, laminated, silty dolomite; light grey, laminated, gypsiferous siltstone; brown, laminated, silty dolomite; and minor amounts of dolomite-pebble orthoconglomerate and sparsely bioclastic or barren, very thinly bedded limestone. Commonly this formation is pervasively solution-brecciated, such that at Cross Bay and North Kent Island (Sections 1 and 2) fully half of the formation is a dark brown, dolomitic, largely amorphous solution breccia. At Norfolk Inlet (Section 6), these dark solution breccias occur somewhat less pervasively, and well to the west, north of the Sutherland River (Section 17), most of the original lithology is preserved, the effects of penecontemporaneous solution-brecciation being, although prevalent, much less intense.

In the past, similar strata immediately overlying the Goose Fiord Formation on southwestern Ellesmere Island have been assigned to the Blue Fiord Formation (McLaren, 1963, and Columnar Section No. 28 therein; Kerr, 1968; Mayr and Okulitch, 1984); however, Thorsteinsson and Uyeno (1980, p. 18-19) have correctly pointed out that this practice is inappropriate on purely lithological grounds. Additionally, Thorsteinsson and Uyeno (op. cit.) have noted the presence of 150 to 200 m of brown dolomite occupying a similar stratigraphic position at Muskox Fiord. Mayr (1982) reported the presence of an unnamed dolomite unit between the Goose and Blue Fiord formations in the Grise Fiord area, but later (Mayr and Okulitch, 1984) included that unit in the Blue Fiord Formation. The basal beds of that unit yielded conodonts of early Zlichovian age (Uyeno, pers. comm., 1982).

The upper contact of the unnamed formation with the overlying Blue Fiord Formation is sharp, and in general irregular (Fig. 4d, f). Much of this irregularity is clearly related to compactional solution (Fig. 4d), so that the possiblity of this upper contact representing an erosional surface cannot be unambiguously assessed on lithological grounds alone. While the consistent thickness of this formation and an increasing abundance of limestone toward its top might together suggest the presence of only a brief hiatus prior to Blue Fiord deposition, it is evident that a long span of Early Devonian time, effectively the entire Lochkovian through Zlichovian, could not be continuously represented by the relatively thin Goose Fiord — unnamed formation sequence in the Norfolk Inlet — Cardigan Strait area. Therefore, it is likely that a significant unconformity exists either below or above the unnamed formation — probably below it (see Figure 3).

In terms of its general lithology and stratigraphic position immediately beneath the Blue Fiord Formation, the unnamed formation bears a strong resemblance to the Vendom Fiord Formation as described by Trettin (1978) from west-central Ellesmere Island. Trettin's Vendom Fiord Lithofacies Group 2 includes silty dolomite, sandstone, siltstone, and lesser amounts of flat-pebble conglomerate, lime mudstone and laminated gypsum/anhydrite; these together constitute about two thirds of the formation, which is roughly 400 m thick in west-central Ellesmere Island. Lithofacies Group 3 includes lime wackestone; a possible equivalent to Trettin's basal, conglomeratic Lithofacies Group 1 is absent from the unnamed formation. Brecciation is rare in the west-central Ellesmere Vendom Fiord Formation. In general, then, this comparison is favourable; a greater prevalence of evaporites and solution breccias, an absence of coarse clastics, and a much attenuated thickness would indicate deposition under much shallower, topographically subdued conditions.

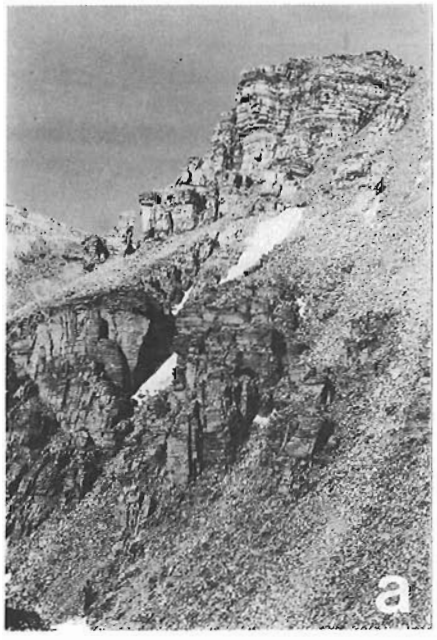
a

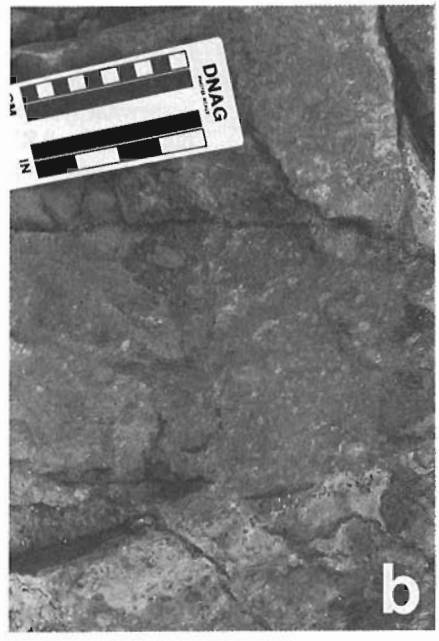
DNAG
IN
b


c


d


e

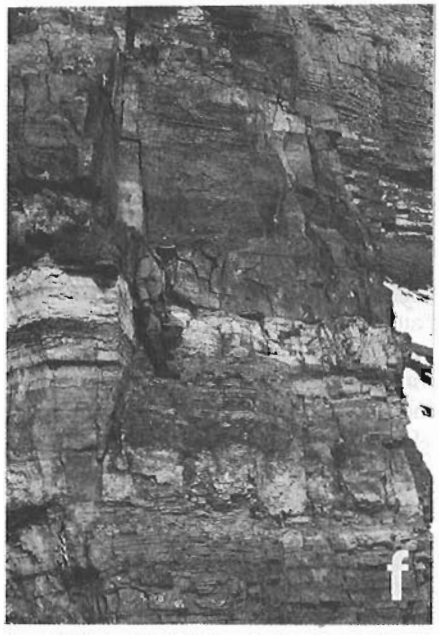
f


g


h

If the unnamed formation is indeed equivalent to the Vendom Fiord Formation, then it is noteworthy that the upper contact of the Vendom Fiord with the Blue Fiord Formation is gradational near Ca non Fiord and Strathcona Fiord (Trettin, 1978).

Alternatively, the unnamed formation may represent a new formation entirely.

Blue Fiord Formation

The Blue Fiord is an important and widely recognized formation in the northwestern Arctic, which records a resumption of quiescent, carbonate-depositing conditions in Zlichovian time, following a period of Early Devonian tectonism (Okulitch et al., 1986). Throughout the area under investigation it prominently overlies the recessive unnamed formation.

In the Norfolk Inlet area, the Blue Fiord Formation is divisible into four informal 'members' (Sections 1, 2, 3, 6, 10 and 12, Figs. 1, 2). The lower, dark coloured limestone 'member' (Blue Fiord 1) is about 100 m thick (Section 6), and is generally composed of a nodular-bedded, dark grey, lime wackestone with irregular silty partings. It is abundantly fossiliferous, and contains colonial rugose corals, crinoid ossicles, brachiopods, gastropods, stromatoporoids, bryozoans, tentaculitid and dacryoconarid tentaculites, ostracodes, bivalves and ammonoids. This 'member' grades into crinoidal wackestone and packstone in the upper 10 m. This same lower, nodular bedded, lime wackestone is present at Sutherland River (Section 17), where 25 m outcrop. At Sections 1 and 2 the basal few metres of the Blue Fiord are dolomitic, and heavily vertically burrowed.

Figure 4. Field photographs of the Devon Island, Goose Fiord, and unnamed formations.

a. Gradational contact between the Devon Island and Goose Fiord formations at Norfolk Inlet (Section 5). In this photograph, the contact occurs in the recessive interval between the lower (Devon Island) and upper (Goose Fiord) cliffs. Person standing at bottom left for scale.
b. Devon Island Formation, bedding plane view, about 25 m below top of formation at Section 5. Planolites-type burrows are visible to the right of the photo-scale; intraformational pebble paraconglomerate occurs in the bed immediately below (lower half of photo).
c. Goose Fiord and unnamed formations at Cross Bay (Section 2). The unnamed formation is the recessive unit at the top of the photo.
d. Solution-accentuated contact between the unnamed formation (lower) and Blue Fiord Formation (upper) at Section 6.
e. Laminated gypsiferous siltstone near the base of the unnamed formation, Section 6. Rod base at 3.3 m above the base of the formation. Rod is 1.5 m high.
f. Contact (person pointing) between the unnamed formation and Blue Fiord Formation at Section 2.
g. Solution-brecciated dolomite in the unnamed formation, Section 2, about 7 m below top of formation.
h. Unnamed formation (58 m thick) at Section 17, north of the Sutherland River. Here the unnamed formation is underlain by the Prince Alfred Formation (beneath dashed line). The upper cliff consists of dark limestone of the Blue Fiord Formation.

Blue Fiord 2 is a light coloured dolomite 'member', and is about 200 to 250 m thick. It weathers somewhat recessively in comparison to the resistant dark limestone 'members' that under- and overlie it, and its upper portion (50-100 m estimated) does not outcrop. At Section 12, on the south side of Norfolk Inlet, some 150 m are preserved. The basal 80 to 90 m consist of a generally massive, buff-grey, crinoidal dolomite. Minor features include digitate corals, brachiopod vugs, pods of solution breccia, and thin beds of laminated dolomite. At Section 12, Blue Fiord 2 is separated from underlying dolomitic, crinoidal, lime wackestones of Blue Fiord 1 by a thin bed of dark solution breccia, but elsewhere (Section 6), the contact between crinoidal limestones and dolomites is gradational, the result of diagenetic dolomitization. The lower crinoidal dolomite grades to a 30 m thick, massive, poorly crinoidal dolomite with abundant thin vertical burrows; the upper 10 m of this unit contain numerous elongate stromatactis features. The highest preserved 30 m of Blue Fiord 2 strata are a light grey, laminated, silty dolomite, with minor crosslamination and thin beds of dolomite-pebble conglomerate.

Blue Fiord 3 (Section 10) is a second, resistant, dark limestone 'member', approximately 100 m thick (Fig. 5a, b). The lower half is composed of dark grey, massive, crinoidal or bioclastic, lime wackestone; thin, silty partings occur in the lowest 20 m. A prolific fauna includes crinoid ossicles, brachiopods, metre-sized favositid and alveolitid corals, solitary Rugosa, and gastropods. The upper half of this 'member' is a generally dolomitic, crinoidal wackestone. Dolomitization commonly produces a dark grey-brown mottled outcrop appearance, and its intensity increases upsection through this 'member'.

Blue Fiord 'member' 4 outcrops very poorly, but its estimated thickness is somewhat in excess of 200 m. It is a generally monotonous sequence of buff-grey, "fenestral" dolomite. The "fenestrae" are demonstrably leached crinoid ossicles. Similar traces of brachiopods, gastropods and corals occur less commonly. Its lower 35 m outcrop at Section 10, where a 1 m thick, cryptalgally-laminated dolomite marks an irregular, erosional base; whatever hiatus this contact represents, however, is not believed to be significant. The highest 80 m of 'member' 4 are adequately exposed at Section 3, where crinoid-"fenestral" dolomite is prevalent. In the uppermost 20 to 25 m, extensively vertically-burrowed dolomite and fossiliferous dolomite with large gastropods occur. The upper contact of Blue Fiord 4 with the overlying Bird Fiord Formation is difficult to precisely establish, as solution-brecciation and zebra- dolomitization occur pervasively near this level (Fig. 5c).

Recently, Smith (1984) proposed that the dolomites and limestones previously included in the Blue Fiord Formation on southwestern Ellesmere Island should be reassigned to the Disappointment Bay Formation. The Disappointment Bay is a coeval formation composed largely of dolomite, and previously confined to Cornwallis and Bathurst islands and areas immediately adjacent (Thorsteinsson, 1958; Thorsteinsson and Kerr, 1968; Kerr, 1974; Thorsteinsson and Uyeno, 1980). Smith (1984, p. 61) contends that the light coloured

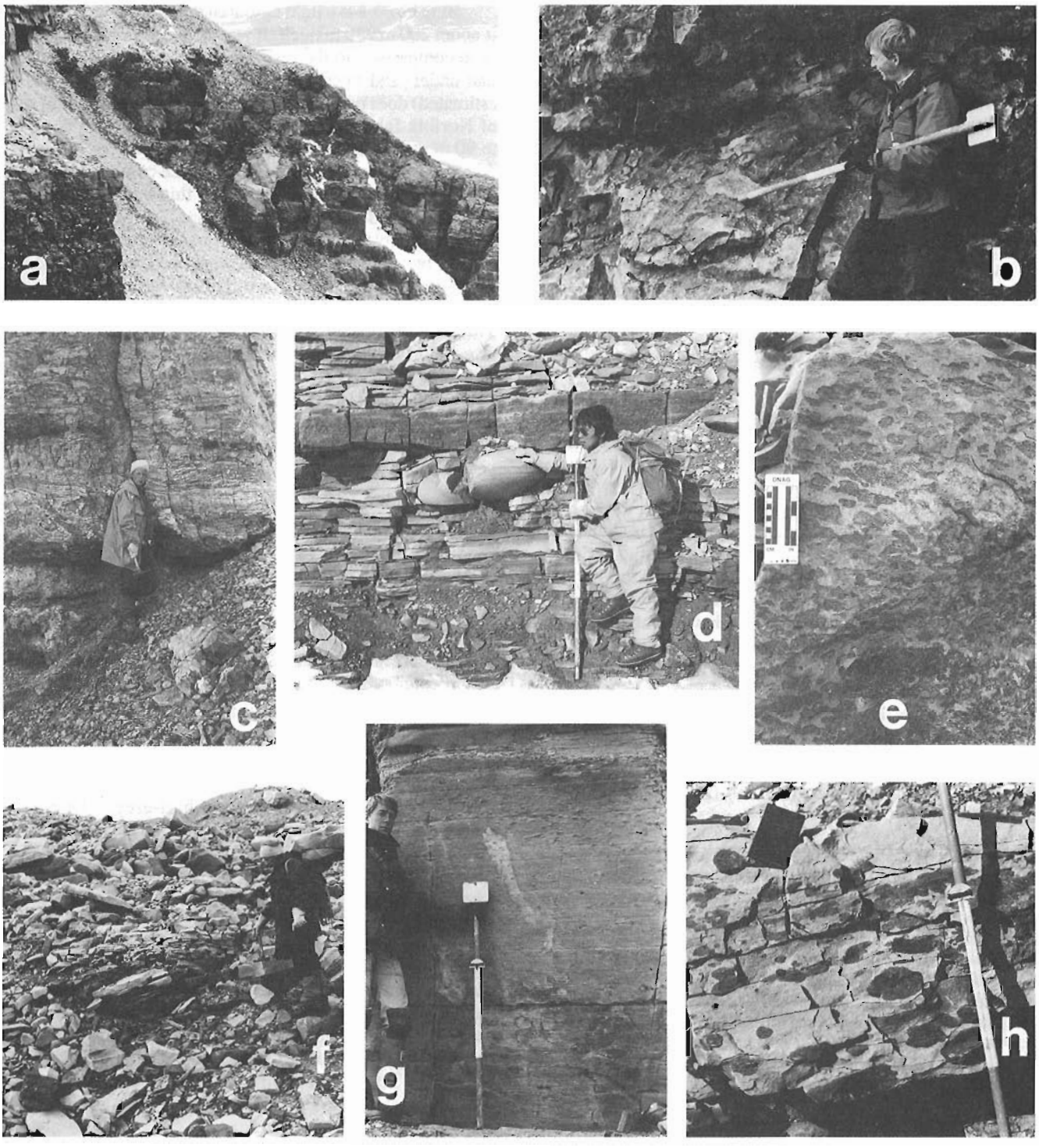

Figure 5. Field photographs of the Blue Fiord, Bird Fiord and Strathcona Fiord formations.

a. Overview of Blue Fiord 3, Section 10 (Cape Harrison).
b. Large alveolitid coral (indicated by rod) in dark fossiliferous limestone, Blue Fiord 3, Section 10.
c. Zebra dolomites near the base of the Bird Fiord Formation, Section 3. At this locality, the uppermost Blue Fiord Formation ('member' 4) consists of massive, crinoidal dolomite bearing large gastropods (just below knees of person standing).
d. Large concretions in Bird Fiord Formation (unit D), Section 9.
e, h. Incipient development of concretions in Bird Fiord D sandstones, Section 9.
f. Large-scale crossbeds in Bird Fiord D, Section 9.
g. Strathcona Fiord Formation, 7 m thick unit of laminated argillaceous siltstone, Section 9. Rod base at lower contact of formation.

carbonates on southern Ellesmere Island are sufficiently distinct from the dark coloured limestones and shales of the Blue Fiord Formation in the type section as to warrant exclusion from that formation.

At its type locality (McLaren, 1963), the Blue Fiord Formation consists of bedded limestones and calcareous shales, with significant biohermal development near by. As is evident from McLaren's (1963, p. 60) descriptions from southwestern Ellesmere and northern Devon islands, and recognized by others (Kerr, 1976; Trettin, 1978; Smith, 1984), facies variation is prevalent, with shallower water, back-reef platform sediments extending to the east and south of a marginal reef belt. Hence platformal, crinoidal and burrowed carbonates are abundant in the Norfolk Inlet area and southwesternmost Ellesmere Island. The Norfolk Inlet dolomites ('members' 2 and 4) are diagenetic in origin, as is indicated by their relationship with the underlying limestone 'members' (1 and 3), which shoal upward and become progressively more dolomitic toward their upper contacts. Dolomitization is facies-specific, occurring preferentially in shallower water, more commonly porous sediments. Various facies of the Blue Fiord Formation are closely interfingering and are gradational to one another, and dolomitization acts to enhance their distinction. Smith's (1984) proposal has merit in as far as that, at the extreme opposites of various Blue Fiord facies belts, the lithologies of the formation are indeed quite different. The interfingering of various facies occurs, however, over a broad area, and exposures with mixed lithologies are much more common than sections exhibiting a single facies type, a fact that makes the application of Smith's proposal impractical.

More significantly, the Blue Fiord dolomites and the Cornwallis Island-type Disappointment Bay dolomites do not appear to be genetically comparable. Both may be described as "fenestral" or vuggy dolomites, but whereas the Blue Fiord dolomites are crinoidal and burrowed in origin, and hence not truly fenestral at all (in the sense of Shinn, 1983), much of the Disappointment Bay vuggy dolomite is of a shrinkage-related, properly fenestral origin (personal observations, ECP). However, thorough petrological study is required in this regard before any firm conclusions can be made.

Because of the largely facies-related distinction between Blue Fiord limestones ('members' 1 and 3) and dolomites ('members' 2 and 4), we do not consider our four-fold subdivision to be widely applicable much beyond the Norfolk Inlet area. Near Prince Alfred Bay, Morrow and Kerr (1977) have recognized a two-fold limestone-dolomite subdivision (their map units Du_1 and Du_2), and at Goose Fiord (McLaren, 1963) and Grise Fiord (Mayr, 1982) three-fold subdivisions can be distinguished.

Bird Fiord Formation

The Bird Fiord Formation in the Cardigan Strait area is about 300 m thick, and a four-fold subdivision (informally designated A-D) can be recognized, following the four units of Goodbody (1985) described from southwestern Ellesmere Island.

At Section 7 (Fig. 1), Bird Fiord A is 168 m thick. It is composed predominantly of light grey-brown, silty, laminated dolomite, in places wave-rippled, and lesser amounts of bedded gypsum, dark, laminated claystone, dolomite-pebble orthoconglomerate, dark solution breccia, and dolomitic sandstone. Evaporites are most common in the lower to middle portions of this unit, and are best developed at Section 3 and immediately west of the head of Norfolk Inlet (not measured). The lower contact is commonly solution-brecciated, and appears to be disconformable (Fig. 5c).

Bird Fiord B is a thin, fossiliferous, limestone unit, roughly 40 m thick. At Sections 7 and 8 its base is recorded by a thin conglomerate incorporating small pebbles of dolomite from unit A. At Section 4 (Fig. 1), near the head of Norfolk Inlet, the transition from A to B is less dramatic, although disconformable nonetheless; at this locality, a poorly bioclastic, silty limestone forms the top of Bird Fiord A. The Bird Fiord B unit is a fairly monotonous, massive to thin bedded, bioclastic lime mudstone to wackestone, with irregular, disrupted, thin, sandy partings. Locally, the limestones grade to biosparites. Observed fauna include crinoid ossicles, brachiopods (dominantly spiriferids), favositid, alveolitid, thamnoporid and solitary rugose corals, gastropods, fish fragments, stromatoporoids, tentaculites and sponges.

Bird Fiord C, estimated to be 50 m thick (Sections 8, 9, Fig. 1), consists of interbedded dark grey, fissile siltstone to claystone, and grey-green, sparry, variably sandy, crinoidal packstone. The abundant, large crinoid ossicles are a distinctive orange- yellow colour, and impart an orangey hue to the packstones when viewed from a distance. Brachiopods occur prolifically in some of these beds, and other fossils include receptaculaceans and fenestellid bryozoans. The uppermost beds of unit C are composed of calcareous, bioclastic (disarticulated brachiopod shells) sandstone.

Bird Fiord D is about 125 m thick (Section 9), and records a transition to nearshore and fluvial, more clastically dominated conditions. The lower 50 m are mostly composed of light grey, laminated, quartz sandstone, which is commonly cross-stratified. In the lower half of this interval, thick interbeds of brown, calcareous, brachiopod shell-rich sandstone are common; these bear abundant, large, fish fragments and are partly conglomeratic. The development of large concretions is a striking feature of this unit; some sandstone beds demonstrate a peculiar, mottled texture indicative of arrested, incipient growth of concretions (Fig. 5d, e, h). The highest 4 m of grey sandstone are pervasively cross-stratified (Fig. 5f), and east-west trending, bipolar paleocurrents suggest a possible tidal influence.

The upper 75 m of unit D are composed of very thinly bedded to laminated, crosslaminated, fine grained quartz sandstone. Hematitic cement imparts a red colour to weathered surfaces, but fresh surfaces are off-white. A 15 m wide, fluvial conglomerate channel occurs at the top of the formation. Most of this reddish sandstone unit is rubbly, but evidence of westerly-directed paleocurrents occurs toward its top.

The Bird Fiord Formation, as used in this report, includes Morrow and Kerr's (1977) map units Du_3, Du_4 and most of Dbi. Units Du_3 and Du_4 correspond approximately to Bird Fiord A and B respectively; Morrow and Kerr's unit Dbi equates with Bird Fiord C and D and the Strathcona Fiord Formation of this report.

Okse Bay Group

The Okse Bay Group on northwesternmost Devon Island includes the Strathcona Fiord, Hecla Bay, Fram and Hell Gate formations.

The Strathcona Fiord Formation at Section 9 (Fig. 1) is 65 m thick. A 7 m thick unit of wavy-laminated, grey-green, argillaceous siltstone (Fig. 5g) forms the basal part of the formation. The remainder (58 m) is composed of interbedded red sandstone, similar to the one in unit D of the Bird Fiord Formation, and laminated, burgundy mudstone. The mudstone beds increase in thickness and abundance upsection. The only macrofossils noted were abundant fish fragments from a single, thin conglomerate bed 15 m above the base of the formation. The Strathcona Fiord Formation forms the uppermost part of Morrow and Kerr's (1977) map unit Dbi.

The overlying Hecla Bay Formation (Sections 9 and 11) is approximately 250 m thick. It is overwhelmingly composed of orange, thin bedded, medium grained quartz sandstone with abundant crossbedding; dark grey, laminated siltstones occur subordinately. The sandstone displays prominent Liesegang-features.

The Fram Formation weathers very recessively, and its estimated thickness (very approximate) is 250 to 300 m. The upper 100 m of the Fram are fairly continuously exposed at Section 15 (Fig. 1), near Cape Derby. At this locality the Fram Formation is composed of alternating beds of recessive, purple weathering siltstone, and greenish grey, laminated, fine grained sandstone. The sandstone beds are commonly crosslaminated, and many contain abundant, large, coaly plant fragments.

The Hell Gate Formation occurs incompletely on northwesternmost Devon Island, where only its lowest portions are preserved. It is composed of salmon pink, crosslaminated, coarse grained quartz sandstone.

REFERENCES

Goodbody, Q.H.
1985: Stratigraphy, sedimentology and paleontology of the Bird Fiord Formation, Canadian Arctic Archipelago; unpublished Ph.D. thesis, University of Alberta, Edmonton, Alberta.

Greiner, H.R.
1963: Southern Goose Fiord, southern Ellesmere Island; Geological Survey of Canada, Memoir 320, p. 292-302.

Kerr, J.Wm.
1968: Geology, southwestern Ellesmere Island, District of Franklin; Geological Survey of Canada, Map 10-1968.
1974: Geology of Bathurst Island Group and Byam Martin Island, Arctic Canada (Operation Bathurst Island); Geological Survey of Canada, Memoir 378.
1976: Stratigraphy of central and eastern Ellesmere Island, Arctic Canada, Part III. Upper Ordovician (Richmondian), Silurian and Devonian; Geological Survey of Canada, Bulletin 260.

Mayr, U.
1982: Lithostratigraphy (Ordovician to Devonian) of the Grise Fiord area, Ellesmere Island, District of Franklin; *in* Current Research, Part A, Geological Survey of Canada, Paper 82-1A, p. 63-66.

Mayr, U. and Okulitch, A.V.
1984: Geology, North Kent Island and south Ellesmere Island, District of Franklin, maps; Geological Survey of Canada, Open File 1036.

McLaren, D.J.
1963: Goose Fiord to Bjorne Peninsula; Geological Survey of Canada, Memoir 320, p. 310-338.

Morrow, D.W. and Kerr, J.Wm.
1977: Stratigraphy and sedimentology of lower Paleozoic formations near Prince Alfred Bay, Devon Island; Geological Survey of Canada, Bulletin 254.

Okulitch, A.V., Packard, J.J. and Zolnai, A.I.
1986: Evolution of the Boothia Uplift, Arctic Canada; Canadian Journal of Earth Sciences, v. 23, p. 350-358.

Shinn, E.A.
1983: Birdseyes, fenestrae, shrinkage pores, and loferites: a re-evaluation; Journal of Sedimentary Petrology, v. 53, p. 619-628.

Smith, G.P.
1984: Stratigraphy and paleontology of the Lower Devonian sequence, southwest Ellesmere Island, Canadian Arctic Archipelago; Unpublished Ph.D. thesis, McGill University, Montreal, Quebec.

Thorsteinsson, R.
1958: Cornwallis and Little Cornwallis islands, District of Franklin, Northwest Territories; Geological Survey of Canada, Memoir 294.
1963: Prince Alfred Bay, Devon Island; Geological Survey of Canada, Memoir 320, p. 221-232.

Thorsteinsson, R. and Kerr, J.Wm.
1968: Cornwallis Island and adjacent smaller islands, Canadian Arctic Archipelago; Geological Survey of Canada, Paper 67-64.

Thorsteinsson, R. and Uyeno, T.T.
1980: Stratigraphy and conodonts of Upper Silurian and Lower Devonian rocks in the environs of the Boothia Uplift, Canadian Arctic Archipelago; Geological Survey of Canada, Bulletin 292.

Trettin, H.P.
1978: Devonian stratigraphy, west-central Ellesmere Island, Arctic Archipelago; Geological Survey of Canada, Bulletin 302.

Geochemistry of Winnipegosis discoveries near Tablelands, Saskatchewan

P.W. Brooks, K.G. Osadetz, and L.R. Snowdon
Institute of Sedimentary and Petroleum Geology, Calgary

Brooks, P.W., Osadetz, K.G., and Snowdon, L.R., Geochemistry of Winnipegosis discoveries near Tablelands, Saskatchewan; in Current Research, Part D, Geological Survey of Canada, Paper 88-1D, p. 11-20, 1988.

Abstract

Recently discovered oils from the Middle Devonian Winnipegosis Formation in southern Saskatchewan have distinctive geochemical compositions characterized by a high saturate/aromatic hydrocarbon ratio and a bimodal n-alkane distribution, and are unlike any previously reported from the Williston Basin. It is possible that these oils represent a mixture of a previously recognized family of oils (commonly restricted to Ordovician reservoirs in southeastern Saskatchewan) and a distinctive oil, not previously recognized in the Williston Basin. Alternatively, these oils may represent a single oil derived from a source rock of complex composition. The abundance and composition of biological marker compounds indicate that these oils do not represent a family of oils derived from previously described potential petroleum source rocks. All or part of these Winnipegosis oils are possibly derived from petroleum sources indigenous to the upper Elk Point Group.

Résumé

Des hydrocarbures récemment découverts dans la formation de Winnipegosis, d'âge dévonien moyen, dans le sud de la Saskatchewan, présentent des compositions géochimiques distinctives, caractérisées par un rapport élevé des hydrocarbures saturés aux hydrocarbures aromatiques, et une distribution bimodale des n-alcanes; ces hydrocarbures sont différents de tous ceux découverts jusque-là dans le bassin de Williston. Il est possible qu'ils représentent un mélange d'une famille d'hydrocarbures déjà identifiée (généralement limitée à des réservoirs ordoviciens du sud-est de la Saskatchewan), et d'un type d'hydrocarbure distinctif jusque-là non identifié dans le bassin de Williston. Il est aussi possible que ces hydrocarbures représentent un seul type de pétrole dérivé d'une roche mère de composition complexe. L'abondance et la composition des constituants repères biologiques indiquent que ces hydrocarbures ne représentent pas une famille de pétroles dérivés de roches mères potentielles déjà décrites. Il est possible qu'une partie ou la totalité de ces hydrocarbures de Winnipegosis dérivent de roches mères autochtones de la partie supérieure du groupe d'Elk Point.

INTRODUCTION

Oils recently discovered in the Middle Devonian Winnipegosis Formation of Saskatchewan (Table 1) have distinctive geochemical compositions. These oils can be distinguished from both existing families of oils currently recognized in the Williston Basin (Brooks et al., 1987; Zumberge, 1983; Williams, 1974) and an oil produced from the Winnipegosis Formation in the American portion of the basin (from Sheridan County, presumed to be from either the Outlook or Redstone fields, sample location not identified by Zumberge, 1983). These distinctions indicate a unique oil-source relationship that affects the hydrocarbon prospectivity of the Winnipegosis oil-play in southern Saskatchewan.

Previous studies of Williston Basin oils

Williams (1974) examined a large number of oils produced from the American and Canadian portions of the Williston Basin. On the basis of carbon isotopes (whole oils and hydrocarbon fractions), gasoline range compounds (C_4-C_7), and heavy saturate fraction compositions (C_{15+}), he distinguished three families of oils of differing stratigraphic distribution. He proposed that the source rocks for these oil families were the Winnipeg (Type I), Bakken (Type II), and Tyler (Type III) formations. His correlation of the majority of oils to a Bakken Formation source rock became a dogmatic axiom of analysis in the Williston Basin (Price et al., 1984, 1986a, 1986b; Dembecki and Pirkle, 1985; Leenheer, 1984; Meissner et al., 1984; Webster, 1984; Schmoker and Hester, 1983). Zumberge (1983) examined another collection of oils from the American portion of the Williston Basin. Using gross composition, carbon isotopes of the heavy saturate fraction (C_{15+}), and selected biological markers (pristane/phytane and diterpanes) he proposed six different families of oils in the basin. Two of the families of oils he described appear to be equivalent to types identified by Williams. Zumberge's Group 1 oils appear to be equivalent to Williams' Type I oils, and his Group 2 oils appear to be the same as Williams'

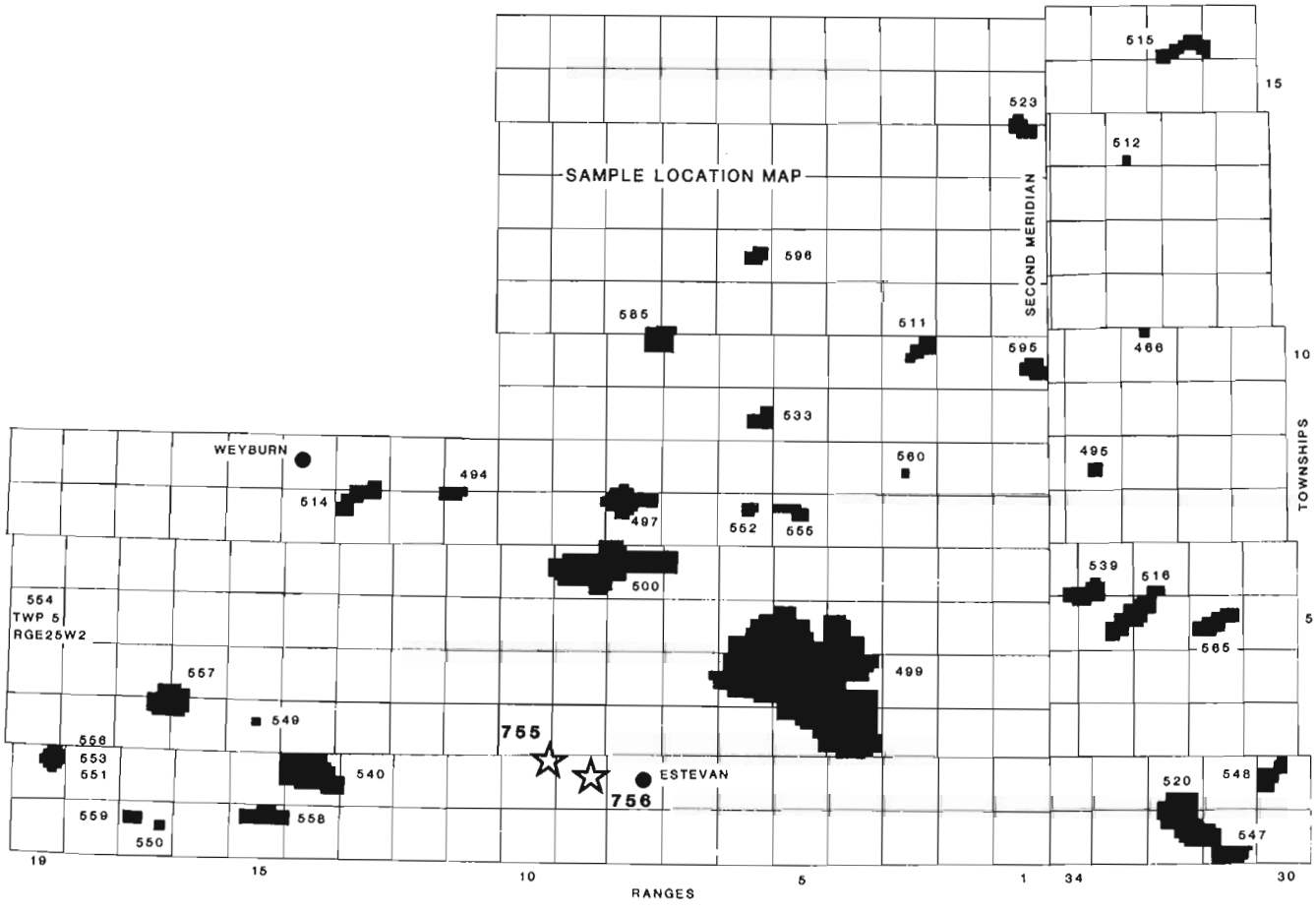

Figure 1. Sample location map indicating the position of samples analyzed for this study (sample nos. 755, 756) and those reported previously by Brooks et al. (1987).

Table 1. Sample location data

Sample no.	Location	Depth (m)	Name
755	04-36-002-10W2	2601 to 2606	Lasmo et al. Tableland 4-36
756	A08-22-002-09W2	2581 to 2584	Home et al. Tableland 8A-22

Type II oils. Zumberge did not study any oils from Pennsylvanian reservoirs, the interval containing Williams' Type 3 oils.

Brooks et al. (1987) studied the composition of a suite of oils from southeastern Saskatchewan. They identified and defined the characteristics of three families of oils. They confirmed the presence of Williams' Type I oils in Ordovician reservoirs within their study area (Family A). The remaining oils they studied resemble most closely Williams' Type II oils. However, they suggested that differences in the biological markers (pristane/phytane and diasterane/regular sterane ratios) of the remaining oils warrant subdivision into two families because of the unlikeliness that their distinctive compositions could be produced from a single source rock (Huang and Meinschein, 1979). A few of the oils, identified as Family B, have compositional characteristics and a stratigraphic distribution that suggest they were derived from a clastic source rock like the Bakken Formation. The majority of the oils, identified as Family C, have compositional characteristics and a stratigraphic distribution that suggest they were derived from an anoxic, clay-starved source interval, possibly like the one identified recently from the Lodgepole Formation (Osadetz and Snowdon, 1986).

EXPERIMENTAL

Two samples of oils (sample nos. 755, 756) produced from recent discoveries in the Winnipegosis Formation were examined in this study (Table 1).

Following distillation, to remove material that boils below 210°C, oils were fractionated according to the method published by Snowdon (1978). Saturate hydrocarbon fractions were examined by capillary column gas chromatography (GC) using a VARIAN 3700 gas chromatographer equipped with a 25 m fused-silica column coated with OV-1, and temperature programmed from 50-280°C at a heating rate of 4 degrees per minute (using He as the carrier gas). Capillary column gas chromatography-mass spectrometry (GC-MS) of the saturate fractions was performed using a VG 70SQ hybrid gas chromatography-mass spectrometer-mass spectrometer (GC-MS-MS) to duplicate GC-MS conditions used by Brooks et al. (1987). Data were collected by multiple ion detection (M.I.D.), monitoring ions at m/z 191.1794 (terpanes) and m/z 217.1950 (steranes).

RESULTS

Table 2 summarizes the significant results of analysis of the two oils produced from the Winnipegosis Formation of southeastern Saskatchewan. The composition of the two oils is essentially identical, although they were obtained from separate pools. The gross composition of the oils is characterized by very high saturate to aromatic ratios — greater than 2.5. Saturate fraction gas chromatograms (SFGC's) of the two samples (Fig. 2) are similar in that they are characterized by a bimodal distribution of compounds about peaks at nC_{15} and nC_{24}. Within the low molecular weight normal alkanes there is a marked odd/even predominance. Through the middle range of compounds, nC_{19} to nC_{21}, the distribution is complex. Higher molecular weight compounds, nC_{22+}, form a bell, centred at nC_{24}, without a clearly developed predominance pattern. There is a baseline hump in the range of nC_{27} to nC_{33}, indicating the presence of terpanes and steranes. Both pristane and phytane are abundant in these oils. The pristane/phytane ratios are both significantly less than one.

Fragmentograms of the terpanes (m/z=191) and steranes (m/z=217), shown in Figure 3, indicate that these compounds are in relatively low abundance in these oils. There is a well developed predominance of the C_{29} steranes over the C_{27} steranes. The S/R and beta beta/R ratios indicate that the oils are fully mature. The ratio of diasteranes/regular steranes is greater than 1.5. The ratio of C_{23}/C_{30} terpanes is very low.

Table 2. Selected compositional data

Sample no.:	755	756
Sat/Arom[1]:	2.6	2.5
Pr/Ph[2]:	0.62	0.75
Terpanes		
23/30[3]:	0.08	0.09
Ts/Tm[4]:	1.12	1.16
27/30[5]:	0.40	0.43
29/30[6]:	0.71	0.73
C_{31}S/R[7]:	1.37	1.41
hop/mor[8]:	6.56	7.64
Steranes		
27/29[9]:	0.43	0.38
27:28:29[10]:	26:15:60	24:13:62
S/R[11]:	1.17	1.09
BB/R[12]:	1.34	1.30
dia/reg[13]:	1.58	1.73

1. ratio of saturate/aromatic hydrocarbons
2. ratio of pristane/phytane
3. ratio of C_{23} tricyclic terpane/C_{30} pentacyclic 17alpha (H)-hopane
4. ratio of T_s[18alpha (H)-trisnorhopane]/T_m [17alpha (H)-trisnorhopane]
5. ratio of C_{27}pentacyclic hopane(T_m)/C_{30} 17alpha (H)-hopane
6. ratio of C_{29} 17alpha (H)-norhopane/C_{30} 17alpha (H)-hopane
7. ratio of (20S) [17alpha (H)-homohopane]/(20R) [17alpha (H)-homohopane]
8. 17alpha (H)-hopane/17beta (H)-moretane
9. C_{27} 5alpha (H), 14alpha (H), 17alpha (H)-cholestane/C_{29}

DISCUSSION

Comparison with existing families of oils

If the SFGC's for the Winnipegosis oils are compared with the SFGC's of the oil families identified previously from southeastern Saskatchewan, it may be seen that the bimodal character of the Winnipegosis oils is unique (Brooks et al., 1987, Fig. 3). This bimodal character is most obvious in the low ratio of nC_{22}/nC_{24}.

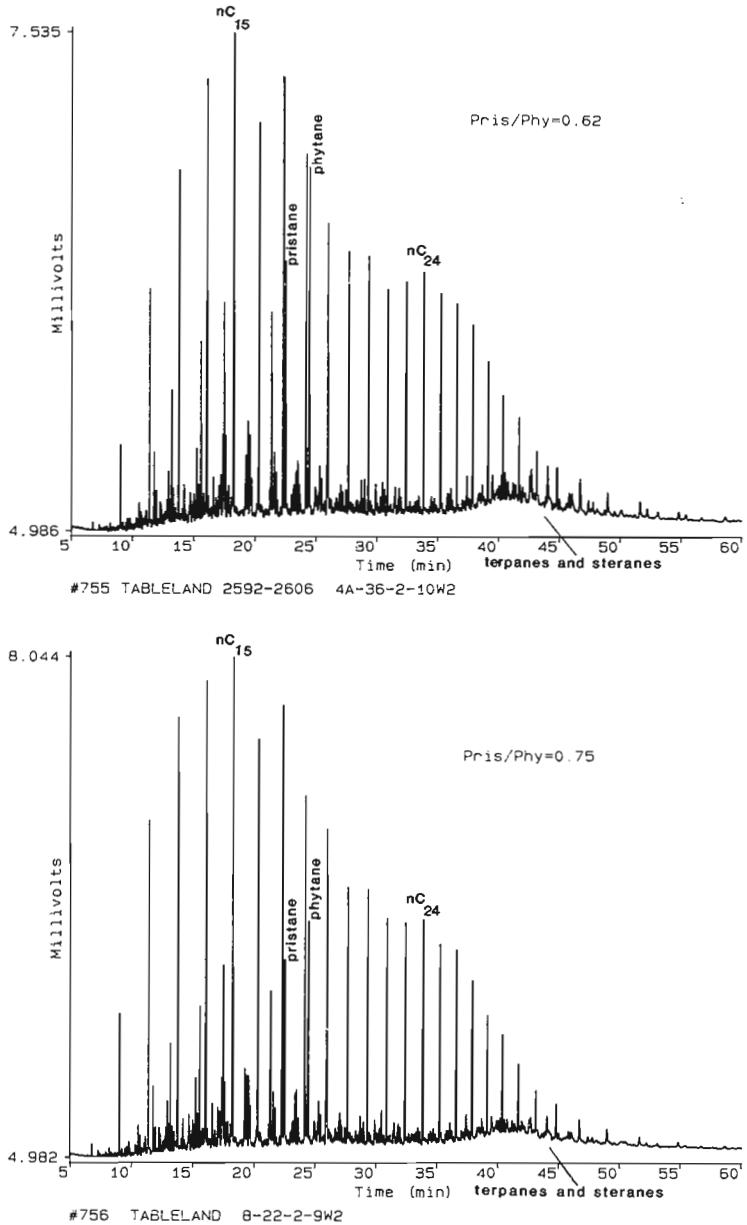

Figure 2. Saturate hydrocarbon fraction capillary gas chromatograms of oils produced from the Winnipegosis Formation in southeastern Saskatchewan.

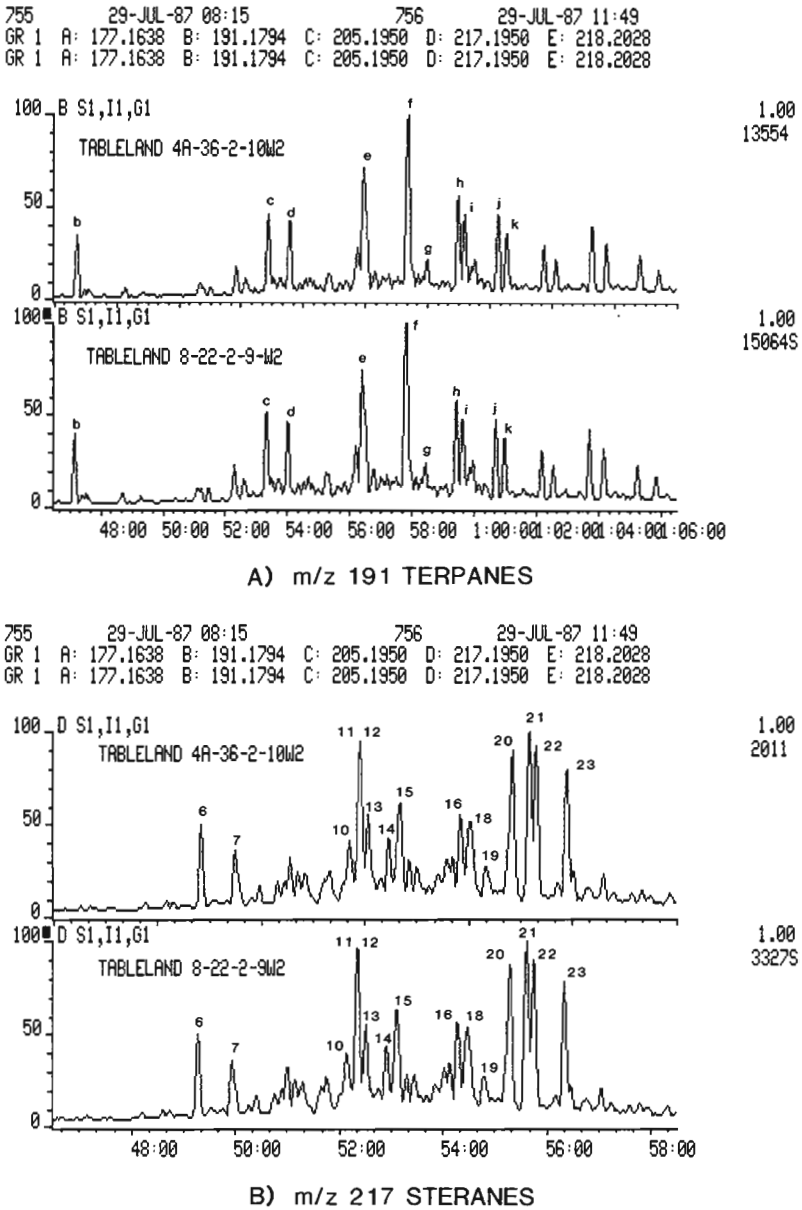

Figure 3. Capillary gas chromatography-mass spectrometry fragmentograms of: a. m/z 191 terpanes, and b. m/z 217 steroidal alkanes. Peaks indicated by letters (terpanes) and numbers (steroidal alkanes) are identified in Tables 3 and 4, respectively.

Brooks et al. (1987) employed several crossplots to discriminate between families of oils. The two Winnipegosis oils are plotted on similar diagrams with the samples described previously by Brooks (ibid.) (Figs. 4, 5, 6). The most diagnostic of the three figures is Figure 6, where the high saturate/aromatic ratio distinguishes these oils from Families A and B, and the high diasterane/regular sterane ratio distinguishes them from Family C. The other two discriminant diagrams plot the pristane/phytane ratio against the diasterane/regular sterane ratio (Fig. 4) and the C_{23}/C_{30} terpane ratio (Fig. 5). The two Winnipegosis oils again occupy a distinctive area on the cross-plots, although they are accompanied by oil sample no. 533, from the Star Valley Frobisher-Alida beds pool, an oil previously assigned to Family B.

The oil produced from the Winnipegosis Formation is compositionally distinct from the other three families of oils (Brooks et al., 1987) produced from southeastern Saskatchewan. The ratio of saturate/aromatic hydrocarbons of these oils is high compared with oils examined by Brooks et al. (1987). These oils are most easily distinguished from the oils of Family A, which are restricted to Ordovician reservoirs in southeastern Saskatchewan. Family A oils are characterized by a very low abundance of pristane and phytane and a pristane/phytane ratio greater than one. In many other respects the Winnipegosis oils resemble the Family A oils, particularly with their low abundance of biomarkers and low C_{23}/C_{30} terpane ratios (Fig. 5). The Winnipegosis oils can be distinguished from the oils of Family C by their high ratio of diasteranes/regular steranes (Figs. 4, 6). The pristane/phytane ratios of both the Winnipegosis oils and Family C oils

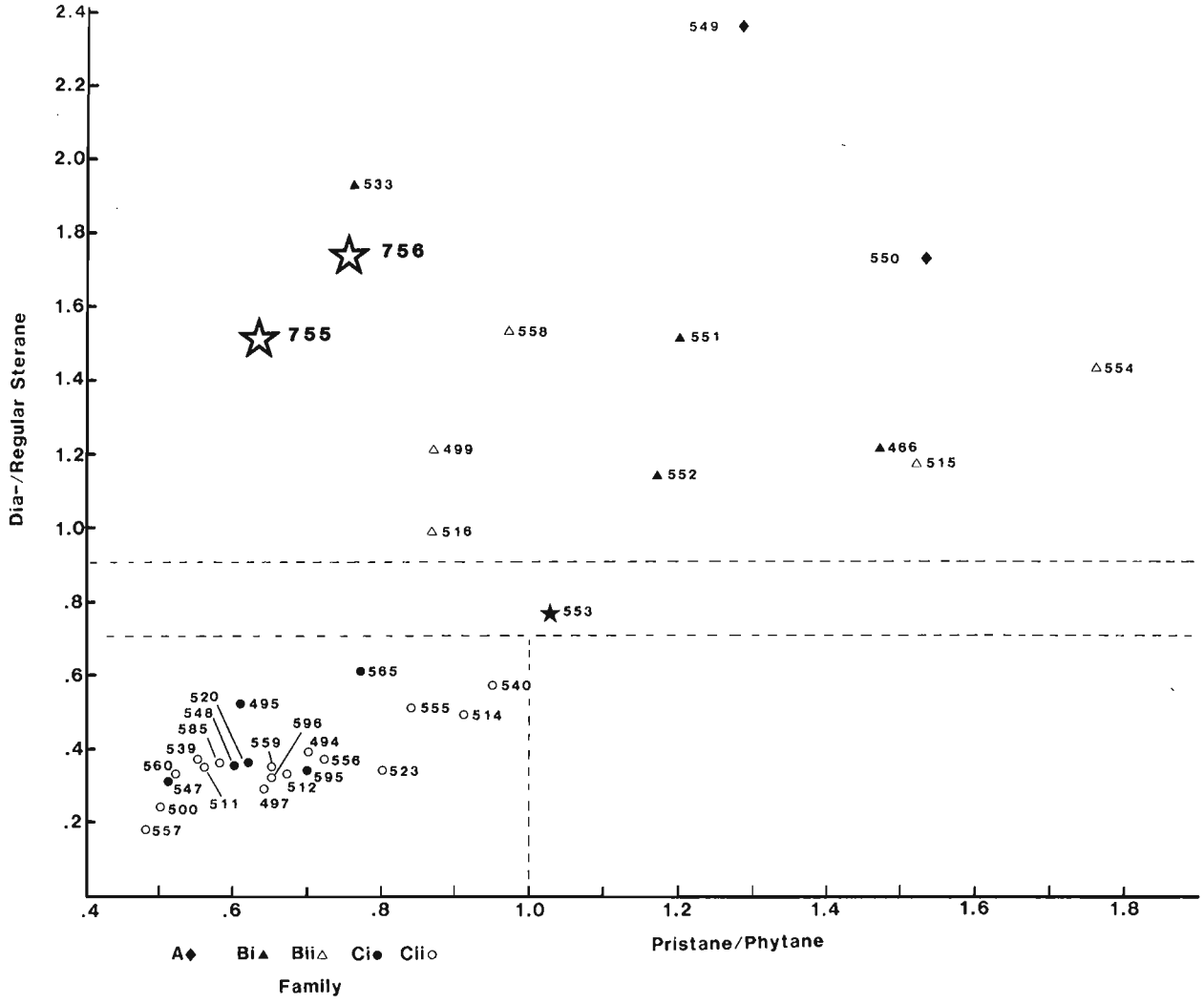

Figure 4. Cross-plot of pristane/phytane ratio versus diasterane/regular sterane ratio for sample nos. 755 and 756 (this study) and oils reported on previously by Brooks et al. (1987). Families of oils as identified by Brooks et al. (ibid.). Oil no. 553 is interpreted as a mixture of Families B and C. Oil no. 533 (Star Valley Frobisher-Alida beds pool), has compositional affinities to sample nos. 755 and 756. See the text for discussion of these similarities.

is less than one. In comparison with Family B oils, both the high saturate/aromatic ratio and character of the SFGC's of the Winnipegosis oils are distinctive. Oils of Family B are distinguished by a pronounced even/odd predominance amongst the higher numbered n-alkanes, a feature not characteristic of the Winnipegosis oils. Commonly, the oils of Family B have pristane/phytane ratios greater than one, yet there are several exceptions, most notably sample no. 533 (Star Valley Frobisher-Alida beds pool) (Brooks et al., 1987). This oil displays several compositional similarities to the Winnipegosis oils (Figs. 4, 5).

The three families of oils recognized by Brooks et al. (1987) represent two of the families identified by Williams (1974). The third family of oils recognized by Williams has a limited geographic and stratigraphic distribution not extending into Canada (Dow, 1974). Zumberge's (1983) oils from the Williston Basin included a number of samples from Devonian reservoirs, including one sample from the Winnipegosis. Two of Zumberge's families of oils are restricted to Devonian reservoirs. However, the Winnipegosis oil examined by Zumberge (1983, Fig. 3, sample II-4) has compositional characteristics like those of the Family A oils of Brooks et al. (1987). There are some superficial resemblances between the Winnipegosis oils and Zumberge's Group 4 oils from Upper Devonian reservoirs, but inspection indicates that there are three strong distinctions between the Winnipegosis oils of this study and the two groups of oils from Devonian reservoirs, identified by Zumberge (1983). The ratio of nC_{17}/pristane is very low in Group 4 oils compared with the Winnipegosis oils. The ratio nC_{22}/nC_{24}, which defines the hump in the SFGC of the Winnipegosis oils, differs. Finally, the Group 4 oils' SFGC's indicate an abundant hopanoid compound eluting just before the nC_{30} peak that is not apparent in the SFGC's of the Winnipegosis oils from Saskatchewan.

Table 3. Peaks identified in m/z 191 terpane traces (Fig. 5)

a. C_{23} tricyclic terpane
b. C_{24} tetracyclic terpane
c. T_s[18alpha(H)-trisnorhopane]
d. T_m[17alpha(H)-trisnorhopane]
e. 17alpha(H)-norhopane
f. 17alpha(H)-hopane
g. moretane
h. (20S)17alpha(H)-homohopane
i. (20R)17alpha(H)-homohopane
j. (20S)17alpha(H)-bishomohopane
k. (20R)17alpha(H)-bishomohopane

Mixed or simple composition?

The oils produced from the Winnipegosis Formation in southeastern Saskatchewan are herein identified as Family D. This family has a unique composition compared with other oils produced from the Williston Basin, as noted above. The complex nature of the SFGC's suggest that Family D oils may be derived from more than one contributing type of organic material. This complexity may have arisen due to either a mixing of oils generated independently from different source rock intervals, or from a mixture of contributing materials from a single source rock. Brooks et al. (1987) found that the SFGC's of Family A oils were characterized by very low abundances of pristane and phytane, a high pristane/phytane ratio, a high abundance of C_{15}, C_{17}, and C_{19} n-alkanes and a low relative abundance of higher homologues ($>nC_{22}$) with an even/odd predominance. These characteristics of the SFGC could be considered similar to that part of the SFGC in the Family D oils representing lower homologues of n-alkanes. Considering that an oil from the Winnipegosis Formation from the American part of the basin is clearly a Family A oil (Zumberge, 1983), it is possible that the oils

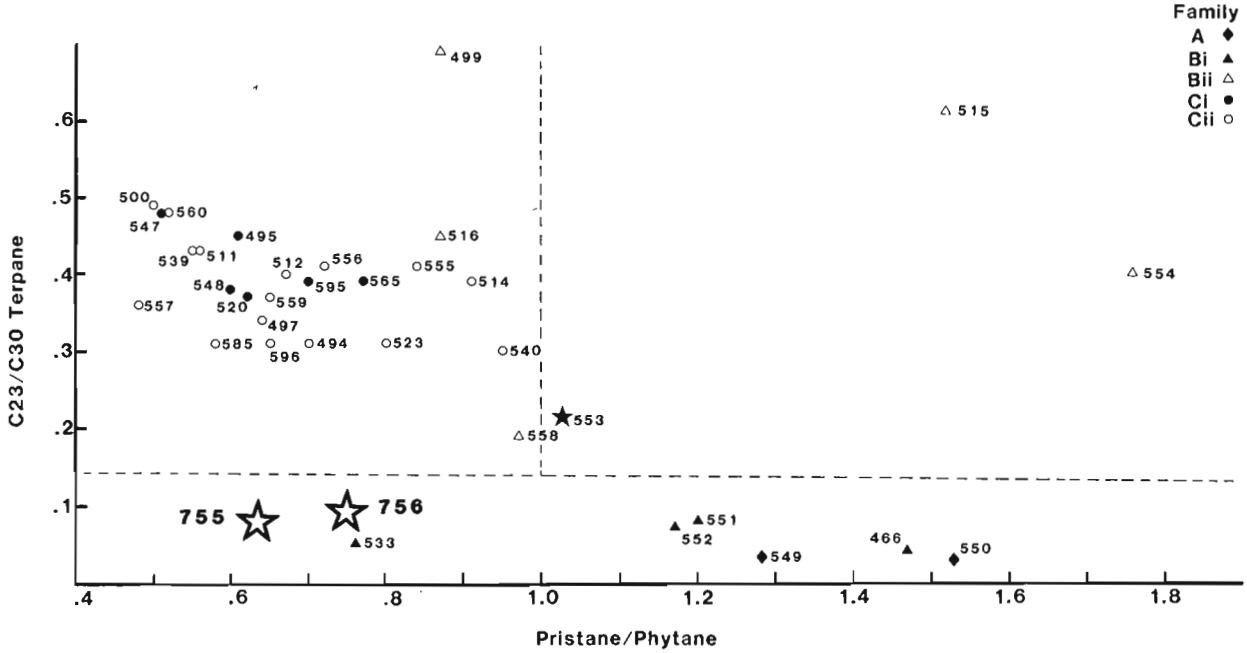

Figure 5. Cross-plot of pristane/phytane ratio versus C_{23}/C_{30} terpane ratio. Symbols identified in Figure 4.

studied here represent a mixture of a Family A oil, commonly attributed to Ordovician sources (Brooks et al., 1987; Kohm and Louden, 1982, 1978; Kendall, 1976), with another oil, having the characteristic of the higher homologues in the n-alkane hump. Alternatively, a single source interval of distinctive composition may have produced these oils with their complex composition of the saturate fraction hydrocarbons.

The latter hypothesis is currently preferred for several reasons. First, there is at present no simple model known whereby fractions or classes of compounds may be preferentially contributed by different source rocks to yield the observed properties. For example, if the higher molecular weight portion were preferentially contributed by an Ordovician source, then the absolute and relative contributions of pristane and phytane should be quite different from those of Family A oils. Commensurate with this, one would expect to find a consistent match between Winnipegosis and Ordovician oils in the higher molecular weight range (i.e. steranes and terpanes). A second point against the theory of two separate source rocks is that the two available samples are from separate pools, yet they have essentially identical compositions. This requires that identical proportions be contributed from different sources in both instances. Third, a dual source hypothesis requires that both sources have similar levels of maturity, because all of the maturation indicators are essentially consistent. It is thus more likely that these oils were derived from a single, as yet unidentified, source rock.

Stratigraphic setting and distribution of Family D oils

At the present time only two pools in southeastern Saskatchewan produce oils with all of the compositional characteristics of Family D (Table 1). These pools occur within a stratigraphic "reef" play in a basinal setting north of the Winnipegosis platform edge (Williams, 1984, Fig. 6; Wardlaw and Reinson, 1971). Oil occurs in Middle Devonian reefs of similar setting and age in northern Alberta, although the evaporitic sub-basins are smaller than the Prairie salt basin of Saskatchewan. Examination of the SFGC's of oils from the Middle Devonian oil pools of northern Alberta indicate that there are some similarities to Family D oils (Powell, 1984). The saturate/aromatic ratio of an oil from the Rainbow area exceeds two and the pristane/phytane ratios are less than one. However, none of the Alberta oils have the bimodal distribution of n-alkanes that is so characteristic of Family D oils. There are no additional data to allow further comparison at present. As discussed above it does not appear that Family D oils are known from the American portion of the Basin.

It is clear that the affinity of sample no. 533 will have to be re-evaluated with the discovery of this new family of oils. Although distinguishable from the oils of the Winnipegosis Formation because of its lower saturate/aromatic ratio, sample no. 533 occurs away from the centre of the Family B distribution on diagrams plotting pristane/phytane ratio against both diasterane/regular sterane ratio and C_{23}/C_{30} terpane ratio. In all three of these compositional ratios, sample no. 533 resembles the oils from the Winnipegosis Formation. The Star Valley pool lies within the geographic region of the Winnipegosis play. Possibly the Star Valley pool represents a mixture of oils from both Family D and Family B. If this is true, then the stratigraphic distribution of these oils extends from the upper Elk Point Group into the overlying Madison Group.

Table 4. Peaks identified in m/z 217 traces (Fig. 4)

2	C_{21} sterane
3	C_{21} sterane
5	C_{22} sterane
6	13(H), 17alpha(H)-diacholestane (20S)
7	13(H), 17alpha(H)-diacholestane (20R)
10	5alpha(H), 14alpha(H), 17alpha(H)-cholestane (20S)
11	5alpha(H), 14(H), 17(H)-cholestane (20R)
12	24-ethyl-13(H), 17alpha(H)-diacholestane (20S)
13	5alpha(H), 14(H), 17(H)-cholestane (20S)
14	5alpha(H), 14alpha(H), 17alpha(H)-cholestane (20R)
15	24-ethyl-13(H), 17alpha(H)-diacholestane (20R)
16	24-methyl-5alpha(H), 14alpha(H), 17alpha(H)-cholestane (20S)
17	24-methyl-5alpha(H), 14(H), 17(H)-cholestane (20R)
18	24-methyl-5alpha(H), 14alpha(H), 17alpha(H)-cholestane (20S)
19	24-methyl-5alpha(H), 14alpha(H), 17alpha(H)-cholestane (20R)
20	24-ethyl-5alpha(H), 14alpha(H), 17alpha(H)-cholestane (20S)
21	24-ethyl-5alpha(H), 14(H), 17(H)-cholestane (20R)
22	24-ethyl-5alpha(H), 14(H), 17(H)-cholestane (20S)
23	24-ethyl-5alpha(H), 14alpha(H), 17alpha(H)-cholestane (20R)

Constraints on source rocks

Family D oils are characterized by low pristane/phytane ratios and high diasterane/regular sterane ratios. The pristane/phytane ratio reflects the extent of oxidation of organic debris at and near the sediment/water interface. Pristane/phytane ratios of less than one can be indicative of an anoxic water column. A high ratio of diasteranes/regular steranes indicates the presence of clay minerals in the source rock, because rearranged steranes in oils are ascribed to clay-catalysed rearrangement reactions of precursor sterols, via unsaturated intermediates (Sieskind et al., 1979; Rubinstein et al., 1975). The source rock of Family D oils is interpreted as a thermally mature argillaceous rock that was deposited in a highly anoxic environment.

The absence of Family D oils from the American portion of the basin suggests: 1. that contributing sources may not be present there; or 2. that oils derived from equivalent source rocks remain to be found.

The stratigraphic setting of this reef play suggests that laterally equivalent basinal laminites could be a potential source, following the model of reef reservoir — source relationships outlined by Stoakes and Creaney (1985). Organic-rich laminites do occur in this formation (Wardlaw and Reinson, 1971), and the transition from starved basin facies to platform carbonates lies largely in the Canadian portion of the upper Elk Point Basin. The starved basin facies is generally absent from the American portion of the basin. If the Winnipegosis laminites are a contributing source, their distribution could explain the absence of Family D oils from the American portion of the basin. Absence of indications of other potential source rocks in Paleozoic strata of the Williston Basin provides a further constraint on the source of these oils.

Two preliminary models of hydrocarbon generation and migration are considered feasible. In the first model, source rocks indigenous to the Winnipegosis Formation have generated the oils and migration has been local into adjoining reefs or suitable traps in the platform edge. In the alternate model, these oils represent a mix of oils from different sources. One component of the oil is a Family A (Ordovician sourced) oil that is similar to the oil produced from the Winnipegosis Formation in the American portion of the basin (Zumberge, 1983). The other portion of the oil was derived from another source interval of similar thermal maturity. The Winnipegosis Formation may also be the source of this component of the oil. The migration and mixing pathways for the second model are more complex, and require a significant component of migration through the stratigraphic column.

GEOCHEMICAL CONSTRAINTS ON EXPLORATION MODELS

The Winnipegosis stratigraphic oil play in Saskatchewan is not new. The stratigraphic configuration of the play was well known in the late 1950's (Edie, 1959), and the high contrast between reef mounds and flanking evaporites makes the targets easily identifiable on reflection seismic lines. The play has been extensively drilled by several operators. Over the last ten years increased attention has been paid to areas of greater burial depth, and exploration activity has been focussed on southeastern Saskatchewan. Wardlaw and Reinson (1971) recognized fifteen years ago that lack of knowledge about source-reservoir relationships was the main reason for exploration failure. Only recently, a major oil company conducted a well-executed though unsuccessful program of exploration just west of the area that is now producing, in a region of greater maximum burial depth than the region of the current discoveries. Recent exploration activity has been only partly successful. The question arises as to how geochemistry can be employed to improve the efficiency of exploration in this play.

There are two basic contributions that can be made by organic geochemistry to the exploration of this play. Examination of the thermal maturity and hydrocarbon generation of the source rock can be used to outline exploration fairways of thermally mature source rock. Alternatively, geochemical identification of source-reservoir relationships separated by vertical migration pathways can lead to the identification of controls on the existing play and the formulation of new plays both within and below the stratigraphic unit of current interest.

If the source is indigenous to the Winnipegosis Formation, the main controls on an exploration play may be the thermal maturity of the Winnipegosis source and the effective draining of the source into suitable trapping configurations of facies or structure. A significant thermal gradient anomaly lying east of Weyburn has recently been identified extending northward from the hinge of the Nesson Anticline (Majorowicz et al., 1986). Within this region, thermal maturities of all Paleozoic source rocks are expected to be elevated compared to settings of similar, and sometimes even greater burial depth (Majorowicz et al., in press). We speculate that this factor may have controlled the failure of a recent drilling program, where burial depth was used as a control on thermal maturity instead of a combination of thermal gradient and burial depth. Levels of thermal maturity and oil

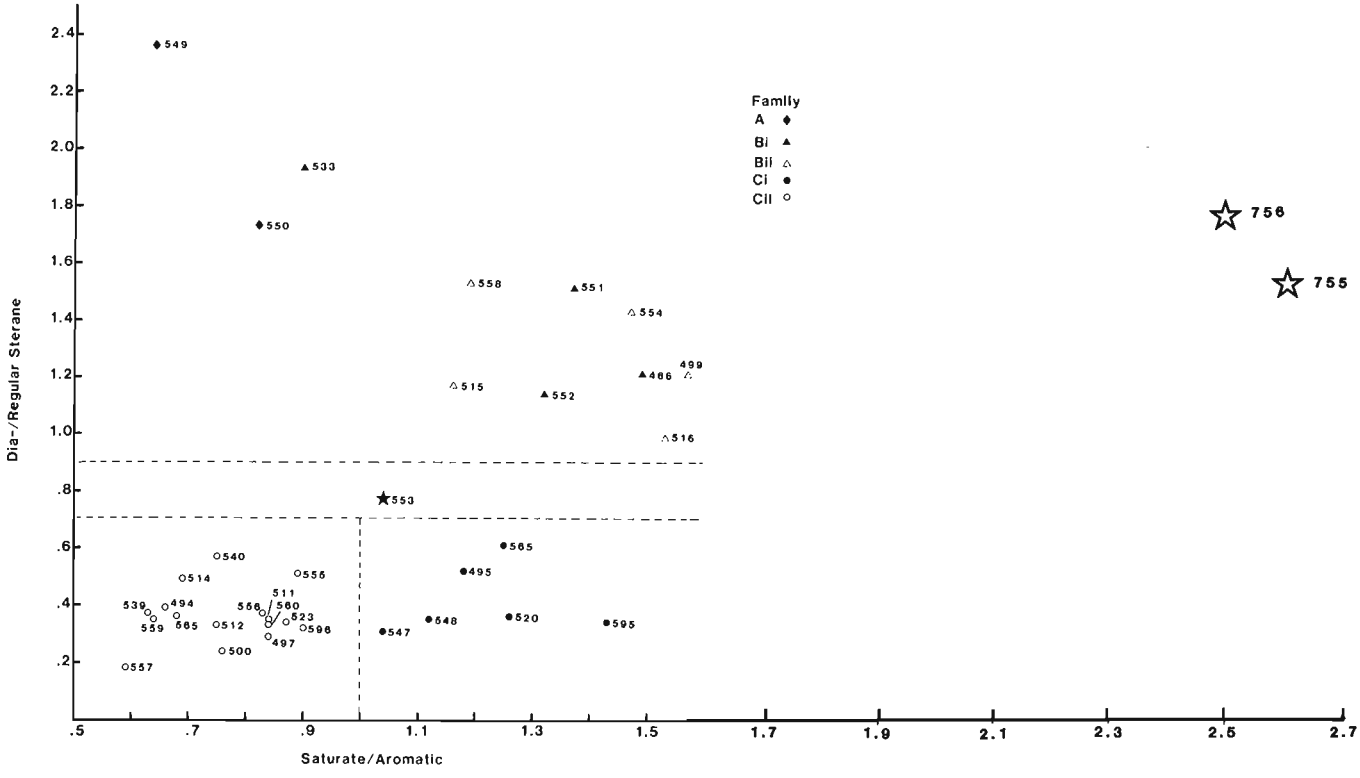

Figure 6. Cross-plot of saturate/aromatic ratio versus diasterane/regular sterane ratio. Symbols as identified in Figure 4.

generation potential derived from techniques such as Rock-Eval pyrolysis and solvent extract yield can be used to map thermal maturation patterns of the effective source rock in detail. This work remains to be done.

The character of the Winnipegosis oil studied by Zumberge (1983), although this oil is trapped in a structure deforming the fringing platform carbonate reservoir, provides evidence for significant migration of Family A (Ordovician) oils vertically through the stratigraphic section. The possibility that Family D oils are a mixture of Family A oils and some other component suggests that the migration pattern may be controlled by vertical migration pathways. If this is true, a major control on the accumulation of oil in the Winnipegosis Formation may be structurally controlled migration along vertical fractures. In such configurations, plays may exist in suitable traps within lower Winnipegosis platform facies in communication with thermally mature Ordovician source rocks. Plays in strata intervening between the source and the Winnipegosis reservoir could also be prospective. Should a Family A oil be discovered in another Winnipegosis pool, it could be indicative of potential at depth. The composition of the Star Valley oil suggests that structurally controlled migration pathways may extend into the Carboniferous succession.

A number of possible oil plays exist in the Winnipegosis Formation of the Williston Basin. The geochemistry of the oils and their sources can be used to define play types and delineate play fairways. Further study of solvent extracts from potential source rocks is underway to attempt to resolve the oil-source correlations.

CONCLUSIONS

1. The oils produced from the Winnipegosis Formation in southeastern Saskatchewan have a unique composition in comparison to other oils produced from the Williston Basin. They may be discretely sourced by strata indigenous to the Elk Point Group, or they may be a mixture of previously unidentified oils and Family A oils.

2. Vertical migration of oils through the Paleozoic succession is a significant process in the basin. An oil produced from the Winnipegosis Formation in the American portion of the basin belongs to Family A and the oil from the Star Valley pool previously assigned to Family B may be a mixture of the Family D and Family B oils.

3. Thermal maturity of potential source rocks and oil-source relationships are significant controls on the distribution of oil in the Winnipegosis Formation in Saskatchewan.

ACKNOWLEDGMENTS

The authors appreciate the collection and donation of oils for this study by Lasmo Exploration Canada Ltd., and Home Oil Ltd., the operating companies of the two discovery wells sampled for this study. Lasmo Exploration Canada Ltd. allowed the preparation and review of this article during the period when their well data were still confidential. This project was set up under the guidance of the O.E.R.D. 6.1.1., Government-Industry Review Committee, and the authors are grateful for this assistance.

REFERENCES

Brooks, P.W., Snowdon, L.R., and Osadetz, K.G.
1987: Families of oils in southeastern Saskatchewan; *in* Proceedings of the fifth international Williston Basin symposium, J.E. Christopher and C.G. Carlson (eds.); Bismarck, North Dakota, June 15-17, 1987, p. 253-264.

Dembicki, H., Jr. and Pirkle, R.L.
1985: Regional source rock mapping using a source potential rating index; American Association of Petroleum Geologists, Bulletin, v. 69, no. 4, p. 567-581.

Dow, W.G.
1974: Application of oil-correlation and source-rock data to exploration in Williston Basin; American Association of Petroleum Geologists, Bulletin, v. 58, no. 7, p. 1253-1262.

Edie, R.W.
1959: Middle Devonian sedimentation and oil possibilities, central Saskatchewan, Canada; Bulletin of the American Association of Petroleum Geologists, v. 43, no. 5, p. 1026-1057.

Huang, W.Y. and Meinschein W.G.
1979: Sterols as ecological indicators; Geochimica and Cosmochimica Acta, v. 43, p. 739-745.

Kendall, A.C.
1976: The Ordovician carbonate succession (Big Horn Group) of southeastern Saskatchewan; Saskatchewan Department of Mineral Resources, Report no. 180, 185 p.

Kohm, J.A. and Louden, R.O.
1982: Ordovician Red River of eastern Montana and western North Dakota: Relationships between lithofacies and production; *in* Fourth International Williston Basin Symposium Proceedings, J.E. Christopher and J. Kaldi (eds.); Saskatchewan Geological Society, Regina, p. 27-28.
1978: Ordovician Red River of Eastern Montana and western North Dakota: relationships between lithofacies and production; *in* 1978 Williston Basin Symposium — the Economic Geology of the Williston Basin, Proceedings of the Montana Geological Society 24th Annual Conference, Billings, Montana, p. 99-117.

Leenheer, M.J.
1984: Mississippian Bakken and equivalent formations as source rocks in the Western Canadian Basin; Organic Geochemistry, v. 6, p. 521-532.

Majorowicz, J.A., Jones, F.W. and Jessop, A.M.
1986: Geothermics of the Williston basin in Canada in relation to hydrodynamics and hydrocarbon occurrences; Geophysics, v. 51, p. 767-779.

Majorowicz, J.A., Jones, F.W. and Osadetz, K.G.
—: Heat flow environment of the electrical conductivity anomalies in the Williston Basin and hydrocarbon occurrence. Bulletin of Canadian Petroleum Geology. (in press)

Meissner, F.F., Woodward, J., and Clayton, J.L.
1984: Stratigraphic relationships and distribution of source rocks in the greater Rocky Mountain region; *in* Hydrocarbon source rocks of the greater Rocky Mountain region, J. Woodward, F.F. Meissner, and J.L. Clayton (eds.); Rocky Mountain Association of Geologists, Denver, p. 1-34.

Osadetz, K.G. and Snowdon, L.R.
1986: Speculation on the petroleum source rock potential of portions of the Lodgepole Formation (Mississippian) of southern Saskatchewan; *in* Current Research, Part B, Geological Survey of Canada, Paper 86-1B, p. 647-651.

Powell, T.G.
1984: Some aspects of the hydrocarbon geochemistry of a Middle Devonian barrier-reef complex, western Canada; *in* A.A.P.G. Studies in Geology no. 18 — Petroleum Geochemistry and Source Rock Potential of Carbonate Rocks, J.G. Palacas (ed.); American Association of Petroleum Geologists, Tulsa, Oklahoma, p. 45-61.

Price, L.C., Daws, T., and Pawlewicz, M.
1986a: Organic metamorphism in the Lower Mississippian — Upper Devonian Bakken shales, Part I: Rock-Eval Pyrolysis and Vitrinite Reflectance; Journal of Petroleum Geology, v. 9, no. 2, p. 125-162.

Price, L.C., Ging, T., Love, A., and Anders, D.
1986b: Organic metamorphism in the Lower Mississippian — Upper Devonian Bakken shales, Part II: Soxhlet Extraction; Journal of Petroleum Geology, v. 9, no. 3, p. 313-342.

Price, L.C., Ging, T., Daws, T., Love A., Pawlewicz, M., and Anders, D.
1984: Organic metamorphism in the Mississippian-Devonian Bakken shale, North Dakota portion of the Williston Basin; *in* Hydrocarbon source rocks of the Greater Rocky Mountain region, J. Woodward, F.F. Meissner and J.L. Clayton (eds.); Rocky Mountain Association of Geologists, Denver, p. 83-134.

Rubinstein, I., Sieskind, O., and Albrect, P.
1975: Rearranged sterenes in a shale: occurrence of simulated formation; Journal of the Chemical Society, Perkin Transactions I, p. 1833-1835.

Schmoker, J.W. and Hester, T.C.
1983: Organic carbon in the Bakken Formation United States portion of Williston Basin. American Association of Petroleum Geologists Bulletin. v. 67/12, p. 2165-2174.

Sieskind, O., Joly, G., and Albrecht, P.
1979: Simulation of the geochemical transformation of sterols: superacid effect of clay minerals; Geochimica and Cosmochimica Acta, v. 43, p. 1675-1679.

Snowdon, L.R.
1978: Organic geochemistry of the Upper Cretaceous/Tertiary delta complexes of the Beaufort Mackenzie Sedimentary Basin; Geological Survey of Canada, Bulletin 291.

Stoakes, F.A. and Creaney, S.
1985: Sedimentology of a carbonate source rock: the Duvernay Formation of Alberta Canada; *in* Rocky mountain carbonate reservoirs: a core workshop, M.W. Longman, K.W. Shanley, R.F. Lindsay and D.E. Eby (eds.); S.E.P.M. core workshop no. 7, Golden, Colorado, August 10-11, 1985; Society of Economic Paleontologists and Mineralogists, Tulsa, Oklahoma, p. 343-375.

Wardlaw, N.C. and Reinson, G.E.
1971: Carbonate and evaporite deposition and diagenesis, Middle Devonian Winnipegosis and Prairie evaporite formations of south-central Saskatchewan; American Association of Petroleum Geologists, Bulletin, v. 55, p. 1759-1786.

Webster, R.L.
1984: Petroleum source rocks and stratigraphy of the Bakken Formation in North Dakota; *in* Hydrocarbon source rocks of the greater Rocky Mountain region, J. Woodward, F.F. Meissner and J.L. Clayton (eds.): Rocky Mountain Association of Geologists, Denver, p. 57-81.

Williams, G.K.
1984: Some musings on the Devonian Elk Point Basin, Western Canada, Bulletin of Canadian Petroleum Geology, v. 32, no. 2, p. 215-231.

Williams J.A.
1974: Characterization of oil types in Williston Basin; American Association of Petroleum Geologists, Bulletin, v. 58, no. 7, p. 1243-1252.

Zumberge, J.E.
1983: Tricyclic diterpane distributions in the correlation of Paleozoic crude oils from the Williston Basin; *in* Advances in Organic Geochemistry 1981, John Wiley & Sons Ltd., p. 738- 745.

Early Namurian (or older) alkali basalt in the Borup Fiord Formation, northern Axel Heiberg Island, Arctic Canada

H.P. Trettin
Institute of Sedimentary and Petroleum Geology, Calgary

Trettin, H.P., Early Namurian (or older) alkali basalt in the Borup Fiord Formation, northern Axel Heiberg Island, Arctic Canada; in Current Research, Part D, Geological Survey of Canada, Paper 88-1D, p. 21-26, 1988.

Abstract

Unmetamorphosed but spilitized amygdaloidal flows, identified as alkali basalt on the basis of stable trace element ratios, occur 16.7 to 48.5 m above the base of the Borup Fiord Formation in an area south of Rens Fiord, northern Axel Heiberg Island. Limestone 35 to 36.5 m above the volcanics has yielded conodonts of early Namurian (Arnsbergian) age. The volcanics constitute a local member within the Borup Fiord Formation that either is correlative with part of the Audhild Formation in northwestern Ellesmere Island or slightly older. Outcrops of these two units occur in a northeasterly trending belt that is parallel to the axis of the Sverdrup Basin. The volcanism was caused by rifting and occurred in nonmarine or shallow marine settings.

Résumé

Des coulées amygdaloïdes non métamorphisées mais spilitisées, identifiées comme étant des basaltes alcalins d'après les rapports entre les oligo-éléments stables, se situent entre 7,7 et 48,5 m au-dessus de la base de la formation de Borup Fiord, dans une région située au sud du fiord Rens, dans le nord de l'île Axel Heiberg. Dans les calcaires situés entre 35 et 36,5 m au-dessus des roches volcaniques, on a recueilli des conodontes d'âge namurien inférieur (Arnsbergien). Les roches volcaniques constituent un membre local à l'intérieur de la formation de Borup Fiord, qui peut être corrélé avec une partie de la formation d'Audhild du nord-ouest de l'île Ellesmere, ou légèrement plus ancien que celle-ci. On rencontre des affleurements de ces deux unités dans une zone d'orientation générale nord-est, parallèle à l'axe du bassin de Sverdrup. Le volcanisme a été causé par la formation d'un fossé tectonique qui eut lieu dans un milieu non marin ou de type marin peu profond.

INTRODUCTION

In 1986, a thin volcanic unit of local extent was discovered in the basal part of the Carboniferous succession in an area south of Rens Fiord, northern Axel Heiberg Island, in the course of a reinvestigation of the lower Paleozoic rocks (Trettin, 1987). The upper Paleozoic rocks in this area had not been studied previously but had been assigned, on the basis of air observation and air photo interpretation (Thorsteinsson and Trettin, 1972b), to an undifferentated map unit that includes the Borup Fiord, Nansen, van Hauen and Degerbols formations. The volcanic rocks form a narrow, northerly and northeasterly trending outcrop belt that is terminated by a fault in the south and by overburden in the northeast (Fig. 1, inset). They are of particular interest because, together with the Audhild Formation of northwestern Ellesmere Island (see below), they represent the oldest known phase of volcanism in the Sverdrup Basin. In order to establish their stratigraphic position and age, a short section was measured that extends from the base of the Carboniferous succession through the volcanics to the lowest overlying fossiliferous limestone. The volcanics were mentioned only very briefly in the earlier report (Trettin, 1987) because laboratory studies relevant for the definition of their age and composition still were in progress. The results of this work are reported and interpreted here.

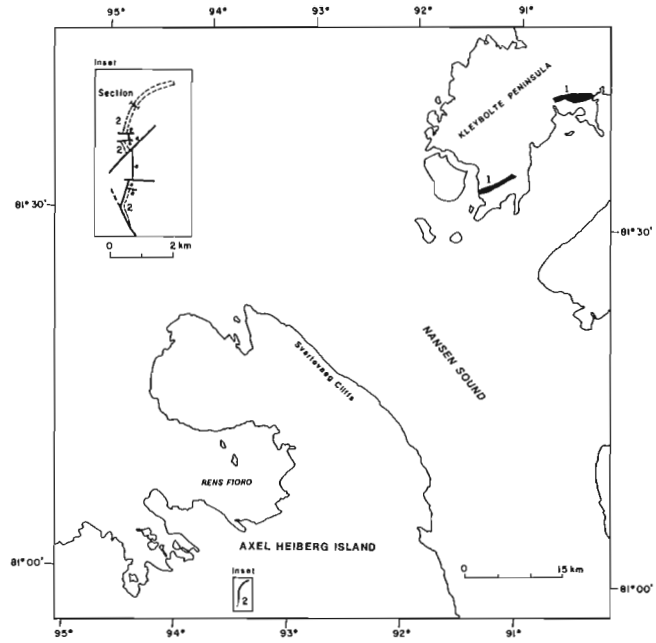

Figure 1. Location of Carboniferous volcanic units; 1: Audhild Formation (from Thorsteinsson and Trettin, 1972a); 2: volcanic member of Borup Fiord Formation (for geological setting see Trettin, 1987, Fig. 36-2B).

LITHOSTRATIGRAPHY

South of eastern Rens Fiord, gently dipping Carboniferous strata lie on tightly folded quarzite and phyllite of the Lower Cambrian Grant Land Formation with angular unconformity. The basal 90 m of the Carboniferous succession are characterized by intermittent exposures of sandstone, basalt, dolostone and limestone (Fig. 2 and Appendix). These strata are overlain by orange and grey weathering carbonate rocks that have not been studied. The composition and origin of the measured strata are discussed below, and their age and stratigraphic assignment in the concluding parts of the paper.

Sandstone occurs at the base of the section (unit 1, at 0-4.7 m) and above the volcanics (unit 7, at 64-65.5 m; unit 9, at 79.5-80 m). Unit 1 is a dusky red to greyish red sandstone that shows flat and undulating lamination and small-scale crosslamination. Its grain size is medium to coarse in the lower part with some granule-bearing beds, and medium to fine near the top. The sandstone is composed mainly of quartz with trace amounts of muscovite and biotite, the latter commonly replaced by opaque minerals (including hematite). The quartz is moderately or well sorted. Some grains are well rounded, but most are more angular owing to pressure solution or marginal replacement.

Units 7 and 9, also reddish, are medium to coarse grained sandstones that display flat or undulating lamination and consist of quartz and chert in a matrix of microcrystalline or fine crystalline dolomite[1]. Some chert grains are slightly schistose and one has inclusion-free spherical structures, reminiscent of radiolarians.

The presence of a dolomitic matrix shows that units 7 and 11 are probably of peritidal or shallow marine origin. Unit 1, lacking such a matrix and overlying an angular unconformity, may be nonmarine, but lacks diagnostic features.

The quartz in these sediments very likely has a long history of recycling. It probably was derived originally from crystalline rocks of the Canadian Shield and has passed through the Lower Cambrian Grant Land Formation and perhaps also through the Lower Devonian Stallworthy Formation. The chert evidently comes from the Hazen Formation (Lower Cambrian to Lower Silurian), which includes a large proportion of slightly metamorphosed radiolarian chert. After the Late Silurian — Early Devonian erosion of the Hazen Formation, detrital grains of the chert may have been incorporated in the Stallworthy Formation before becoming part of the Carboniferous strata (cf. Trettin, 1969; 1979, Figs. 29, 30).

Two units of **dolostone** (9-10, at 70.5-79.5 m; and 12, at 80-83.5 m) are reddish and composed of predominantly fine crystalline dolomite with varying amounts of unsorted, floating quartz, ranging in grain size from silt to very coarse sand. These strata probably were deposited in peritidal or shallow marine settings.

A single unit of brownish grey, massive **limestone** occurs near the top of the measured section (unit 13, at 83.5-91.5 m). The limestone is a skeletal wackestone composed of a variety of invertebrates, foraminifera, and algae. Very fine

[1] The following terms are used for size grades of crystals: microcrystalline = 0.004 to 0.062 mm; very fine crystalline = 0.0625 to 0.125 mm; fine crystalline = 0.125 to 0.25 mm. This classification, which conforms with the Wentworth scale, has been adapted from Leighton and Pendexter (1962) and Drummond (1963), and has been applied in most reports of this writer (e.g. Trettin, 1979).

to fine crystalline dolomite euhedra are scattered throughout the rock. The following organic components were identified in thin sections by Dr. B. Beauchamp:

brachiopods (spines common)
pelecypods
gastropods
echinoderms
apterinellid, bradyinid, staffellid, and tuberetinid foraminifera
Girvanella sp.
beresellid and ungdarellid algae
?Tubiphytes sp.

In addition, there are present intact silicified brachiopods of Composita-type. This "biota", according to Beauchamp, "is in general characteristic of schizohaline restricted (e.g. lagoonal) environment".

The **volcanics** occur in two units (unit 3, at 4.7-16.7 m; and unit 5, at 48.0-48.5 m) that are separated by a covered interval of 4.5 m. Ten specimens examined in thin section (with the aid of some whole-rock X-ray diffractograms) are all mafic amygdaloidal rocks that have been altered to spilite. The plagioclase has been altered to albite and the mafic silicates (presumably pyroxene and (?) olivine) are almost entirely replaced by chlorite, altered glass, opaque minerals and carbonate. Carbonate veinlets or replacements are common. The amygdules contain carbonate, chlorite, chalcedony, quartz, and opal.

Duplicate analyses of three specimens of basalt are listed in Table 1. The results have been recalculated to 100 percent, omitting the weight loss on ignition, which varies from 7.7 to 12.5 percent. The material lost on ignition probably consisted mainly of CO_2, which has subsequently been determined separately, and H_2O, which has not been determined directly. The water (probably between 4 and 7 percent) occurs mainly in the crystal structure of the chlorite.

Classification on the basis of major elements would be meaningless because of the alteration state and amygdaloidal character of the rocks. Average ratios of stable trace elements (Fig. 3) indicate that all three specimens are alkali basalt (cf. Winchester and Floyd, 1977, Fig 6). The tectonic environment — a continental intraplate setting (see below) — is well enough known to test the validity of the most recent plot of tectonic environments based on three of these elements (Meschede, 1986, Fig. 1). The results are acceptable; one lies in the field of alkalic intraplate basalt and the two others lie in a field of predominantly intraplate basalt that is shared by alkali basalt and tholeiite (Fig. 4). In continental settings, both alkali basalt and tholeiite are extruded during doming or rifting regimes; the specific significance of alkali basalt in these settings is a complex and controversial problem (cf. Kampunzu et al., 1986) that requires special chemical and isotopic studies for its solution (e.g. Perry et al., 1987).

Evidence for deposition in an aqueous environment, such as pillow structure or abundant brecciation, was not observed.

Table 1. Chemical analyses of volcanic rocks.

	86TM1-20.5 m				86TM1-27.0 m				86Tm1-30.0 m			
	118-86-1	Method	118-86-10	Method	118-86-2	Method	118-86-11	Method	118-86-3	Method	118-86-12	Method
SiO_2 %	47.0	1	46.9	1	52.2	1	52.0	1	47.6	1	47.5	1
Al_2O_3%	12.8	1	12.7	1	14.0	1	14.0	1	15.4	1	15.7	1
TiO_2 %	1.87	1	1.87	1	1.80	1	1.79	1	3.08	1	3.02	1
Fe_2O_3%	5.2	1	5.2	1	8.6	1	8.8	1	7.7	1	7.5	1
FeO %	5.0	4	5.0	4	2.4	4	2.3	4	5.2	4	5.1	4
MnO %	0.13	1	0.13	1	0.08	1	0.08	1	0.06	1	0.06	1
MgO %	6.35	1	6.43	1	6.65	1	6.71	1	6.37	1	6.29	1
CaO %	9.58	1	9.66	1	5.29	1	5.29	1	4.97	1	4.88	1
Na_2O%	3.65	1	3.52	1	4.45	1	4.41	1	4.78	1	4.86	1
K_2O %	0.56	1	0.56	1	0.39	1	0.41	1	1.05	1	1.17	1
P_2O_5 %	0.20	1	0.21	1	0.21	1	0.22	1	3.2	1	3.2	1
CO_2 %	7.6	4	7.8	4	3.9	4	4.0	4	0.61	4	0.66	4
Total	99.9		100.0		100.0		100.0		100.0		99.9	
As ppm	0	2	0	2	4	2	3	2	6	2	0	2
Ba ppm	110	1	230	1	100	1	230	1	240	1	250	1
Br ppm	0	2	0	2	0	2	6	2	0	2	0	2
Mo ppm	5	2	5	2	6	2	4	2	5	2	5	2
Nb ppm	17	2	18	2	15	2	15	2	58	2	61	2
Rb ppm	11	2	11	2	1	2	6	2	11	2	12	2
Sr ppm	74	2	77	2	75	2	73	2	130	2	130	2
Th ppm	0	2	0	2	0	2	0	2	0	2	0	2
U ppm	0	2	0	2	0	2	0	2	0	2	0	2
Y ppm	20	2	18	2	18	2	14	2	22	2	21	2
Zr ppm	120	2	120	2	110	2	110	2	290	2	290	2

Method 1: wave-length dispersive X-ray fluorescence.
Method 2: energy dispersive X-ray fluorescence, using Compton scatter.
Method 4: rapid chemical techniques (FeO by modified Wilson method; CO_2 by combustion and infrared detection).

If the rocks were deposited in a nonaqueous environment, the spilitization must have been caused by groundwater, probably soon after deposition when the lavas were still hot. The highly vesicular texture of the rocks would have facilitated this process. Alternatively, the spilization could have been caused by lacustrine or sea water that was present during the deposition of the volcanics, or by lagoonal or sea water that invaded the area immediately afterwards.

AGE

A limestone sample collected 83.5 to 85.0 m above the base of the section (GSC locality C-97213) yielded conodonts, identified as follows by Dr. A.C. Higgins:

Cavusgnathus sp.
Gnathodus bilineatus bollandensis Higgins and Bouckaert

Age: Gnathodus bilineatus bollandensis Zone, Arnsbergian Stage, early Namurian.

The Arnsbergian is the second of seven stages distinguished in the Namurian of western Europe, and the Gnathodus bilineatus bollandensis Zone is coextensive with that stage (Higgins, 1985). The fact that the interval between the conodont-bearing limestone and the volcanics is only 35 m thick suggests that the volcanics themselves are no older than Namurian (Pendleian or Arnsbergian) although they could be Viséan in age if deposition was slow or if there was a hiatus.

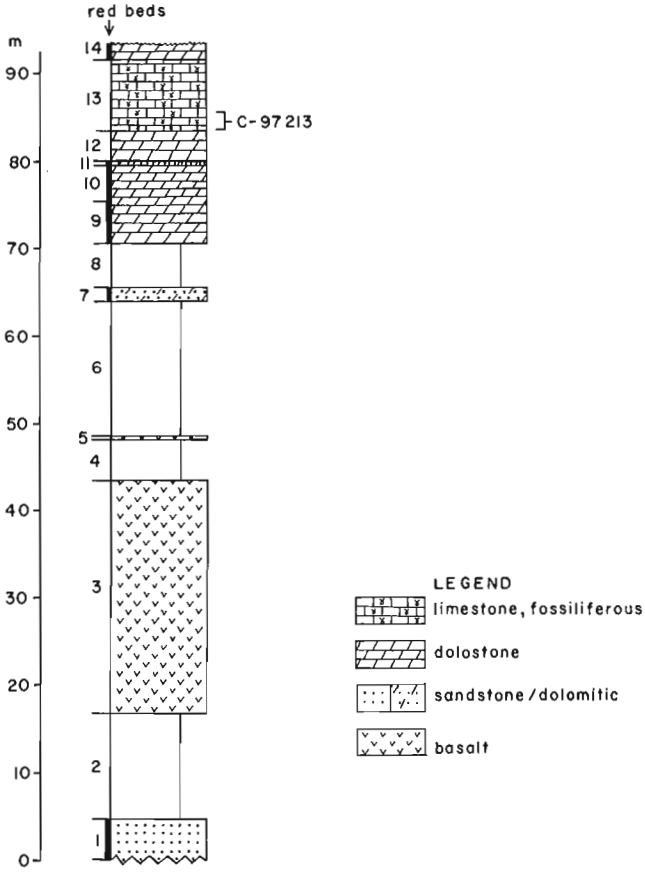

Figure 2. Stratigraphy of lowermost part of the Carboniferous succession south of eastern Rens Fiord. Units 1 to 7 are unequivocally assigned to the Borup Fiord Formation; units 8 to 14 belong either to the Borup Fiord Formation or to the Nansen Formation.

REGIONAL RELATIONSHIPS

The upper Paleozoic succession of the Arctic Islands (Thorsteinsson and Tozer, 1970; Thorsteinsson, 1974; Nassichuk and Davies, 1980; Davies and Nassichuk, in press) lies unconformably on Devonian and older strata of the Ellesmerian Orogen and forms the basal part of the Sverdrup Basin fill. The oldest deposits are nonmarine clastic sediments of Viséan age (Emma Fiord Formation) that are preserved at a few localities only, including the Svartevaeg Cliffs of northern Axel Heiberg Island and Kleybolte Peninsula of northwestern Ellesmere Island (Fig. 1). In most of the region the basal Carboniferous deposits consist of variegated clastic and

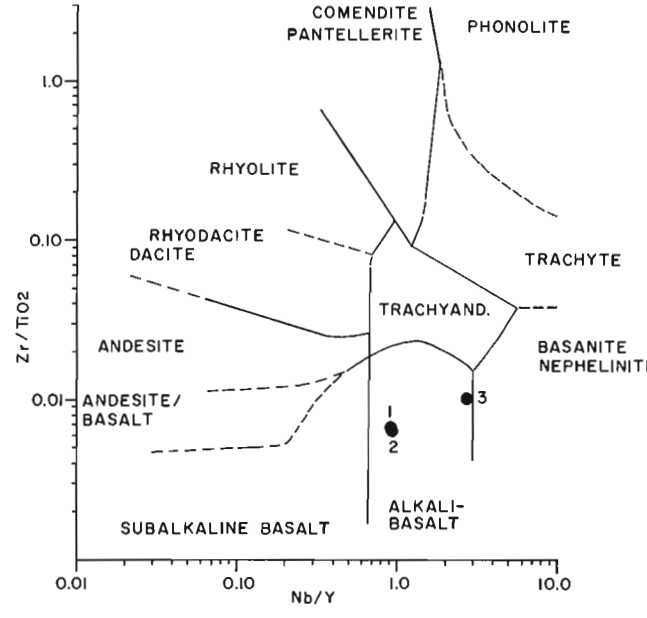

Figure 3. Classification of three samples of basalt (based on Winchester and Floyd, 1977, Fig. 6).

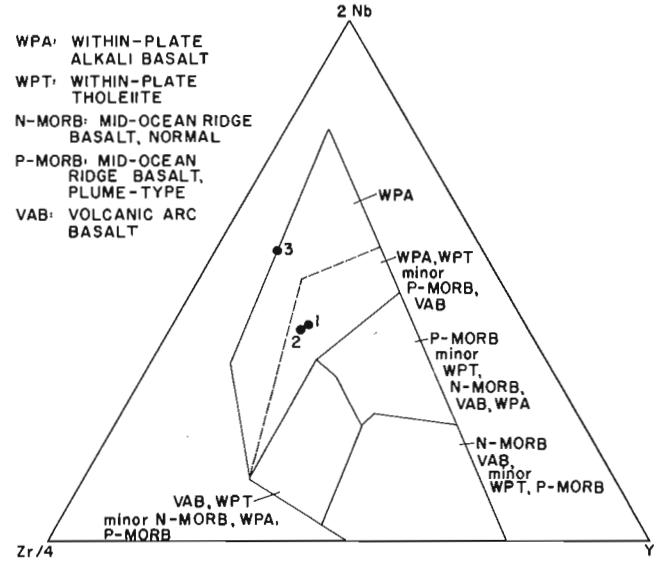

Figure 4. Tectonic environment of analyzed samples (based on Meschede, 1987, Fig. 1).

minor carbonate sediments, that have been assigned to the Borup Fiord Formation in northern Axel Heiberg Island and northwestern Ellesmere Island, and to the Canyon Fiord Formation in the rest of the region. The coarse grade of these two formations, which ranges up to boulder conglomerate at many localities, and their association with listric normal faults at some localities indicate a major rifting event that created the Sverdrup Basin. The diachronous character of this event is apparent from the facts that the Borup Fiord Formation is older than the Canyon Fiord Formation in general and that the latter is highly diachronous.

The Borup Fiord Formation ranges in thickness from "a feather edge" to 460 m and is characterized by marked facies changes over short distances. The upper part has yielded foraminifera of Arnsbergian age at Borup Fiord, northwestern Ellesmere Island, but the age of the largely nonmarine lower and middle parts is uncertain. The base of the formation has been tentatively placed in the late Viséan (Lower Bollandian) on Kleybolte Peninsula, and in the earliest Namurian (middle Pendleian) in northwestern Ellesmere Island and northern Axel Heiberg Island (Nassichuk and Davies, 1980, Fig. 4).

In most of the region, the Borup Fiord Formation is overlain either by carbonate strata of the Nansen Formation or by evaporitic, carbonate and clastic sediments of the Otto Fiord Formation. However, a thick (560 m) volcanic unit, The Audhild Formation, is intercalated between the Borup Fiord and Nansen formations on Kleybolte Peninsula (Fig. 1). The age of the Audhild Formation is poorly constrained but fossil collections from the Borup Fiord and Nansen formations in the Hare Fiord region suggest that it may be Arnsbergian (Nassichuk and Davies, 1980, Fig. 4).

Establishment of a stratigraphic nomenclature for the area south of Rens Fiord requires more fieldwork. It is obvious however, that not only the clastic redbeds below the volcanics but also the reddish carbonate and minor clastic sediments immediately above them can be assigned to the Borup Fiord Formation. The latter, for example, are similar to strata in the upper part of the formation at Emma Fiord (cf. Thorsteinsson, 1974, p. 24). The volcanics therefore constitute a local member within the Borup Fiord Formation. The position of the upper contact of Borup Fiord Formation has not yet been determined in the area south of Rens Fiord. It could be placed at the top of unit 7 or at some higher level, possibly above the measured section, as other redbeds are present above unit 13.

Present fossil evidence permits — but does not prove — partial correlation of the volcanic member of the Borup Fiord Formation with the Audhild Formation if an Arnsbergian age is accepted for the latter. This correlation implies that the base of the Borup Fiord Formation is somewhat older on Kleybolte Peninsula, where the volcanics are underlain by 380 m of Borup Fiord strata, than south of Rens Fiord, where they are underlain by only 17 m of Borup Fiord strata. Alternatively, the volcanic member of the Borup Fiord Formation may be slightly older than the Audhild Formation. Regardless of this problem, the two units are close enough in age to be considered together as manifestations of the earliest known phase of volcanism in the Sverdrup Basin, a phase that was associated with the Borup Fiord — Canyon Fiord rifting event. It is interesting to note that the outcrop areas of the two volcanic units are aligned in a northeasterly direction that is roughly parallel with the axis of the Sverdrup Basin (cf. Nassichuk and Davies, 1980, Fig. 1).

ACKNOWLEDGMENTS

The faunal and floral identifications, as mentioned, were made by A.C. Higgins and B. Beauchamp, and the chemical analyses by the Analytical Chemistry Section of the Geological Survey at Ottawa under the direction of G.R. Lachance. I thank G. Check for able assistance in the field, and the Director, officers and pilots of the Polar Continental Shelf Project for transportation in the field and courtesies. The manuscript has benefitted from critical reading by B. Beauchamp and R. Thorsteinsson.

REFERENCES

Davies, G.R. and Nassichuk, W.W.
—: Carboniferous and Permian history of the Sverdrup Basin, Arctic Islands; *in* Innuitian Orogen and Arctic Platform: Canada and Greenland; H.P. Trettin, (ed.); Geological Survey of Canada, Geology of Canada, no. 3 (also Geological Society of America, The Geology of North America, v. E). (in press)

Drummond, J.M.
1963: Carbonates and grade size; Bulletin of Canadian Petroleum Geology, v. 11, p. 33-53.

Higgins, A.C.
1985: The Carboniferous System: Part 2 — Conodonts of the Silesian Subsystem from Great Britain and Ireland; *in* A Stratigraphical Index of Conodonts, A.C. Higgins and R.L. Austin (eds.); Ellis Horwood Limited Publishers for The British Micropaleontological Society, Chichester, England, p. 210-227.

Kampunzu, A.B., Caron, J.-P.H., and Lubala, R.T.
1986: The East African Rift, magma genesis and astheno-lithospheric dynamics; Episodes, v. 9, p. 211-215.

Leighton, W.M. and Pendexter, C.
1962: Carbonate rock types; *in* Classification of carbonate rocks, W.E. Ham (ed.); The American Association of Petroleum Geologists, Memoir 1, p. 33-61.

Meschede, M.
1986: A method of discriminating between different types of mid-ocean ridge basalts and continental tholeiites with the Nb-Zr-Y diagram; Chemical Geology, v. 56, p. 207-218.

Nassichuk, W.W. and Davies, G.R.
1980: Stratigraphy and sedimentation of the Otto Fiord Formation — a major Mississippian-Pennsylvanian evaporite of subaqueous origin in the Canadian Arctic Archipelago; Geological Survey of Canada, Bulletin 286.

Perry, F.V., Baldridge, W.S., and DePaolo, D.J.
1987: Role of asthenosphere and lithosphere in the genesis of Late Cenozoic basaltic rocks from the Rio Grande rift and adjacent regions of the southwestern United States; Journal of Geophysical Research, v. 92, p. 9193-9213.

Thorsteinsson, R.
1974: Carboniferous and Permian stratigraphy of Axel Heiberg Island and western Ellesmere Island, Canadian Arctic Archipelago; Geological Survey of Canada, Bulletin 224.

Thorsteinsson, R. and Tozer, E.T.
1970: Geology of the Arctic Archipelago; *in* Geology and Economic Minerals of Canada, R.J.W. Douglas (ed.); Geological Survey of Canada, Economic Geology Report no. 1, p. 547-590.

Thorsteinsson, R. and Trettin, H.P.
1972a: Geology, Cape Stallworthy; Geological Survey of Canada, Map 1305A (1:125,000).
1972b: Geology, Bukken Fiord, District of Franklin; Geological Survey of Canada, Map 1310A (1:125,000).

Trettin, H.P.
1969: Pre-Mississippian geology of northern Axel Heiberg and northwestern Ellesmere islands, Arctic Archipelago; Geological Survey of Canada, Bulletin 171.
1979: Middle Ordovician to Lower Devonian deep-water succession at southeastern margin of Hazen Trough, Canön Fiord, Ellesmere Island; Geological Survey of Canada, Bulletin 272.
1987: Investigations of Paleozoic geology, northern Axel Heiberg and northwestern Ellesmere islands; *in* Current Research, Part A, Geological Survey of Canada, Paper 87-1A, p. 357-367.

Winchester, J.A. and Floyd, P.A.
1977: Geochemical discrimination of different magma series and their products using immobile elements; Chemical Geology, v. 20, p. 325-343.

APPENDIX

Stratigraphic section

Location: about 8 km south of eastern Rens Fiord, northern Axel Heiberg Island; NTS 560 A; UTM Zone 15X, 492300E, 8991900 N

Underlying strata: quartzite and phyllite of Grant Land Formation (Lower Cambrian)

- angular unconformity -

Unit 1: 0 to 4.7 m (4.7 m)

Sandstone: composed mainly of quartz with small amounts of muscovite, biotite, feldspar; moderately to well sorted; quartz is well rounded to subangular (pressure solution); grain size medium to very coarse in lower part with some granule-bearing layers, and medium to fine grained at top; beds 4 to 7 cm thick, planar or undulating lamination with some low-angle crosslamination; dusky red to greyish red.

Unit 2: 4.7 to 16.7 m (12.0 m)

Covered, recessive; drift of reddish sandstone in lower part.

Unit 3: 16.7 to 43.5 m (26.8 m)

Basalt: amygdaloidal, spilitic.

Unit 4: 43.5 to 48.0 m (4.5 m)

Covered.

Unit 5: 48.0 to 48.5 m (0.5 m)

Basalt: amygdaloidal, spilitic.

Unit 6: 48.5 to 64.0 (15.5 m)

Covered.

Unit 7: 64.0 to 65.5 m (1.5 m)

Sandstone: composed of quartz and subordinate chert (1 fragment with ghosts of radiolarians?), medium to coarse grained, well sorted, in matrix of fine crystalline dolomite; quartz subangular to rounded; pale red to greyish red; undulating beds 0.5 to 1 cm thick.

Unit 8: 65.5 to 70.5 m (5.0 m)

Covered.

Unit 9: 70.5 to 75.5 m (5.0 m)

Dolostone: mainly fine crystalline, with floating silt and sand of quartz; massive; moderate red-orange.

Unit 10: 75.5 to 79.5 m (4.0 m)

Outcrop and rubble of **dolostone**: very fine to fine crystalline with floating quartz of silt to very coarse sand grade, rounded, unsorted; greyish red.

Unit 11: 79.5 to 80.0 m (0.5 m)

Sandstone: composed of quartz and chert (partly schistose), medium to coarse grained, poorly sorted in matrix of dolomite, microcrystalline to fine crystalline; horizontal bedding; pale red.

Unit 12: 80.0 to 83.5 m (3.5 m)

Dolostone: fine crystalline, with small amounts of floating quartz, silt to fine sand grade; laminated to thin bedded; pale red.

Unit 13: 83.5 to 91.5 m (8.0 m)

Skeletal lime wackestone: dolomitic; scattered euhedral dolomite, very fine and fine crystalline; massive; light brownish grey. GSC locality C-97213 from 83.5 to 85.0 m: conodonts, Arnsbergian Stage, early Namurian.

Unit 14: 91.5 to 93.5 m (2.0 m)

Dolostone: massive, pale red.

Top of measured section; intermittent exposures of Carboniferous rocks continue.

Geographic variations in relationships between random and maximum vitrinite reflectance, Western Canadian coals

K.C. Pratt
Institute of Sedimentary and Petroleum Geology, Calgary

Pratt, K.C., Geographic variations in relationships between random and maximum vitrinite reflectance, Western Canadian coals; in Current Research, Part D, Geological Survey of Canada, Paper 88-1D, p. 27-32, 1988.

Abstract

Linear relationships between random and maximum vitrinite reflectance are defined on the basis of analysis of 54 coal samples from Western Canada. Equations are developed representing three major coal-producing areas of the region as well as one for the entire region. Variations in the nature of the equations and difficulties in their use are discussed. The need for strict control of data and the difficulty in achieving accuracy, which may restrict the usefulness of such equations in routine analysis, are shown. Although the results from regression analysis offer a good graphic representation of the linearity between values measured, calculated values may be affected by a number of factors that are difficult to control in practical situations.

Résumé

On a défini, en fonction de l'analyse de 54 échantillons de charbon provenant de l'ouest du Canada, des relations linéaires entre les valeurs aléatoires et les valeurs maximales de la réflectance de la vitrinite. On a élaboré les équations représentant trois grands secteurs houillers de la région, et une équation applicable à la région toute entière. On étudie les variations des propriétés des équations et la difficulté d'application de celles-ci. On démontre le besoin d'un strict contrôle des données et la difficulté à atteindre un degré suffisant de précision, difficulté qui peut réduire l'utilité de telles équations lors de l'analyse de routine. Bien que les régressions offrent une bonne représentation graphique de la linéarité entre les valeurs mesurées, il est possible qu'un certain nombre de facteurs difficiles à contrôler dans des situations pratiques influencent les valeurs calculées.

INTRODUCTION

It has long been known that the relationship between maximum vitrinite reflectance ($\overline{Ro}_{max}$) and random vitrinite reflectance ($\overline{Ro}$ random) is strongly linear. Variations of this relationship have been reported, including those of Ting (1978), Neavel et al. (1981), Bustin (1984) and Weiss (1985). Since their equations differ somewhat, it was decided that development of an equation of this type for Western Canada would be appropriate. As well, the recent work of Kilby (1986) indicates that the optical nature of a coal may vary depending on the types of tectonic stress to which it has been subjected, which, in turn, has a direct effect on the relationship between $\overline{Ro}_{max}$ and $\overline{Ro}$ random.

With this in mind, the present study attempts to define a relationship between $\overline{Ro}_{max}$ and $\overline{Ro}$ random for a suite of Western Canadian coals. The data are arranged according to geographic origin in order to define possible variations related to sample location. The data represent three major coal producing areas; 1. southeastern British Columbia, 2. northeastern British Columbia, and 3. the Rocky Mountain Foothills of Alberta. In terms of rank, the coals range from high volatile A to medium volatile bituminous in southeastern British Columbia, high volatile A to low volatile bituminous in northeastern British Columbia, and from high volatile bituminous C to high volatile bituminous A in the Rocky Mountain Foothills.

The data used were selected largely from existing files that have been compiled during the course of several projects. Since the main objective of this report is to compare $\overline{Ro}_{max}$ with $\overline{Ro}$ random, detailed discussion of geological factors such as age and tectonic style is not presented. However, these factors, particularly tectonic style, have probably had a significant influence in the production of some of the variations shown. In age the samples range from Late Jurassic to Paleocene.

EXPERIMENTAL

The microscopes used for data generation included two Leitz MPV2 systems, (one equipped with an Apple II computer for data acquisition), a Zeiss MPM II Zonax microcomputer system, as well as a Zeiss IBAS II image analysis system, which uses the vitrinite mode of a grey level histogram to determine $\overline{Ro}$ random. Goodarzi (1987) described the IBAS system in some detail, and showed that it provides good correlation between manual and automated $\overline{Ro}$ random determinations. At the outset, there was some concern that the variety of equipment used could be a possible source of error; however, a review of previous in-house checks showed excellent agreement between all systems.

Data from 54 of the 82 samples initially considered were finally used. Only samples that had clean, high quality, and recently polished surfaces at the time of original analysis were used, because reflectance values can be severely influenced by the quality of the polish. A number of samples with high mineral content and inadequate polished surfaces were eliminated. Several low rank samples were eliminated because structure, which was visible in the telinite, might have resulted in a lowering of results in IBAS $\overline{Ro}$ random determinations. Several samples of low rank coal were also eliminated because of weathering effects.

RESULTS AND DISCUSSION

Table 1 lists the data used to compare maximum and random reflectances by regression analysis. The samples marked with asterisks were not included in the final analysis because they may have been weathered, but are included for referral in subsequent discussion. Figure 1 shows regression plots of the data with random reflectance on the abscissa and maximum reflectance on the ordinate for all three areas of interest (Fig. 1a, b, c) as well as a composite plot for all the data (Fig. 1d). Equations derived from the regression analyses of the data shown in Figure 1 are presented in Table 2. Also in Table 2, the equations are used to determine maximum reflectance from random reflectance for hypothetical random values of 0.5, 1.0, 1.5, and 2.0. This is intended to show the variations in predicted values depending on the equation used.

Examination of Table 2 and the plots given in Figure 1 indicate that, for the data used, relationships are quite linear. It is interesting to note the behavior of the equations when various values are used in each, as shown in Table 2. The equation for northeastern British Columbia and the overall equation (labelled "Total") are in good agreement in terms of predicted values. The Rocky Mountain Foothills equation, which uses only lower values as data, is in good agreement with the overall equation in the lower ranges (0.50) but gives low results in the higher ranges. The southeastern British Columbia equation, using a range of values in the middle of the total reflectance data set, gives poor results at each extreme, mainly because of a major difference in slope compared with the other three equations. These results demonstrate the potential error that can occur when extrapolating results from regression analysis to predict maximum reflectance values from random data. Equations based on a relatively narrow range of reflectance values should not be applied to a much broader range for predictive purposes. Also, it appears that equations based on the same range of reflectance values may differ if the data are from different geographic localities with different geological histories.

Variations in the slopes of the regression lines are particularly interesting. The slope of the southeastern British Columbia data is quite different from all the others, which vary to a much smaller degree. Kilby (1986) reported biaxial reflectance indicatrices in coals of the Peace River coalfield, suggesting the influence of tectonic stress. This phenomenon would influence any relationship between reflectance parameters. It is possible that the differing tectonic style of the southern Cordillera, which includes more thrust faulting than the northern Cordillera, may contribute to the difference in the slopes of the equations reported here. In the south, thrust faulting would result in sudden increases in overburden adding vertical pressure, whereas in the north, fold generation would be accompanied by an increase in lateral pressure. These differences in principal stress directions could affect the resulting optical configuration (i.e. uniaxial negative vs. biaxial) to varying degrees.

Weathering, and mineral matter and maceral contents are some of the factors that affect measured reflectances in coal (Bustin et al., 1983). Figure 2 is a plot of the reflectance measurements for samples from the Alberta Foothills before

Table 1. Summary of sample information and data used in regression analysis subdivided according to geographic origin.

Sample	GSC locality C-number	$\bar{R}o_{max}$	$\bar{R}o$ random
	Northeastern British Columbia		
360/85	135515	0.93	0.85
904/82	97518	0.96	0.87
533/82	135507	0.97	0.89
227/86	113798	1.00	0.89
689/81	113797	1.00	0.89
610/81	104028	1.05	0.96
341/85	135517	1.11	1.02
450/80	89336	1.15	1.02
722/81	104086	1.20	1.09
604/81	104021	1.20	1.07
453/80	89339	1.26	1.18
524/85	135503	1.27	1.19
327/82	89309	1.38	1.32
313/82	89304	1.39	1.32
436/80	89317	1.41	1.26
116/81	72268	1.45	1.33
114/81	72268	1.51	1.44
325/82	89309	1.54	1.43
499/83	120944	1.65	1.50
503/85	120948	1.70	1.58
901/82	97520	1.70	1.56
98/81	72267	1.81	1.69
125/81	72270	1.81	1.69
127/81	72270	1.84	1.73
129/81	72270	1.91	1.73
1236/82	113796	1.96	1.76
	Southeastern British Columbia		
806/83	112755	0.98	0.89
67/84	113782	0.99	0.90
68/84	113783	1.07	0.97
71/84	113786	1.09	1.05
753/83	113757	1.10	1.02
750/83	113753	1.12	0.99
825/83	108907 113787	1.12	1.08
766/83	113788, 89, 90	1.13	0.99
796/83	112781, 82	1.17	1.14
800/83	112804	1.20	1.17
1257/86	108634	1.21	1.13
1265/86	108634	1.22	1.11
1294/86	108634	1.24	1.18
783/83	112987, 88	1.24	1.18
1283/86	108634	1.27	1.19
772/83	112510, 11	1.30	1.25
787/83	112994	1.33	1.26
790/83	108941, 42	1.33	1.28
785/83	112991	1.42	1.34
	Alberta Foothills		
282/83	113777	0.53	0.52
289/85	113775	0.58	0.53
256/83	113777	0.58	0.58
1446/86	112711	0.58	0.49*
92/85	113774	0.62	0.58
255/83	113777	0.62	0.58
1449/86	112713	0.63	0.53*
183/85	113776	0.67	0.58
247/83	113777	0.69	0.63
87/85	113774	0.70	0.63
1443/86	113799	0.73	0.64*
120/85	113774	0.74	0.72
1442/86	129234	0.81	0.66*
1456/86	142432	0.85	0.75*

* Denotes sample disqualified due to weathering

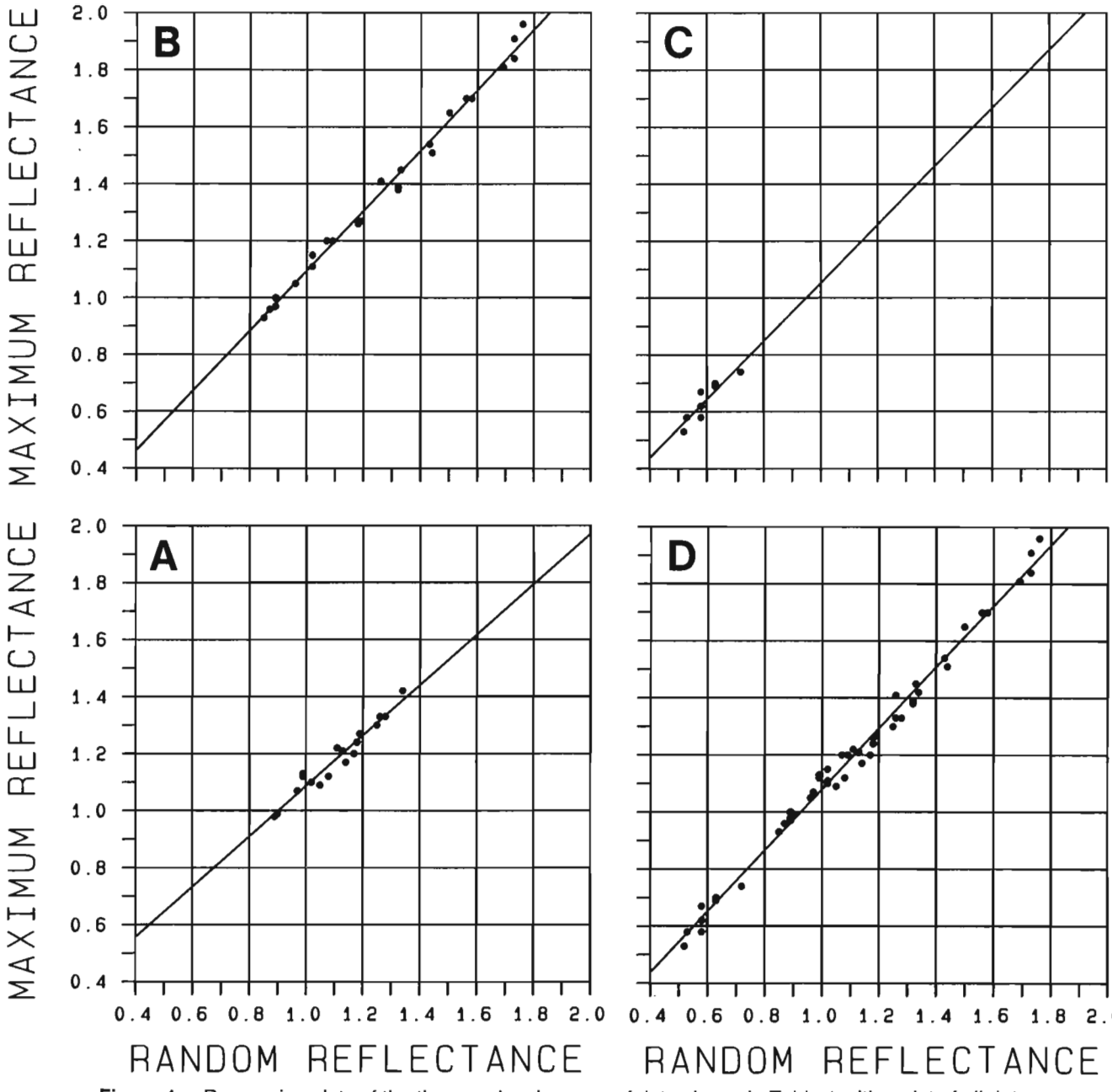

Figure 1. Regression plots of the three regional groups of data shown in Table 1 with a plot of all data. Clockwise from bottom left: A) Southeastern British Columbia, B) Northeastern British Columbia, C) The Alberta Foothills, and D) The total of all three regions.

the effects of weathering are considered. The scatter of data in Figure 2 was thought to be highly unusual in view of the well-known fact that the difference between $\overline{R}o_{max}$ and $\overline{R}o$ random in low rank coals is usually quite small (see also Table 1). In a higher rank coal, such a scatter would be expected due to increased anisotropy, and greater variations in the difference between $\overline{R}o_{max}$ and $\overline{R}o$ random (Stach et al., 1982; Bustin et al., 1983). Closer examination of these data and their origins shows that the data marked with asterisks in Table 1 came from outcrops that may have been severely weathered. When the outcrop data are excluded, the resulting plot shows considerably less scatter. Although this is not conclusive proof that weathering is a factor in such a relationship, it was decided that these samples should be excluded from further analysis. Therefore, Figure 1 excludes these samples from both of the plots in which the Alberta Foothills data are included.

Weathering, the problem of mineral matter causing inferior polishes, and the possibility that telinitic structure may affect results from IBAS automated analysis, all produce data control problems. Furthermore Kalkreuth (1982) has identified coals in northeastern British Columbia in which reflectance may have been suppressed due to the presence of high amounts of liptinite. It is possible that this may also affect the relationships between $\overline{R}o_{max}$ and $\overline{R}o$ random. It is obvious that regression equations may do well in illustrating ideal situations, but many of the samples encountered in routine analysis have to be disqualified on the basis of the above problems.

Table 2. Summary of predictive equations obtained from regression analysis of data in Table 1, where x represents $\bar{R}o$ random. The value predicted represents $\bar{R}o_{max}$. Correlation coefficients are shown, as well as values obtained when hypothetical values of 0.05, 1.00, 1.50, and 2.00 are used in the equations.

Region	Predictive equation	Correlation coefficient	Examples of predicted values 0.50	1.00	1.50	2.00
S.E. British Columbia	0.884 × + 0.203	0.972	0.64	1.08	1.52	1.96
N.E. British Columbia	1.055 × + 0.040	0.996	0.57	1.10	1.62	2.15
Alberta Foothills	1.025 × + 0.027	0.904	0.54	1.05	1.57	2.08
TOTAL	1.071 × + 0.008	0.996	0.54	1.08	1.62	2.15

Table 3. Examples of actual sample data being used to predict $\bar{R}o_{max}$ from $\bar{R}o$ random using both the overall equation and the appropriate regional equation. Measured $\bar{R}o_{max}$ values are included for comparison.

Region	Sample	Random reflectance	Maximum reflectance	Predicted[1] value	Predicted[2] value
S.E. British Columbia	67/84	0.90	0.99	1.00	0.97
	1265/86	1.11	1.22	1.18	1.20
	785/83	1.34	1.42	1.39	1.44
N.E. British Columbia	360/85	0.85	0.93	0.94	0.92
	327/82	1.32	1.38	1.43	1.42
	503/85	1.58	1.70	1.71	1.70
Alberta Foothills	282/83	0.52	0.53	0.56	0.57
	247/83	0.63	0.69	0.67	0.68
	120/85	0.72	0.74	0.77	0.78

[1] Using equation from appropriate region data
[2] Using equation from complete data set

Table 3 shows actual data, selected at random, used to predict maximum reflectance values using both the appropriate regional equation and the overall equation. Measured maximums are included for comparison. At the Institute of Sedimentary and Petroleum Geology, the maximum acceptable error for comparing reflectance data between various microscopes and operators is 0.03 %. Comparing measured maximum values to predicted values, Table 3 indicates that 15 of 18 predictions meet this criterion. In routine analysis, however, there is no way of knowing which samples are anomalous. When this criterion is increased to 0.04 %, examination of the residuals given in the computer output showed that 21 of 54 data pairs were unacceptable in the overall equation, with a maximum error of 0.07 %. There were 2 of 9 (maximum error 0.05 %), 7 of 19 (maximum error 0.05 %), and 6 of 26 (maximum error 0.06 %) unacceptable cases in the Rocky Mountain Foothills, southeastern British Columbia, and northeastern British Columbia data, respectively. It is clear that in practice the overall equation is less reliable than the others. In all four cases the inaccuracies may be due in some part to the relatively low number of data pairs used, but they do show the problem of possible error in the use of regression analysis. Even with a wide interval to fall into (i.e. predicted maximum ± 0.04 %, equivalent to a band of 0.08 %), a considerable number of data fail in all four cases.

DIFFICULTIES IN RELATING $\bar{R}o_{max}$ TO $\bar{R}o$ RANDOM USING REGRESSION ANALYSIS

It becomes evident when working with the actual data that there is a fundamental dilemma that must be considered. If it is necessary to break down the data to represent smaller regions, a confusing abundance of equations could result. Use of wider-ranging equations, subject to the influence of greater numbers of factors, may increase the possibility of error. It should also be noted that a basic assumption of regres-

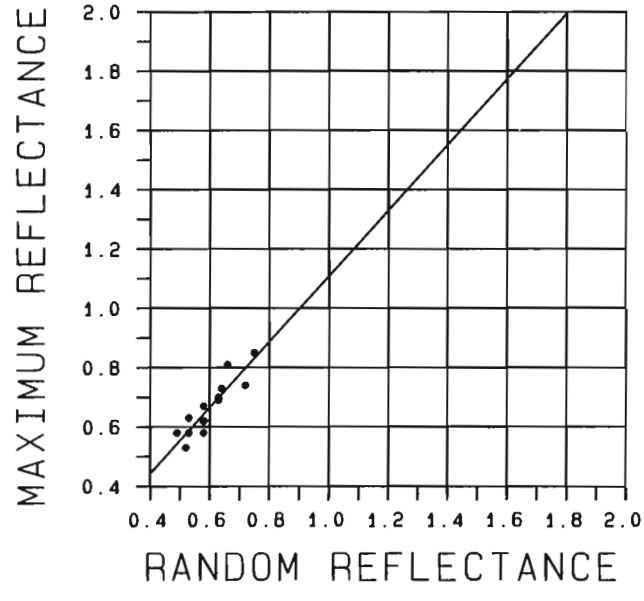

Figure 2. Regression plot of data from the Alberta Foothills region to show abnormal amount of scattering before elimination of weathered samples (marked with asterisks in Table 1). Note that the weathered samples are excluded from the final regression analysis.

sion analysis is that the variance remains constant throughout the data range. It is commonly known that over a wide range of coal ranks, this is not the case.

It is felt that in many cases, too much is being expected from regression analysis. Any predicted dependent variable is in fact a mean value and any use of such values must recognize this property and accommodate possible errors. Often, correlation coefficients are used to imply that linearity between variables is significant. This statistic, no matter how convincing, only serves to quantify the shape of the data and makes no implications regarding cause and effect. Furthermore, in no way does it offer any measure of the reliability of predicted values. Other forms of statistical analysis are available for this purpose.

$\overline{Ro}_{max}$ is often used to predict other parameters. It is hazardous to use a predicted value to predict yet another. Error factors compounded in this way could increase substantially, perhaps exponentially. For this reason, any predictive model requiring maximum reflectance values should use either a properly measured $\overline{Ro}_{max}$, or should be redefined on the basis of $\overline{Ro}$ random if maximum values are unavailable.

A good example of random reflectance being used in a predictive model is that of Pearson (1986). This study uses histogram class frequencies generated by an automated photometry system to predict the Coke Stability Index and $\overline{Ro}_{max}$ of coals by using multiple regression.

Regression analysis does provide a good graphic illustration of the relationships between $\overline{Ro}_{max}$ and $\overline{Ro}$ random but the use of resulting equations to predict maximum reflectance may produce anomalous results. If predicted values are used in further predictive models, the significant amounts of error possible should be reported. In the present study, several possible factors have been suggested that may affect the relationship between $\overline{Ro}_{max}$ and $\overline{Ro}$ random; these include weathering, mineral content, maceral content, tectonic stress, and geographic origins. Further investigations monitoring these factors using more ideal datasets are warranted. It is felt that a multivariate approach may be necessary.

CONCLUSIONS

An attempt was made to: 1. define a linear relationship between maximum vitrinite reflectance and random vitrinite reflectance for coals of Western Canada; and 2. establish specific linear relationships for three major coal producing areas within this region. Although these relationships are linear, difficulties encountered indicate routine use may have limited validity. Weathering and tectonic factors may contribute to variations in the nature of these relationships.

It is concluded that such relationships illustrate ideal situations; however, a large number of samples, routinely examined, would have to be disqualified in order to maintain and control data quality. Even with this increased data control, fairly substantial amounts of error still occur when predicted values are calculated. For this reason, it is suggested that relationships established by regression analysis not be used for further research unless analytical methods chosen can accommodate such error.

A more desirable approach would be to redefine the models used on the basis of random vitrinite reflectance alone, which would then avoid the use of maximum values altogether. To obtain analytically precise results a multiple regression or multivariate approach may be necessary.

ACKNOWLEDGMENTS

The author would like to thank A.R. Cameron, W.D. Kalkreuth and L.D. Stasiuk for advice and critical review of the text.

REFERENCES

Bustin, R.M.
1984: Coalification levels and their significance in the Groundhog coalfield, North central British Columbia; International Journal of Coal Geology, v. 4, p. 21-44.

Bustin, R.M., Cameron, A.R., Grieve, D.A., and Kalkreuth, W.D.
1983: Coal petrology — Its principles, methods and applications; Geological association of Canada, Short course notes, v. 3, 273 p.

Goodarzi, F.
1987: The use of automated image analysis in coal petrology; Canadian Journal of Earth Science, v. 24, no. 5, p. 1064-1069.

Kalkreuth, W.D.
1982: Rank and petrographic composition of selected Jurassic-Lower Cretaceous coals of British Columbia, Canada; Bulletin of Canadian Petroleum Geology, v. 30, no. 2, p. 112-139.

Kilby, W.E.
1986: Biaxial reflecting coals in the Peace River coalfield; British Columbia Ministry of Energy Mines and Petroleum Resources, Geological Fieldwork, Paper 1986-1, p. 127-137.

Neavel, R.C., Smith, S.E., Hippo, E.J., and Miller, R.N.
1981: Optimum classification of coals; *in* Proceedings, International conference on coal science, Dusseldorf; Verlag Gluckauf, p. 1-15.

Pearson, D.E.
1986: Development of a reflectogram based coke strength prediction technique applicable to Western Canadian coking coals, final report; prepared for CANMET Energy Research Laboratories, DSS file 07SQ.23440-4-9280, 16 p.

Stach, E., Mackowsky, M.Th., Teichmüller, M., Taylor, G.H., Chandra, D., and Teichmüller, R.
1982: Coal Petrology; third edition, Gebrüder Borntraeger, Berlin, Stuttgart.

Ting, F.T.C.
1978: Petrographic techniques in coal analysis; *in* Analytical methods for coal and coal products; C. Karr (ed.); v. 1, Academic Press, p. 3-26.

Weiss, H.M.
1985: Geochemische und petrographische Untersuchungen am organischen Material kretazischer Sedimentgesteine aus dem Deep Basin, Westkanada; Ph.D. thesis, Aachen, (unpublished), 261 p.

Geological processes interpreted from gasoline range analyses of oils from southeast Saskatchewan and Manitoba

L.R. Snowdon and K.G. Osadetz
Institute of Sedimentary and Petroleum Geology, Calgary

Snowdon, L.R. and Osadetz, K.G., Geological processes interpreted from gasoline range analyses of oils from southeast Saskatchewan and Manitoba; in Current Research, Part D, Geological Survey of Canada, Paper 88-1D, p. 33-40, 1988.

Abstract

Correspondence and factor analysis of the distribution of 28 gasoline range compounds in about 140 crude oils from the Canadian portion of Williston Basin indicates that formation of this range of hydrocarbons has been most strongly controlled by post oil-generation processes, including migration, water washing, and biodegradation. One family of oils can be clearly distinguished on the basis of gasoline range data, but other genetic affinities and the effect of thermal maturation are not obvious from the analysis.

Résumé

L'analyse de correspondance et l'analyse de facteurs concernant la distribution de 28 composés de la gamme des essences, que l'on trouve dans environ 140 huiles brutes provenant de la portion canadienne du bassin de Williston, indique que la formation de ces hydrocarbures a été très étroitement régie par des processus ultérieurs à la phase de génération du pétrole, en particulier par la migration, le lessivage par l'eau et la biodégradation. On peut clairement distinguer une famille de pétroles d'après les données sur les gammes d'essences, mais d'autres affinités génétiques et l'effet de la maturation thermique ne sont pas évidents d'après l'analyse.

INTRODUCTION

As part of an ongoing, systematic study of the potential source rocks and crude oils of Saskatchewan (Osadetz and Snowdon, 1986 a, b; Brooks et al., 1987 a, b; Snowdon et al., in press; Brooks et al., 1988), the gasoline range (C_5 to C_8) has been chromatographically analyzed for over 140 crude oil samples representing essentially all of the fields in the northeastern (Canadian) portion of the Williston Basin.

The primary objective of the overall program is to construct a petroleum generation, migration, accumulation, and alteration model sufficiently comprehensive to both explain all of the available geological and geochemical observations, and also to be useful as a prediction tool to delimit favourable exploration fairways. A useful model would be one that could be successfully applied to both exploration (in the case of untested plays) and explanation (in the case of both successful and unsuccessful tests).

Williams (1974) relied extensively on gasoline range data to identify his types of oils and to correlate oil types with solvent extract data from potential sources. Our study has produced essentially the same results as those of Williams. A family of oils in Middle Devonian (Winnipegosis) reservoirs is not present in the U.S. portion of the basin (Brooks et al., this volume) and the oils described by Williams from Pennsylvanian reservoirs (Tyler Formation) are not present in the Canadian part of the basin. More detailed study of the saturate fraction of the oils has indicated that most of them, not separable using gasoline range compounds, can be assigned to two families of distinctive composition that cannot be derived from a single source rock.

Statistical analysis of the distribution of gasoline range compounds has been applied to the interpretation of both the level of thermal maturity and the genetic affinity of crude oils (Thompson, 1979; Snowdon and Powell, 1979; Powell and Snowdon, 1979). This group of hydrocarbons has also been noted as being very sensitive to migration (Leythaeuser et al., 1983), water washing, and biodegradation (Snowdon and Powell,1979). Similar statistical techniques have thus been applied to the Saskatchewan gasoline range data in order to extract as much information as possible about the genetic relationships of the oils and also the nature and extent of various postdepositional processes including maturation, expulsion/migration, and post-emplacement alteration by water washing, inspissation and biodegradation.

SAMPLE SET

The samples analyzed in this study (Appendix A) include over 140 oils from southeast Saskatchewan and Manitoba, representing essentially all of the fields currently producing in the area (Fig. 1). These samples comprise a superset of those studied by Brooks et al. (1987) using gas chromatography-mass spectrometry, and thus the assignment to families of oils from the Canadian portion of the basin has been done and comparisons and contrasts made with similar studies done largely in the U.S. portion of the basin (Williams, 1974; Dow, 1974; Zumberge, 1983; Leenheer, 1984).

The reservoirs from which the oils were obtained range in age from Ordovician to Carboniferous, with a few samples from Mesozoic reservoirs in the northeastern part of the study area, which have apparently migrated across the unconformity.

METHODS AND RESULTS

The gasoline range (C_5 to C_8) hydrocarbons were obtained and analyzed chromatographically using techniques similar to those of Thompson (1979) and Snowdon and Powell (1979). Briefly, an aliquot of the whole crude oil was mixed with an inert solid (water saturated alumina or Ottawa sand) and placed into a sample chamber through which a fixed volume of helium was passed at room temperature. The effluent was then passed onto a piece of fused-silica chromatography column held at the temperature of liquid nitrogen. When the liquid nitrogen was removed, the gasoline range hydrocarbons were allowed to proceed onto a 60m DB-1 fused-silica chromatography column for analysis using a flame ionization detector and Nelson Analytical integration system.

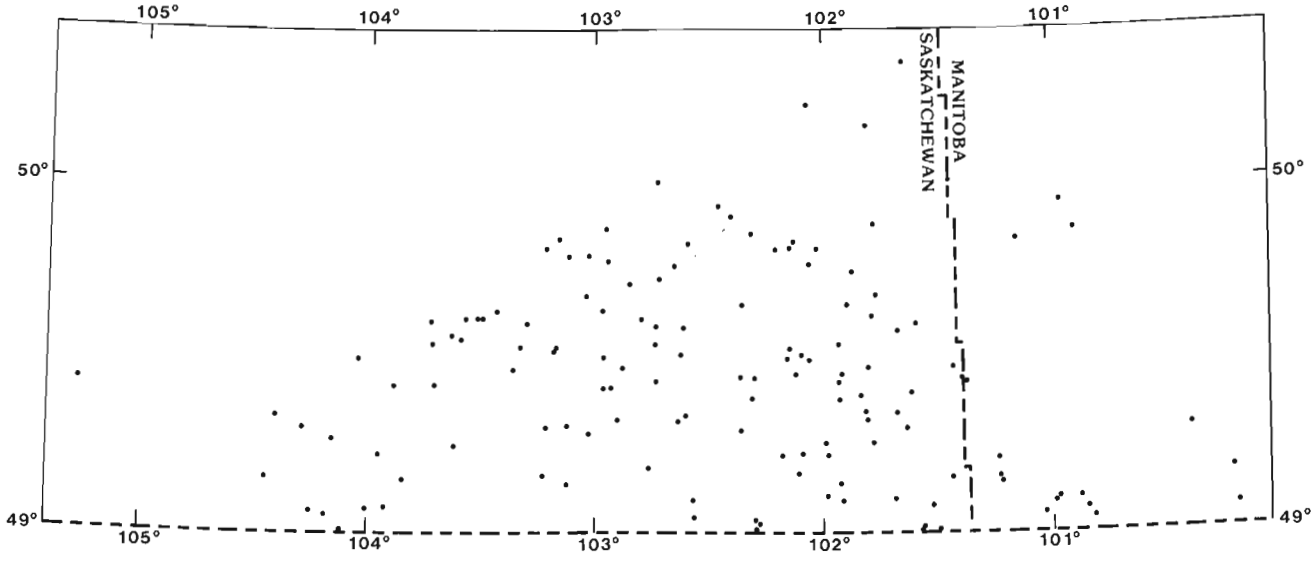

Figure 1. Map of the oil fields sampled in southeast Saskatchewan and Manitoba.

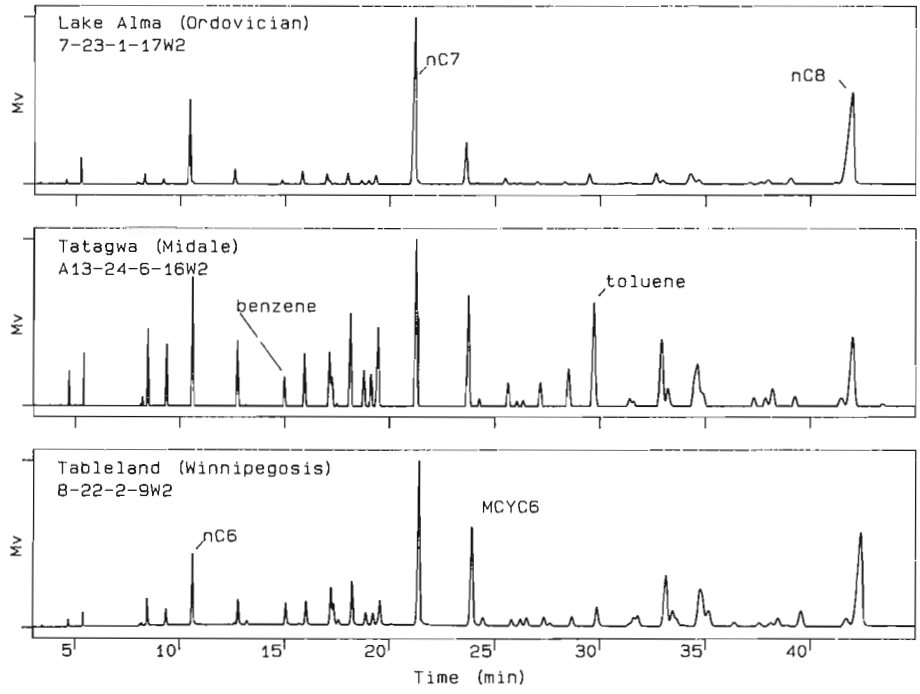

Figure 2. Examples of gasoline range chromatograms for three families of oils.

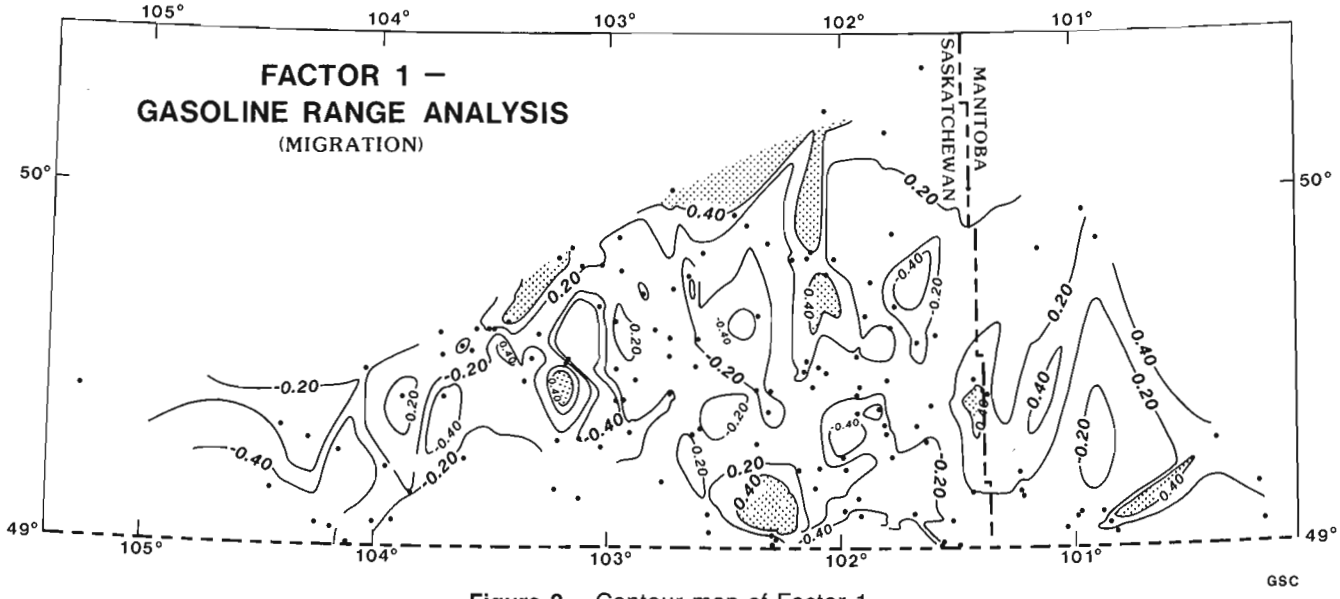

Figure 3. Contour map of Factor 1.

Twenty-eight of the peaks eluting between iso-pentane and n-octane have been identified by comparison with authentic standards and, although the identities of most of the other peaks are available from the literature, these have not been included in the statistical treatment of the results. Similarly, some of the peaks co-elute on the column used; these peaks were simply identified as one of the contributing pair, and no attempt was made to apportion the peak area. Examples of the gas chromatograms for members of three previously identified families of oils (Brooks et al., 1987) are shown in Figure 2. Calculated Heptane values are very similar to those reported by Thompson (1983) for five fields in southeast Saskatchewan.

The resulting matrix of 28 variables for more than 140 samples was analyzed by cluster and factor analysis (Davis, 1973), and also by correspondence analysis (Lebart and Fenelon, 1975), a technique that allows both variables and samples to be plotted in the same factor space. Gasoline range and other parameters, as well as factor loadings were mapped and contoured using a commercial computer program (Surface II Terraplot).

DISCUSSION

The assignment of controls (genetic predisposition or geological process) to the various factors was made by observing which samples had extreme loadings on the various factors and which variables contributed most heavily to the factor scores. The Family A oils of Brooks et al. (1987) and those oils that were extensively biodegraded (notably in the Mesozoic reservoirs) have gasoline range properties that are very different from all other oils in southeast Saskatchewan. As a result, all the factors were more or less completely controlled by the properties of very few samples, and the remaining 130 or so samples all fell into a large group identified as different from the extremes. In order to examine the variability within the remainder of the sample set, correspondence and factor analysis was repeated after the Family A oils and those occurring above the unconformity had been removed from the data set. It is quite clear that the gasoline range analysis is a very simple and powerful tool for identifying Family A (Ordovician) oils in this basin. The following discussion is based on the reduced data set and is therefore only applicable to oils below the unconformity and in Families B and C of Brooks et al. (1987).

Factor 1 carried 36.5 % of the eigenvalue (Table I), and samples with high factor loadings were rich in volatile components and depleted in benzene, toluene and higher molecular weight components of the gasoline range. Since the low molecular weight components would be expected to be preferentially removed by the effects of water washing due to higher water solubilities, water washing has been discounted in the interpretation of this factor. Similarly, loss of the volatile components due to sample collection, handling, and analysis procedures has been discounted because of the low scores of benzene and toluene. Genetic control does not appear to be a plausible explanation because the families identified on the basis of other data have not been separated by this factor. It should be noted, however, that all other parameters have been measured on the $C_{15}+$ fraction and it is possible that the volatile components have different genetic affinities than the heavier ends. The preferred explanation is that high Factor 1 loadings correspond to more extensively migrated hydrocarbons. The results of Leythaeuser and others (1983) indicate that the low molecular weight fractions should move more quickly and easily and hydrocarbons that have moved farther may reasonably be expected to have encountered more gas-unsaturated water along the way. Thus, competition between losses through dissolution, and enrichment due to preferential movement, could have resulted in the loss of benzene, toluene and the heavier components. Factor 1 has thus been attributed to a complex set of interactions associated with migration, but with no control on the extent of migration in terms of kilometres or tens to hundreds of kilometres. This assignment has clearly been made by precluding a number of other possible geological processes and is thus less than compelling.

The geographic distribution of Factor 1 loadings (Fig. 3) suggests that samples near the subcrop edge and in a few locations in the central portion of the study area have the highest loadings. This distribution is not inconsistent with the attribution of the extent of migration as a control on this factor.

Table 1. Correspondence Analysis results and interpreted factor attributions.

FACTOR	EIGENVALUE %	NEGATIVE LOADING	POSITIVE LOADING	INTERPRETATION
1	36.5	BENZENE TOLUENE	VOLATILES (ESPECIALLY BRANCHED)	MIGRATION ?
2	29.0	VOLATILES BENZENE, TOLUENE (NORMALS <nC8)	HEAVIES	WATERWASHING SAMPLE HANDLING (BIODEGRADATION)
3	14.2	NORMAL ALKANES	BENZENE, TOLUENE BRANCHED	ORDOVICIAN OILS (BIODEGRADATION)
4	6.2	BENZENE	22DMC4, TOLUENE (CYC6, 23DMC5, MCYC6)	GENETIC ?
5	4.8	TOLUENE (CYC5, DMCYC5'S)	BENZENE (CYC6, 2MC6, 1,1DMCYC5)	GENETIC ?
6	2.2	1C2DMCYC5, 1C4DMCYC6 (2,3DMC4)	(2,2,3TMC5, nC5)	INDICATED ANALYTICAL ERROR
	92.9			GSC

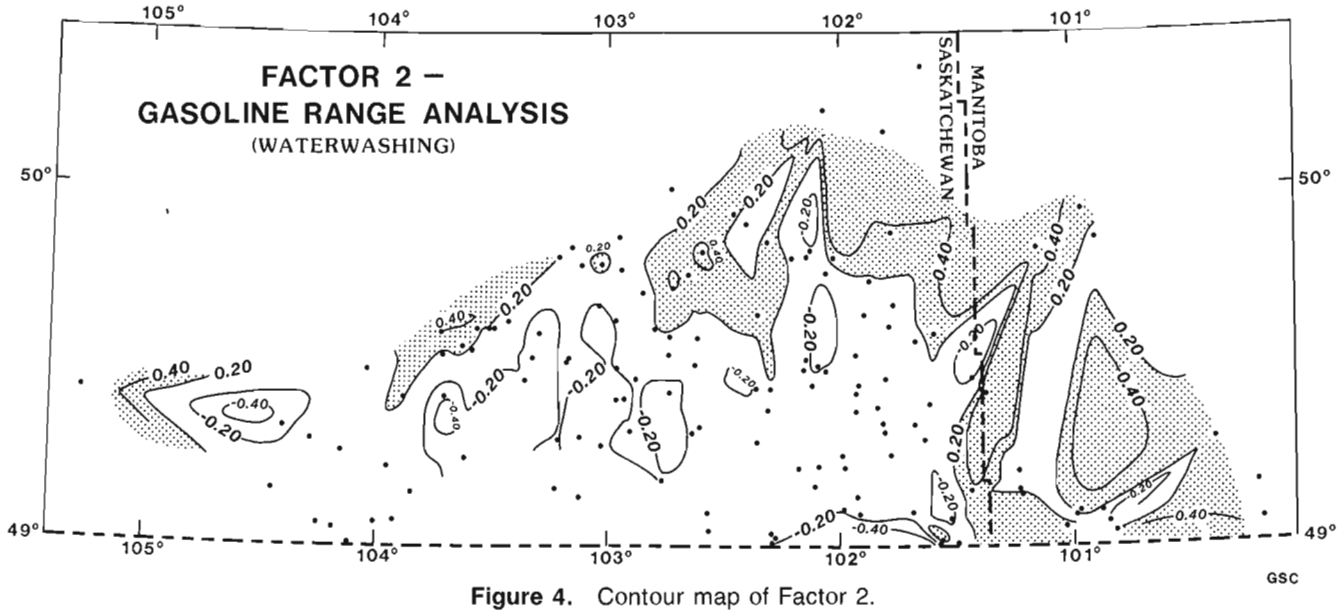

Figure 4. Contour map of Factor 2.

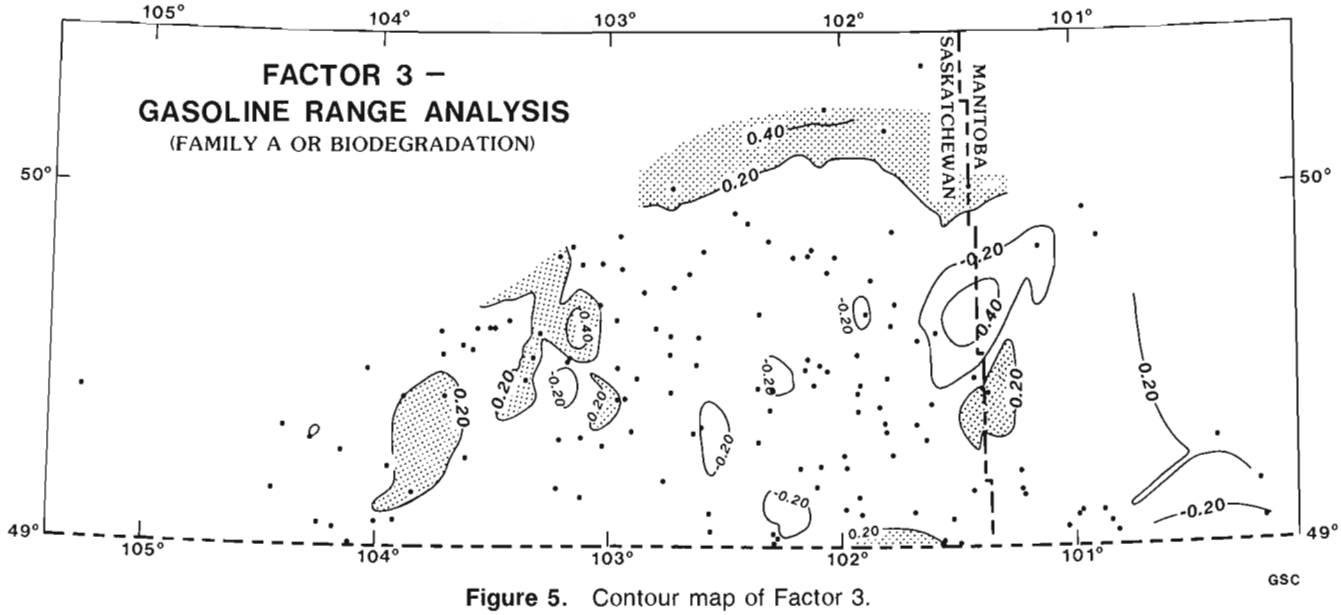

Figure 5. Contour map of Factor 3.

Samples with a high loading on Factor 2 (Fig. 4) were noted to occur close to the Paleozoic subcrop edge and also to contain low amounts of benzene and toluene, the most water soluble compounds in the gasoline range. Thus Factor 2 was attributed to water washing. Similarly, Factor 3 was attributed to biodegradation on the basis of the geographic distribution (Fig. 5) and the fact that n-alkanes were preferentially removed from samples with a high Factor 3 loading. Locations with high loadings on Factor 2 and low loadings on Factor 3 (that is, water washed but not biodegraded) are interpreted as areas of flushing by water with little or no oxygen, probably connate water.

Factors 4 and 5 are again difficult to attribute because there is no obvious link between the chemistry of the high and low factor loading samples and any reasonable geological process. These factors may have a genetic control, but again, the samples do not correspond with previously identified families of genetically related oils. Factor 6 accounted for 2.2 % of the eigenvalue and had only a single sample with a high loading. The factor score was essentially controlled by a single variable, which on detailed inspection proved to be incorrectly entered into the data matrix. This error was left in the data to demonstrate the usefulness of the technique for locating transcription errors of this sort.

With the exception of the separation of Family A oils from the others, there appears to be little genetic information in the gasoline range distribution for this group of oils. Similarly, thermal maturation has not been assigned to any of the factors that explain the variance in this data set. A plot of Heptane value versus Isoheptane value (Thompson, 1983) shows that the Heptane value is between 20 and 30 for almost all of the samples. Isoheptane values, on the other hand, indicate a fairly wide range of maturity, with values from about 0.5 to 2.0. Other maturity indicators, such as biomarker ratios and phenanthrene indices, are in agreement with the Heptane value; that is, little difference in the level of maturity.

REFERENCES

Brooks, P.W., Osadetz, K.G. and Snowdon, L.R.
1987: Origin of compositional differences amongst oils from the Hummingbird Field (Paleozoic), southeast Saskatchewan; *in* Current Research, Part A, Geological Survey of Canada, Paper 87-1A, p. 331-336.
1988: Geochemistry of Winnipegosis discoveries near Tablelands, Saskatchewan; *in* Current Research, Part D, Geological Survey of Canada, Paper 88-1D.

Brooks, P.W., Snowdon, L.R., and Osadetz, K.G.
1987: Families of oils in southeastern Saskatchewan; Proceedings of the Fifth International Williston Basin Symposium, Bismark, North Dakota, p. 253-264.

Davis, J.C.
1973: Statistics and data analysis in geology; John Wiley and Sons, 550 p.

Dow, W.G.
1974: Application of oil-correlation and source rock data to exploration in Williston Basin; American Association of Petroleum Geologists Bulletin, v. 58/7, p. 1253-1262.

Lebart, L. and Fenelon, J.P.
1975: Statistique et informatique appliquees; Bordas Dunod, Paris.

Leenheer, M.J.
1984: Mississippian Bakken and equivalent formations as source rocks in the Western Canadian Basin; Organic Geochemistry, v. 6, p. 521-532.

Leythaeuser, D., Schaefer, R.G., and Pooch, H.
1983: Diffusion of light hydrocarbons in subsurface sedimentary rocks; American Association of Petroleum Geologists Bulletin, v. 67/6, p. 889-895.

Osadetz, K.G., and Snowdon, L.R.
1986a: Speculation on the petroleum rock potential of portions of the Lodgepole Formation (Mississippian) of southern Saskatchewan; *in* Current Research, Part B, Geological Survey of Canada Paper 86-1B, p. 647-651.

1986b: Petroleum source rock reconaissance of southern Saskatchewan; *in* Current Research, Part A, Geological Survey of Canada Paper 86-1A, p. 609-617.

Powell, T.G. and Snowdon, L.R.
1979: Geochemistry of crude oils and condensates from the Scotian Basin, Offshore eastern Canada; Bulletin of Canadian Petroleum Geology, v. 27/4, p. 453-466.

Snowdon, L.R., Brooks, P.W., Williams, G.K., and Goodarzi, F.
in press: Canol and Bluefish shales: Source of the Norman Wells Oil; Organic Geochemistry.

Snowdon, L.R. and Powell, T.G.
1979: Families of crude oils and condensates in the Beaufort-Mackenzie Basin; Bulletin of Canadian Petroleum Geology, v. 27/2, p. 139-162.

Thompson, K.F.M.
1979: Light hydrocarbons in subsurface sediments; Geochimica et Cosmochimica Acta, v. 43/5, p. 657-672.
1983: Classification and thermal history of petroleum based light hydrocarbons; Geochimica et Cosmochimica Acta, v. 47, p. 303-316.

Williams, J.A.
1974: Characterization of oil types in Williston Basin, American Association of Petroleum Geologists Bulletin, v. 58/7, p. 1243-1252.

Zumberge, J.E.
1983: Tricyclic diterpane distributions in the correlation of Paleozoic crude oils from the Williston Basin; *in* Advances in Organic Geochemistry 1981, John Wiley & Sons Ltd., p. 738-745.

APPENDIX A

Names, locations and lab numbers of sample set

WELL NAME	DEPTH (m)	LAB NO.	LOCATION
BIRDBEAR	?	#466	05-33-010-32W1
ALAMEDA	1279.2-1291	#490	13-14-003-02W2
WILLMAR	1230-1232.6	#491	02-02-006-03W2
HUNTOON	1344-1344	#492	03-04-007-09W2
WEYBURN SOUTH	1350.5-1368.9	#493	05-18-007-12W2
INNES WEST	1335.2-1335.6	#494	13-31-007-11W2
SOUTH PARKMAN	3577-3581	#495	16-09-008-33W1
HUME	1343-1346	#496	15-33-007-12W2
VIEWFIELD	1349-1350.5	#497	13-33-006-09W2
HUNTOON	1345-1350	#498	07-32-006-09W2
STEELMAN	1391.1-1399	#499	13-27-004-05W2
BENSON	1334.7-1335.9	#500	05-25-006-08W2
WEYBURN NORTH	1367-1388	#501	09-08-007-12W2
STEELMAN	1444-1446	#502	15-20-004-05W2
INNES	1320.75-1330.41	#503	15-28-007-10W2
GRIFFIN	1304.24-1310.64	#504	01-09-008-11W2
HUME	1338.51-1340	#505	13-36-007-12W2
GLEN EWEN	1282.6-1289	#506	05-21-003-01W2
QUEENSDALE	1185-1185.75	#507	09-29-006-01W2
WEYBURN	1368-1373.3	#508	14-04-007-13W2
CANTAL SOUTH	1143-1145	#509	08-12-005-34W1
ARCOLA	1179.5-1185	#510	11-21-008-32W1
KENOSEE	1195-1198	#511	12-26-010-03W2
RED JACKET	663-666	#512	10-04-014-32W1
FLORENCE	1288.7-1291.7	#513	13-04-002-34W1
RALPH	1306.7-1314.3	#514	01-32-007-13W2
ROCANVILLE	653-655.6	#515	02-11-016-13W1
NOTTINGHAM	1129.2-1137	#516	04-14-005-33W1
SILVERTON	1149.1-1154.6	#517	02-31-003-32W1
CANTAL	1120-1123	#518	16-25-005-34W1
INGOLDSBY	1082-1084	#519	16-07-004-31W1
WORKMAN	1207-1218	#520	03-03-002-32W1
ELMORE	1211-1214	#521	02-04-001-31W1
ANTLER NORTH	1146-1149	#522	08-01-001-31W1
WAPELLA	668.43-682.08	#523	13-34-014-01W2
ROSEBANK	1086-1094	#524	04-14-005-03W2
SHERWOOD	1241-1244	#525	05-01-001-03W2
PARKMAN	1030.5-1038.5	#526	01-15-009-33W1
CARNDUFF	1265.2-1276.2	#527	01-23-002-34W1
WORKMAN	1177-1181	#528	15-18-007-31W1
MOOSE MNT.	1198-1200	#529	08-09-010-02W2
CARNDUFF	1255-1257	#530	09-15-003-34W1
QUEENSDALE E.	1165-1168	#531	11-22-006-01W2
HAZELWOOD	1135-1140	#532	16-22-011-04W2
STAR VALLEY	3817.75-3804	#533	13-11-009-06W2
HASTINGS	1235.65-1236.57	#534	14-27-003-34W1
WEYBURN	1451-1458	#535	B12-28-005-13W2
OAKLEY	1141.8-1143.3	#536	04-36-004-33W1
BIENFAIT	1587.5-1592	#537	08-05-006-03W2
FREESTONE	1191-1194.25	#538	A14-02-009-07W2
ALIDA WEST	1136-1334.2	#539	06-06-006-33W1
OUNGRE	1820-1826.5	#540	03-29-002-14W2
HASTINGS	1144.5-1145.5	#541	06-24-004-33W1
MIDALE	1402-1420.6	#542	15-12-006-11W2
PARKMAN	1147.9-1151.5	#543	10-12-010-02W2
SOURIS FTS.	1337.7-1338.2	#544	13-36-001-34W1
FLETWODE SOUTH	1160-1161	#545	14-07-011-03W2
FREDA LAKE	1701-1705.5	#546	16-30-004-18W2
ELMORE	1177-1183.6	#547	09-04-001-31W1
GAINSBOROUGH	1064	#548	07-28-002-30W1
OUNGRE WEST	2932	#549	04-22-003-15W2
LAKE ALMA	?	#550	07-23-001-17W2
HUMMINGBIRD	2309-2318	#551	10-26-002-19W2
KISBEY	1616-1625	#552	07-27-007-06W2
HUMMINGBIRD	2223-2229	#553	05-26-002-19W2
RONCOTT	1823-1825	#554	09-34-005-25W2
KISBEY	1230-1233	#555	05-29-009-05W2

WELL NAME	DEPTH (m)	LAB NO.	LOCATION
HUMMINGBIRD	1876-1904	#556	11-26-002-19W2
NEPTUNE	1748.5-1755.5	#557	04-06-004-16W2
RATCLIFFE	6349-6382	#558	05-30-001-15W2
LAKE ALMA	1981-1987	#559	04-29-001-17W2
FREEMANTLE	3900-3907	#560	11-16-008-03W2
CLARILAW	1222M-1224.5	#561	01-28-007-05W2
MACOUN WEST	1562M-1564	#562	05-18-004-09W2
TATAGWA	1429.5-1432.9	#563	A13-24-006-16W2
FRAYS	978.9-981.5	#564	04-26-007-31W1
STORTHOAKS	3412-3422	#565	A09-17-005-31W1
LOST HORSE H.	1168-1176.5	#566	07-04-010-08W2
BRYANT	1433-1434	#567	05-25-005-08W2
HOFFER	1943-1946	#568	09-27-001-15W2
BROMHEAD	1693-1694	#569	13-30-003-12W2
STOUGHTON	1269-1270	#570	11-12-008-08W2
STOUGHTON	1267.3-1268	#571	05-28-008-08W2
VIEW HILL	1542-1549	#572	05 09-004-08W2
HANDSWORTH	1180.5-1182.5	#573	A09-21-010-09W2
LOUGHEED	1382-1387	#574	12-30-005-14W2
BRYANT	1412-1413	#575	07-30-005-07W2
WAUCHOPE	1125.5-1130	#576	04-05-007-33W2
FLAT LAKE	1974-1976	#577	06-05-001-16W2
PINTO	1606-1608.1	#578	02-02-002-05W2
SKINNER LAKE	1878-1900	#579	05-18-004-17W2
NORTHGATE	1570-1574	#580	01-14-001-03W2
WINMORE	1143.5-1146.75	#581	A15-26-001-31W1
MINARD	1337-1339	#582	01-16-006-07W2
ROSEBANK SOUTH	3516-3529	#583	13-25-004-32W1
EDENVALE	1130-1132.3	#584	10-12-006-33W1
HANDSWORTH	1177.25-1179.5	#585	9A-36-010-08W2
MACOUN	1522.8-1526.1	#586	13-14-004-09W2
PINTO	1684.3-1686.2	#587	16-14-001-05W2
NORTHGATE	1596.2-1597.8	#588	07-12-001-03W2
FERTILE	948.4-954	#589	08-36-005-30W1
WEIR HILL	1352.3-1352.7	#590	11-34-005-06W2
WARMLEY	1242-1247	#591	09-15-010-05W2
WHITEBEAR	3678-3710	#592	16-31-007-06W2
MIDALE CENTRAL	1395-1398	#593	03-05-007-10W2
FREESTONE	1170-1171	#594	05-31-009-07W2
PARKMAN	1082-1083	#595	08-11-010-01W2
MOOSE VALLEY	1182-1185	#596	12-14-012-06W2
LAKE ALMA	3058-3065	#597	07-23-001-17W2
BIENFAIT	1584-1588	#598	09-05-003-06W2
MORRISVIEW	1259.4-1260	#599	14-03-007-06W2
HARTHAVEN	1189.9-1211	#600	01-02-010-09W2
AUBURNTON	1197-1199.75	#601	15-06-006-01W2
GLEN EWAN	1334.7-1336.2	#602	03-32-002-01W2
KINGSFORD WEST	1485-1487.4	#603	01-29-061-07W2
ALAMEDA WEST	1351.5-1367	#604	13-09-004-03W2
WILDWOOD	1178.6-1179.1	#605	15-36-006-02W2
FERTILE	961-965	#606	16-10-006-30W1
CREELMAN	1197-1207.3	#607	11-07-010-09W2
WHITEBEAR	1122.9-1126.5	#608	06-27-009-01W2
CRYSTAL HILL	3661-3668	#609	14-18-010-01W2
QUEENSDALE W.	1198.7-1201	#610	13-24-006-02W2
LIGHTNING CR.	1079-1081.5	#611	10-32-007-32W1
BROWNING	1264.6-1265.2	#612	13-28-006-05W2
WASKADA	921-926	#711	A16-13-001-26W1
SOURIS HARTNEY	650.13-652.88	#712	08-17-004-22W1
LULU LAKE	1008-1015	#713	16-27-001-21W1
WASKADA	928-932	#714	05-03-002-26W1
SOUTH PIERSON	993-1000	#715	08-25-002-29W1
TILSTON	947-949	#716	15-30-005-29W1
WASKADA	925.5-933	#717	04-25-001-26W1
PIERSON	983-986	#718	01-18-003-28W1
COULTER	945-963	#719	11-21-001-27W1
SOUTH PIERSON	976.3-990	#720	12-19-002-28W1
DALY	?	#721	10-13-010-28W1
VIRDEN	?	#722	09-26-010-26W1
WHITEWATER	819-823	#723	16-33-002-21W1
KIRKELLA	?	#724	04-18-012-29W1
VIRDEN	?	#725	04-27-011-26W1
TABLELAND	2601-2606	#755	A04-36-002-10W2
TABLELAND	?	#756	08-22-002-09W2

Field observations on the structural and depositional history of Prince Patrick Island and adjacent areas, Canadian Arctic Islands

J.C. Harrison, A.F. Embry, and T.P. Poulton
Institute of Sedimentary and Petroleum Geology, Calgary

Harrison, J.C., Embry, A.F., and Poulton, T.P., Field observations on the structural and depositional history of Prince Patrick Island and adjacent areas, Canadian Arctic Islands; in Current Research, Part D, Geological Survey of Canada, Paper 88-1D, p.41-49, 1988.

Abstract

Structural observations from Prince Patrick Island and adjacent areas obtained during the 1987 field season have led to new conclusions concerning the five tectonic phases associated with the Devonian-to-recent geological history of the western Canadian Arctic Islands.

New data show that Parry Islands Fold Belt (latest Devonian or earliest Carboniferous, and Permian deformations) continues with a change of trend into southeastern Prince Patrick Island. The Mesozoic tectonic history is subdivisible into two phases: 1. an early phase, associated with the evolution of the Sverdrup Basin (Permian to early Middle Jurassic); and 2. a later phase, associated with east-west extension and rifting (Middle Jurassic to Late ? Cretaceous). Folds related to the regional impact of the Eurekan Orogeny (Paleogene) are now known throughout Eglinton Island and central and northern Prince Patrick Island. The magnitude and sense of slip of post-Eurekan tectonic elements on the Arctic Coastal Plain remain unknown.

Résumé

Les résultats d'observations sur le terrain, faites en 1987, des structures caractérisant l'île du Prince-Patrick et les régions adjacentes nous ont amenés à de nouvelles conclusions à propos des cinq phases tectoniques associées à l'histoire géologique de la portion occidentale de l'archipel Arctique canadien, du Dénovien à l'Holocène.

De nouvelles données montrent que la zone plissée des îles Parry (déformation allant du sommet du Dénovien au début du Carbonifère, et déformations survenues au Permien) se prolonge dans le sud-est de l'île du Prince-Patrick, en changeant d'orientation générale. On peut subdiviser l'évolution survenue au Mézosoïque en deux phases: 1. une phase initiale, associée à l'évolution du bassin de Sverdrup (Permien au début du Jurassique moyen); et 2. une phase ultérieure, associée à un épisode d'extension et de formation d'un fossé tectonique (Jurassique moyen au Crétacé supérieur ?). Les plis résultant de l'impact régional de l'orogénèse de l'Euréka (Paléogène) sont maintenant identifiés dans l'ensemble de l'île Eglinton ainsi que les portions centrale et septentrionale de l'île du Prince-Patrick. On n'a pas encore pu déterminer la grandeur et la direction du rejet des éléments tectoniques ultérieurs à l'Eureka, dans la plaine côtière de l'Arctique.

INTRODUCTION

As part of the ongoing interest by the Geological Survey of Canada in continuing the geological mapping program in the Canadian Arctic Islands, helicopter-supported field activities were carried out on Prince Patrick and Eglinton islands and parts of northwestern Melville Island during June and July, 1987.

The project objectives are to produce a set of 1:250 000 scale geological maps (NTS 88G, 89B, 98H, 99A, and small portions of NTS 89A, and 89D) and structural cross-sections, as well as a complete reassessment of the lithostratigraphy (Q.H. Goodbody, A.F. Embry), biostratigraphy (T.P. Poulton, J. Wall), seismic stratigraphy (T. Brent), structural history (J.C. Harrison), and general aspects of hydrocarbon and resource potential of the area.

This paper presents some initial geological observations arising from the summer field activities, with special emphasis on the structural and tectonostratigraphic history of the area.

Although geological observations in the area date back to the 1850's (Mecham, 1855; M'Clintock, 1857) an overall understanding of the geology was not available until the latter half of this century (Tozer, 1956; Tozer and Thorsteinsson, 1964). These data were later incorporated into the first key summary article on the Canadian Arctic Islands, by Thorsteinsson and Tozer (1970). The Prince Patrick Island area was recognized as being near the intersection of four geological provinces: the Arctic Platform underlain by undisturbed Cambrian to Devonian platform carbonates and Middle and Upper Devonian siliciclastic rocks; the Parry Islands Fold Belt underlain by platform- and basinal-facies rocks of the same age, involved in the Ellesmerian Orogeny (latest Devonian or earliest Carboniferous), and also underlain by Permo-Carboniferous redbeds involved in the Melvillian Disturbance (Permian); the Carboniferous to Paleogene strata of the Sverdrup Basin involved in the Eurekan Orogeny; and the Arctic Coastal Plain, which is the exposed portion of a Neogene, post-tectonic sedimentary wedge deposited on the shelf and slope of the Arctic Ocean Basin. A smaller structural feature within the Prince Patrick Island area is the Eglinton Graben: a northeast trending Jurassic and Cretaceous depocentre downfaulted against the Blue Hills Fault Belt on the east, and the Prince Patrick Uplift on the west.

This article addresses four aspects of the structural history of the Prince Patrick Island area as presented by Thorsteinsson and Tozer (1970) that now require re-evaluation in light of observations obtained during the 1987 field season. These include:

1. The apparent westward termination of the Parry Islands Fold Belt east of Prince Patrick Uplift

2. The timing of motion on north striking normal faults and related extensional features in the vicinity of Eglinton Graben and Prince Patrick Uplift

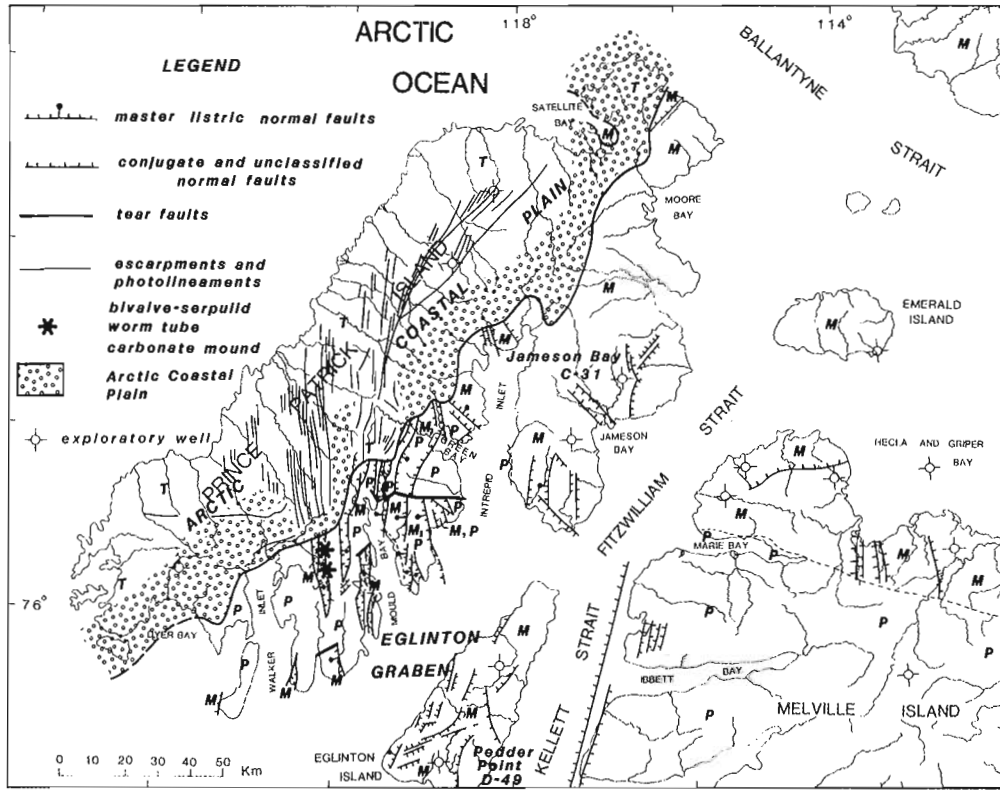

Figure 1. Simplified geology of Prince Patrick Island and adjacent areas with distribution of normal faults, tear faults, hydrothermal travertine mounds, and unclassified linear tectonic elements. P, Paleozoic strata; M, Mesozoic strata; T, Tertiary strata. Reverse slip on some faults on Eglinton Island is likely.

3. The distribution of structures attributable to the Eurekan Orogeny.

4. The significance of linear tectonic elements on the Arctic Coastal Plain.

STRATIGRAPHIC OVERVIEW

Strata exposed at the surface on Prince Patrick and Eglinton islands include rocks of Middle to Upper Devonian, Upper Triassic to Upper Cretaceous, and Neogene ages (Fig. 1). Mappable Devonian units include 1. the Weatherall and Cape De Bray formations (marine shale with lesser siltstone and sandstone), 2. the Beverley Inlet Formation (deltaic and nonmarine sandstone, siltstone, and shale), and 3. the Parry Islands Formation (nonmarine sandstone and conglomerate; Embry and Klovan, 1976).

Understanding of the Mesozoic stratigraphy of the Canadian Arctic Islands has evolved rapidly in the last ten years. As a result, many of the formations identified in the Prince Patrick Island area by Tozer (1956) and Tozer and Thorsteinsson (1964) have been either abandoned, redefined, or raised to group status. In addition, certain formations previously identified elsewhere are now known to be present in the project area. Major contributions to this evolution of knowledge have been made by Embry (1983, 1984a, b, 1985, in press) for the Upper Triassic to Lower Cretaceous section, and Plauchut and Jutard (1976) for the Upper Cretaceous section. The subdivision, age, thickness, gross lithology and distribution of Mesozoic strata in the project area are summarized in Figures 2 and 3. These figures also incorporate much new data collected during the 1987 field season.

The detailed subdivision of Mesozoic units has permitted a greatly improved understanding of the way in which sea level fluctuations and periodic tectonic events have influenced the final distribution of time-stratigraphic units. The variations in paleogeographic distribution of selected Carboniferous to Lower Cretaceous rock units are displayed in Figures 4 to 7. These diagrams also incorporate some subsurface information from exploratory wells drilled in the area by the resource sector. Poorly consolidated sandstones, conglomerates, peat, and deposits of uncoalified wood that unconformably overlie Devonian to Cretaceous rocks on Prince Patrick Island and that are exposed at the surface throughout the Arctic Coastal Plain were assigned to the Beaufort Formation by Tozer (1956). Generally similar rocks on Banks Island have been dated as Early to Middle Miocene by Hills et al. (1974). Quaternary glaciofluvial gravels, and glaciomarine and glaciolacustrine silt deposits have also been identified at various scattered localities on Prince Patrick Island.

LIMITS OF PARRY ISLANDS FOLD BELT

Parry Islands Fold Belt was first identified and named by Fortier and Thorsteinsson (1953). The east trending fold belt was defined on the east by the Boothia Uplift and on the west by the limits of folding in Paleozoic strata on Melville Island.

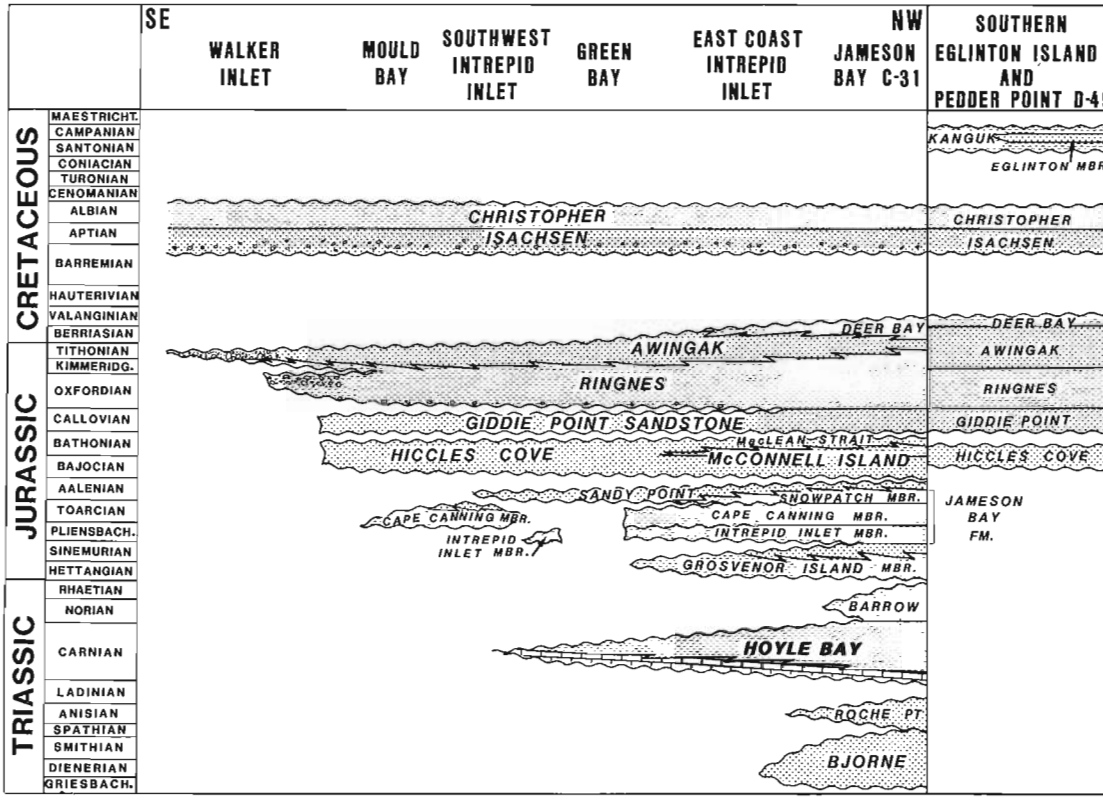

Figure 2. Correlation chart of Mesozoic strata on Prince Patrick and southern Eglinton islands as determined by surface measured sections and two exploratory wells (Jameson Bay C-31 and Pedder Point D-49).

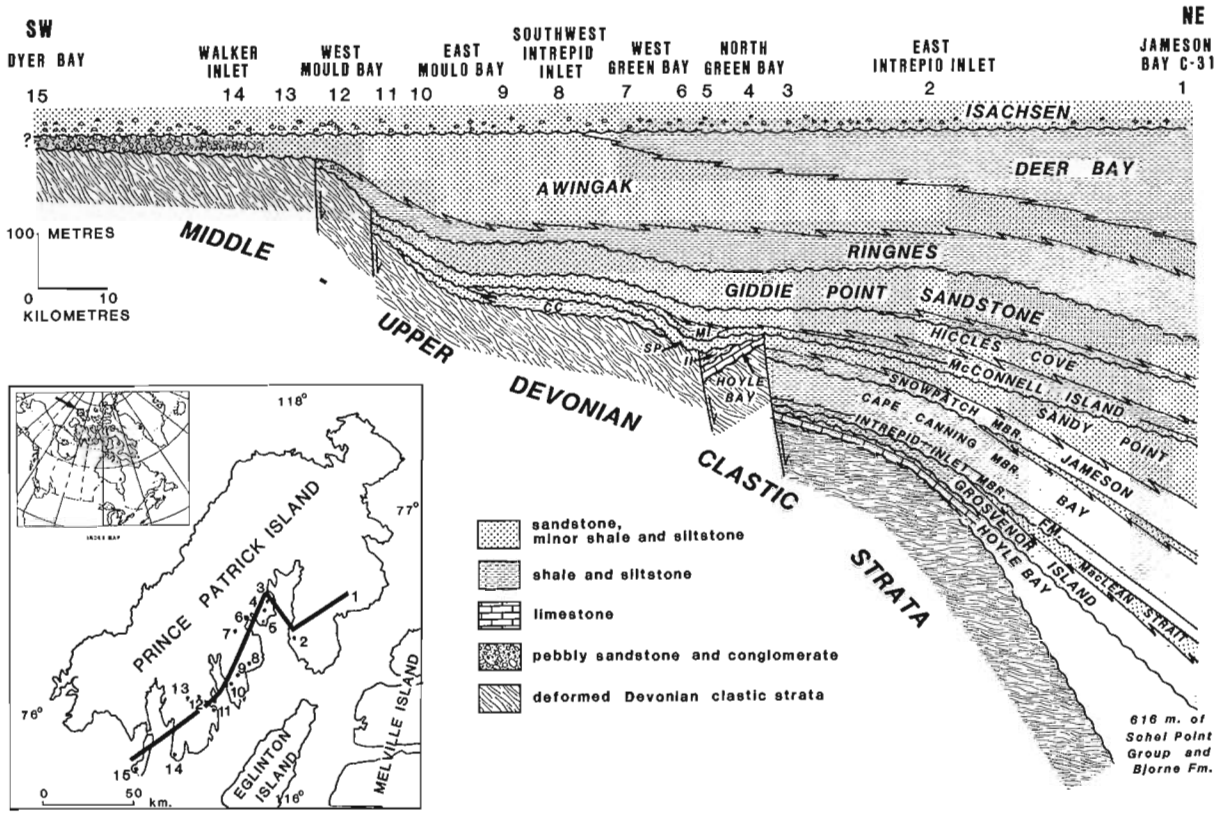

Figure 3. Schematic stratigraphic cross-section of exposed Upper Triassic to Lower Cretaceous strata on southeastern Prince Patrick Island.

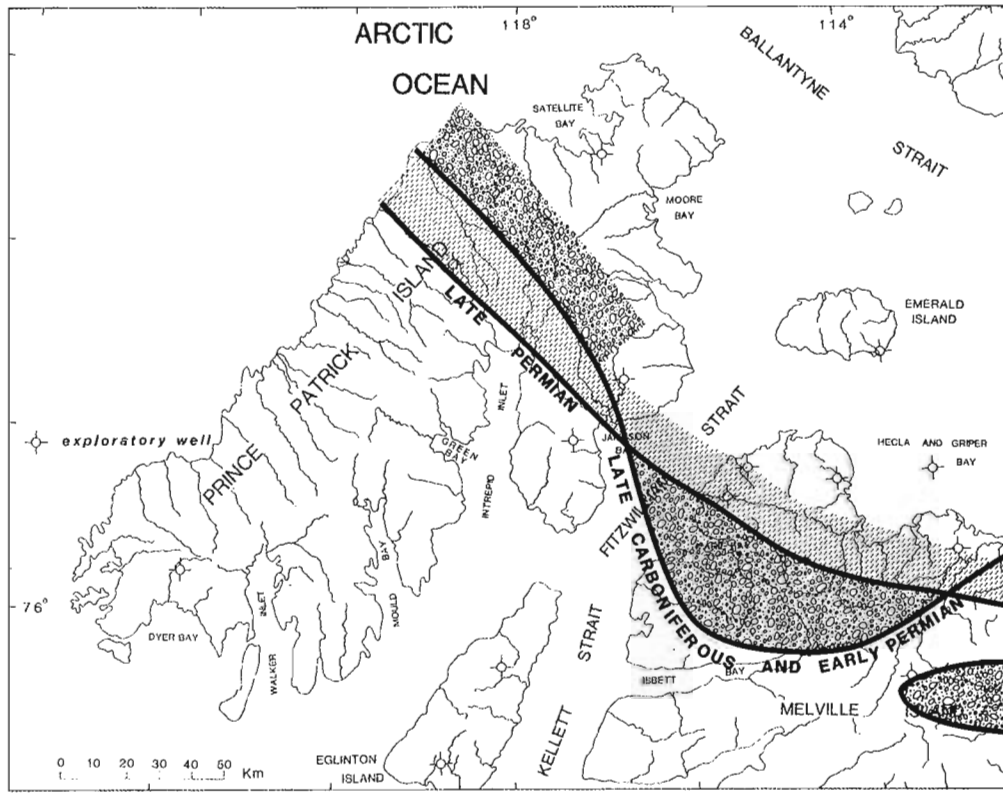

Figure 4. Limits and distribution of Carboniferous and Permian strata, Prince Patrick Island area.

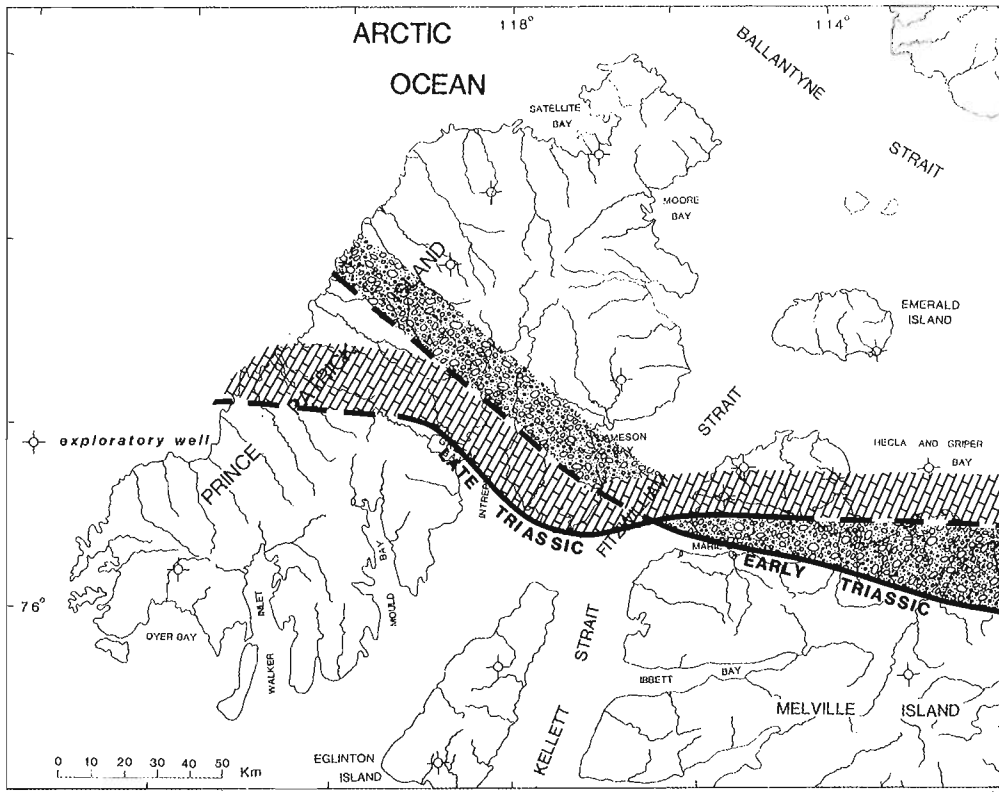

Figure 5. Limits and distribution of Lower Triassic and Upper Triassic strata, Prince Patrick Island area.

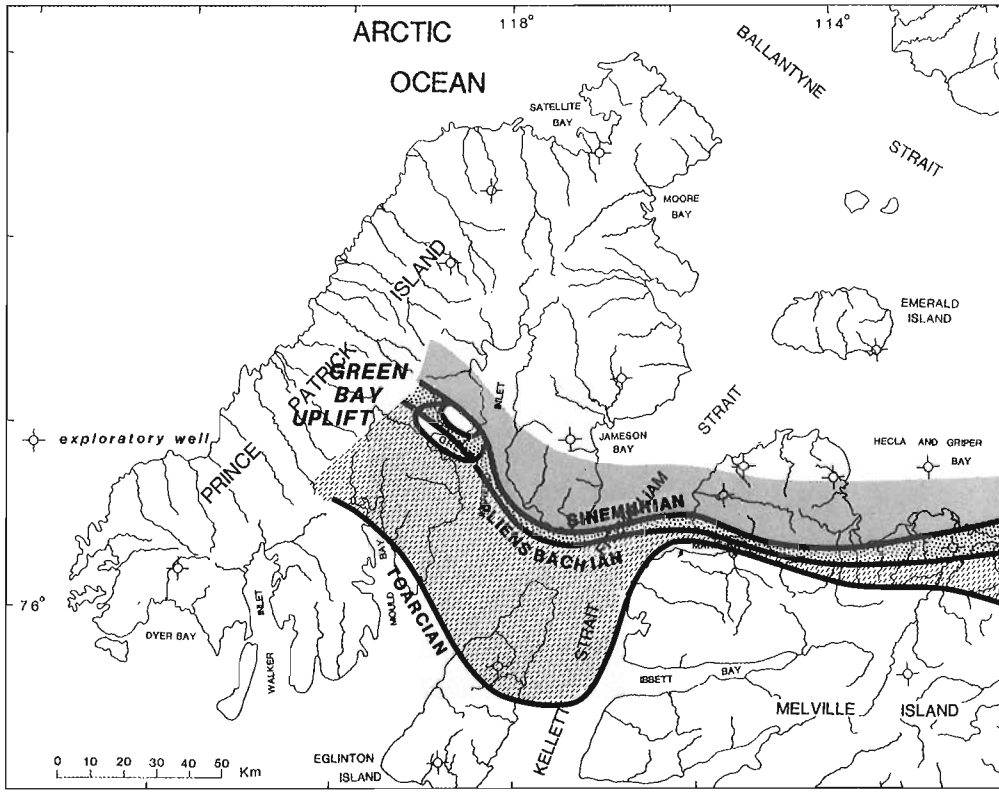

Figure 6. Limits and distribution of Lower Jurassic strata, Prince Patrick Island area.

Apart from a possible northwest trending anticline at the head of Mould Bay, no westward continuation of the fold belt onto Prince Patrick Island was recognized in the course of fieldwork in the area by Tozer and Thorsteinsson (1964). They suggested that the tilting (to about 30°) of the Devonian rocks beneath the sub-Mesozoic angular unconformity could have been caused by block rotation associated with faulting.

To explain the abrupt westward disappearance of the fold belt, Thorsteinsson and Tozer (1970) proposed that a dextral strike-slip fault was responsible for a northward displacement of the deformed terrain. Thus both the Paleozoic fault and the offset fold belt were conveniently swept under the cover of younger strata.

In the course of the more recent fieldwork on Melville Island (Harrison, et al., 1985; Harrison and Bally, in press) three significant observations were made concerning this problem. First, the characteristic tight folding in the Canrobert Hills is restricted to basinal-facies strata of lower Paleozoic age. The tight folds pass upsection into a widespread unit of ductile flow in the Cape De Bray Formation and, above that, the south facing Purchase Bay Homocline in Devonian siliciclastic rocks. Secondly, the terrain south of the Canrobert Hills and upsection from the Cape De Bray Formation ("Blue Hills Fault Belt" of Tozer and Thorsteinsson, 1964) was found to be a region of monoclinal flexures and associated faults of contractional character. Thus, the thinned- skinned style of folding characteristic of the Parry Islands Fold Belt of eastern Melville Island changes westward into regions exhibiting thick-skinned, basement-involved deformational styles. Harrison and Bally (in press) suggested that all regions of foreland deformation should be included in the Parry Islands Fold Belt. It was further proposed that the term Canrobert Hills Fold Belt should be applied to areas having the distinctive style of deformation associated with basinal facies rocks.

Thus the problem before the start of the 1987 field season concerned the westward disappearance of the Parry Islands Fold Belt of southwest Melville Island, the westward disappearance of Purchase Bay Homocline, and the westward disappearance of Canrobert Hills Fold Belt.

The observations made during the past field season indicate that the structural elements on Melville Island in fact do continue onto Prince Patrick Island.

The Paleozoic deformation is indicated by an angular unconformity (up to 90°) beneath Triassic and younger strata at the surface, and beneath Carboniferous to Permian strata in the subsurface. The compressional tectonic elements found in Famennian and older strata beneath the unconformity include seven north to northwest trending anticlines with six intervening synclines (Fig. 8), small reverse faults, and intraformational thrust faults with unknown but probably limited displacement. The synclines are wide, upright, gently-plunging folds, whereas the anticlines tend to be narrow, upright structures faulted axially or on one limb. In cross-section the anticlines are cuspate, with upward-steepening limbs and an axial zone with a very small radius of curvature. Outcrops of the axial region display a pronounced slaty cleavage, eastward and westward verging minor folds and minor thrusts, and numerous low angle and bedding-parallel

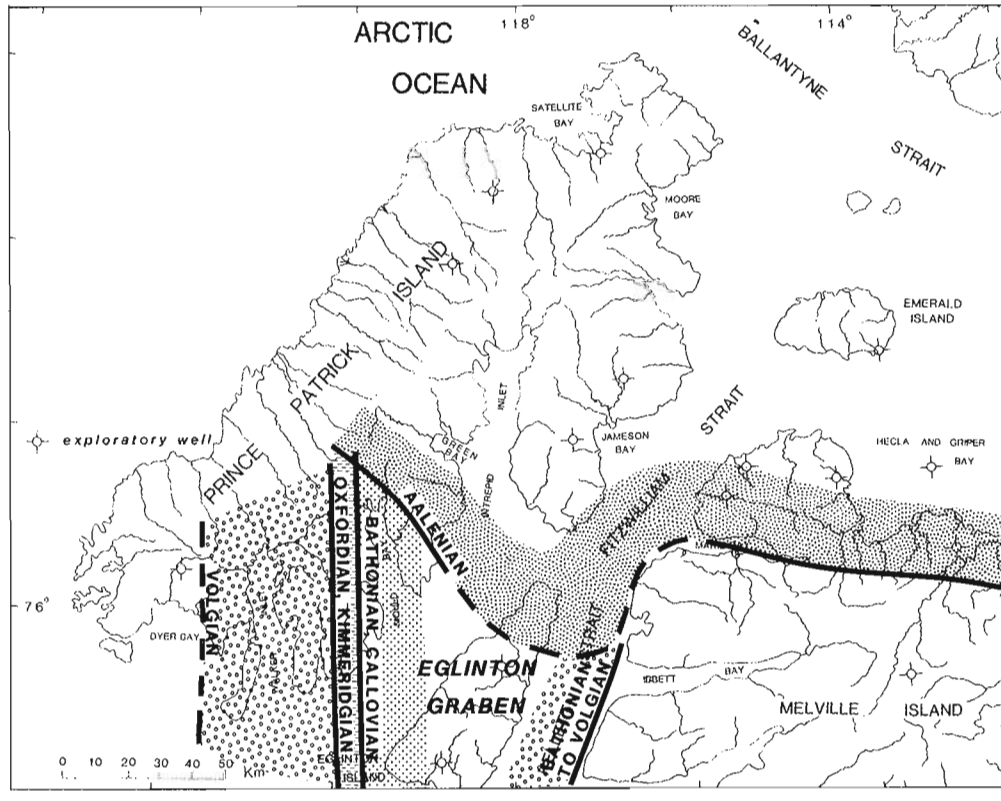

Figure 7. Limits and distribution of Middle and Upper Jurassic strata, Prince Patrick Island area.

slickenside surfaces. The cuspate nature of the anticlines testifies to a shallow decoupling level, presumably located at the top of the Cape De Bray Formation. Estimated visible shortening is 5 to 10 percent.

The change in orientation of the fold belt between Melville and Prince Patrick islands is attributed to a tectonic reentrant centred on northern Eglinton Island, and the buttressing effect of platform carbonates (or other competent strata) that define a salient beneath southwestern Prince Patrick Island. The change in orientation of Parry Islands Fold Belt is probably paralleled by a reentrant in Canrobert Hills Fold Belt, which plunges west beneath Fitzwilliam Strait and northwest beneath Intrepid Inlet and Green Bay areas. The southern and western limits of Canrobert Hills Fold Belt are defined by the south facing Purchase Bay Homocline south of Ibbett Bay on Melville Island and by a similar southwest facing homocline west of Intrepid Inlet on Prince Patrick Island.

MESOZOIC TECTONICS

North striking normal faults were identified by Tozer and Thorsteinsson (1964) throughout the Mould Bay and Walker Inlet areas of Prince Patrick Island. The bulk of the movement was identified as postdating the deposition of Lower Cretaceous strata but predating the Neogene Beaufort Formation. Based on a regional understanding of faulting in the Arctic Islands, Thorsteinsson and Tozer (1970) suggested that the normal faulting was penecontemporaneous with the Eurekan Orogeny in the mid-Cenozoic.

Balkwill and Fox (1982), reviewing regional geophysical and other data from the Sverdrup Basin, noted that northeast striking normal faults may have been active during the emplacement of a Jurassic and Cretaceous subsurface dyke swarm identified throughout the western Arctic Islands.

Data collected from Prince Patrick Island during the 1987 field season indicate that there were two distinct phases in the tectonic evolution of the area during the Mesozoic prior to the Eurekan Orogeny. The first phase postdated the Melvillian Disturbance (Permian; Thorsteinsson and Tozer, 1970) and continued into the Middle Jurassic. During this phase, facies belts, depositional and erosional zero isopachs, and some tectonic elements were influenced by northwest trending lines of uplift and subsidence (Figs. 4-7).

One of the northwest trending structural elements active during the Early Jurassic is a small area of uplift documented in the Green Bay area, which is here referred to as the Green Bay Uplift (Fig. 6). Along the axis of the uplift Pleinsbachian and Toarcian strata of the Jameson Bay Formation have been eroded prior to onlap of the uplift by Aalenian strata of the Sandy Point Formation. Pre-Aalenian tilting can be attributed to block rotation of strata during down-to-the-basin slip on northwest striking, listric extensional faults identified in the Green Bay area.

The dominance of northwest trending tectonosedimentary elements continued through the Aalenian in the Prince Patrick Island area. However, north to northeast trending structural and depositional elements were first present in the Middle Jurassic after the Aalenian, were periodically active from the Middle Jurassic to the Late (?) Cretaceous, and were reactivated after deposition of the Beaufort Formation.

Evidence for this second distinct phase of Mesozoic tectonism has been obtained from both structural and stratigraphic observations. Paired north to northeast striking faults, which we interpret as graben boundary faults, are common throughout the Mould Bay and southern Intrepid Inlet areas (Fig. 6). Reverse drag of strata on the downthrown side of many of these faults serves to establish the extensional and listric character of the master slip surfaces (Bally et al., 1981). The faults east and west of Mould Bay are typified by west dipping master listric faults and east dipping conjugates. Near the head of Mould Bay, sublatitudinal tear faults (or transfer faults) link up east dipping master listric faults found around Green Bay with their oppositely dipping counterparts to the south.

Timing of faulting is suggested by patterns of stratigraphic overlap and the sedimentological record. Uplift and erosion of highlands west of Mould Bay are responsible for the occurrence of Devonian sandstone clasts in the Ringnes and Awingak formations. This uplift was probably accompanied by faulting. Timing of the faulting is indicated by the east-to-west overstepping of Bathonian and Callovian strata by the Ringnes Formation between the first and second grabens west of Mould Bay. A younger period of faulting is also indicated by the overstepping of the Ringnes Formation by the Volgian Awingak Formation between the second and third grabens west of Mould Bay (see Figure 3, and compare Figures 1 and 7).

The discovery of travertine mounds and associated marine vent communities in (or overlying?) the Christopher Formation along the trace of one of these sub-longitudinal faults (see Figure 1) indicates a continuation or renewal of extensional tectonism during (or after?) the Early Cretaceous. Since these faults also offset the Christopher, tectonism also continued after the Early Cretaceous but terminated prior to the deposition of the Beaufort Formation.

Comparison of Middle Jurassic zero edges in Figure 7 and the supporting data in Figure 1 suggests that the Middle Jurassic saw a major shift in patterns of basin margin sedimentation, which we believe is associated with a dramatic change in structural style. The dominance of north trending stratigraphic limits beginning after the Aalenian suggests the beginning of east-west extension that is coplanar and coincident with the emplacement of the subsurface gabbro dyke swarm documented in the western Arctic Islands by Balkwill and Fox (1982). It may also be coincident with rifting events that presumably predated the creation of the Canada Basin.

THE EUREKAN OROGENY IN THE WESTERN ARCTIC ISLANDS

Tozer and Thorsteinsson (1964) recognized the impact of the Eurekan Orogeny in the western Arctic Islands by the northwest trending Moore Bay Anticline and the adjacent synclines on northern Prince Patrick Island.

The 1987 survey indicates that there are at least three other anticlines and two synclines on the west side of Intrepid Inlet, and a series of minor folds and spatially associated faults on Eglinton Island that may also be attributed to the Eurekan Orogeny (Fig. 8). Shorter wavelengths and limited strike-lengths distinguish these Eurekan folds from the older folds

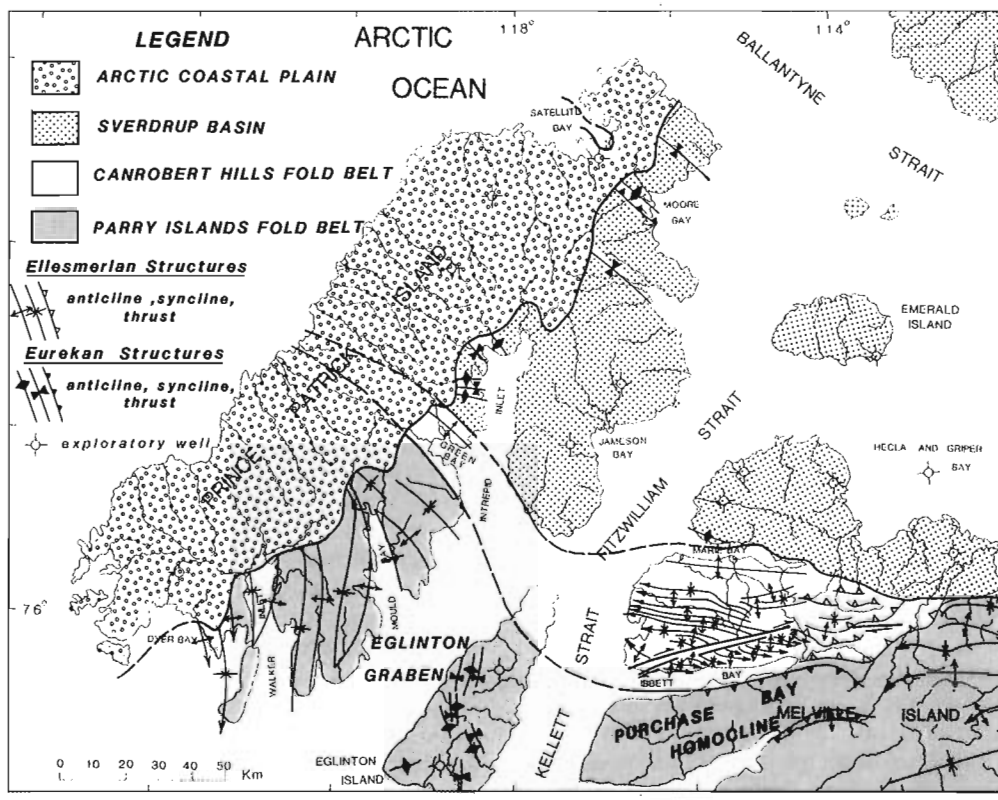

Figure 8. Tectonostratigraphic provinces and distribution of Paleozoic (Ellesmerian and Melvillian) and Tertiary (Eurekan) folds and some associated reverse faults, Prince Patrick Island area. Reverse faults are associated with some folds on Eglinton Island but are not shown.

in the Devonian siliciclastic succession. Shortening attributed to Tertiary folding is estimated to be less than 5 percent. The parallelism of Eurekan folds and faults to pre-existing normal faults is noteworthy and may indicate that reactivation of slip on the pre-existing anisotropic fabric in the Mesozoic rocks may be responsible for the location and orientation of the younger contractional structures. Plateau uplift and peneplanation of marine Cretaceous and older rocks throughout the western Arctic Islands may also be attributed in part to the widespread influence of the Eurekan Orogeny.

NEOGENE TO RECENT TECTONIC ELEMENTS

Tozer and Thorsteinsson (1964) recognized the existence of structural dislocations and linear tectonic features on the Arctic Coastal Plain that signified the occurrence of post-Beaufort deformation on western Prince Patrick Island. They also suggested the probability that reactivation of pre-existing planes of slip was responsible for the location of the linear features. Since earthquake activity still occurs in the area, recent fault motion seems likely.

A compilation of all major photolineaments on the Arctic Coastal Plain is shown in Figure 1. Although local tilting of the Beaufort Formation to about 15° may be associated with slip on these lineaments (Devaney, pers. comm., 1987), the magnitude and sense of slip on these structures remains unknown.

REFERENCES

Balkwill, H.R. and Fox, F.G.
1982: Incipient rift zone, western Sverdrup Basin; *in* Arctic Geology and Geophysics, A.F. Embry and H.R. Balkwill (eds.); Canadian Society of Petroleum Geologists, Alberta, p. 171-187.

Bally, A.W., Bernoulli, D., Davis, G.A., and Montadert, L.
1981: Listric normal faults; Oceanologica Acta, v. 4, supplement, p. 87-101.

Embry, A.F.
1983: The Heiberg Group, western Sverdrup Basin, Arctic Islands; *in* Current Research, Part B, Geological Survey of Canada, Paper 83-1B, p. 381-389.
1984a: The Schei Point and Blaa Mountain groups (Middle-Upper Triassic) Sverdrup Basin, Canadian Arctic Archipelago; *in* Current Research, Part B, Geological Survey of Canada, Paper 84-1B, p. 327-336.
1984b: The Wilkie Point Group (Lower-Upper Jurassic), Sverdrup Basin, Arctic Islands, *in* Current Research, Part B, Geological Survey of Canada, Paper 84-1B, p. 299-308.
1985: New stratigraphic units, Middle Jurassic to lowermost Cretaceous succession, Arctic Island, *in* Current Research, Part B, Geological Survey of Canada, Paper 85-1B, p. 269-276.
— Jurassic-lowermost Cretaceous Stratigraphy, Melville Island; *in* Geology of Melville Island, R.L. Christie (ed.); Geological Survey of Canada, Paper (in press).

Embry, A.F. and Klovan, J.E.
1976: The Middle-Upper Devonian clastic wedge of the Franklinian Geosyncline; Bulletin of Canadian Petroleum Geology, v. 24, p. 485-639.

Fortier, Y.O. and Thorsteinsson, R.
1953: The Parry Islands Folded Belt in the Canadian Arctic Archipelago; American Journal of Science, v. 251, p. 259-267.

Harrison, J.C. and Bally, A.W.
— Cross-sections of the Parry Islands Fold Belt on Melville Island, Canadian Arctic Islands; Bulletin of Canadian Petroleum Geology (in press).

Harrison, J.C., Goodbody, Q.H., and Christie, R.L.
1985: Stratigraphic and structural studies on Melville Island, District of Franklin; *in* Current Research, Part A, Geological Survey of Canada, Paper 95-1A, p. 629-637.

Hills, L.V., Klovan, J.E., and Sweet, A.R.
1974: Juglans eocinerea n. sp., Beaufort Formation (Tertiary), southwestern Banks Island, Arctic Canada; Canadian Journal of Botany, v. 52, p. 65-90.

M'Clintock, Sir F.L.
1857: Reminiscences of Arctic Ice Travel in Search of Sir John Franklin and his Companions; Journal of the Royal Society, Dublin, v 1, p. 183-280.

Mecham, G.F.
1855: Travelling Journal of Lieutenant Mecham; *in* British Parliamentary papers (1855), p. 499-540

Plauchut, B.P. and Jutard, G.G.
1976: Cretaceous and Tertiary stratigraphy, Banks and Eglinton Islands and Anderson Plain (N.W.T.); Bulletin of Canadian Petroleum Geology, v. 24, no. 3, p. 321-371.

Thorsteinsson, R. and Tozer, E.T.
1970: Geology of the Arctic Archipelago; *in* Geology and economic minerals of Canada, R.J.W. Douglas (ed.); Geological Survey of Canada, Economic Geology Report no. 1, Fifth edition, p. 548-589.

Tozer, E.T.
1956: Geological Reconnaissance, Prince Patrick, Eglinton, and Western Melville islands, Arctic Archipelago, Northwest Territories; Geological Survey of Canada, Paper 55-5.

Tozer, E.T. and Thorsteinsson, R.
1964: Western Queen Elizabeth Islands, Arctic Archipelago; Geological Survey of Canada, Memoir 332, 242 p.

Preliminary source rock evaluation of the Nordegg Member (lower Jurassic), Alberta

L.D. Stasiuk[1], K.G. Osadetz, and F. Goodarzi
Institute of Sedimentary and Petroleum Geology, Calgary

Stasiuk, L.D., Osadetz, K.G., and Goodarzi, F., Preliminary source rock evaluation of the Nordegg Member (lower Jurassic), Alberta; in Current Research, Part D, Geological Survey of Canada, Paper 88-1D, p. 51-56, 1988.

Abstract

The hydrocarbon source rock potential of the Lower Jurassic Nordegg Member of western Alberta is currently under investigation. Thermal maturity of the Nordegg ranges from 0.42 % (Tmax = 432 °C) to 0.83 % Ro (Tmax = 447°C) to 1.58 % Ro (Tmax = 487°C). This trend reflects the increasing depth of its burial from northwestern to southern Alberta. Kerogen in the Nordegg is Type I, comprising mainly matrix bituminite, exsudatinite/bitumen, and a phosphatic-bitumen-like substance. Total organic carbon content ranges from approximately 3 to 24 percent by weight. The Nordegg Member thus exhibits properties typically associated with good to excellent hydrocarbon source rocks.

Résumé

On étudie actuellement le potentiel des roches mères d'hydrocarbures du membre de Nordegg, qui appartient au Jurassique inférieur, dans l'ouest de l'Alberta. La maturité thermique du membre de Nordegg se situe entre 0.42 pour cent (Tmax = 432 °C) et 0,83 pour cent Ro (Tmax = 447°C) et même 1,58 pour cent Ro (Tmax = 487°C). Cette évolution reflète l'augmentation de la profondeur d'enfouissement du membre de Nordegg, du nord-ouest au sud de l'Alberta. Dans le membre de Nordegg, le kérogène est de type I, et comprend une matrice composée de bituminite, une exsudatinite ou un bitume, et une substance phosphatée rappelant le bitume. La teneur totale en carbone organique se situe entre environ 3 et 24 pour cent, en poids. Le membre de Nordegg présente donc des propriétés typiquement associées à des roches mères d'hydrocarbures de qualité bonne à excellente.

[1] Department of Geology — Energy Research Unit, University of Regina, Regina, Saskatchewan, S4S 0A2

INTRODUCTION

As part of a thermal maturation and burial history study of the Alberta and Saskatchewan portions of the Western Canada Sedimentary Basin, attention has been paid to certain potential source rock intervals. This brief report will discuss preliminary results of studies of the Lower Jurassic Nordegg Member (Lower Jurassic) of Alberta.

The Nordegg forms the lowermost part of the Fernie Formation (Fig. 1) and consists predominantly of black limestones and calcareous black shales with abundant chert fragments and locally phosphatic nodules (Spivak, 1949). Frebold (1957) reported a change from dark, massive shales in southwestern Alberta to dark, cherty limestone in central northwest Alberta. Thickness of the Nordegg Member reaches approximately 40 m in the subsurface, near Stolberg, Alberta.

The Nordegg Member has been recognized as a potential source of phosphate used in the production of agricultural fertilizers (e.g. Century and Christie, work in progress). High concentrations of phosphates presumably represent paleogeographic zones of upwelling of open ocean currents with a correspondingly high production of plankton. The potential of phosphate-rich sediments as hydrocarbon source rocks was initially speculated on by Brongersma-Sanders (1948; *in* Powell et al., 1975), and later systematically studied by Powell et al. (1975), Maughan (1980; Permian Phosphoria Formation, western United States), Fournié (1980), and Burollet and Oudin (1980), who worked on the Paleocene and Eocene of Tunisia.

A suite of phosphorites, studied by Powell et al. (1975), ranging in age from Tertiary to Precambrian, were not found to be abnormally rich in organic carbon, but contained very high proportions of extractable asphaltic material. The authors (ibid.) suggested that this was evidence for possible migration of heavy oil at an early stage of diagenesis.

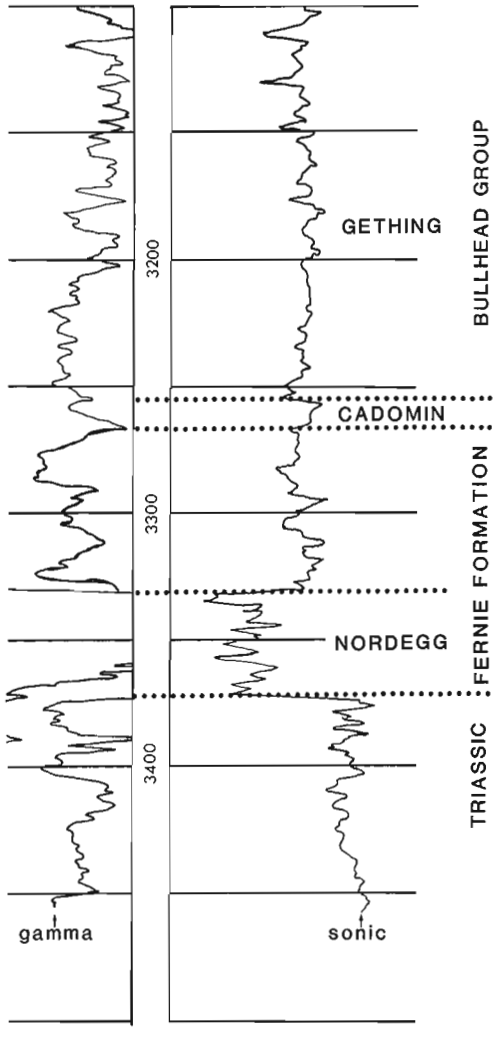

Figure 1. General stratigraphy of the Nordegg Member illustrated by log response in 9-26-87-7W6. Note the strong gamma-ray deflection; this is often a characteristic of fine-grained sediments rich in organic carbon (Russell, 1985).

ACKNOWLEDGMENTS

Rock-Eval pyrolysis was performed under the supervision of L.R. Snowdon, who, along with R.W. Macqueen, critically reviewed the manuscript.

CURRENT INVESTIGATION

Nordegg Member core samples were collected from a number of Alberta locations (Fig. 2), the analysis and spacing of which provide a preliminary regional perspective of the thermal maturity level and hydrocarbon source rock potential of this unit.

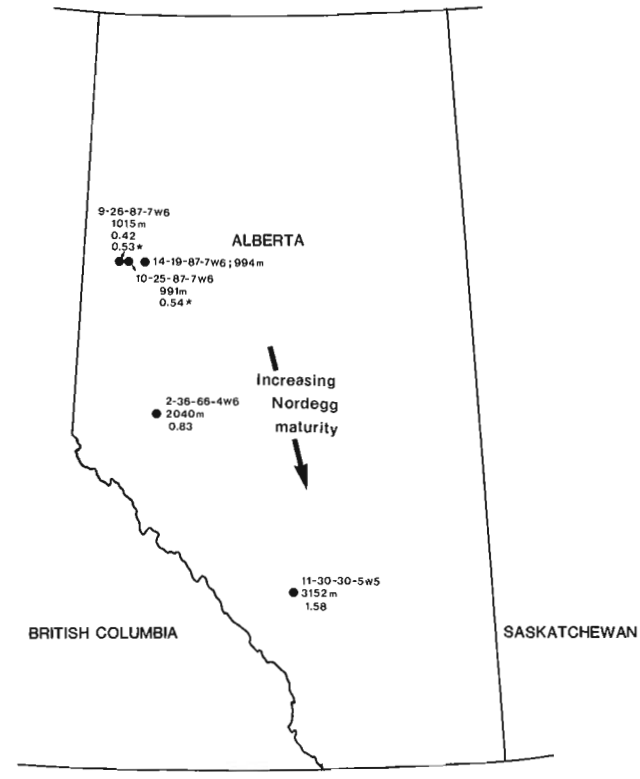

Figure 2. Borehole locations, depth to the Nordegg Member (m) and the percent reflectance in oil of vitrinite/Type III kerogen in the Nordegg Member and Gething (*) Formation.

Table 1. Rock-Eval parameters and their definition and significance in source rock evaluation (compiled from Tissot and Welte, 1978).

Rock-Eval Parameter	Definition Significance
S1	mg free and adsorbed hydrocarbons/gm of rock volatilized at moderate pyrolysis temperatures (300°C).
S2	mg hydrocarbons/gm of rock liberated during pyrolysis at elevated temperatures (300-600°C).
S3	mg CO_2/gm of rock generated from kerogen during pyrolysis.
TOC	Total Organic Carbon in weight per cent.
Tmax	temperature corresponding to maximum hydrocarbon generation (S2) during pyrolysis.

METHODS OF STUDY

Organic petrography (Type III kerogen/vitrinite reflectance in oil; oemax and Red/Green quotients of fluorescing kerogen compounds) and Rock-Eval pyrolysis were used to initially assess the source rock potential and thermal maturity.

Microscopic examination of polished blocks, using oil immersion objectives, was performed with a Zeiss MPM II reflected-light microscope fitted with: 1. a Hewlett Packard 300/9000 microcomputer; a Ziess Coflex software package was used for reflectance measurements; 2. a halogen white light source; and 3. an ultra-high pressure mercury lamp, ultraviolet light source.

Powell and Snowdon (1983) proposed a modified hydrocarbon generation model for Type II, III and IV organic matter, recognizing that distinctive organic matter types generate distinctive hydrocarbon products at different levels of thermal maturity. Like Vassoevich et al. (1974), they correlated the thermal maturity of organic material with vitrinite reflectance (%Ro vitrinite/Type III kerogen). Their studies suggest that Type II and resinite- or liptinite-rich Type III oil source materials begin to generate oils at thermal maturity levels betweeen 0.5 to 0.7 % Ro depending upon the type of source material. Peak oil generation is predicted to occur over the interval 0.7 to 1.2 % Ro, again depending upon the organic matter type. At reflectances of 1.2 % Ro, the thermal cracking of $C_{15}+$ hydrocarbons becomes significant. This process is largely complete at a level of 1.6 % Ro, and at 1.8 % Ro, a marked decline in the production of wet gas signifies the onset of dry gas generation in the overmature zone. Type II sources do not generate significant amounts of gas until they reach the overmature zone (1.2-1.8 % Ro); Type III organic materials generate significant proportions of gaseous hydrocarbons at the same level of thermal maturity as the onset of liquid hydrocarbon generation (0.7-1.2 % Ro) (Monnier et al., 1981; Powell and Snowdon, 1983). Type I source rocks and kerogens from the Green River Shale studied by Espitalié et al. (1985) exhibit a significant decrease in Hydrogen Index at approximately 0.85 % Ro, and a peak yield of solvent extracted saturate hydrocarbons at approximately 1.0 % Ro, which can both be interpreted to represent the onset and peak generation of liquid hydrocarbons.

Rock-Eval pyrolysis-organic carbon analysis may be used to assess the quantity of hydrocarbon ultimately derivable from a sample of sediment, the oil and gas generation potential and thermal maturity, and also to approximate the organic matter type in potential petroleum source rocks (Tissot and Welte, 1978). Rock-Eval estimates five parameters: S1, S2, S3, TOC and Tmax. Table 1, assembled from Tissot and Welte (1978), summarizes the significance of each of the parameters.

RESULTS

Though a limited number of samples have been analyzed for %Ro, and by Rock- Eval analysis, the results soundly establish the Nordegg Member as a potential hydrocarbon source rock in the Alberta Basin.

THERMAL MATURITY/ORGANIC PETROLOGY

The thermal maturity level of the Nordegg sediments (Table 2) ranges from an average minimum of 0.42 % Ro in northwest Alberta, to 0.83 % Ro in central northwest Alberta, to a maximum of 1.58 % Ro in the deep basin northwest of Calgary. The %Ro increases in value with increasing depth of burial of the Nordegg Member. The maturity level within Township 87, Range 6W6, may be somewhat higher than the measured %Ro of 0.42, since overlying Gething coal is at a %Ro ranging from 0.51 to 0.57 %. Reflectance is susceptible to supression in extremely hydrogen-rich sediments (Hutton and Cook, 1980; Goodarzi et al., 1987) and this may be occurring within the Nordegg Member.

Two 'kerogen facies' appear to be consistently present in the Nordegg sediments in boreholes 14-19-87-7W6, 13-25-87-7W6, 9-26-87-7W6 and 3-36-68-4W6. Facies 1 is distinct in that it contains both phosphatic nodules and fossils, and a 'soft' phosphatic- bitumen-like amorphous material (Fig. 3a). Facies 2 is characterized by the absence of phosphatic-kerogen assemblages. Both facies consist predominantly of matrix bituminite (lipoid substances adsorbed onto mineral surfaces; Creaney, 1980), which under ultraviolet irradiation displays very strong positive alteration. After only 30 seconds of ultraviolet exposure, oil-like substances, soluble in immersion oil, begin to exude out of the mineral matrix. This results in a unique and anomalous, brown, murky field of view.

Morphologically intact hydrogen-rich kerogen is rare in the Nordegg sediments, with only Campenia-like marine alginite positively identified. Rare examples of mineralized Pterosphaeridia-like alginite are also present. Fluorescing kerogen also includes variable amounts of liptodetrinite.

A second feature common to both facies is the presence of exsudatinite/bitumen in pores and fractures. In facies 1

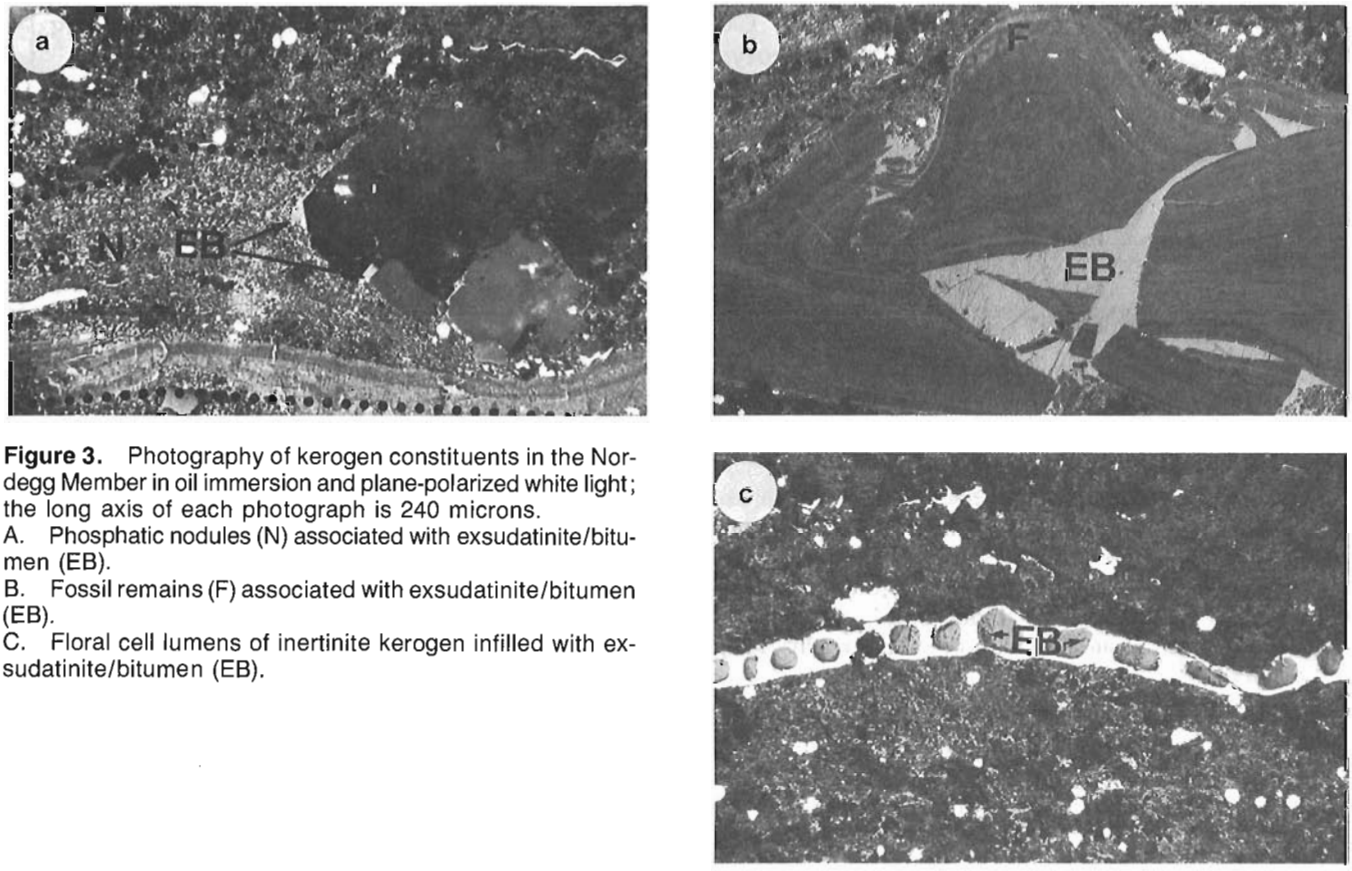

Figure 3. Photography of kerogen constituents in the Nordegg Member in oil immersion and plane-polarized white light; the long axis of each photograph is 240 microns.
A. Phosphatic nodules (N) associated with exsudatinite/bitumen (EB).
B. Fossil remains (F) associated with exsudatinite/bitumen (EB).
C. Floral cell lumens of inertinite kerogen infilled with exsudatinite/bitumen (EB).

Table 2. Reflectance in oil of vitrinite/type III kerogen in the Nordegg Member and overlying Gething coal(*)

Location	Depth (m)	%Ro	Standard Deviation	Tmax (°C)
9-26-87-7W6	948.2	0.53*	0.04	436
	1022.0	0.44	0.07	431
	1027.5	0.40	0.04	435
10-25-87-7W6	983.0	0.51*	0.05	432
	984.8	0.57*	0.04	431
2-36-68-4W6	2056.6	0.81	0.05	446
	2060.3	0.84	0.04	442
11-30-30-5W5	3176.4	1.58	0.07	487

Table 3. Rock-Eval results for the Nordegg Member and overlying Gething Formation (*) sediments. For definition of parameters, see Table 1; HI, Hydrogen Index; OI, Oxygen Index

Location	Depth (m)	TOC	Tmax (°C)	S1	S2	S3	HI	OI
14-19-87-7W6	914.4*	8.34	436	0.70	26.61	1.73	319	21
9-26-87-7W6	935.4*	1.42	436	0.37	1.23	0.41	80	29
	948.2*	1.55	436	0.70	1.48	1.53	96	99
	1022.0	23.62	431	9.92	151.84	1.33	643	6
	1027.5	9.32	435	3.33	64.52	0.61	692	7
	1028.4	22.12	433	6.79	166.58	1.02	753	5
10-25-87-7W6	983.0*	4.91	432	1.18	12.13	0.55	247	11
	984.8*	11.23	431	2.68	20.93	0.70	186	6
2-36-68-4W6	2056.6	14.37	446	3.08	44.83	0.83	312	6
	2060.3	9.20	447	1.66	34.72	0.42	377	5
11-30-30-5W5	3176.4	3.24	487	0.16	0.74	0.41	23	13

the exsudatinite/bitumen is primarily associated with 'phosphatic kerogen'; for example, infilling fractures in teeth/fossils and phosphate nodules (Fig. 3b). To a lesser extent in facies 1, exsudatinite/bitumen infills cell lumens in the traces of floral inertinite kerogen. Facies 2 is, on the other hand, characterized by exsudatinite/bitumen uniquely infilling only cell lumens of floral inertinite kerogen (Fig. 3c).

Overmature kerogen in borehole 11-30-30-5W5 is hosted by an extremely pyrite-rich, silty to sandy shale, and consists of trace amounts of inertinite and vitrinite-like kerogen.

ROCK-EVAL ANALYSIS

Nordegg Member Rock-Eval results are listed in Table 3; also included are results from overlying Gething Formation sediments. Total organic carbon in the Nordegg ranges from 3.24 to 23.62 wt. %; S1 from 0.16 to 9.92 mg HC/gm rock; S2 from 0.74 to 166.58 mg HC/gm rock. Using the criteria of Osadetz and Snowdon (1986) for rating potential source rocks, the Nordegg in boreholes 14-19-87-7W6, 9-26-87-7W6 and 2-36- 68-4W6 must be considered as a good to excellent potential source rock.

The thermal maturity level, as defined by Tmax, ranges from an average 434°C in northwest Alberta (Tp 87-R7W6), to 447°C in central northwest Alberta (Tp 68-R4W6), to a maximum of 487°C in the deep basin northwest of Calgary (Tp 30-R5W5). The increase in Tmax from north to south reflects both increasing %Ro (Fig. 2) and depth of burial for the Nordegg Member.

It is often convenient to plot the Hydrogen Index ([S2/Org C]x100) against the Oxygen Index ([S3/Org

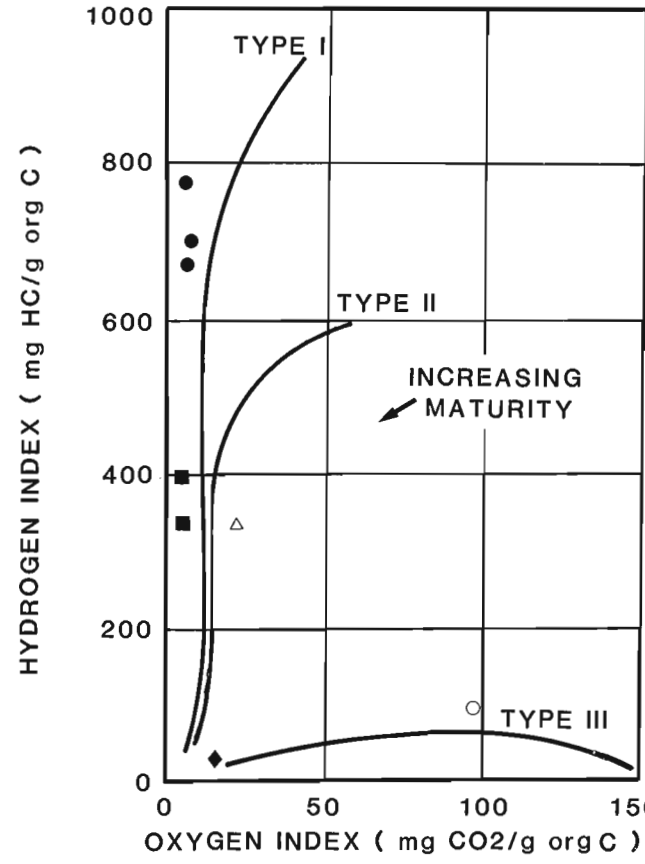

Figure 4. Hydrogen Index-Oxygen Index plot of Nordegg Member sediments (● 9-26-87-7W6, ■ 2-36-68-4W6, ◆ 11-30-30-5W5) and Gething Formation sediments (△14-19-87-7W6, ○9-26-87-7-W6).

C]x100), in order to infer the type of organic matter in potential source rocks (Macauley et al., 1985). The two indices establish the Nordegg Member as comprising Type I kerogen (Fig. 4). The evolution of Type I kerogen in the Nordegg with increasing maturity (decreasing Hydrogen and Oxygen indices) (Fig. 4), reflects increasing %Ro, Tmax and depth of burial from northern to southern Alberta.

DISCUSSION AND CONCLUSIONS

Preliminary results of the organic petrology and Rock-Eval analysis of the Nordegg Member point to its high potential as a petroleum source rock in west-central to northwest Alberta. The predominantly Type I kerogen (Hydrogen Indices of 300 to >700), consisting of matrix bituminite, 'phosphatic-kerogen' and exsudatinite/bitumen, is considered marginally mature in regions near Township 87, Range 7W6. This is indicated by a vitrinite/Type III kerogen %Ro near 0.50 % (Monnier et al., 1981) and a Tmax approaching 435°C (430° to 435°C = marginally mature sediments, Osadetz and Snowdon, 1986).

In the region of borehole 2-36-68-4W6, the Nordegg Member still maintains excellent Type I kerogen, source rock potential. The thermal maturity level of the Nordegg in this borehole (%Ro mean = 0.83; Tmax = 447°C) is moderate and the sediments are probably within the peak zone of liquid hydrocarbon generation (criteria of Macauley et al., 1985). Within the deep basin the Nordegg is overmature (%Ro >1.30) and has no remaining liquid hydrocarbon potential and only a restricted gas potential. Thus maturation of the Nordegg Member increases from north to south in the study area.

Further, detailed studies with much greater geographic control are necessary to define the lateral limits of potential source rocks and their thermal maturity level in the Nordegg Member. In conjunction, detailed organic geochemistry studies should be pursued to establish a possible oil-source rock correlation for Nordegg sediments.

REFERENCES

Burollet, P. and Oudin, J.-P.
1980: Paléocène et Eocène en Tunisie – Pétrole et phosphates; *in* Géologie Comparée des Gisements de Phosphates et de Pétrole, J.-C. Dumort (ed.); Editions B.R.G.M., Orléans Cedex, p. 205-216.

Creaney, S.
1980: The organic petrology of the Upper Cretaceous Boundary Creek Formation, Beaufort-Mackenzie basin; Bulletin of Canadian Petroleum Geology, v. 28, p. 112-129.

Espitalié, J., Deroo, G., and Marquis, F.
1985: Rock-Eval pyrolysis and its applications; Institut Français du Pétrole,.Paris, preprint series, Geologie no. 27299, Project B41 79008, 72 p.

Fournié, D.
1980: Phosphates et pétrole en Tunisie; *in* Géologie Comparée des Gisements de Phosphates et de Pétrole, J.-C. Dumort (ed.); Editions B.R.G.M., Orléans Cedex, p. 156-166.

Frebold, H.
1957: The Jurassic Fernie Group in the Canadian Rocky Mountains and Foothills; Geological Survey of Canada, Memoir 287, 197 p.

Goodarzi, F., Davies, G.R., Nassichuk, W.W., and Snowdon, L.R.
1987: Organic petrology and Rock-Eval analysis of the Lower Carboniferous Emma Fiord Formation in Sverdrup Basin, Canadian Arctic Archipelago; Marine and Petroleum Geology, v. 4, p. 132-145.

Hutton, A.C. and Cook, A.C.
1980: Influence of alginite on the reflectance of vitrinite from Joadja, NSW, and some other coals and oil shales containing alginite; Fuel, v. 59, p. 711-714.

Macauley, G., Snowdon, L.R., and Ball, F.D.
1985: Geochemistry and Geological Factors Governing Exploitation of Selected Canadian Oil Shale Deposits; Geological Survey of Canada, Paper 85-13, 65 p.

Maughan, E.K.
1980: Relation of phosphorite, organic carbon and hydrocarbons in the Permian Phosphoria Formation (western U.S.A.); *in* Géologie Comparée des Gisements de Phosphates et de Pétrole, J-C. Dumort (ed.); Editions B.R.G.M., Orléans Cedex, p. 63-91.

Monnier, F., Powell, T.G., and Snowdon, L.R.
1981: Qualitative and quantitative aspects of gas generation during maturation of sedimentary organic matter. Examples from Canada frontier basins; *in* Advances in Organic Geochemistry 1981, M. Bjoro/y et al. (eds.); John Wiley and Sons Ltd., p. 487-495.

Osadetz, K.G. and Snowdon, L.R.
1986: Petroleum source rock reconnaissance of southern Saskatchewan; *in* Current Research, Part A, Geological Survey of Canada, Paper 86-1A, p. 609-617.

Powell, T.G. and Snowdon, L.R.
1983: A composite hydrocarbon generation model; Erdöl und Kohle, v. 36, p. 163-170.

Powell, T.G., Cook, P.J., and McKirdy, D.M.
1975: Organic Geochemistry of Phosphorites: Relevance to Petroleum Genesis; American Association of Petroleum Geologists, Bulletin, v. 59, p. 618-632.

Russell, D.J.
1985: Depositional analysis of a black shale by using gamma-ray stratigraphy: the Upper Kettle Point Formation of Ontario; Bulletin of Canadian Petroleum Geology, v. 33, p. 235-252.

Spivak, J.
1949: Jurassic sections in Foothills of Alberta and Northeastern British Columbia; American Association of Petroleum Geologists, Bulletin, v. 33, p. 533-546.

Tissot, B.P. and Welte, D.H.
1978: Petroleum formation and occurrence; Springer-Verlag, Berlin, 538 p.

Vassoevich, N.B., Akramkhodzhqev, A.M., and Geodekyan, A.A.
1974: Principal zone of oil formation; *in* Advances in Organic Geochemistry, B.P. Tissot and F. Bienner (eds.); 1973, Editions Technip, Paris, p. 309-314.

Field studies at 'fossil forest' sites in the Arctic Islands

R.L. Christie
Institute of Sedimentary and Petroleum Geology, Calgary

Christie, R.L., Field studies at 'fossil forest' sites in the Arctic Islands; in Current Research, Part D, Geological Survey of Canada, Paper 88-1D, p. 57-60, 1988.

Abstract

Field studies continue at a recently discovered fossil wood locality on Axel Heiberg Island. Fossilized logs and stumps in the lower Tertiary Eureka Sound Group are known at widely scattered Arctic localities.

Alteration of the organic matter at the new site, however, is minimal and the site may be an important one in the study of plant remains.

Résumé

On poursuit actuellement des recherches sur le terrain dans une localité récemment découverte, caractérisée par la présence de bois fossile, dans l'île Axel Heiberg. On connaît l'existence de troncs et de souches fossilisés en d'autres endroits très dispersés de l'Arctique, situés dans le groupe d'Eureka Sound datant du Tertiaire inférieur.

Toutefois, dans la nouvelle localité découverte, l'altération de la matière organique est minimale et cet endroit pourrait s'avérer d'une grande importance à l'étude des restes végétaux.

INTRODUCTION

Concentrations of petrified logs with, in places, relict stumps in growth position have been found in beds of the Tertiary Eureka Sound Group at several localities on Ellesmere Island in the course of the past 100 years. In 1985, attention was focussed on a new locality, on Axel Heiberg Island. Here, in-place stumps, associated logs and smaller wood fragments, and forest-floor litter have been preserved without significant petrification or mineralization. The fossil material, although compressed and slightly coalified, is still mainly wood- or leaf-like. Intensive field study of the forest layers at the site near the Geodetic Hills, Axel Heiberg Island, was carried out in 1986 (see Basinger, 1986; McMillan, 1986; Francis and McMillan, 1987). Geological Survey of Canada research and cooperating research on this and other "fossil forests" were organized in 1986 as a Survey project under R.L. Christie. Fieldwork, reported here, was continued in 1987 at the Geodetic Hills site and at a site near Strathcona Fiord, Ellesmere Island (see Figure 1).

HISTORY OF STUDIES

Terrigenous plant remains of early Tertiary age were discovered in 1875 in the Canadian High Arctic, at 'Watercourse Valley', by Captain G.S. Nares, Royal Navy. An extensive collection of fossil leaves from this northern Ellesmere locality was studied by O. Heer (1878). Members of the Greely Expedition of 1881-83 noted fossil logs (Fig. 2A) on Judge Daly Promontory, to the south of Watercourse Valley, and the new locality became known as "Brainard's Fossil Forest", named for the discoverer (Brainard, *in* Greely, 1886, v. II, p. 419, 420). Another forest locality, with stumps in growth position (Fig. 2B), was discovered by Per Schei (1903, 1904) at Stenkul Fiord, southern Ellesmere Island, and this locality was later described by Nathorst (1915) (see also Riediger and Bustin, 1987).

The fossil leaves, logs, and rarer stumps occur in a sandstone-mudstone unit with coal beds that was named the Eureka Sound Group by J.C. Troelsen (1950, p. 78). Eureka Sound beds have been mapped over the years at widely scattered localities in the Arctic Islands. The formation is considered to be dominantly nonmarine in origin, but marine indicators have been noted in some beds (West et al., 1975, 1977; West and Dawson, 1979). The fossil wood is typically more or less petrified (silicified or calcified) and coalified.

'Fossil forests' (layers with stumps preserved in growth position) (Fig. 2C) were discovered at Hot Weather Creek near Eureka Weather Station, Ellesmere Island, in 1955 by N.J. McMillan (1963). A third 'fossil forest' locality south of Strathcona Fiord, Ellesmere Island was discovered by M. Dawson and others during fieldwork in 1973 and later (Dawson et al., 1975). At this site, orange weathering stumps occur in black coal, providing one of the more photogenic occurrences (Fig. 2D).

The most recent, and in certain ways the most spectacular, 'fossil forest' discovery is that near the Geodetic Hills, Axel Heiberg Island, discovered during stratigraphic studies by B.D. Ricketts, Geological Survey of Canada. The site

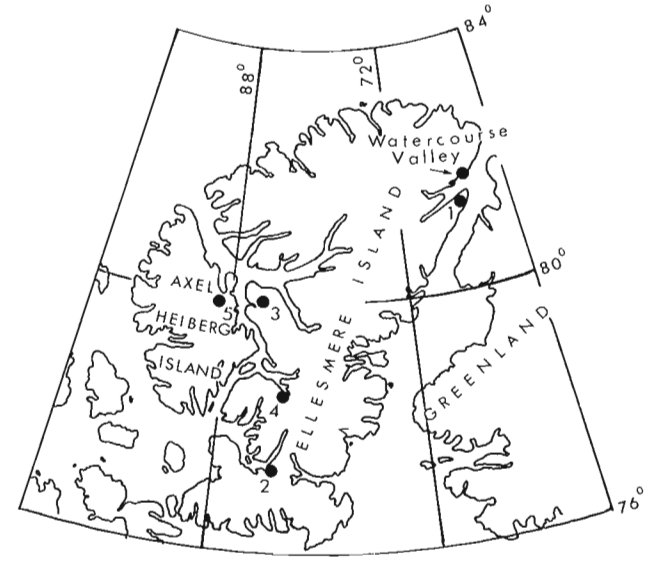

Figure 1. Index map showing the localities at which early Tertiary 'fossil forests' or concentrations of fossil logs are known. 1. Brainard's Fossil Forest; 2. Stenkul Fiord; 3. Hot Weather Creek; 4. Strathcona Fiord; 5. Geodetic Hills.

was studied intensively during 1986, with paleobotanical collections obtained by J.E. Basinger of the University of Saskatchewan and 'paleo-wood' material collected by J.E. Francis of Adelaide, Australia (see Basinger, 1986). It became apparent during collection and excavation of the in-place stumps, the undisturbed forest-floor mats (Fig. 2E), and the paleosol and bleached-zone layers that the site may be a unique one for study in several fields of science.

FIELD ACTIVITIES IN 1987

Fieldwork was carried out in July, 1987 at the Geodetic Hills and the Strathcona Fiord fossil forest sites. Several teams camped together at the Axel Heiberg Island locality; participants included J. Basinger, B. Lepage, J.E. Francis, L.V. Hills, R. Day, S. Cumbaa, D. Grattan, B.D. Ricketts, D.J. McIntyre, M.R. Dawson, M. McKenna, C. Howard, J.H. Hutchison, and R.L. Christie. Associated with the geological, paleobotanical, and paleozoological studies was a film group: Breakthrough Films and TV., Inc., of Toronto. Ira Levy, Rachel Low, John Dyer, Ted McLelland, and Gordon Thompson filmed and interviewed scientists working at the site. Others who visited included Hans Dommasch, photographer, Eli Bornstein, artist, and Roger and Rowena Winkler, photographer and assistant.

The locality near Strathcona Fiord on Ellesmere Island was studied later in July by Francis and Christie.

Air and other field support for all groups was provided by the Polar Continental Shelf Project.

RESEARCH AND PUBLICATIONS

Stratigraphic studies by B.D. Ricketts of the sequence of beds containing fossil forest layers in the Geodetic Hills continues, with biostratigraphic control provided through palynological study by D.J. McIntyre. Paleobotanical research by J.

Basinger, B. Lepage, and L.V. Hills continues. Tree rings and forest dynamics measurements are being undertaken by J.E. Francis in Adelaide, Australia. Paleosol samples collected by R.L. Christie are under study by R. Protz, University of Guelph, supported by certain laboratory analyses by A. Foscolos at the Institute of Sedimentary and Petroleum Geology, Calgary.

A multi-paper GSC publication is now being prepared, and will comprise preliminary reports on the fossil forest at Geodetic Hills.

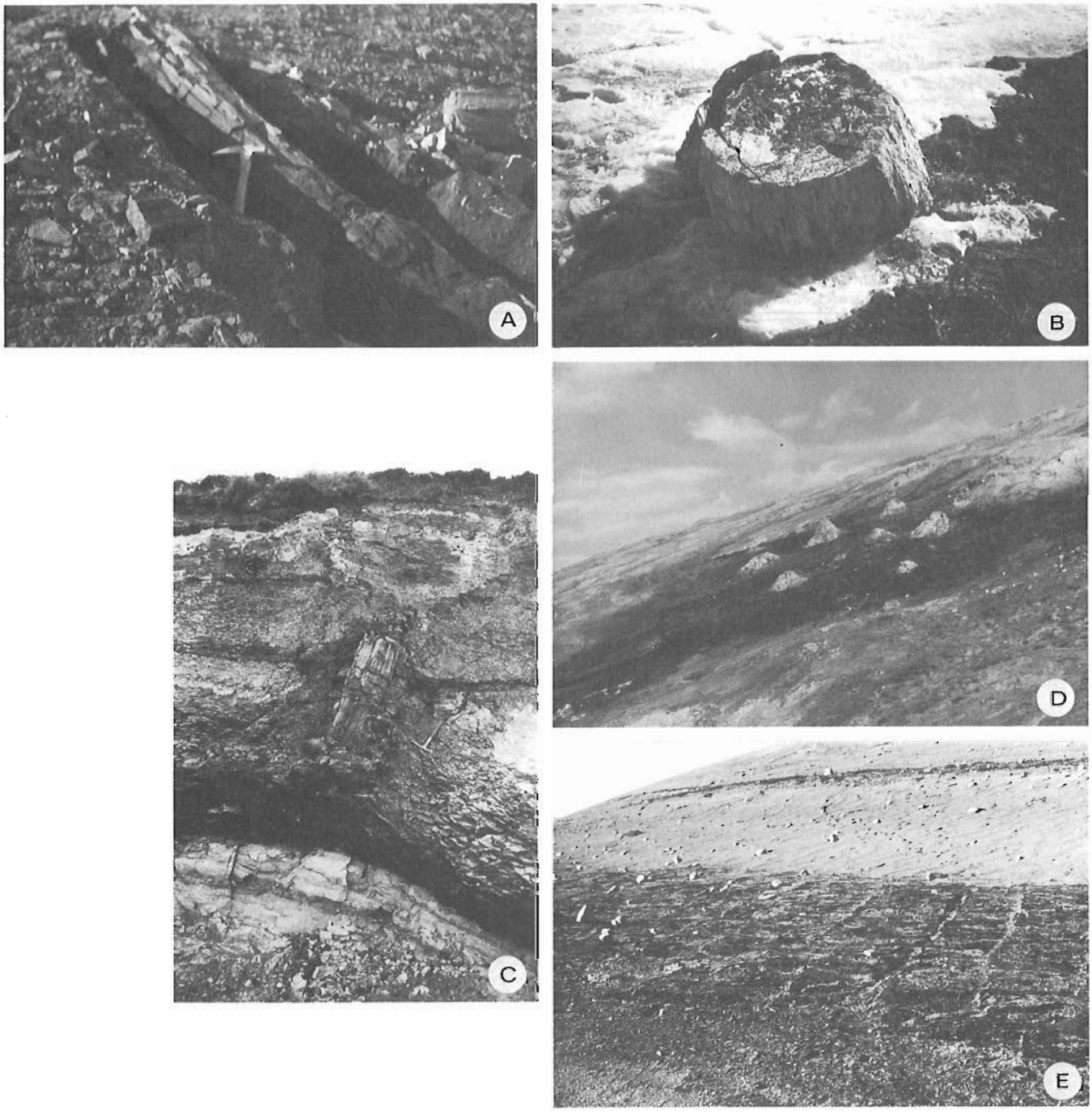

Figure 2. Some view of 'fossil forests' of Ellesmere and Axel Heiberg Islands. **A**, Judge Daly Promontory, R.L. Christie, GSC 124974; **B**, Stenkul Fiord, C.L. Riediger, 1983; **C**, Near Hot Weather Creek, J.F. Basinger, 1986; **D**, Strathcona Fiord, R.L. Christie, 1987; E, Geodetic Hills: forest floor 'mat', R.L. Christie, 1987.

REFERENCES

Basinger, J.F.
1986: Our 'tropical' Arctic; Canadian Geographic, v. 106, no. 6, p. 28-37.

Dawson, M.R., West, R.M., Ramaekers, P., and Hutchison, J.H.
1975: New evidence on the paleobiology of the Eureka Sound Formation, Arctic Canada; Arctic, v. 28, p. 110-116.

Francis, J.E. and McMillan, N.J.
1987: Fossil forests in the Far North; Geos, v. 16, no. 1, p. 6-9.

Greely, A.W.
1886: Three years of Arctic Service, volumes I and II; Charles Scribner's Sons, New York.

Heer, O.
1878: Notes on fossil plants discovered in Grennell Land by a Captain H.W. Feilden; Quarterly Journal of the Geological Society of London, v. 34, p. 66-72.

McMillan, N.J.
1963: Slidre River; *in* Geology of the north-central part of the Arctic Archipelago, Northwest Territories (Operation Franklin), Fortier et al. (eds.); Geological Survey of Canada, Memoir 320, p. 400-407.
1986: Tertiary fossil forests in the Arctic; Episodes, v. 9, p. 169-170.

Nathorst, A.G.
1915: Tertiare pflazenreste aus Ellesmere-land; Report of the second Norwegian Arctic Expedition in the *Fram*, 1898-1902, No. 35; The Society of Arts and Sciences of Kristiania, v. 4.

Riediger, C.L. and Bustin, R.M.
1987: The Eureka Sound Formation, southern Ellesmere Island; Bulletin of Canadian Petroleum Geology, v. 35, p. 123-142.

Schei, Per
1903: Summary of geological results, the Second Norwegian Polar Expedition in the *Fram*; Geographical Journal, v. 22, p. 56-65.
1904: Preliminary account of the geological investigations made during the Second Norwegian Polar Expedition in the Fram; Appendix I *in* O. Sverdrup, New Land, v. II, London, Longman, Green and Company.

Troelsen, J.C.
1950: Contribution to the geology of Northwest Greenland, Ellesmere and Axel Heiberg Islands; Meddelelser om Gr/onland, v. 149, no. 7, 85 p.

West, R.M. and Dawson, M.R.
1979: Vertebrate paleontology and the Cenozoic history of the North Atlantic region; Polar-forschung, v. 48 1/2, p. 103-119.

West, R.M., Dawson, M.R., and Hutchinson, J.H.
1977: Fossils from the Paleogene Eureka Sound Formation, Northwest Territories, Canada: occurrence, climatic and paleogeographic implications; *in* Paleontology and Plate Tectonics, R.M. West (ed.); Milwaukee Public Museum, Special Papers in Biology and Geology, v. 2, p. 79-93.

West, R.M., Dawson, M.R., Hutchinson, J.H., and Ramaekers, P.
1975: Paleontologic evidence of marine sediments in the Eureka Sound Formation of Ellesmere Island, Arctic Archipelago, Northwest Territories, Canada; Canadian Journal of Earth Sciences, v. 12, p. 574-579.

Depositional setting of the Maastrichtian Cuesta Creek Member, Tent Island Formation, northern Yukon

J. Dixon
Institute of Sedimentary and Petroleum Geology, Calgary

Dixon, J., Depositional setting of the Maastrichtian Cuesta Creek Member, Tent Island Formation, northern Yukon; in Current Research, Part D, Geological Survey of Canada, Paper 88-1D, p.61-65, 1988.

Abstract

Early descriptions and interpretations of the depositional setting of the Maastrichtian Cuesta Creek Member, Tent Island Formation, identified the clastics as fluvial deposits prograding over prodelta sediments. Some of the clastics were attributed to braided river deposition. The facies types, sedimentary structures and regional setting favour a drastic revision of the original interpretations. The generally thin bedded nature of the succession, small- to large-scale scours, Bouma-type cyclothems, debris-flow-type deposits and a lack of sedimentary structures produced by traction currents all point to an origin as sediment-gravity flow deposits on a submarine fan.

Résumé

Grâce aux premières descriptions et interprétations du milieu sédimentaire dans lequel s'est formé le membre maastrichtien de Cuesta Creek, qui appartient à la formation de Tent Island, on a identifié les roches clastiques comme étant des dépôts fluviatiles en progression sur des sédiments prodeltaïques. On a attribué l'existence de quelques-unes des roches clastiques à une sédimentation dans un cours d'eau anastomosé. En raison des types de faciès, des structures sédimentaires et du milieu régional, il semble que l'on doive réviser à fond les interprétations initiales. Le caractère généralement finement lité de la succession, les affouillements de petites à grandes dimensions, les cyclothèmes de type Bouma, les dépôts du type coulées de boue, et l'absence de structures sédimentaires produites par des courants de traction, sont des détails indiquant tous qu'il s'agit de roches sédimentaires déposées par des courants de gravité sur un cône alluvial sous-marin.

INTRODUCTION

Cuesta Creek strata were formally named by Young in 1975, prior to which they had been informally recognized as "the basal chert conglomerate and sandstone division" (Fig. 1; Young, 1972, 1973). Holmes and Oliver (1973) informally included the strata in an expanded Moose Channel Formation and called them unit 1. Young (1972, 1973, 1975) and Holmes and Oliver (1973) attributed deposition of Cuesta Creek strata to a delta plain/delta front setting possibly with braided rivers as well as meandering rivers.

Re-examination of Cuesta Creek strata at Fish River (locality 87-5, Fig. 2; the type section), along Hornet Creek, on the east side of Rapid Creek, and at a few isolated areas west of Deep Creek (Fig. 2) has led to the reassessment of previous interpretations of depositional setting. The bulk of the detailed descriptions are from the section along Fish River, where the succession is well exposed and sedimentary features readily seen. Strata were measured on the southeast side of the canyon, rather than the north, because of their better access and exposure.

Acknowledgments

I would like to thank Ruth Peach for her assistance in gathering the data during 1987 and the Polar Continental Shelf Project for their helicopter support. Larry Lane provided base-camp facilities at Shingle Point. Brian Ricketts offered useful comments that led to improvements in the text.

STRATIGRAPHY

The Cuesta Creek Member contains the lowest strata of the Maastrichtian Tent Island Formation (Young, 1975; Sweet, 1978). It erosionally overlies shale of the Boundary Creek Formation and is gradationally succeeded by the mudstone member of the Tent Island Formation. Tent Island strata are succeeded by the sandstone-dominant Moose Channel Formation. At the type area, near the junction of Boundary Creek with Fish River (locality 87-5, Fig. 2), Young (1975) recognized a local stratigraphy in the Cuesta Creek Member, consisting of four units, which are, in ascending order: 1. a basal sandstone and shale unit, 2. a lower sandstone and conglomerate unit, 3. a mudstone unit, and 4. an upper sandstone and conglomerate unit.

In Figure 1, Holmes and Oliver's (1973) unit 1 plus their unit C are shown as the Cuesta Creek Member. Unit C was considered to be separated from overlying strata by a probable unconformity. Unit C is equivalent to Young's (op. cit.) basal sandstone and shale unit of the Cuesta Creek Member. Holmes and Oliver's (op. cit.) unit 2 is the mudstone member of the Tent Island Formation.

Cuesta Creek strata are gradationally overlain by a 60 to 100 m thick interval of interbedded shale and sandstone, which is in turn overlain relatively abruptly by a thick mudstone-dominant succession. Both sequences are assigned to the mudstone member.

<table>
<tr><th>YOUNG 1972, 1973</th><th colspan="2">HOLMES & OLIVER 1973</th><th colspan="2">YOUNG 1975</th></tr>
<tr><td rowspan="2">Moose Channel Fm</td><td>4</td><td rowspan="3">Moose Channel Fm</td><td colspan="2">Moose Channel Fm</td></tr>
<tr><td>3</td><td rowspan="3">mudstone mbr</td><td rowspan="3">Tent Island Fm</td></tr>
<tr><td>'Upper Cretaceous shale'</td><td>2</td></tr>
<tr><td>'conglomerate and sandstone division'</td><td>1</td><td rowspan="2">Cuesta Creek Mbr</td></tr>
<tr><td>'yellow-weathering shale division'</td><td colspan="2">'Unit C'</td><td>Boundary Creek Fm</td></tr>
</table>

Figure 1. Comparison of Upper Cretaceous stratigraphic terminology used in the northern Richardson Mountains.

FACIES ASSEMBLAGES

Sandstone-shale facies assemblage

The sandstone-shale assemblage consists of interbedded very fine to fine grained sandstone and shale in beds that generally do not exceed 1 m in thickness and are mainly 0.5 m or less. Commonly the sandstones and shales form cyclic couplets similar to Bouma sequences. The bases of the sandstone beds invariably are abrupt and erosional. Load structures are commonly present on the base of the sandstone beds. Other sole marks, such as flutes and grooves, are locally present but not very common. In some of the thicker beds, sideritized, small mud-chip clasts occur in the basal few centimetres. Typically the lower few centimetres of each cycle are massive, grading up into subhorizontal laminae, which are in turn overlain by current-ripple laminae that grade up into finely laminated shale. The shale intervals may contain thin beds (up to 10 cm) of ripple laminated siltstone and/or very fine grained sandstone. Thickness of the sandstone units varies from a few millimetres to about 1 m; however, some of the thicker units appear to be amalgamated beds.

Within this assemblage there are thick intervals of thinly interbedded shale and sandstone, in which the sandstone beds are a few millimetres to a few centimetres thick, and generally are ripple or horizontally laminated. Intervening shale beds tend to be slightly thicker (a few centimetres to several decimetres).

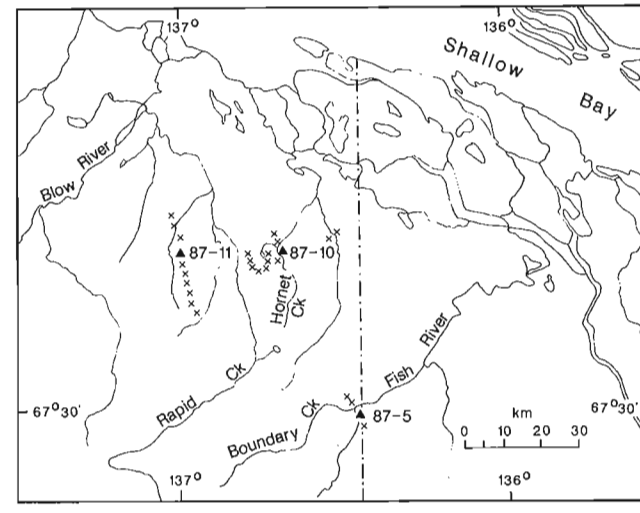

Figure 2. Location map and distribution of Cuesta Creek outcrops.

Thick intervals of the sandstone-shale facies assemblage occur at the base of the member at the type area, near the junction of Boundary Creek and Fish River (locality 87-5, Fig. 2). This assemblage is also found as thin intercalations within intervals dominated by the sandstone-conglomerate facies assemblage. The lowest 60 to 100 m of the mudstone member consists of this facies assemblage.

Sandstone-conglomerate facies assemblage

The sandstone-conglomerate facies assemblage is characterized by interbedded fine to coarse grained sandstone, granulestone and conglomerate (Fig. 3). Individual units of sandstone or conglomerate have been measured up to 6 m thick, but they consist of amalgamated beds. Individual beds are generally less than 1 m in thickness.

The sandstone units tend to appear massive, although a few beds with fine, subhorizontal laminae were noted. Basal contacts are abrupt and erosional, and locally loaded. Mud clasts are present in some beds. Laterally the beds tend to lens out due to erosion by overlying strata (Fig. 4).

Conglomerate units tend to consist of amalgamated beds, with individual beds usually 50 cm thick or less. However, in some units it is difficult to recognize individual beds because of the uniform clast size. Most clasts are small pebbles, 5 cm or less in diameter, although clasts up to 30 cm in long diameter are present. Most of the clasts are chert of various colours, although black and brown chert clasts are dominant. Vein quartz and quartzite are sub-dominant clast types. A few examples of mud clasts in conglomerates were noted and at least one bed consists entirely of mud clasts in a mud matrix (seen at Fish River, locality 87-5, Fig. 2). Most of the conglomerates are clast supported with a matrix of very fine to granular sand. Most of the small pebbles are subspherical; the larger clasts tend to be oblate to discoidal. Because of the tendency of many beds to contain a relatively uniform clast size, clast grading is not always apparent. However, examples of normal and inverse grading were noted in some thin conglomerate beds (Fig. 3). Individual beds and units of amalgamated beds are lens-shaped and rapidly pinch out laterally due to erosion by overlying beds. Where conglomerates rest on shale beds, load structures may be present (Fig. 5).

Figure 3. Sandstone-conglomerate facies asemblage. Fish River locality (87-5). Note inverse grading in the conglomerate beds. Hammer head approximately 12 cm. ISPG photograph 2846-18.

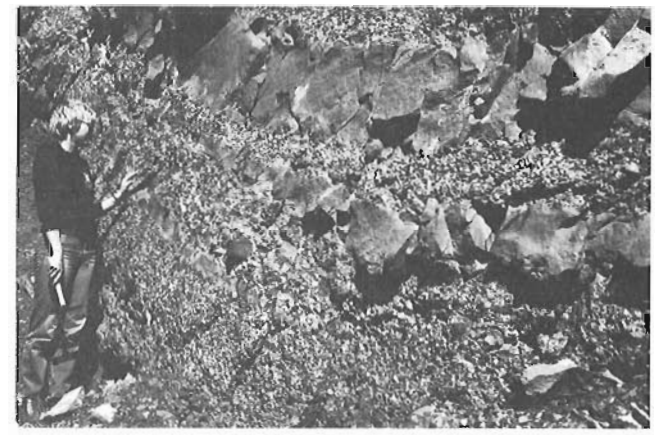

Figure 4. Lateral pinch-out and amalgamation of beds in the sandstone-conglomerate facies assemblage. Fish River locality (87-5). ISPG photograph 2846-16.

Figure 5. Load structures on the base of a conglomerate bed. Fish River locality (87-5). Hammer approximately 30 cm long. ISPG photograph 2846-19.

Strata of the sandstone-conglomerate assemblage are present at Fish River, Rapid Creek, and at Hornet Creek, where they are a prominent component of the succession.

Sandstone facies assemblage

The sandstone facies assemblage consists of thick intervals of sandstone beds with only minor amounts of interbedded conglomerate or shale. This asssemblage was noted only at Rapid Creek (location 87-11, Fig. 2) where an estimated 30 m or more of fine grained sandstone occur at the top of the exposed succession. Sand grade size ranges up to coarse, although fine is the dominant grade. Scattered throughout the talus are small pebbles, suggesting the presence of either thin conglomerate beds or pebbly sandstones. The sandstones weather into platy to flaggy talus, and no sedimentary structures were seen by the author in the poor quality exposures.

Other sedimentary attributes

The contact with the underlying Boundary Creek strata is not exposed in the type area but was noted at Hornet Creek (locality 87-10). Young (1975, fig. 5) illustrated an erosional contact on Rapid Creek. At the Hornet Creek locality the contact is erosional, but unlike the contact at Rapid Creek it is a shale-on-shale contact with a channel-like scour between the shales.

At Fish River the lowest strata of the Cuesta Creek Member consist of the sandstone-shale facies assemblage, which exhibits very distinct, large-scale, internal geometrical relationships seen only from a distance. Bundles of strata form wedge-shaped packages, and succeeding bundles crosscut the lower sets at low angles (Fig. 6). These features have the appearance of low-angle foresets.

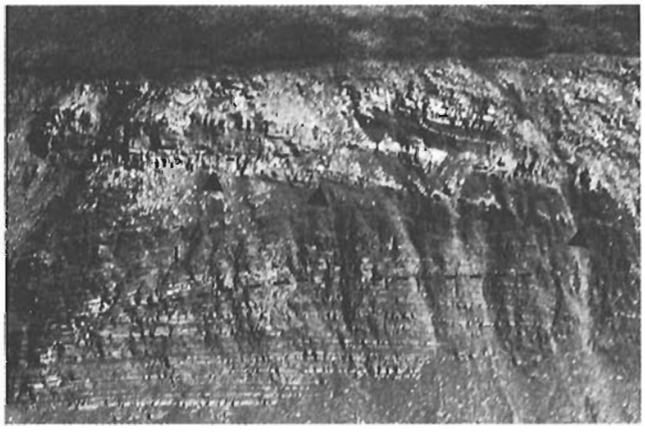

Figure 6. Cross-cutting relationships in strata of the sandstone-mudstone and sandstone-conglomerate facies assemblages. Channel-scour within the sandstone-mudstone assemblage indicated by a dashed line. The base of the sandstone-conglomerate facies assemblage (arrows) also is a channel scour. Fish River locality (87-5). ISPG photograph 2846-23.

Figure 7. Character of the channel margin (arrows) at the base of the sandstone-conglomerate facies assemblage at Fish River (locality 87-5). ISPG photograph 2846-20.

The foreset-like beds are erosionally overlain by beds of the sandstone-conglomerate assemblage (Fig. 6) that fill a broad, channel-like feature. The southern margin of this channel is exposed along the cliff face (Fig. 7), where up to 8 m of relief is visible on the channel margin (however, the channel margin is not completely exposed and elsewhere there are 10 to 15 m of channel-filling sediment). Strata of the sandstone-conglomerate facies assemblage onlap the channel margins (Fig. 7). Within the channel-fill there is much local scouring, and small-scale channels are common.

Examples of small slump folds in incompetent shaly strata within the Cuesta Creek Member and the immediately overlying mudstone member are common at the Fish River locality. One notable example from strata immediately above the Cuesta Creek Member has involved a thrust fault (Fig. 8). This example also has been illustrated by Holmes and Oliver (1973, plate 2, fig. B), who identified it as an angular discordance, and by Young (1975, fig. 11), who correctly identified it as a fault.

Also important to the reinterpretation of the depositional setting is the presence of pebbly mudstone beds within the lowermost strata of the mudstone member (Young, 1975, p. 19), attributable to debris flow deposition. Also, the same interval contains beds of the sandstone-shale facies assemblage, which exhibit Bouma-like cyclothems.

DEPOSITIONAL SETTING

In an earlier publication I suggested (Dixon, 1986) that the Cuesta Creek succession was a product of sediment gravity-flow deposition, but did not fully document the criteria for this conclusion. The attributes of the three facies assemblages described here point to deposition as sediment gravity-flow deposits, rather than as sediments of traction currents in a fluvial system. Bouma-like cycles are typical deposits of turbidity currents; the conglomerates display many features of resedimented conglomerates (Walker, 1975, 1977), and mud-matrix-supported conglomerates are products of debris flow.

Figure 8. Syndepositional thrust faults (arrows) in Cuesta Creek and lowermost strata of the mudstone member, Tent Island Formation. Fish River locality (87-5). ISPG photograph 2846-15.

The Bouma-like turbidites of the sandstone facies assemblage in the lower Cuesta Creek at Fish River could represent levee deposits or prograding lobe deposits on a submarine fan complex. Young (1975, p. 19) attributed them to delta-front sedimentation. The overlying sandstone-conglomerate facies assemblage obviously comprises channel-fill sediments. The complex fill of this channel is comparable to many sequences described from other submarine fan deposits (e.g. Arnott and Hein, 1986), whereas it is unlike many fluvial deposits (see Miall, 1978, for an extensive review of fluvial deposits). The lack of sedimentary structures more typical of fluvial deposits — planar and trough crossbedding — also favours a sediment gravity-flow origin.

The underlying Boundary Creek Formation consists of organic-rich marine shales deposited on an outer shelf-to-slope setting (Dixon, 1986). In order to create a subaerial unconformity as envisaged by Holmes and Oliver (1973) and Young (1975), a major uplift would be required, yet there is very little evidence for such a major tectonic event in the northern Yukon. Alternatively, the unconformity could have resulted from a major lowering of sea level, subsequent shelf-edge erosion and the formation of submarine canyons and fans. Later transgression and rise in relative, or absolute, sea level would create a setting in which the submarine fan and canyon would become less active and begin to fill with muddier deposits as the supply of sediment reaching the outer shelf and slope was curtailed. This latter scenario would better fit the known stratigraphic succession and the sedimentary characteristics of the Cuesta Creek and enclosing strata. Also, the succession of depositional environments and unconformities from the Boundary Creek Formation up to the Moose Channel Formation is comparable to the depositional models such as those described in the sequence concept of Vail and co-workers (*in* Payton, 1977).

REFERENCES

Arnott, R.W. and Hein, F.J.
1986: Submarine canyon fills of the Hector Formation, Lake Louise, Alberta: Late Precambrian syn-rift deposits of the proto-Pacific miogeocline; Bulletin of Canadian Petroleum Geology, v. 34, p. 395-407.

Dixon, J.
1986: Cretaceous to Pleistocene stratigraphy and paleogeography, northern Yukon and northwestern District of Mackenzie; Bulletin of Canadian Petroleum Geology, v. 34, p. 49-70.

Holmes, D.W. and Oliver, T.A.
1973: Source and depositional environments of the Moose Channel Formation, Northwest Territories; Bulletin of Canadian Petroleum Geology, v. 21, p. 435-478.

Miall, A.D. (ed.)
1978: Fluvial Sedimentology; Canadian Society of Petroleum Geologists, Memoir 5, 859 p.

Payton, C.E. (ed.)
1977: Seismic stratigraphy — Applications to hydrocarbon exploration; American Association of Petroleum Geologists, Memoir 26, 516 p.

Sweet, A.R.
1978: Palynology of the lower part, type section, Tent Island Formation, Yukon Territory; *in* Current Research, Part B, Geological Survey of Canada, Paper 78-1B, p. 31-37.

Walker, R.G.
1975: Generalized facies models for resedimented conglomerates of turbidite association; Geological Society of America, Bulletin, v. 86, p. 737-748.
1977: Deposition of upper Mesozoic resedimented conglomerates and associated turbidites in southwestern Oregon; Geological Society of America, Bulletin, v. 88, p. 273-285.

Young, F.G.
1972: Cretaceous stratigraphy between Blow and Fish rivers, Yukon Territory; *in* Report of Activities, Part A, Geological Survey of Canada, Paper 72-1A, p. 229-235.
1973: Mesozoic epicontinental, flyschoid and molassoid depositional phases of Yukon's North Slope; *in* Canadian Arctic Geology, J.D. Aitken and D.J. Glass (eds.); Geological Association of Canada — Canadian Society of Petroleum Geologists, p. 181-202.
1975: Upper Cretaceous stratigraphy, Yukon Coastal Plain and northwestern Mackenzie Delta; Geological Survey of Canada, Bulletin 249, 83 p.

Compositional characteristics of anthracitic coals in the Hoidahl Dome area, northern Yukon Territory[1]

A.R. Cameron, C. Boonstra, and K.C. Pratt
Institute of Sedimentary and Petroleum Geology, Calgary

Cameron, A.R., Boonstra, C., and Pratt, K.C., Compositional characteristics of anthracitic coals in the Hoidahl Dome area, northern Yukon Territory; in Current Research, Part D, Geological Survey of Canada, Paper 88-1D, p. 67-74, 1988.

Abstract

In the Hoidahl Dome area of the northern Yukon Territory the observed occurrence of coal in the Mississippian Kayak Formation has been extended along strike for a distance of approximately 4 km from the original exposure discovered in 1985. Structural complications make lateral tracing of beds difficult but it would appear that there are more seams than the 5 m thick bed originally described. Petrographic and chemical analyses of the samples collected in 1987 indicate that the coal has the same high quality as that sampled in 1985 with sulphur contents average 0.5 to 0.6 percent on most samples, and ash contents average 7.0 percent. One series of samples which may be from a different seam than the 5 m thick bed gave higher ash and sulphur values. Reflectance data indicate that the coals sampled in the most easterly exposure visited in 1987 have higher reflectance values than those collected in 1985 with reflectances averaging about 3.20% $R_o$max on some of the recent samples compared with 2.89 to 2.95 % $R_o$max for the 5 m thick bed. These reflectances indicate ranks close to the semianthracite/anthracite boundary.

Résumé

Dans la région du dôme de Hoidahl, dans la partie nord du Yukon, de nouvelles observations ont indiqué des venues de charbon dans la formation mississipienne de Kayak, le long de la direction de ce gisement, sur une distance d'environ 4 km à partir de l'affleurement initial découvert en 1985. En raison du caractère complexe de la structure, il est difficile de retracer latéralement les couches, mais il semblerait qu'il existe davantage de filons que la couche de 5 m d'épaisseur initialement décrite. Les analyses pétrographiques et chimiques des échantillons recueillis en 1987 indiquent que le charbon est d'aussi bonne qualité que celui échantillonné en 1985; la teneur en soufre est en moyenne de 0,5 à 0,6 pour cent dans la majorité des échantillons, et leur teneur en cendres est en moyenne de 7,0 pour cent. Une série d'échantillons qui pourraient provenir d'un filon autre que la couche de 5 m d'épaisseur sont caractérisés par de plus fortes teneurs en cendres et en soufre. Les résultats des mesures de réflectance indiquent que les charbons échantillonnés dans l'affleurement le plus à l'est, visité en 1987, présentent de plus fortes valeurs de la réflectance que ceux recueillis en 1985. Les réflectances se situent en moyenne aux alentours de 3,20 pour cent $R_o$max dans certains des récents échantillons, comparativement à 2,89-2,95 pour cent $R_o$max pour la couche de 5 m d'épaisseur. Ces réflectances indiquent un rang proche de la limite entre le semi-anthracite et l'anthracite.

[1] Contribution to the Frontier Geoscience Project.

INTRODUCTION

A single outcrop of a 5 m thick seam of semianthracite coal was described and sampled in the Hoidahl Dome area in 1985 (Cameron et al., 1986). The coal occurs in the Kayak Formation of Mississippian age and has low ash and sulphur contents. Fieldwork in 1987 revealed that additional outcrops of coal occur at several localities in the area over a distance of about 4 km. The outcrops are found in stream gullies near the northern edge of a wedge-shaped exposure of Kayak on the south flank of a structural high identified as Hoidahl Dome (Fig. 1). The area is near the headwaters of the Blow River, and can be located on NTS Map 117 A, approximately 80 km south of Shingle Point on the Arctic coast and 118 km west of Aklavik, NWT. The geology of the area has been mapped by Norris (1981).

In the most recent fieldwork, coals exposed in outcrop were measured, and sampled in detail for chemical and petrographic analyses. All the coal exposures found to date and sampled are on the northern edge of the Kayak Formation fringing the Hoidahl Dome. No additional outcrops were found in the more southerly part of the area underlain by Kayak (see Figure 1) despite helicopter fly-bys and some ground traversing. In general the coal beds observed dip to the south and may exist in the subsurface in the southern part of the study area. Some cursory examination of the narrow belt of Kayak, shown on Figure 1 as girdling Hoidahl Dome to the east and northeast, failed to reveal additional outcrops.

SAMPLING AND ANALYTICAL PROCEDURES

The coals in outcrop were sampled by a series of minichannels which, when aggregated, represent the total thickness of the exposed coal. Where possible, natural lithological breaks within the seam; that is, rock partings, were used to mark the boundaries of samples; otherwise, and in most cases, the seams were sampled at 0.5 m intervals. Table 1 summarizes identification and location data for each series of samples, and Figure 2 shows schematic seam sections with sample positions identified in their correct stratigraphic position. A total of 41 samples were collected in 1987, including rock partings and roof and floor specimens. All the coals appeared to be little affected by weathering, an observation later confirmed by microscopy. At two of the sampling stations (3 and 3A) the coals were moderately to highly sheared, indicating localized structural deformation.

In the laboratory, the samples were crushed to minus 20 mesh (840) and small portions split out for pelletizing and polishing in preparation for microscopic analyses. Another portion was submitted for proximate analysis and determination of sulphur content according to ASTM procedures (ASTM, 1979). For the chemical analysis some of the coal samples were combined, but for the petrographic determinations each of the coal samples was analyzed separately. A check of each sample including roof and floor specimens and partings with a scintillometer revealed no abnormal radioactivity.

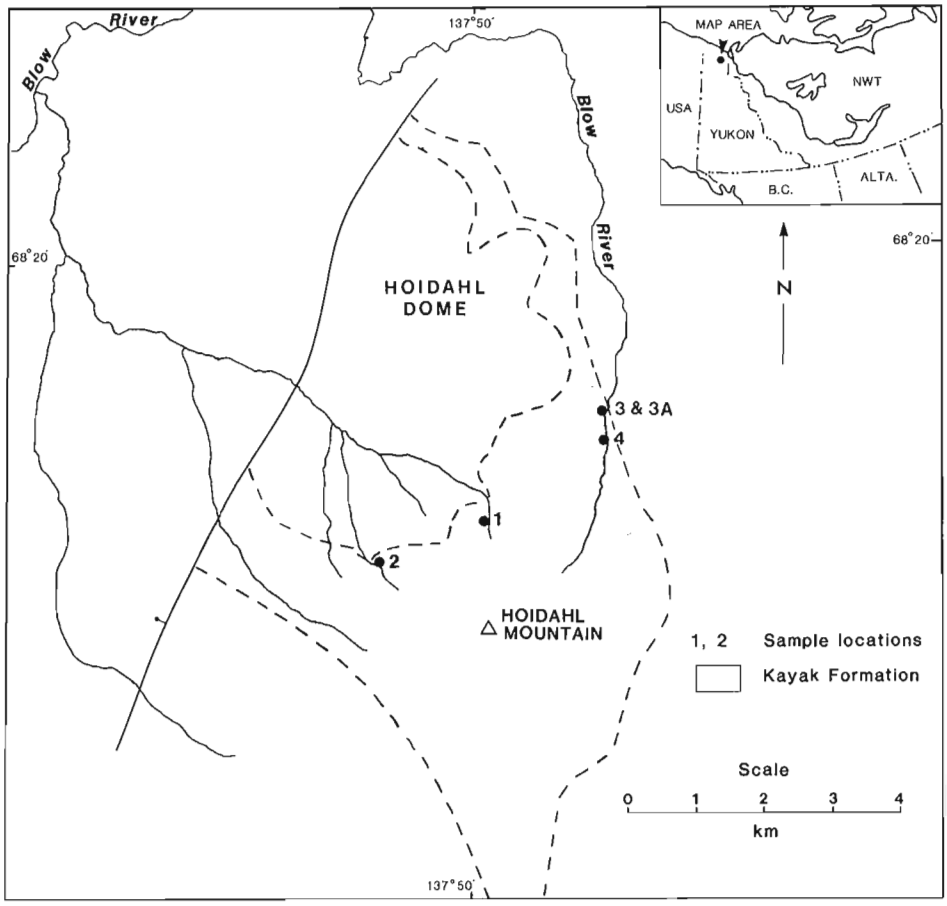

Figure 1. Location map of sampling stations in study area.

Petrographic analyses consisted of determination of maceral content (500 point counts per sample) and reflectance measurements (50 points maximum and 50 points minimum per sample). Maximum and minimum reflectances were both determined so as to obtain the bireflectance, which is an index of the anisotropy of the coal. Bireflectance is maximum reflectance ($\%R_o max$) minus minimum reflectance ($\%R_o min$). Coals matured under normal geological conditions will have a certain range of bireflectance depending on their rank. Abnormal coalification, such as that caused by igneous intrusion, will express itself in abnormally high bireflectances.

Both reflectance and maceral analyses were carried out on a Leitz Orthoplan microscope equipped with MPV II photometric accessories. Reflectance measurements were made on vitrinite A, and all analyses were made at a magnification of X650, using partly polarized light.

RESULTS

Chemical analyses

Chemical compositional data from proximate analysis are presented in Table 2 for the samples collected in 1987. Along with these are tabulated proximate analysis data determined on the HD series of samples collected in 1985. In the analyses of the 1987 material, a number of field samples were combined, as for example in series CQ 660, where samples 3 through 9 were combined and analyzed as a single sample. As with the HD series, the newer samples, in most cases, showed very low ash and sulphur contents. An exception was sample series CQ 663, for which average ash and sulphur values were 13.6 and 1.24 percent, respectively, considerably higher than most of the other Hoidahl Dome coals studied to date. The significance of this difference will be discussed later. Sample series CQ 660 from Station 2 (see Figure 2) is probably from the same seam as the HD samples. In both cases the sulphur contents are low and the ash contents in many of the intervals are extraordinarily low. In the HD series, the average ash content over the 5.6 m thickness of the seam (exclusive of a 14 cm thick parting) is 7.2 percent whereas the CQ 660 samples, which together total 6.0 m of coal, average 6.0 percent ash for the seam. Certain intervals within each exposure are even lower, for example, intervals 7 through 11 in the HD samples, and intervals 2 through 9 in CQ 660. In the HD series, intervals 7 through 11 represent 2.5 m of coal with an average ash content of about 4.0 percent, and intervals 2 through 9 represent 4.0 m of coal with an ash content of 4.7 percent. Such low ash contents on a raw coal basis are rarely encountered. In both series, somewhat higher ash contents were found in samples adjacent to partings or to the roof and floor; for example, samples 2, 5, 12 and 13 in the HD series and sample 10 in the CQ 660 series. The coals represented by CQ 662 and CQ 664 are also low in both ash and sulphur. Fixed carbon contents on the dry mineral- matter free basis indicate semianthracite rank for most of these coals, and many are close to the semianthracite/anthracite boundary. Rank data based on reflectance will be discussed later.

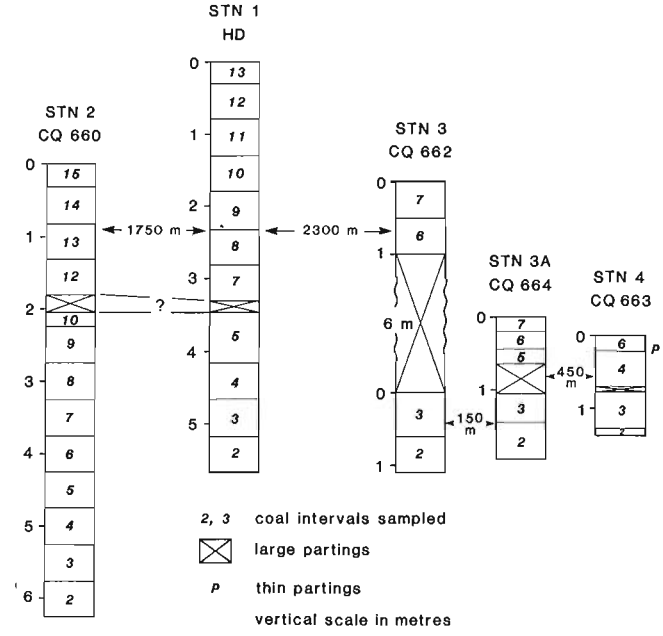

Figure 2. Schematic seam sections of coals sampled in Hoidahl Dome area showing intervals sampled and sample numbers.

Table 1. Location data for Hoidahl Dome samples.

Station	Map area	NTS	Easting/Northing all in zone 8W	GSC locality C-number	Field number
1	Blow River	117A	383300/7578850	C-099883	HD
2	Blow River	117A	381700/7578250	C-098801	CQ660
3	Blow River	117A	385150/7580350	C-098803	CQ662
3A	Blow River	117A	385100/7580350	C-098805	CQ664
4	Blow River	117A	385150/7579900	C-098804	CQ663

MACERAL COMPOSITION

Maceral distribution data are reported in Tables 3 and 4. Because of the high rank of these coals, the liptinite group cannot be identified, so that petrographic variation is expressed in different proportions of the vitrinite and inertinite macerals. Maceral distribution in the HD series of samples is included in Table 3 for comparison with CQ 660 samples because both sets are believed to be from the same seam. Nearly all of the samples show relatively high inertinite and low vitrinite, most averaged values show vitrinite contents ranging from 58 to 67 percent. Individual samples within series show some variation when compared to one another. For example, vitrinite contents within the HD series range from 50 to 70 percent and within CQ 660 from 46 to 67 percent. However, overall, the seam or seams display high inertinite and relatively low vitrinite contents, with little vertical change within the seam.

Table 2. Chemical data on coals of Hoidahl Dome area (data in weight percent).

Sample	Moisture AR*	Ash AR	Sulphur AR	Volatile matter AR	Volatile matter DMMF*	Fixed carbon AR	Fixed carbon DMMF	Sampled interval thickness (m)
13	2.1	10.9	0.50	12.8	13.7	74.2	86.3	0.33
12	1.7	11.6	0.46	10.8	11.3	75.9	86.7	0.50
11	1.6	6.5	0.52	11.2	11.5	80.7	88.5	0.50
10	1.5	2.6	0.53	11.7	11.8	84.2	88.2	0.50
9	1.5	2.4	0.57	11.7	11.8	84.4	88.2	0.50
HD 8	1.6	3.8	0.55	11.1	11.3	83.5	88.8	0.50
7	1.6	5.0	0.52	11.7	12.0	81.7	88.0	0.50
6**	0.7	63.6	0.21	5.7		30.0		
5	1.6	7.8	0.48	11.8	12.3	78.8	87.8	0.70
4	1.6	5.4	0.54	10.7	11.0	82.3	89.1	0.50
3	1.5	4.3	0.58	11.0	11.2	83.2	88.8	0.50
2	1.5	21.5	0.47	11.2	12.3	65.8	87.7	0.50
Av.	1.6	7.2	0.52	11.3	11.9	79.9	88.1	
15	3.5	6.6	0.69	8.8	9.0	81.1	91.0	0.30
13-14	2.3	11.5	0.56	8.5	8.7	77.7	91.3	1.00
CQ 12	2.8	5.4	0.65	8.7	8.8	83.1	91.2	0.50
660 10	2.5	12.9	0.53	9.2	9.6	75.4	90.4	0.20
3-9	2.7	4.8	0.58	8.8	8.9	83.7	91.1	3.50
2	2.5	3.7	0.74	12.2	9.8	81.6	90.2	0.50
Av.	2.7	6.2	0.60	9.1	9.3	82.0	90.7	
6-7	4.1	4.2	0.55	8.6	8.8	83.1	91.2	1.00
CQ 2-3	3.8	6.6	0.58	8.1	8.3	81.5	91.7	1.10
662 Av.	3.9	5.5	0.57	8.3	8.5	82.3	91.5	
6	2.7	13.2	1.17	9.5	9.7	74.6	90.3	0.20
CQ 4	3.1	11.0	1.30	9.3	9.4	76.6	90.6	0.50
663 3	2.5	13.7	1.23	9.3	9.4	74.5	90.6	0.50
2	2.2	26.2	1.09	8.5	8.5	63.1	91.5	0.10
Av.	2.7	13.6	1.24	9.3	9.4	74.4	90.6	
CQ 5-7	3.2	4.5	0.64	7.9	8.0	84.4	92.0	0.65
664 2-3	3.6	6.2	0.56	8.0	8.1	82.2	91.9	0.90
Av.	3.4	5.5	0.59	8.1	8.2	83.0	91.8	

*AR - As received basis; DMMF - Dry, mineral-matter free
**Sample 6 not included in calculating average for HD series

Table 3. Maceral composition (MMF) of sample series HD and CQ 660; data in volume percent.

Sample	Vitrinite A	Vitrinite B	Total vitrinite	Semi-fusinite	Fusinite	Macrinite	Inerto-detrinite	Micrinite	Sclerotinite	Total inertinite
HD 13	22.0	38.0	60.0	13.2	3.0	11.4	10.6	1.4	0.4	40.0
HD 12	12.4	56.4	68.8	6.1	1.2	10.4	9.8	3.7	0.0	31.2
HD 11	25.4	45.2	70.6	7.4	0.8	12.4	6.2	2.6	0.0	29.4
HD 10	13.6	36.4	50.0	7.6	0.8	21.4	15.6	4.6	0.0	50.0
HD 9	16.0	39.8	55.8	8.2	1.2	23.4	9.4	1.8	0.2	44.2
HD 8	10.5	43.4	53.9	11.5	0.0	23.3	9.4	1.5	0.4	46.1
HD 7	11.2	43.8	55.0	10.0	0.4	18.9	12.5	3.0	0.2	45.0
HD 6					NOT ANALYZED					
HD 5	18.0	51.9	69.9	6.6	1.2	12.1	6.8	3.4	0.0	30.1
HD 4	10.7	41.2	51.9	9.5	0.6	17.9	13.3	6.2	0.6	48.1
HD 3	26.2	39.1	65.3	8.7	1.8	12.5	8.3	2.8	0.6	34.7
HD 2	23.4	41.2	64.6	12.4	4.4	9.4	8.2	1.0	0.0	35.4
Av.	17.0	43.6	60.6	8.9	1.9	15.7	9.8	2.9	0.2	39.4
CQ 660 15	16.6	49.0	65.6	15.2	2.4	10.4	6.0	0.4	0.0	34.4
CQ 660 14	8.8	50.2	59.0	9.2	2.0	19.0	9.2	1.0	0.4	41.0
CQ 660 13	8.4	52.6	61.0	7.0	1.6	17.4	9.4	2.6	0.0	39.0
CQ 660 12	20.8	46.1	66.9	11.6	1.5	12.7	6.4	0.9	0.0	33.1
CQ 660 11					NOT ANALYZED					
CQ 660 10	7.8	58.6	66.4	11.4	3.4	10.2	6.8	1.8	0.0	33.6
CQ 660 9	13.6	47.4	61.0	8.4	1.0	18.4	8.8	2.0	0.0	38.6
CQ 660 8	4.6	51.7	56.3	6.1	1.2	28.1	6.1	2.0	0.2	43.7
CQ 660 7	8.4	38.0	46.4	7.8	2.2	32.2	8.6	2.6	0.2	53.6
CQ 660 6	9.4	42.4	51.8	13.4	7.2	20.6	5.8	0.8	0.4	48.2
CQ 660 5	7.6	45.2	52.8	5.0	2.0	30.0	8.4	1.4	0.0	47.2
CQ 660 4	13.9	47.2	61.1	4.9	2.7	22.1	6.1	2.5	0.6	38.9
CQ 660 3	6.0	42.0	48.0	8.2	1.2	35.2	4.4	2.2	0.0	52.0
CQ 660 2	19.4	39.8	59.2	11.8	0.8	16.2	11.0	0.4	0.6	40.8
Av.	11.2	46.5	57.7	8.9	2.2	21.8	7.6	1.6	0.2	42.3

Table 4. Maceral composition (MMF) of sample series CQ 662, 663, and 664; data in volume per cent.

Sample	Vitrinite A	Vitrinite B	Total vitrinite	Semi - fusinite	Fusinite	Macrinite	Inerto - detrinite	Micrinite	Sclerotinite	Total inertinite
CQ 662 7	17.8	42.4	60.2	9.4	2.7	22.0	4.9	0.8	0.0	39.8
CQ 662 6	22.0	39.8	61.8	8.8	0.8	21.1	6.5	0.6	0.4	38.2
CQ 662 4, 5					NOT ANALYZED					
CQ 662 3	7.4	46.6	54.0	6.2	0.8	27.8	7.6	3.6	0.0	46.0
CQ 662 2	7.8	55.4	63.2	4.8	2.2	20.4	8.2	0.8	0.4	36.8
Av.	13.4	46.0	59.4	7.3	1.6	23.1	6.8	1.6	0.2	40.6
CQ 663 6	15.0	46.8	61.8	13.4	5.4	13.6	5.2	0.6	0.0	38.2
CQ 663 5					NOT ANALYZED					
CQ 663 4	24.2	48.2	72.4	8.4	1.2	13.0	4.4	0.4	0.2	27.6
CQ 663 3	17.6	48.8	66.4	15.0	2.0	12.2	3.2	1.2	0.0	33.6
CQ 663 2	16.2	36.2	52.4	21.8	4.6	13.8	5.8	1.6	0.0	47.6
Av.	19.6	47.3	66.9	12.7	2.4	12.9	4.2	0.8	0.1	33.1
CQ 664 7	9.4	60.8	70.2	4.4	1.0	19.4	3.6	1.4	0.0	29.8
CQ 664 6	20.5	47.6	68.1	7.4	1.2	6.7	6.2	0.4	0.0	31.9
CQ 664 5	33.6	36.0	69.6	9.0	2.6	12.2	5.6	0.8	0.2	30.4
CQ 664 4					NOT ANALYZED					
CQ 664 3	7.8	51.0	58.8	10.2	0.4	20.6	8.2	1.2	0.6	41.2
CQ 664 2	17.0	48.0	65.0	4.4	0.8	20.2	7.4	2.2	0.0	35.0
Av.	16.3	48.8	65.1	7.0	1.0	18.6	6.7	1.4	0.2	34.9

The most abundant inertinite macerals are semifusinite and macrinite. Fusinite, at least the pyrofusinite variety, is relatively low in abundance. Some difficulty was encountered in distinguishing semifusinite from macrinite. By definition, semifusinite is supposed to exhibit structure believed to be derived in part from original tissue structure in the parent plant material. At the Hoidahl Dome locality, coals display all gradations between undisputed semifusinite with good cell structure and totally structureless macrinite. The problem lies in establishing the boundary, based on structure, between the two macerals. The high inertinite content of these coals suggests an environment of deposition that was conducive to some oxidation of the peat material for very long periods of time, with some variation, over the life of the swamp. A condition that would produce such an environment might be a water level in the swamp somewhat more shallow than usual. The very low ash content of these coals also suggests an environment that must have been well shielded from influx of clastic sediments. The parting(s) at the HD site and in CQ 660 probably represent splay deposits occurring at a time of flood.

REFLECTANCE ANALYSES

Reflectance data for these samples are shown in Table 5. The data for the HD series are also shown for comparison with values obtained on the 1987 material.

The data may be separated into two populations, one comprising the HD and CQ 660 suites of samples, and the other encompassing the samples collected at Stations 3, 3A and 4 in the most easterly of the creeks examined (see Figure 1). Average $R_o$max for the HD suite is 2.95 % and for CQ 660, 2.89 %. These values are very similar and to be expected if these two series, which are 1.7 km apart, represent the same seam. Within each suite there is some variation; the HD samples range from 2.86 to 3.01 %, and the spread in CQ 660 samples is from 2.84 to 2.96 %. These reflectances indicate that practically all of these samples fall into the semianthracite rank class based on the value of 3.00 % $R_o$max proposed by Davis (1978) for the semianthracite/anthracite boundary. In contrast, the material from the most eastern outcrops sampled (series CQ 662, 663 and 664) all show significantly higher $R_o$max values, with averages of 3.27, 3.21 and 3.19 % respectively. Based on the boundary proposed above, these coals are anthracites. However, based on volatile matter values determined by proximate analysis [dry mineral-matter free (DMMF) volatile matter between 8 and 14 %] nearly all the samples fall into the semianthracite class. Note that the CQ 660 through CQ 664 suites have DMMF volatile contents between 8 and 9 % indicating a rank classification, based on chemistry, just below the semianthracite/anthracite boundary.

The reflectance and volatile matter content of the CQ 660 samples vis-a-vis the other samples is somewhat anomalous. Although CQ 660 reflectance values are very similar to those of the HD series, the corresponding volatile matter contents of the CQ 660 samples are more similar to those of the samples collected at Stations 3, 3A and 4, and these have higher reflectances, as Table 5 shows. Volatile matter content for the HD samples averages about 11 %, whereas the average for CQ 660 samples is about 9 %, and their average reflectances are 2.95 and 2.89 %, respectively. At present we have no explanation for this apparent discrepancy.

Bireflectances determined on the Hoidahl Dome samples range from 0.47 to 0.93 %. These values do not appear abnormal when compared to values published elsewhere for coals of this rank (Stach et al., 1982). Therefore, it does not appear that the Hoidahl Dome coals have matured in any other way than by normal coalification.

CORRELATION OF SAMPLED BEDS

The number of seams present in the Kayak Formation in the Hoidahl Dome area is uncertain at present, but it would appear that there are at least two. The outcrops sampled at Stations 1 and 2 are most likely parts of the same seam. Similar coal thicknesses, rank and petrographic composition support this interpretation. At each locality, there is one fairly prominent parting in the seam, but its stratigraphic position within the seam is different (see Figure 2). At Station 2 (CQ 660 site) it is much nearer the top of the seam than at the HD site (Station 1). Nevertheless, on Figure 2 the partings have been tentatively correlated. Differences in coal thicknesses above and below the parting at the two sites may reflect some localized structural thickening/thinning. Also, variations in original peat thicknesses for different parts of the seam at the two localities cannot be ruled out on the basis of present information.

The stratigraphic position of the beds sampled at Stations 3 and 3A relative to the thick seam discussed above is unknown. Chemical and petrographic compositions are roughly comparable, but the structural situations at both Stations 3 and 3A make correlation difficult at this time. Faulting at both stations has clearly distorted original bed thickness.

The higher sulphur and ash contents, and the presence of several thin partings in the seam sampled at Station 4 suggest that this may be a different seam than the one containing the beds discussed above.

Figure 3 is a plot of maceral compositions for these Hoidahl Dome samples. It does not show any clear-cut differences between the seams.

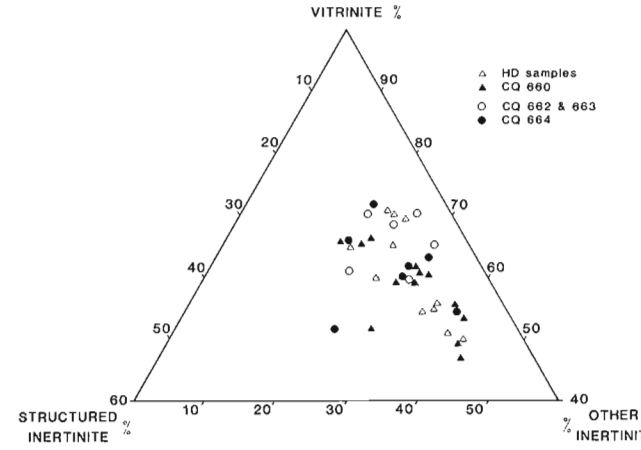

Figure 3. Maceral distribution plot for Hoidahl Dome samples; data on mineral-free basis.

Table 5. Reflectance data on coals of Hoidahl Dome.

Sample series	Sample number	Ro_{max}	Standard deviation	Ro_{min}	Standard deviation	Bireflectance Ro_{max}-Ro_{min}
HD	13	2.99	0.07	2.39	0.18	0.60
	12	3.01	0.09	2.51	0.21	0.50
	11	2.95	0.07	2.36	0.19	0.59
	10	2.95	0.10	2.45	0.20	0.50
	9	2.86	0.08	2.29	0.17	0.57
	8	3.00	0.08	2.45	0.26	0.55
	7	2.99	0.07	2.43	0.26	0.56
	5	2.99	0.10	2.42	0.26	0.57
	4	2.94	0.08	2.43	0.23	0.51
	3	2.93	0.08	2.38	0.24	0.55
	2	2.88	0.10	2.21	0.22	0.67
	Av.	2.95		2.39		0.56
CQ 660	15	2.86	0.13	2.20	0.17	0.65
	14	2.94	0.12	2.33	0.25	0.62
	13	2.93	0.14	2.36	0.20	0.57
	12	2.86	0.14	2.20	0.18	0.65
	10	2.87	0.11	2.29	0.16	0.59
	9	2.93	0.10	2.31	0.17	0.62
	8	2.96	0.10	2.33	0.19	0.62
	7	2.87	0.07	2.36	0.14	0.52
	6	2.84	0.11	2.28	0.14	0.56
	5	2.88	0.10	2.41	0.17	0.47
	4	2.89	0.10	2.30	0.22	0.59
	3	2.90	0.11	2.36	0.21	0.54
	2	2.88	0.10	2.24	0.19	0.64
	Av.	2.89		2.31		0.58
CQ 662	7	3.19	0.12	2.51	0.23	0.68
	6	3.28	0.13	2.39	0.33	0.90
	3	3.31	0.11	2.54	0.30	0.78
	2	3.28	0.12	2.44	0.30	0.84
	Av.	3.27		2.47		0.80
CQ 663	6	3.24	0.10	2.30	0.32	0.94
	4	3.24	0.09	2.32	0.26	0.93
	3	3.20	0.09	2.46	0.28	0.74
	2	3.17	0.09	2.34	0.31	0.83
	Av.	3.21		2.35		0.86
CQ 664	7	3.17	0.12	2.56	0.25	0.61
	6	3.19	0.13	2.49	0.24	0.70
	5	3.13	0.11	2.54	0.25	0.59
	3	3.21	0.14	2.45	0.29	0.79
	2	3.24	0.14	2.54	0.26	0.70
	Av.	3.19		2.52		0.67

There may be additional exposures of coal farther north along the gully on which Stations 3, 3A and 4 are located. Black beds were observed from the helicopter at a distance no greater than 1 km north of Station 3. However, because of time constraints these were not investigated by ground traversing.

SUMMARY AND CONCLUSIONS

Fieldwork in 1987 has extended the observed occurrences of coal in the Hoidahl Dome area for about 4 km beyond the single discovery made in 1985. Samples collected from these new occurrences provided chemical and petrographic data that compare favorably with results from the original suite of samples collected by Norris and Cameron (Cameron, et al., 1986). Most of the new samples confirm the presence of high rank (semianthracite/anthracite) coal with attractive quality characteristics (low ash and sulphur). The 1987 fieldwork and resulting analyses suggest that there may be one or more seams in addition to the 5 to 6 m thick seam discovered in 1985 and sampled at another location in 1987.

REFERENCES

American Society for Testing and Materials (ASTM)
1979: Part 26, Gaseous fuels; coal and coke; atmospheric analysis; American Society for Testing and Materials, Philadelphia, Pennsylvania.

Cameron, A.R., Norris, D.K. and Pratt, K.C.
1986: Rank and other compositional data on coals and carbonaceous shale of the Kayak Formation, northern Yukon Territory; *in* Current Research, Part B, Geological Survey of Canada, Paper 86-1B, p. 665-670.

Davis, A.
1978: The reflectance of coal; *in* Analytical methods for coal and coal products, v. 1; C. Kar (ed.); Academic Press, New York, p. 27-81.

Norris, D.K.
1981: Geology Blow River and Davidson Mountains, Yukon Territory, District of Mackenzie; Geological Survey of Canada, Map 1516A (1:250,000).

Stach, E., Mackowsky, M. Th., Teichmuller, M., Taylor, G.H., Chandra, D., and Teichmuller, R.
1982: Textbook of Coal Petrology; Third Edition, Gebruder Borntraeger, Berlin, Stuttgart.

The Devonian sequence on Grinnell Peninsula and in the region of Arthur Fiord, Devon Island, Arctic Archipelago

Q.H. Goodbody, T.T. Uyeno, and D.C. McGregor[1]
Institute of Sedimentary and Petroleum Geology, Calgary

Goodbody, Q.H., Uyeno, T.T., and McGregor, D.C., The Devonian sequence on Grinnell Peninsula and in the region of Arthur Fiord, Devon Island, Arctic Archipelago; in Current Research, Part D, Geological Survey of Canada, Paper 88-1D, p. 75-82, 1988.

Abstract

On eastern Grinnell Peninsula, 3400 m of Devonian strata are preserved. The lower portion of this sequence is dominated by carbonates, which range in age from the Silurian-Devonian boundary to early Eifelian, and include the Devon Island Formation (Silurian to Early Devonian), Sutherland River Formation (Early Devonian), Prince Alfred Formation (Early Devonian), unnamed formation (Early Devonian), and undivided Devonian carbonates (Early to Middle Devonian). A disconformable overstepping of progressively younger Devonian rocks over lower Paleozoic carbonates in a southwest direction across Grinnell Peninsula is apparent. Complex stratigraphy on northwest Grinnell Peninsula reflects uplift of the Cornwallis Foldbelt.

The carbonates are overlain conformably by clastics of early Eifelian to early Famennian age that are assigned to the Bird Fiord (mixed carbonate/clastic shelf to clastic paralic), Strathcona Fiord (meandering stream), Hecla Bay (meandering/braided stream), Fram (meandering stream), Hell Gate (meandering/braided stream), Nordstrand Point (meandering stream), and Parry Islands (meandering stream/coastal plain to paralic shelf) formations.

Résumé

Dans l'est de la péninsule de Grinnell, sont conservés 3400 m de strates dévoniennes. La portion inférieure de cette séquence est dominée par des carbonates, dont l'âge se situe de la limite du Silurien et du Dévonien à l'Eifélien inférieur, et comprend la formation de Devon Island (d'âge silurien à dévonien inférieur); la formation de Sutherland River (Dévonien inférieur); la formation de Prince-Alfred (Dévonien inférieur); une formation non dénommée (Dévonien inférieur); et des carbonates non subdivisés du Dévonien (Dévonien inférieur à moyen). Il apparaît que dans une direction sud-ouest, à travers la péninsule de Grinnell, des roches dévoniennes progressivement plus récentes sont transgressives sur un niveau discordant composé de carbonates du Paléozoïque inférieur. La stratigraphie complexe du nord-ouest de la péninsule de Grinnell reflète le soulèvement de la zone de plissements de Cornwallis.

Les carbonates sont recouverts en concordance par des roches clastiques d'âge eifélien inférieur à famennien inférieur, que l'on place dans les formations de Bird Fiord (plate-forme à sédimentation mixte avec carbonates et roches clastiques passant à un milieu paralique avec des roches clastiques), de Strathcona Fiord (cours d'eau à méandres), d'Hecla Bay (cours d'eau à méandres/anastomosés), de Fram (cours d'eau à méandres), de Hell Gate (cours d'eau à méandres/anastomosés), de Nordstrand Point (cours d'eau à méandres), et de Parry Islands (cours d'eau à méandres/plaine côtière à plate-forme paralique).

[1] Institute of Sedimentary and Petroleum Geology, Ottawa

INTRODUCTION

Up until now, the Devonian rocks of northwest Devon Island have been studied only on a reconnaissance basis (Thorsteinsson, McLaren, in Fortier et al., 1963; Morrow and Kerr, 1977, 1986; Embry and Klovan, 1976, Table 1). In the course of the present study the entire preserved Devonian sequence, with a maximum thickness of 3400 m, was examined and sampled. Four sections were measured, and spot samples were taken at two other localities. The results of this work will enable detailed lithostratigraphic and biostratigraphic correlation with Devonian strata in other areas, and give insights into local uplift within the Cornwallis Foldbelt. Preliminary results are presented in this paper.

This work has two aspects, reflecting the dual nature of Devonian stratigraphy in this area. One aspect involves the lower portion of the Devonian sequence (Early to Middle Devonian age) which is dominated by carbonates. Movements of the Boothia Uplift resulted in localized clastic influx and complex local changes in stratigraphy. Detailed lithostratigraphic and biostratigraphic work is being done to elucidate the stratigraphy, and to enable correlation with adjoining areas. This work is part of a larger project, being conducted by Goodbody and Uyeno, to study the stratigraphy and sedimentology of Lower to Middle Devonian carbonates across the Arctic Islands (Goodbody, 1985, 1987, in press a, b, c).

The other aspect of the work involves the mainly nonmarine Middle to Upper Devonian rocks that form a local part of the regional clastic wedge. Prior to this study, the general stratigraphy of these rocks was described for the area (McLaren, in Fortier et al., 1963; Embry and Klovan, 1976, see Table 1), but no measured sections and few biostratigraphic age determinations were available. This aspect of the work forms part of a regional study of the sedimentology, lithostratigraphy, and biostratigraphy of the clastic wedge, being conducted by Goodbody and McGregor (Goodbody, 1985, 1987, in press a, b; Richardson and McGregor, 1986; McGregor, in press).

This preliminary report is based on fieldwork by Goodbody in 1986 and by Goodbody and McGregor in 1987, done in conjunction with a regional mapping project led by U. Mayr. Goodbody is responsible for the sedimentology and lithostratigraphy, Uyeno for the conodont studies, and McGregor for the study of the spores.

PRELIMINARY RESULTS

Devonian carbonate sequence

Three complete sections (2, 3 and 5) were measured and an additional section (1) was traversed and sampled (Figs. 1, 2).

Devon Island Formation

The upper portion of the Devon Island Formation was traversed and spot sampled in section 5. Interbedded, bioclastic, rubbly bedded limestones and poorly exposed shales of latest Silurian (Pridolian) to Early Devonian (Lochkovian) age grade up into the overlying Sutherland River Formation.

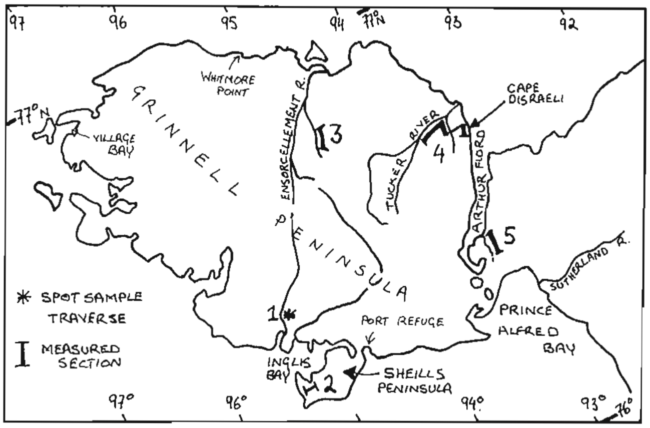

Figure 1. Section and spot sample locations.

Sutherland River Formation

The formation is 32 m thick in section 5. The basal contact with the Devon Island Formation is gradational and apparently conformable. The upper contact with the Prince Alfred Formation is drawn at the top of a distinct ridge of thin bedded, massive textured, white to light grey, locally vuggy and thinly laminated dolostones typical of the Sutherland River Formation at this location. No age determinations for the Sutherland River have as yet been obtained from this section.

Table 1. Comparison of stratigraphic nomenclature between this and previous studies. Corresponding lithostratigraphic units level between columns. Variation in vertical time axes between columns represent changes in biostratigraphic age determination.

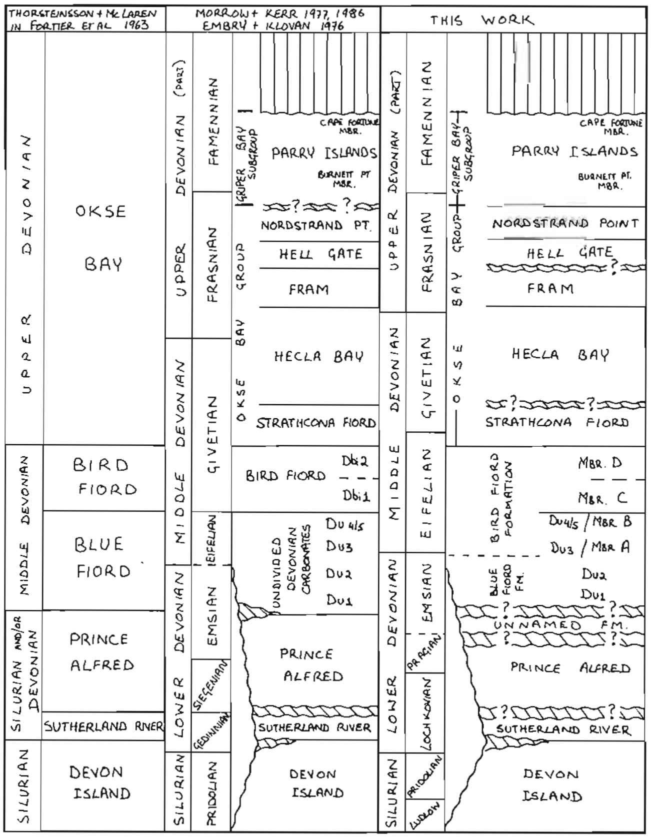

Prince Alfred Formation

The formation is 146 m thick in section 5. Exposure is poor. The lowermost 31.5 m consist of thin to medium bedded, light grey to pinkish, dolomitic siltstones that locally are intraclastic, mudcracked, and contain grey-green argillaceous stringers. These beds are assigned to the Prince Alfred Formation rather than to the Sutherland River Formation because of their silt content. There is no exposed evidence in this section of an unconformity between the Sutherland River and Prince Alfred formations as suggested by Prosh et al. (1988). The upper 115 m of the Prince Alfred Formation consist of crossbedded, noncalcareous, light grey, fine to medium grained sandstone.

Near the base of measured section 3, 15 m of poorly exposed, silty, dolomitic breccia are tentatively assigned to the Prince Alfred Formation due to similarity of the overlying rocks in sections 3 and 5. In section 3, the breccias lie unconformably on Ordovician siliceous limestones of the Eleanor River Formation.

Unnamed formation

Prosh et al. (this volume) describe an unnamed formation of laminated silty dolostone and gypsiferous siltstone with minor amounts of dolomite, intraclastic conglomerate and sparsely bioclastic to barren limestone that overlies the Goose Fiord Formation in the Norfolk Inlet-Cardigan Strait area. This unit overlies the Prince Alfred Formation 25 km east of Arthur Fiord (Prosh et al., 1988).

In section 5, a recessive covered interval 20 m thick overlies sandstones of the Prince Alfred Formation and underlies prominent bioclastic limestones of unit 1 of the undivided Devonian carbonates (see below). This covered interval is believed to represent the unnamed formation. Thorsteinsson (in Fortier et al., 1963, p. 230) noted the presence of a covered interval between the Prince Alfred and Blue Fiord formations, and commented on the apparent abruptness of the contact between these formations. Prosh et al. (1988) present evidence of a regional disconformity at the Prince Alfred

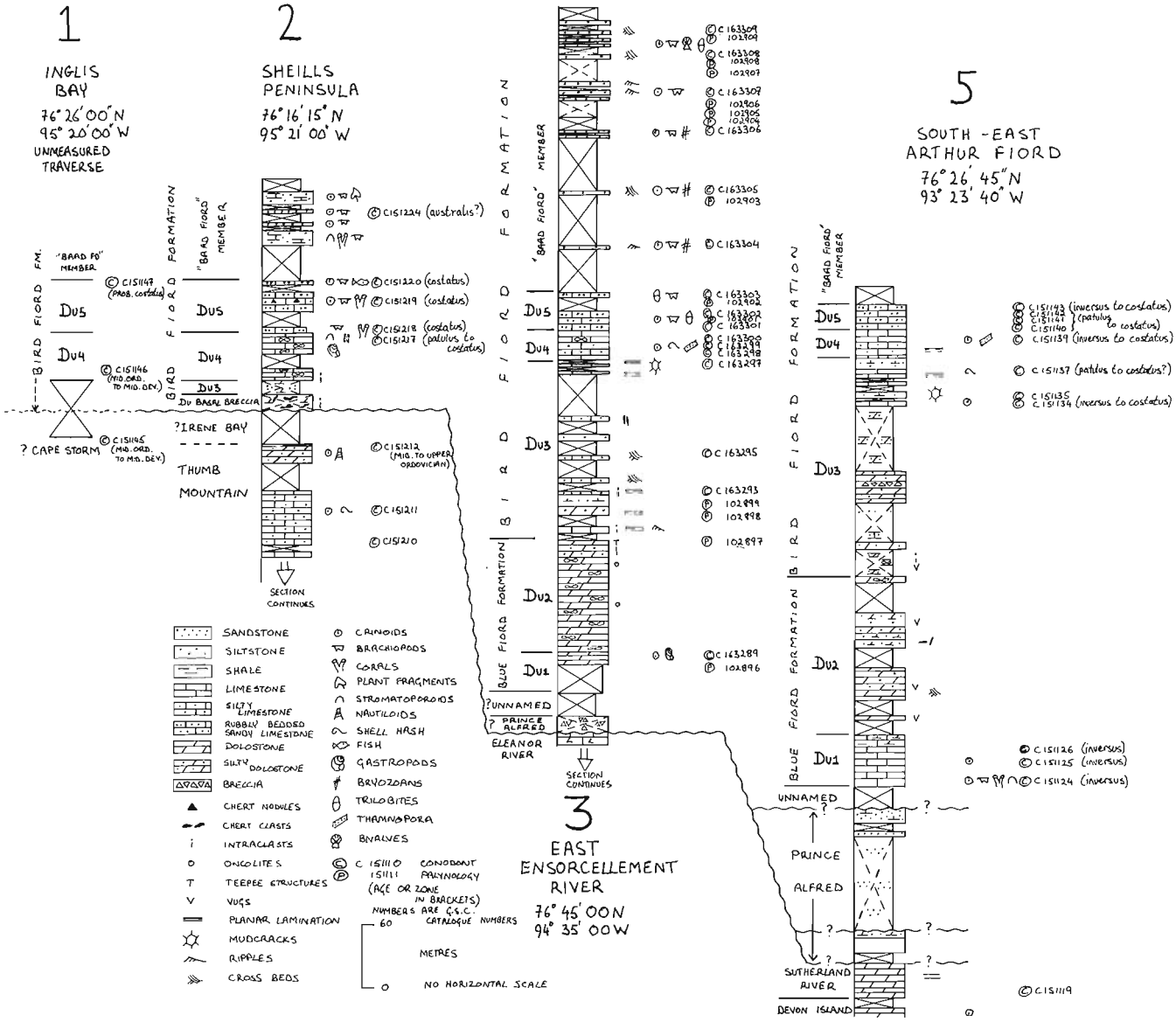

Figure 2. Carbonate stratigraphy, section 1 and measured sections 2, 3, 5.

Formation — unnamed formation contact, and discuss the possibility of a disconformity between the Blue Fiord and unnamed formations.

In section 3 a distinct recessive bench representing 22.5 m of section overlies the basal breccia unit. This interval, assigned tentatively to the unnamed formation because of its stratigraphic position, is overlain by a more prominent, scree-covered interval that is assigned to unit 1 of the undivided Devonian carbonates for reasons discussed below.

Undivided Devonian carbonates

Limestones and dolostones overlying the Prince Alfred Formation and conformably overlain by shales, siltstones and calcareous sandstones of the Bird Fiord Formation were assigned by Thorsteinsson and McLaren (in Fortier et al., 1963, p. 230, 231, and 245-247, respectively) to the Blue Fiord Formation on the basis of macrofaunal and lithological comparisons with the type Blue Fiord Formation on southwestern Ellesmere Island. Thorsteinsson, in Thorsteinsson and Uyeno (1981), referred these rocks to the Disappointment Bay Formation. Morrow and Kerr (1977, 1986) chose not to assign these rocks to previously named stratigraphic units; instead they termed them 'Undivided Devonian Carbonates'. Morrow and Kerr (1977, Map 1412A) recognized four divisions which are, in ascending order: Du1, limestone; Du2, dolomite; Du3, sandy limestone, anhydrite, dolomite; and Du4, limestone. Morrow and Kerr (1986) refined this subdivision to include five stratigraphic divisions. Their map descriptions (1986) of the five units are quoted here with supporting comments based on preliminary results of our fieldwork. These results indicate that units Du1 and Du2 are correlatable with the Blue Fiord Formation, and units Du3 to Du5 with the lower part of the Bird Fiord Formation on southwestern Ellesmere Island.

Du1: "limestone, bluish grey and fossiliferous with abundant corals and crinoids, in some places a quartz pebble bearing interval of cream weathering dolomite is present at the base of the unit". In section 5 Du1 (40 m) overlies the recessive, covered unnamed formation, and consists of prominent weathering, highly bioclastic, rubbly bedded, medium grey limestone. Conodonts indicate an Emsian (inversus Zone) age. The contact with the overlying Du2 is gradational. In section 3 a covered interval 27 m thick expressed by light grey fenestral dolostone and dark brown bioclastic limestone scree is tentatively assigned to Du1, and 7.7 m of thin rubbly bedded, bioclastic, dark brown dolostone overlying the scree is assigned to Du1. In section 3, Du1 appears to consist of both restricted and more open marine carbonates.

Morrow and Kerr's (1986) Du2 and Du3 units are described and discussed together due to difficulties we have experienced in choosing the boundary between them in measured sections. Similarity in principal rock types associated with regional facies changes, and generally poor exposures hamper consistent recognition of this boundary, the position of which is undoubtedly variable by several tens of metres between sections. Mayr (pers. comm., 1987), using airphotes, places the Du2/Du3 boundary at the change from the relatively resistant, ridge-forming rock types of Du2 to the mostly covered, recessive rock types of Du3.

Du2: "dolomite, cream weathering vuggy, finely to medium crystalline 'sucrosic' thick bedded dolomite and thin bedded silty dolomicrite. Du3: dolomite, sandstone, limestone and anhydrite, mainly a sandy dolomite and dolomitic sandstone with sandy dolomite conglomerate, interbedded anhydrite occurs locally in the vicinity of Grave Mount near Arthur Fiord".

In section 5 there is a gradational change upsection from the bioclastic limestones of Du1 to less bioclastic, vuggy, increasingly dolomitic limestones. The boundary between Du1 and Du2 is drawn at the base of a covered interval above which dolostones occur. In this section, Du2 (145 m) is patchily exposed. Prominent, vuggy, thin bedded, light grey dolostones locally show large-scale crossbedding. Silty dolostones and dolomitic siltstones exhibit pervasive bioturbation. The boundary with the overlying Du3 is drawn at the top of a distinct, fenestral, light grey dolostone interval.

Du3 (212 m) is mostly covered, but isolated exposures show that the unit consists of variably silty dolostones indicating a shallow water, restricted depositional environment. Brecciated dolosiltites and silty dolostones, possibly of evaporite solution origin, were encountered. Limestones and silty limestones, mainly of restricted, shallow water facies, but locally with crinoidal debris indicative of more open marine settings, make up the uppermost 44 m and grade abruptly into the bluff-forming limestones of Du4. Conodonts obtained from the upper portion of Du3 in section 5 indicate an Emsian to early middle Eifelian age range (inversus to costatus Zones).

In section 3, Du2 (110.7 m) consists entirely of prominent weathering, light grey, medium bedded, highly fenestral dolostones. Oncolites and intraclasts occur in some horizons. Beds are thinner and silt content greater at the very top of the unit, where mudcracks and teepee structures are present. The upper contact with Du3 is drawn at the base of a covered interval above which rock types are dominated by limestones. Du3 in this section (169 m) is poorly exposed. The covered intervals are apparently underlain by variably silty limestones and calcareous siltstones of shallow water restricted facies, as evidenced by scree lithologies and isolated exposures. Prominent ridges are composed of variably silty, crossbedded limestones. The contact with the overlying bluff-forming Du4 is gradational, but distinct.

It should be apparent from the above discussion that Du2 and Du3 are not lithologically or texturally consistent between sections, and the choice of positioning the boundary between them in measured sections is somewhat arbitrary. However, on the scale of airphoto mapping, and on 1:250,000 scale maps, this boundary is distinct, and is placed at the topographic change from the generally resistant Du2 to the recessive Du3.

This stratigraphy is consistent from Cardigan Strait west to a line between Whitmore Point and Port Refuge. West of this line the stratigraphy is complicated by onlapping onto a Cornwallis Foldbelt paleohigh in the Inglis Bay area (sections 1 and 2, Figs. 1, 2). In section 2, 15 m of poorly exposed dolomitic siltstones overlying a basal Devonian? breccia are assigned to Du3 because they are overlain by good Du4 and Du5 lithologies. To the northwest, in the vicinity of Village Bay, this part of the stratigraphy is complex and requires further investigation (Mayr, pers. comm., 1987).

Du4: "limestone, a bluish grey cliff and ledge former of tan pelletal lime-mudstone (pelmicrite); medium bedded". Du4 is a distinct ridge-former in all the sections measured. The basal contact with Du3 is gradational; the upper contact with Du5 abrupt, in some places, erosional.

In section 5, Du4 (28.4 m) consists of silty limestones and pure limestones. The lower 12.4 m are semi-recessive, with an obvious, rhythmic PAC (Punctuated Aggradational Cycle) sedimentary signature. The upper 16 m are more massive and bluff-forming. Bioclastic debris is sparse, consisting of Thamnopora fragments, crinoid ossicles and unidentified shell debris, and increases slightly toward the top of the unit. The contact with the overlying Du5 is abrupt and erosional.

In section 3, the base of Du4 (28 m) is placed at the appearance of light grey, locally pinkish, micritic limestones. The lower 14 m of this unit show distinct PAC-style facies succession, variably silty lithologies, and copious shallow water, restricted- environment features (planar lamination, cryptalgal lamination, sparse Thamnopora, Favosites and ostracod hash). The upper 14 m are bluff-forming, and consist of mostly massive, pinkish brown, micritic limestone. Fenestral layers occur within the upper part of the unit, as do scour-based hashes of crinoid ossicles and fine shell debris. The contact with the overlying Du5 is abrupt, planar, and distinct.

In section 2, 44 m of semi-prominent light grey-brown and pinkish micritic limestone, mainly massive, but with fenestral layers and common stylolites, are assigned to Du4. There is a cyclic variation in bedding thickness at this location. The contact with Du5 is sharp.

Conodonts obtained from Du4 indicate an early Eifelian age (patulus to costatus Zones).

Du5: "limestone, a brownish grey weathering argillaceous skeletal crinoid-bearing wackestone, corals and brachiopods scattered throughout".

The basal boundary with Du4 is in all cases abrupt, and is, locally, demonstrably erosive. The upper contact with the clastic, upper part of the Bird Fiord Formation is taken to be at the first significant shale interval (nearly always covered). Du5 is characterized by its extremely high bioclastic content (spiriferid, atrypid and rhynchonellid brachiopods, crinoid ossicles, solitary and colonial corals), by high amounts of silt and fine sand impurities, and by pervasive rubbly bedding textures. Argillaceous lenses between beds are common. Conodonts indicate an early middle Eifelian (costatus Zone) age for this unit.

Regional stratigraphic relationships of undivided devonian carbonates

Age determinations based on conodonts indicate that Du1 is equivalent to the central portion of the type Blue Fiord Formation on southwestern Ellesmere Island (Emsian, inversus Zone), and to the Disappointment Bay Formation of Cornwallis and Lowther islands (Thorsteinsson and Uyeno, 1981).

On lithostratigraphic grounds it seems reasonable to equate Du2 (dominated by fenestral dolostones) with fenestral dolostones capping the Blue Fiord Formation in the Goose Fiord area ('member' 4 of Prosh et al., 1988). Examination by us of these dolostones at Blubber Point, southwest Ellesmere Island, lead us, unlike Prosh et al. (1988), to contend that the vugs in the dolostones capping the Blue Fiord Formation on southwesternmost Ellesmere Island represent a true fenestral fabric, as seen in Du2 on Grinnell Peninsula.

Du3 (silty dolostones, locally evaporitic) is lithologically correlatable with the evaporite-rich Member A of the Bird Fiord Formation (Goodbody, 1985; equivalent to Unit 1 of the 'Goose Fiord Member' in Goodbody, 1987; Unit 1 'Cross Bay Member' in Goodbody, in press c) on southwestern Ellesmere Island and in the Norfolk Inlet area of northern Devon Island. A possible correlative is an unnamed formation consisting of anhydrite, gypsum, sandstone, siltstone, and dolomite, which overlies the Disappointment Bay Formation on Lowther Island (see Thorsteinsson and Uyeno, 1981).

Du4 is equated lithostratigraphically with Unit 3, Member A of the Bird Fiord Formation on southwestern Ellesmere Island south of the Schei syncline axis (Goodbody, 1985; equivalent to Unit 3 'Goose Fiord Member' of Goodbody, 1987; Unit 3 'Cross Bay Member' of Goodbody, in press c).

Du5 is closest lithostratigraphically to Member B of the Bird Fiord Formation south of the Schei syncline axis on southwest Ellesmere Island (Goodbody, 1985: equivalent to 'Blubber Point Member' of Goodbody, 1987; in press c).

Both Du4 and Du5 are age equivalent to Member B of the Bird Fiord Formation (Goodbody, 1985; equivalent to 'Blubber Point Member', Bird Fiord Formation in Goodbody, 1987; in press c) in the Goose Fiord region of southwestern Ellesmere Island (Eifelian, costatus Zone). They are age equivalent to a limestone unit assigned to the Blue Fiord Formation overlying the Disappointment Bay Formation on Cornwallis Island (Thorsteinsson and Kerr, 1968) and on Bathurst Island (Kerr, 1974). Thorsteinsson (in Thorsteinsson and Uyeno, 1981, p. 19) commented on this limestone unit and suggested it represents a separate, as yet unnamed formation. Smith (1987) presumably refers to this unit as his unsubstantiated 'Moses Robinson River Formation'.

On the basis of these known stratigraphic relationships, and the consistency of surface expression of these units from southwestern Ellesmere to at least central Grinnell Peninsula, it seems reasonable to include Morrow and Kerr's (1986) Du1 and Du2 in the Blue Fiord Formation, and their Du3, Du4 and Du5 in the Bird Fiord Formation (Figs. 2, 3, Table 1).

Devonian clastic wedge

A section through the entire preserved clastic wedge was measured along the Tucker River and between this river and Cape Disraeli (section 4, Fig. 1). Palynological, conodont, and lithological samples were taken for the purposes of dating the formations, and comparing their petrographic characteristics for source-area studies. This section was first examined by McLaren (in Fortier et al., 1963) and was traversed, but not measured or sampled, by Embry and Klovan (1976).

Bird Fiord Formation *(upper clastic part; 475 m)*

The contact with the carbonate-dominated Du5 is gradational, and is picked at the first significant covered (shale?) interval above the carbonate section. Two stratigraphic divisions, or members, are distinguished (Fig. 3; Table 1). The lower (Dbi1 of Morrow and Kerr, 1986; Member C of Goodbody, 1985; 'Baad Fiord Member' of Goodbody, 1987; in press c) is poorly exposed, 320 m thick, and consists of interbedded shales, siltstones and calcareous sandstones. It is characterized by a coarsening-upward facies pattern, with rhythms 2 to 6 m thick. Bioturbation is intense in the coarser grained rock types. Fossils are abundant; brachiopods, crinoid ossicles, corals, trilobites, plant fragments, and bivalves are present. The upper clastic division (Dbi2 of Morrow and Kerr, 1986; Member D of Goodbody, 1985; 'Cardigan Strait Member' of Goodbody, 1987; in press c) is 155 m thick, and is made up of crossbedded, mostly unfossiliferous, fine to medium grained arkosic sandstones. Rare, poorly preserved bivalve coquinas occur.

Conodonts from beds at the top of the underlying Du5 carbonates indicate an Emsian to early middle Eifelian age (inversus to costatus Zones). Lithostratigraphic correlation of these beds with other sections dated by conodonts on southwest Ellesmere Island (see Goodbody, 1985, 1987) indicates an early middle Eifelian age (costatus Zone). Beds low in the formation on Sheills Peninsula contain spores representing the devonicus- naumovii Zone, of late early Eifelian age. Spores from two stratigraphic levels in the lower half of the lower member at localities 102827 and 102832 indicate mid-Eifelian age, low in the devonicus-naumovae Zone.

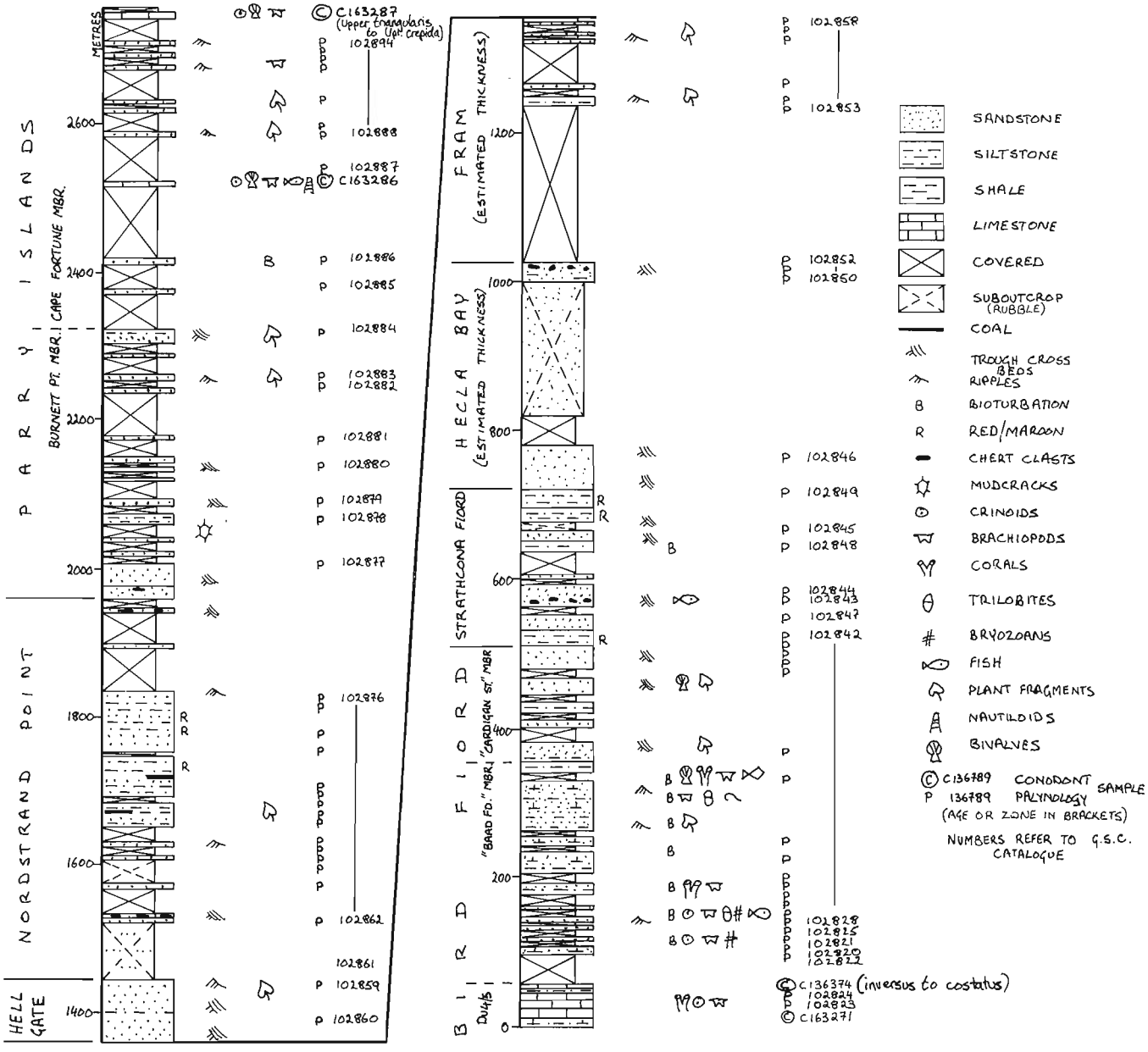

Figure 3. Clastic stratigraphy, measured section 4.

Strathcona Fiord Formation (225 m).

The basal contact with the Bird Fiord Formation is taken at the first appearance of red/maroon coloration. This boundary is sharp, and easily seen in a meander cut along Tucker River. The Strathcona Fiord Formation consists of crossbedded, fine to medium grained, light grey-brown sandstones and siltstones, and grey-green and maroon shales and silty shales. Fining-upward facies sequences with erosional bases are apparent. Chert pebbles locally line scours; shale rip-up clasts are common in these settings. The finer grained rock types are locally bioturbated, and commonly show nodular (paleosol- like) textures. The upper contact with the Hecla Bay Formation is covered, but is apparently abrupt. The abruptness of this boundary is suggestive of erosion, hence the depiction of a possible disconformity between these formations in Table 1. Spores of late Eifelian age (devonicus-naumovae Zone) occur at the base of the Strathcona Fiord Formation on Tucker River at locality 102840, and late Eifelian or early Givetian spores (high in the devonicus-naumovae Zone) are present close to the top of the formation in the same section, at locality 102849.

Hecla Bay Formation (estimated 300 m)

The Hecla Bay Formation is poorly exposed in this area. The basal 60 m are exposed in a river gorge, and consist of crossbedded, multichannel sandstones with rare siltstone partings. Plant fragments are abundant along certain foresets. Above this exposure, a recessive, covered interval approximately 45 m thick leads to a distinct scree-covered ridge forming the upper two thirds of the formation. Scattered outcrops show crossbedded fine to medium grained orange and cream coloured quartz sandstones that contain plant debris and shale rip-up clasts. The upper 40 m of the formation are exposed along Tucker River; lithologies and sedimentary structures are like those of the scattered outcrops below. Chert pebbles are present on some scour surfaces.

Poor outcrop and the lack of fine grained strata hamper age determinations. Spores of early late Givetian age (high in the lemurata-magnificus Zone) were recovered from near the top of the Hecla Bay Formation at locality 102851 in section 4.

Fram Formation (estimated 300 m)

The Fram Formation is very poorly exposed. Only the uppermost 124 m outcrop intermittently along a north flowing tributary of the Tucker River in the vicinity of Cape Disraeli. These exposures consist of interbedded sandstones, siltstones and shales. Fining upward facies sequences are characteristic. Plant fragments are common. Shales are locally maroon. Palynological samples, obtained from the very base of the formation during a brief helicopter stop on the west coast of North Kent Island, await processing. Samples from localities 102853 and 102858, high in the formation in section 4, contain spores of early to mid Frasnian and late Frasnian age respectively (ovalis-bulliferus Zone).

Hell Gate Formation (83 m)

The basal contact with the Fram Formation is abrupt. The abruptness of this boundary is suggestive of erosion, hence the depiction of a possible disconformity between these two formations in Table 1. The Hell Gate Formation, expressed as a distinct light coloured scree ridge, is dominated lithologically by crossbedded light yellow-cream, medium grained sandstones that show ubiquitous crossbedding. Scattered chert pebbles and clay rip-up clasts occur at scour bases. Fining-upward facies sequences are apparent; siltstone intervals are mostly covered, but are locally accessible with some digging. Age determinations are as yet unavailable.

Nordstrand Point Formation (510 m)

The basal contact with the Hell Gate Formation is taken to be where a distinct change in slope and lithology occur. The Nordstrand Point Formation consists of prominent weathering, sand-dominated intervals separated by recessive silt/shale dominated intervals. The former are made up of scour-based, fining-upward sequences of grey-green feldspathic sandstone, grey-green siltstone and grey-green to dark grey shale. Rip-up clasts and large, plant fragments are common on scour bases; chert pebbles are rare, but present on some surfaces. The recessive intervals, dominated by fine grained lithologies, exhibit interbedding of siltstones and shales, which is either planar, or displays definite coarsening-upward successions 0.5 to 1.0 m thick. Root traces are common in the siltstones. The shales are dark grey to maroon and locally contain coal partings 2 to 5 cm thick. Spores from the Nordstrand Point Formation at locality 102876 in section 4 are late Frasnian (upper ovalis-bulliferus Zone).

Parry Islands Formation (788+ m)

The basal contact with the Nordstrand Point Formation is drawn at the base of a distinct ridge-forming crossbedded sandstone. This boundary is of special interest in that it was tentatively interpreted by Embry and Klovan (1976) as a regional unconformity. However, there is no physical evidence of an unconformity in this section. Chert pebbles are not concentrated within this zone and there is no obvious change in grain size or petrology of the sandstones across this boundary. Biostratigraphy will be of extreme importance in clarifying the nature of the boundary.

The Parry Islands Formation is divisible into two members. The lower, Burnett Point Member (Embry and Klovan, 1976) is 366 m thick, and consists of interbedded sandstone, siltstone and shale. Scour-based fining-upward sequences are common in the lower part of the member. The sandstones are trough cross-stratified and channelled; the finer grained lithologies show ripples, mudcracks and root traces, and locally contain thin coals. Higher in the member, the fining-upward sequences are less apparent; sandstone intervals are finer grained, better sorted, and generally planar bedded. Burrowing becomes more common, root traces and coals were not seen. The contact with the Cape Fortune Member (422+ m) is taken to be at the top of a thick sandstone interval,

above which the section is dominated by shale and siltstone. The Cape Fortune Member is largely covered, with ridges of bioturbated, rippled, fine to medium grained sandstone. Lithologies are apparently arranged in coarsening-up successions. Marine fossils occur in two coquinoid layers, one near the centre of the exposed section of the member, the other at the top. Plant fragments are ubiquitous throughout the formation. Conodonts from the highest coquinoid bed within the Cape Fortune Member suggest an early Famennian age (Upper triangularis to Upper crepida Zones). Early Famerrian spores of the Torquata-gracilis Zone were recovered from beds at locality 102885, near the base of the Cape Fortune Member in section 4.

REFERENCES

Embry, A.F. and Klovan, J.
1976: The Middle-Upper Devonian Clastic Wedge of the Franklinian Geosyncline; Bulletin of Canadian Petroleum Geology, v. 24, p. 85-639.

Fortier, Y.O. et al.
1963: Geology of the north-central part of the Arctic Archipelago, Northwest Territories (Operation Franklin); Geological Survey of Canada, Memoir 320, 676 p. + maps and figures.

Goodbody, Q.H.
1985: Stratigraphy, sedimentology and paleontology of the Bird Fiord Formation, Canadian Arctic Archipelago; Unpublished Ph.D. thesis, University of Alberta, 386 p. + maps and figures.
1987: Local geology; southeastern Arctic Islands, Middle Devonian; *in* Stratigraphy, sedimentology and hydrocarbon potential of the Devonian sequence, central and eastern Arctic Archipelago, G.P. Smith, G.H. Goodbody and R.R. Rice (eds.); Second International Symposium on the Devonian System, Canadian Society of Petroleum Geologists, Field Excursion A1 Guidebook, p. 39-63.
a: Lower and middle Paleozoic stratigraphy of Melville Island, Northwest Territories; *in* Geological Reports, Melville Island, District of Franklin, R.L. Christie (ed.); Geological Survey of Canada Paper (in press).
b: Devonian shelf systems on Melville Island, Canadian High Arctic; *in* Proceedings, Second International Symposium on the Devonian System; Canadian Society of Petroleum Geologists, Memoir (in press).
c: Stratigraphy of the Lower to Middle Devonian Bird Fiord Formation, Canadian Arctic Archipelago; Canadian Society of Petroleum Geologists, Bulletin (in press).

Kerr, J. Wm.
1974: Geology of Bathurst Island Group and Byam Martin Island, Arctic Canada; Geological Survey of Canada, Memoir 378, 152 p.

McGregor, D.C.
—: Palynological correlation of Middle and Upper Devonian rocks of Melville Island, Arctic Canada; *in* Geological Reports, Melville Island, District of Franklin, R.L. Christie (ed.); Geological Survey of Canada, Paper. (in press)

Morrow, D.W. and Kerr, J. Wm.
1977: Stratigraphy and sedimentology of lower Paleozoic formations near Prince Alfred Bay, Devon Island; Geological Survey of Canada, Bulletin 254 (includes Map 1421A — Geology of the Prince Alfred Bay Area, Devon Island), 122 p. + maps and figures.
1986: Geology of Grinnell Peninsula and the Prince Alfred Bay area, Devon Island, District of Franklin, Northwest Territories; Geological Survey of Canada, Open File 1325, 45 p. + map.

Prosh, E.C., Lesack, K.A., and Mayr, U.
1988: Devonian stratigraphy of northwestern Devon Island, District of Franklin; *in* Current Research, Part D, Geological Survey of Canada, Paper 88-1D, p. , 1988.

Richardson, J.B. and McGregor, D.C.
1986: Silurian and Devonian spore zones of the Old Red Sandstone continent and adjacent regions; Geological Survey of Canada, Bulletin 364, 79 p. diagrams.

Smith, G.P.
1987: Devonian carbonates of the Canadian Arctic Islands (Abs.); *in* Programs and Abstracts, Second International Symposium on the Devonian System, Calgary, Alberta, p. 207.

Thorsteinsson, R. and Kerr, J.Wm.
1968: Cornwallis and adjacent smaller islands, Arctic Archipelago; Geological Survey of Canada, Paper 67-64.

Thorsteinsson, R. and Uyeno, T.T.
1981: Stratigraphy and conodonts of Upper Silurian and Lower Devonian rocks in the environs of the Boothia Uplift, Canadian Arctic Archipelago; Geological Survey of Canada, Bulletin 292, 75 p.

Catastrophic lake drainage, Tuktoyaktuk Peninsula area, District of Mackenzie

J. Ross Mackay[1]
Terrain Sciences Division

Mackay, J.R., Catastrophic lake drainage, Tuktoyaktuk Peninsula area, District of Mackenzie; in Current Research, Part D, Geological Survey of Canada, Paper 88-1D, p. 83-90, 1988.

Abstract

In the 36 year period from 1950 to 1986 about 65 lakes in the Tuktoyaktuk Peninsula area have undergone at least partial drainage. Data on lake drainage have been obtained from field studies and a comparison of NTS 1:250 000 maps prepared from 1950 air photographs with 1986 Landsat imagery. The majority of the lakes have drained rapidly, if not catastrophically, by erosion of ice-rich terrain at their outlets. Most erosion has been along ice-wedge systems. One lake probably drained as a result of the disturbance of a bulldozed winter road that crossed the outlet creek.

Résumé

Durant la période de 36 ans qui s'étend de 1950 à 1986, ont subi un drainage au moins partiel environ 65 lacs de la région de la péninsule de Tuktoyaktuk. On a obtenu des données sur le drainage des lacs en effectuant des relevés in situ, et en comparant des cartes SNRC au 1/250 000e préparées à partir de photographies aériennes de 1950, aux images transmises par le satellite Landsat en 1986. La majorité des lacs ont subi un drainage rapide, et parfois même catastrophique, causé par l'érosion de terrains très englacés à leur déversoir. L'érosion a principalement eu lieu le long des réseaux de coins de glace. Un lac s'est probablement vidé à la suite d'une perturbation du terrain par la construction au bulldozer d'une route d'hiver qui traverse le ruisseau au déversoir de ce lac.

[1] Department of Geography, University of British Columbia, Vancouver, B.C. V6I 1W5

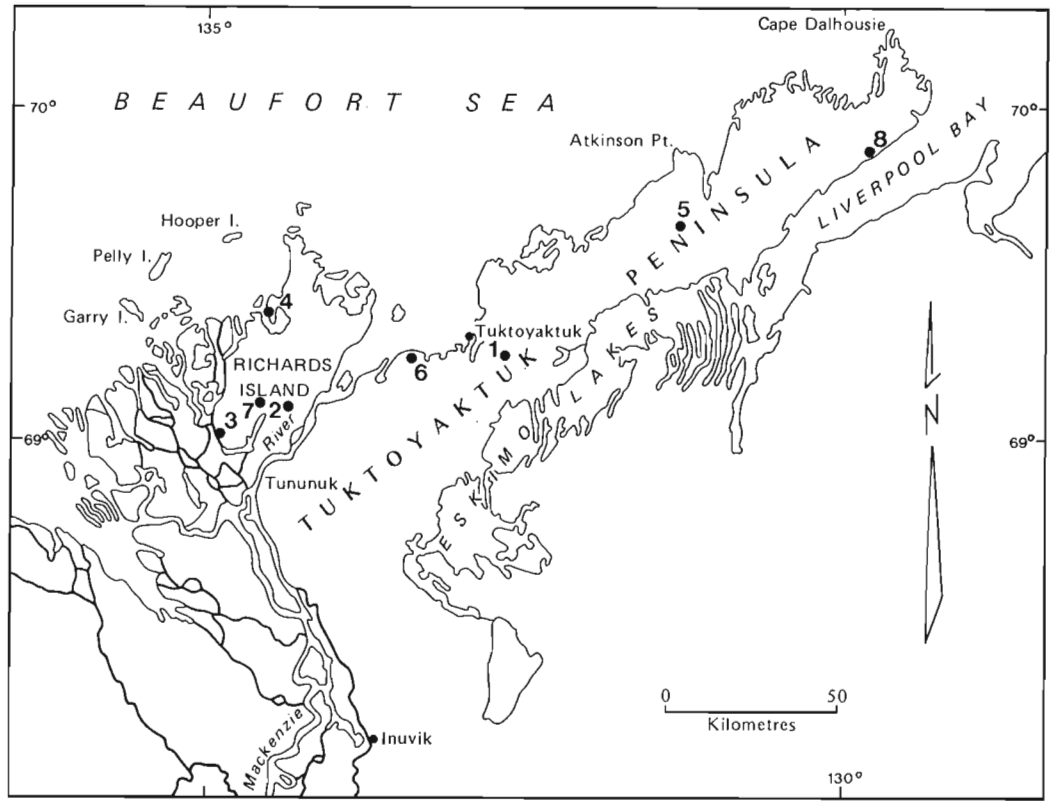

Figure 1. Location map. The numbers 1 to 6 refer to sites that have been used in a previous publication (Mackay, 1985). Site 7 and 8 are new to this paper.

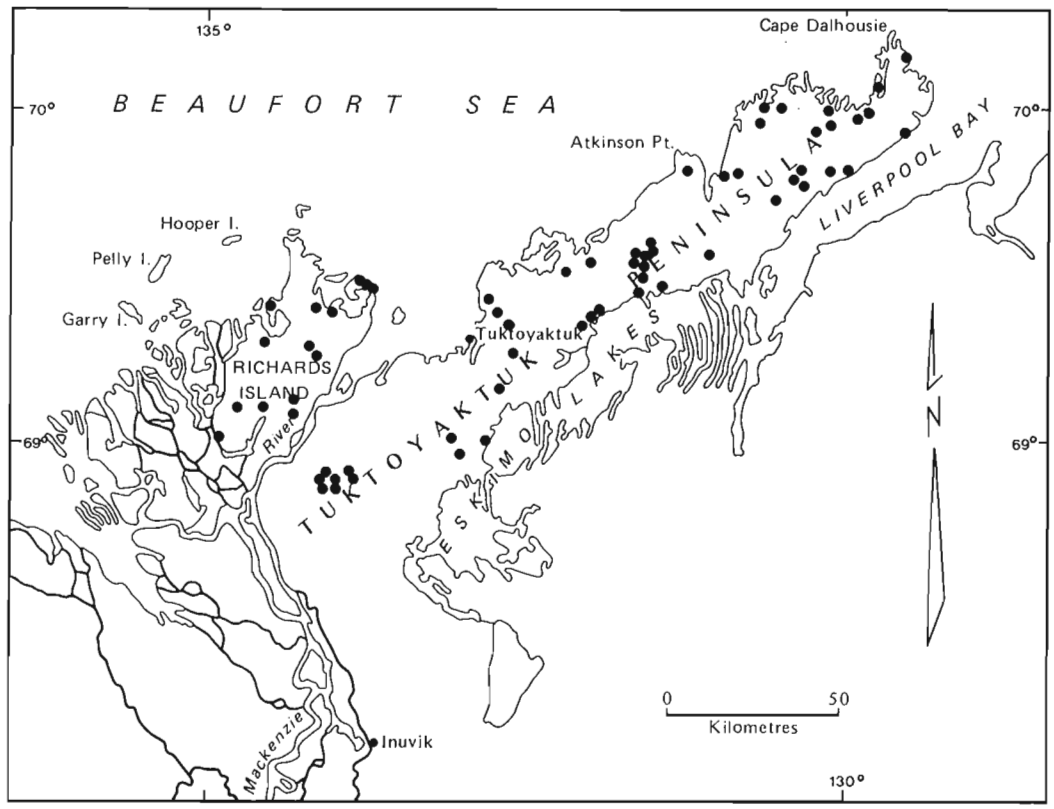

Figure 2. Each dot represents one lake that has been partially or totally drained between 1950 and 1986 (*see* text). Although some subjectivity has been involved in the identification of the lakes, probably 65 lakes or more have been drained in whole or in part between 1950 and 1986 for a nearly 2 lakes per year.

INTRODUCTION

The Tuktoyaktuk Peninsula area of the western Arctic coast, District of Mackenzie (Fig. 1) is in an area of continuous permafrost. Thousands of large and small lakes cover from 15 to 50% of any given large area. Although there are a variety of lake types, many are of thermokarst origin (Rampton and Bouchard, 1975). There is abundant evidence from old abandoned shorelines around most of the larger lakes to show that lake drainage has been taking place for thousands of years. Although lake drainage decreases the total lake area, the number of lakes may increase where the drainage of one large lake leaves behind several residual lakes. Ice-wedge ice is extremely abundant (Pollard and French, 1980). Catastrophic lake drainage is usually associated with the erosion of channels along interconnecting ice-wedge systems. Lake drainage has been mentioned briefly in several previous publications (e.g. Mackay, 1979, 1985). This report discusses catastrophic lake drainage in the Tuktoyaktuk Peninsula area for the 1950 to 1986 period. Numbers are used in the absence of names for lakes (Fig. 1). Lake numbers 1 to 6 have been used in a previous publication (Mackay, 1985) while numbers 7 and 8 are new ones.

Acknowledgments

The fieldwork has been supported by the Geological Survey of Canada, the Natural Sciences and Engineering Research Council of Canada, the Polar Continental Shelf Project, Energy, Mines and Resources Canada, and the Inuvik Scientific Resource Centre, Inuvik, N.W.T.

METHODS

During the course of fieldwork in the Tuktoyaktuk Peninsula area, those lakes showing signs of recent drainage were checked against the NTS 1:250 000 maps prepared from 1950 air photography, to determine if drainage took place before or after 1950, In addition, 1986 Landsat imagery at a scale of about 1:250 000 has been compared with the NTS maps

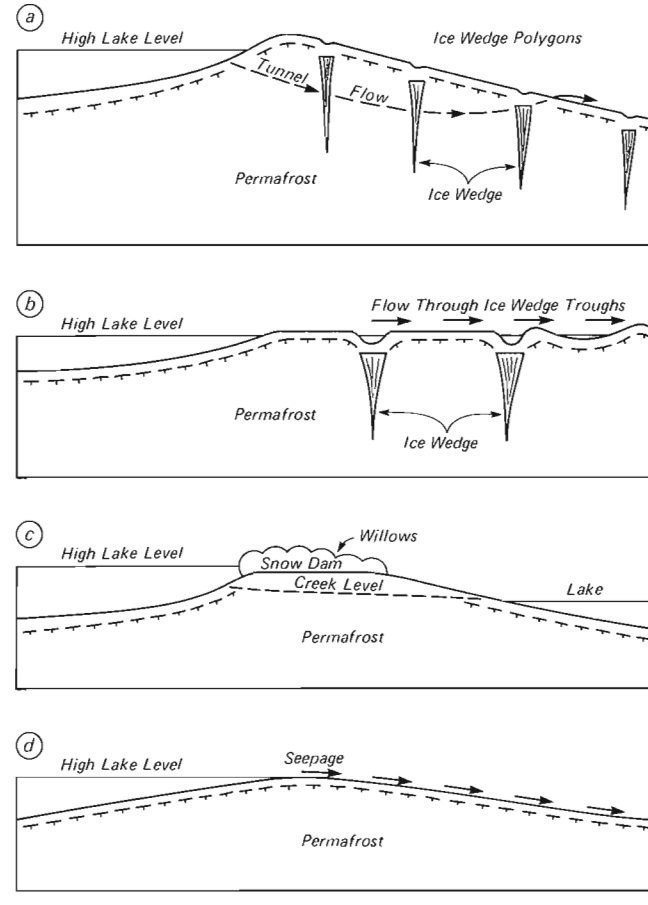

Figure 3. The diagram shows schematically, four common methods of lake drainage. (a) At high water, flow through interconnecting ice-wedge cracks (i.e. thermal contraction cracks) can result in lake drainage. (b) At high water, flow through the troughs of ice-wedge polygons can result in drainage. (c) At high water, a snow dam at the outlet can result in a rise in lake level, overtopping, and drainage. (d) Lakes with seepage channels may drain, particularly if water is diverted along an ice-wedge system.

Figure 4. The photograph was taken in June 1974, a few weeks after drainage. The larger lake is about 150 m wide.

Figure 5. The photo of the outlet channel was taken in June 1974, only a few weeks after the two lakes in Figure 4 drained. Note the jumbled debris, two pools, and signs of thaw slumping of ice-rich permafrost. The arrow points to a man for scale.

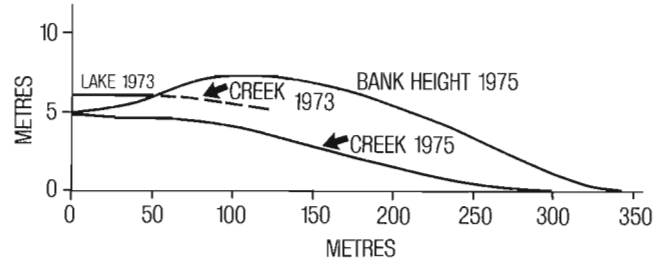

Figure 6. The channel profile marked "creek 1973" was the inferred profile of the pre-drainage channel of the lakes of Figure 4 prior to drainage; the channel was surveyed in 1975, one year after drainage, and is marked "creek 1975".

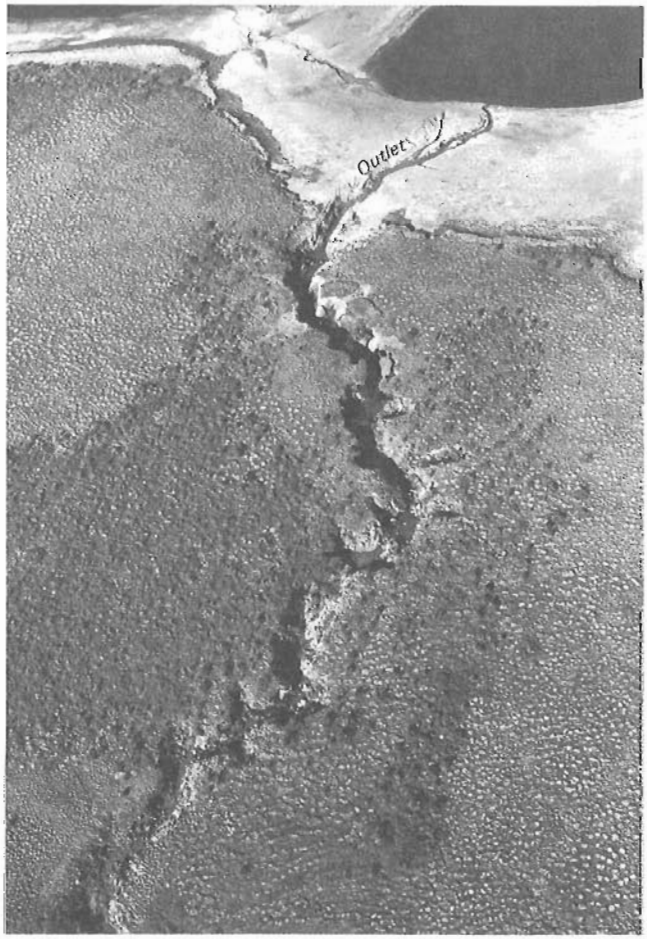

Figure 7. The drainage channel of the lakes of Figure 4 taken in June 1974 a few weeks after drainage. The angularity and freshness of the channel indicate recent catastrophic drainage.

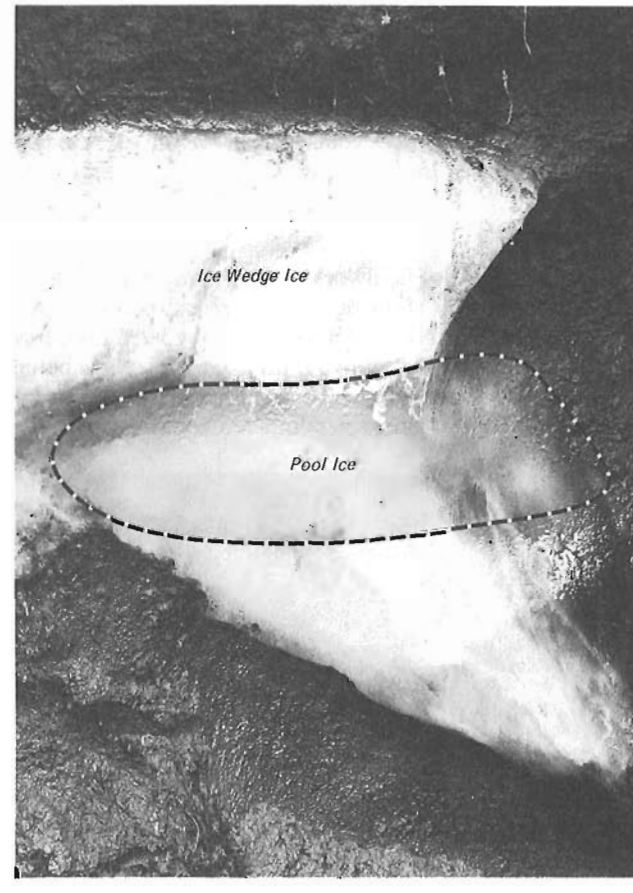

Figure 8. The photo was taken in June 1974 to the left of the man standing in Figure 5. The pool ice formed by the freezing of water in a tunnel eroded in ice-wedge ice and the adjacent permafrost. The horizontal dimension of the pool ice is 1 m. The ice-wedge ice is vertically foliated. The poll ice represents an episode of near drainage prior to actual drainage. Tunnel erosion is shown in Figure 3a.

to see if any differences in lakes sizes or shapes could be detected that would suggest drainage. The results of the 1950 to 1986 comparisons are plotted in Figure 2. About 65 lakes have shown signs of drainage in the 1950 to 1986 period. Of these, at least 20 are known from field studies to have drained catastrophically. The principal drainage processes, with emphasis on permafrost related processes, are discussed below.

UNDERGROUND TUNNEL FLOW

A frequent cause of catastrophic lake drainage is underground tunnel flow through interconnected ice-wedge cracks (thermal contraction cracks) in the snowmelt period of May and June as shown in Figure 3a. An example is given in Figure 4 where two adjoining lakes were drained between 18 September 1973 and 1 June 1974. The larger lake was 350 m long and 150 m wide. Drainage lowered the lake levels by about 1 m to leave a 70 to 80 m wide bare-exposed lake bottom zone around two smaller residual lakes. Figure 5, taken a few weeks after drainage, shows the chaotic nature of the drainage channel where it leaves the larger lake. The discharge was so great that the old drainage channel was deepened by several metres (Fig. 6). Figure 7, an air photograph of the drainage channel taken a few weeks after drainage, indicates, by its freshness, the rapidity of channel erosion.

Underground tunnel flow occurs frequently without lake drainage (Mackay, 1974). Often, in the high water snowmelt period of May and June of after a torrential summer rainstorm, water will flow underground in areas with ice-wedge polygons for a few metres or tens of metres and then emerge downslope as a spring (Fig. 3a). The water that remains trapped in the underground channels and pools then freezes to give a distinctive type of ground ice for which an accepted English language term is lacking. The descriptive words poll ice are used here. The ice has been described frequently in the Russian literature (e.g. Kunznetsova, 1972) where it is sometimes referred to as thermokarst cave ice (Shumskiy, 1959). Pool ice, like intrusive ice, lake ice, or river ice often has a columnar structure indicative of the freezing of bulk water. The columns are similar to the candle ice of lake ice. The preferred orientation of the c-axis is normal to the columns (cf. Michel and Ramseier, 1971). When the freezing is inward from the sides of a tunnel, the columns tend to point inward and the last part to freeze is often discoloured from solute concentration (Gell, 1976). Where the tunnel has eroded through frozen ground, peat, roots, fragments of soil etc. may dangle down from the tunnel roof to appear as if suspended in the clear pool ice. Figures 8 and 9 show pool ice formed from the freezing of water-filled tunnels at the outlet locations pictured in Figure 5. The great abundance of old pre-drainage pool ice exposed along the freshly eroded drainage channel shows that lake drainage nearly occurred at least once previous to 1974. The age of pool ice can, at times, be estimated if pool ice is in an active ice-wedge because the annual ice-wedge veinlets will cut through the pool ice.

Figure 9. The photo was taken in June 1974 to the right of the man standing in Figure 5. The pool ice and ice-wedge ice were eroded when the lake drained. The top of the pool ice is 2 m below the ground surface. The ice-wedge is vertically foliated; the pool ice is horizontally banded.

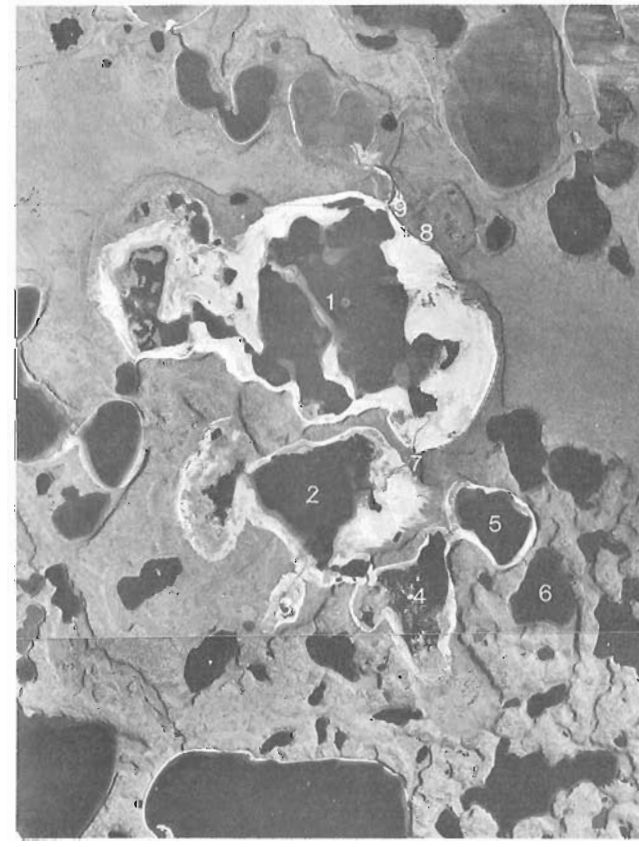

Figure 10. The location is shown in Figure 1, site 5. The partially drained lake, labelled 1, is 4 km long. *See* text for description.

Figure 11. The location is shown in Figure 1, site 8. See text for description.

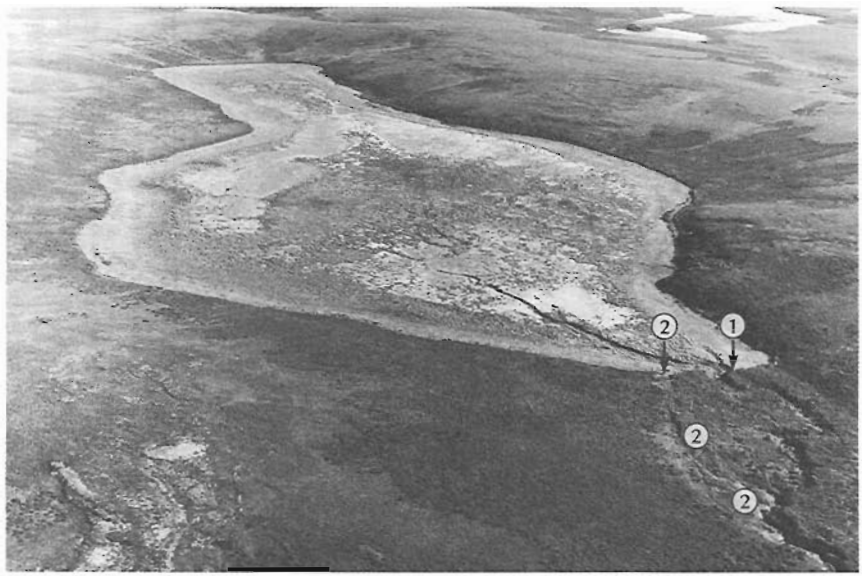

Figure 12. The location is shown in Figure 1, site 2. The lake, prior to drainage in about 1962 or 1963, was 1 300 m long. The present drainage channel is labelled 1, the pre-drainage channel is labelled 2.

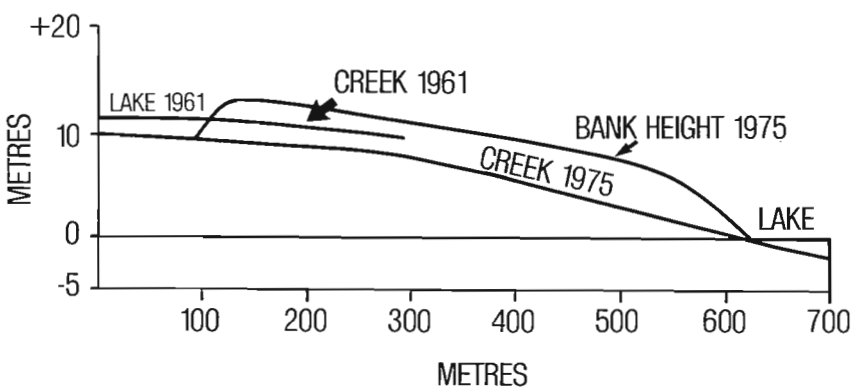

Figure 13. The profiles are for the drainage channels 1 and 2 of the drained lake of Figure 12. The long profile of the present drainage channel as surveyed in 1975 is labelled "creek 1975"; that of the abandoned drainage channel in about 1961 is labelled "creek 1971".

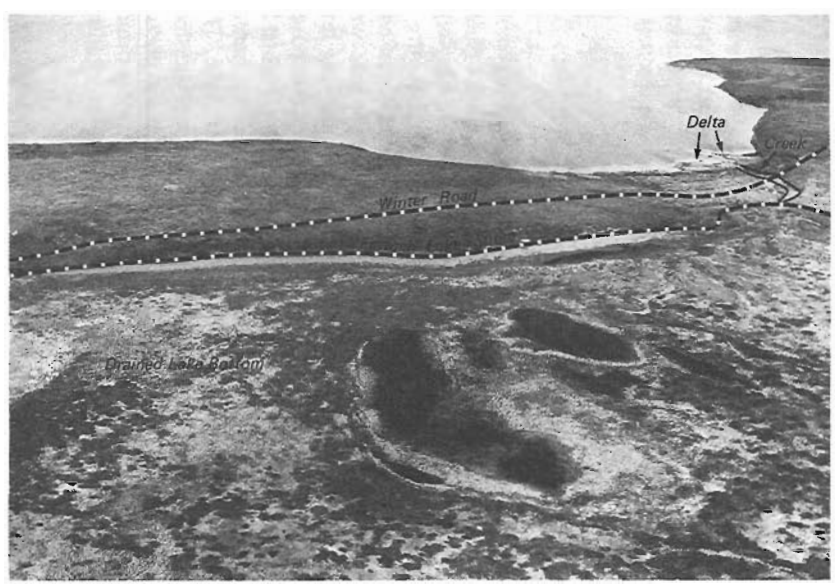

Figure 14. The location is shown in Figure 1, site 1. The lake drained between 18 July 1971 and 30 July 1972 several years after a winter road (see route marked on photo) was bulldozed across the outlet creek. See text for description.

FLOW THROUGH ICE-WEDGE TROUGHS

Probably the majority of first order lakes (i.e. lakes without inflow from a higher lake) have negligible outlet flow after the snowmelt period of May and June. Therefore, first order lakes often lack a drainage channel. The comparative absence of stream flow from first order lakes, even for those lakes whose area exceeds one or two square kilometres, can be attributed to a combination of a low precipitation and a high percent of the total area in lakes. The mean annual precipitation normal for the 1951-1980 period for the Tuktoyaktuk Peninsula area was about 10 to 15 cm, with the amount of rain slightly exceeding that of snow (Environment Canada, 1982). The mean annual water equivalent of the snowpack was about 5 to 10 cm. In view of the fact that a high percentage of the area tends to be in lakes in the first place, the contribution of snowmelt runoff from the adjacent land areas will rarely be enough to raise the water level more than 20 to 40 cm. Consequently, streams tend to be absent and overflow in thermokarst lakes is often through ice-wedge troughs at their outlets (Fig. 3b). Sustained flow through an ice-wedge trough system can lead to lake drainage.

SNOW DAMS AND OVERTOPPING

In the winter, snow blown across lake ice will often accumulate in large snowdrifts along the windward lake shore. Because the outlets of lakes are favoured places for the growth of willows, an outlet on a windward shore may then be blocked by a large snowdrift. Large snowdrifts with high density wind-packed snow can be very effective dams. An excellent example of lake drainage from overtopping of such a snow dam is shown in Figure 10. Lake drainage took place between 1950 and 1955. Referring to the numbers in Figure 10 for locations, a snow dam at location 7 raised the level of lake 2 about 0.5 m above that of the highest lake shoreline. The field evidence comes from waterborne debris trapped on willows to a height of about 0.5 m above the highest shoreline. Overtopping at the snow dam caused rapid erosion of the high centred polygon area along the drainage channel connecting lake 2 to lake 1. Discharge from lake 2 into lake 1 raised the level of lake 1 about 0.3 m. Lake 1, which normally overflowed through an outlet at location 8 then discharged through an outlet at location 9. Rapid erosion at location 9 resulted in abandonment of the outlet at location 8. The levels of both lakes 1 and 2 were lowered by about 2.5 m. As a result of drainage of lakes 1 and 2, lakes 3, 4 and 5 also drained. Lake 6 is now on the verge of draining. The magnitude of lake drainage can be put into perspective when it is realized that lake 1 prior to drainage was about 4 km long, lake 2 about 3 km long, and the levels of both lakes were lowered about 2.5 m.

SEEPAGE OUTLETS

Many lakes that lack drainage channels overlow by way of seepage outlets at times of high water as shown in Figure 3d. For example, Illisarvik (unofficial name), a lake at Figure 1, site 4, was 600 m long and 300 m wide before it was artificially drained in 1978 (Mackay, 1981). Prior to drainage, overflow was by way of a sedgy swale. After the lake was drained along an artificial channel in an area of ice-wedge polygons several hundred metres away from the seepage outlet, much pool ice was exposed along the artificial drainage channel. From this evidence, it is clear that Illisarvik must have narrowly escaped drainage by underground tunnel flow at least once, and more likely several times, in the past.

An example of drainage from erosion of a seepage outlet is shown in Figure 11. Prior to drainage, the lake was 1 300 m long and 700 m wide with a shoal area surrounding a central deep. On 25 June 1969, when the outlet was first seen in the field, water was seeping out over a sedgy divide less than 1 m wide. A few minutes shovelling could have started lake drainage, which, in fact occurred naturally within less than a year. Drainage was catastrophic. The lake level was lowered about 1 m and a box-like channel 5 to 10 m wide was eroded in sands. Although few interlake drainage divides are as narrow and steep as that of the lake of Figure 11, at least half a dozen lakes have been seen in the field where a day's shovelling by one person could initiate drainage.

OUTLET DIVERSION

Two examples are known of lakes that have drained by diversion from one outlet to another. In each case, rapid erosion of the younger outlet through an area of high centered ice-wedge polygons caused lake drainage. The first example for lake 1 in Figure 10 has already been discussed. The second example is shown in Figure 12. The lake, prior to drainage, was 1 300 m long with a maximum width of about 600 m (Mackay, 1985). The present channel is labelled 1 in Figure 12, an older pre-diversion channel is labelled 2. In 1962 or 1963, rapid erosion of channel 1, as surveyed in 1975, is shown in Figure 13 and the profile of channel 2 as it was in 1961 before abandonment is also plotted.

ARTIFICIAL DISTURBANCE

The lake in Figure 14 drained in 1971 or 1972 several years after a winter road was bulldozed across the outlet creek. Drainage was so rapid that a delta was built 0.3 m above normal water level in the receiving lake. This implies that the level of the receiving lake was raised rapidly by about 0.3 cm because of catastrophic drainage. Probably the disturbance of the winter road that crossed the outlet creek caused drainage, but this cannot be proven.

CONCLUSION

In the 36 years period from 1950 to 1986, approximately 65 lakes have undergone at least partial drainage in the Tuktoyaktuk Peninsula area for a rate of about 2 lakes per year. Drainage in most instances was rapid, probably catastrophic, and was caused mainly by diversion of water through interconnecting ice-wedge systems. Frequently, drainage of one lake has resulted in raising the water level of the downstream receiving lake to trigger its drainage and conversely, an upstream source lake may be drained by headward erosion of the connecting creek. Thus, it is not unusual to find drained lakes clustered in groups of two to five or more. Lake drainage has occurred by permafrost related processes such as: underground tunnel flow through ice-wedge cracks (thermal contraction cracks); surface flow through ice-wedge troughs;

overtopping of a snow dam followed by rapid erosion at the outlet; erosion along seepage outlets; and outlet diversion through ice-wedge systems. One lake has probably drained from construction of a bulldozed winter road at the lake outlet, but this cannot be proven. However, the sensitivity of lakes to easy ice-wedge drainage is a most important factor to be considered in any future development activities such as road building, burial of pipelines, etc.

REFERENCES

Environment Canada
1982: Canadian Climate Normals, 1951-1980, Temperature and Precipitation, the North Y.T. and N.W.T.; Atmospheric Environment Service, 55 p.

Gell, W.A.
1976: Underground ice in permafrost, Mackenzie Delta-Tuktoyaktuk Peninsula; unpublished PhD thesis, The University of British Columbia, Vancouver, B.C., 258 p.

Kuznetsova, T.P.
1972: Some morphological features of polygonal-veined ice of the Holocene deposits in central Yakutia. (In Russian.) *in* Problems of Cryolithology No. 2, ed. A.I. Popov; Moscow University Press, Moscow. (Translated by U.S. Joint Publications Research Service for U.S. Army Cold Regions Research and Engineering Laboratory, Draft Translation 433, 1974, p. 49-53.)

Mackay, J.R.
1974: The rapidity of tundra polygon growth and destruction, Tuktoyaktuk Peninsula-Richards Island area, N.W.T.; *in* Report of Activities, Part A, Geological Survey of Canada, Paper 74-1A, p. 391-392.
1979: Pingos of the Tuktoyaktuk Peninsula area, Northwest Territories; Géographie Physique et Quaternaire, v. 33, p. 3-61.
1981: An experiment in lake drainage, Richards Island, Northwest Territories: a progress report; *in* Current Research, Part A, Geological Survey of Canada, Paper 81-1A, p. 63-68.
1985: Permafrost growth in recently drained lakes, Western Arctic Coast; *in* Current Research, Part B, Geological Survey of Canada, Paper 85-1B, p. 177-189.

Michel, B. and Ramseier, R.O.
1971: Classification of river and lake ice; Canadien Geotechnical Journal, v. 8, p. 36-45.

Pollard, W.H. and French, H.M.
1980: A first approximation of the volume of ground ice, Richards Island, Pleistocene Mackenzie delta, Northwest Territories, Canada; Canadian Journal of Earth Sciences, v. 17, p. 509-516.

Rampton, V.N. and Bouchard, M.
1975: Surficial geology of Tuktoyaktuk, District of Mackenzie; Geological Survey of Canada, Paper 74-53, 17 p.

Shumskiy, P.A.
1959: Ground (subsurface) ice. (In Russian.) *in* Principles of Geocryology, Part 1, General Geocryology, Chapter IX, Academy of Sciences of the U.S.S.R., V.A. Obruchev Institute of Permafrost Studies, Moscow. (Translated (1964) by the National Research Council of Canada, Ottawa, TT-1130, 118 p.)

The effect of forest fires on permafrost terrain stability, Little Chicago-Travaillant Lake area, Mackenzie Valley, N.W.T.

David G. Harry and Kaye L. MacInnes[1]
Terrain Sciences Division

Harry, D.G. and MacInnes, K.L., The effect of forest fires on permafrost terrain stability, Little Chicago-Travaillant Lake area, Mackenzie Valley, N.W.T.; in Current Research, Part D, Geological Survey of Canada, Paper 88-1D, p. 91-94, 1988.

Abstract

Permafrost degradation and slope failures, initiated by the effects of forest fire, have occurred on the east bank of the Mackenzie River between Little Chicago and Travaillant Lake. This area is traversed by a potential oil and gas pipeline corridor. Two forest fires in 1986 affected an area of approximately 1 300 km^2, part of which is underlain by ice-rich glacial and glaciolacustrine sediments. Changes in the surface energy balance have resulted in a 50-150% increase in active layer thickness, triggering the development of skin flows on slopes. In some cases, massive ice and icy sediments are exposed at the surface in retrogressive thaw slumps, which are continuing to grow one year following the fire event. Fire-initiated terrain instability represents a significant hazard to development activities in the Mackenzie Valley. The response of ice-rich terrain to forest fires also underlines its susceptibility to other forms of disturbance.

Résumé

Une dégradation du pergélisol et des ruptures de talus, provoquées par les effets des incendies de forêt, se sont produites sur la rive est du fleuve Mackenzie entre Little Chicago et le lac Travaillant. Cette zone pourrait être traversée par un couloir pour oléoducs et gazoducs. En 1986, les incendies de forêt ont touché une région d'environ 1 300 km^2, dont une partie du sous-sol contient des sédiments glaciaires et glaciolacustres riches en glace. Les variations du bilan énergétique de surface ont eu pour conséquence un accroissement de 50 à 150% de l'épaisseur du mollisol, et ont donc donné naissance à des écoulements pelliculaires sur les pentes. Dans certains cas, la glace massive et des sédiments englacés affleurent en surface à l'intérieur de coulées régressives de dégel, qui continuent à se développer une année après l'incendie. L'instabilité du terrain provoquée par les incendies constitue un danger important durant les activités d'aménagement du terrain dans la vallée du Mackenzie. La réponse du terrain riche en glace vis-à-vis des incendies de forêt souligne sa sensibilité aux autres formes de perturbation.

[1] Land Resources Division, Indian and Northern Affairs, Canada, Yellowknife, N.W.T.

INTRODUCTION

Within regions underlain by ice-rich permafrost, physical or thermal disturbance of the ground surface may result in terrain instability and thermokarst (Mackay, 1970). A mechanism resposible for such disturbances is the effect of forest fires (e.g. Heginbottom, 1978; Johnson and Viereck, 1983; Viereck, 1982). Long term changes in ground thermal regime may occur as a result of modification to surface albedo following vegetation loss. For example, analysis of active layer conditions following the Inuvik forest fire of 1968 indicated thaw depths 100-150 % greater in burned areas compared to undisturbed areas, eight years after the fire event (Mackay, 1977). These changes may result in melt-out of ground ice within near-surface permafrost, mobilization of unconsolidated surficial sediments, and thermokarst subsidence and erosion of terrain.

This report describes permafrost terrain response to forest fires which occurred during the summer of 1986, on the east bank of the Mackenzie River in the vicinity of Little Chicago, approximately 150 km northwest of Inurik. (Fig. 1). Following observations by staff of Inland Waters, Environment Canada, and Department of Renewable Resources, Government of the N.W.T. in July 1987 (T.J. Day, pers. comm.), a helicopter reconaissance and brief ground investigations were undertaken by the present authors on September 1987. Information on the fire events has been provided by R. Lanoville, Department of Renewable Resources, Government of the Northwest Territories. The evaluation of terrain stability in this area is particularly important, since it forms part of a proposed transportation corridor for future Beaufort Sea — Alberta oil and gas pipelines (e.g. Polar Gaz, 1984) and for the proposed Mackenzie Highway extension.

TERRAIN CONDITIONS AND FIRE HISTORY OF DISTURBED AREA

North of Little Chicago, the east bank of the Mackenzie River is bordered by a discontinuous glaciolacustrine plain. A zone of low-relief hummocky moraine merges with upland terrain to the east and north. Southeast of Travaillant Lake, the plain is incised by the narrow, steep-sided valley of the Thunder River. Within the lowland area, glacial, glaciolacustrine and colluvial sediments are frequently ice-rich, containing 10-40 % ice by volume (Hughes et al., 1973). The widespread occurrence of thermokarst lakes, in some cases showing indications of active bank collapse, provides further evidence of ice-rich permafrost conditions. Active layer detachment slides and retrogressive thaw flow slides commonly occur on slopes, especially following disturbance or removal of the vegetation cover (Hughes et al., 1972).

On 29 June 1986, several forest fires were ignited by lightning strikes on both sides of the Mackenzie River in the area between Little Chicago and Travaillant Lake, following an extremely dry winter and spring. Those on the northeast side coalesced into two major fires, catalogued as EV016 and EV019. Firefighting effort focused upon limiting the spread of EV019 to the northwest and EV016 to the south. The burned zone is nearly contiguous and covers an area of approximately 130 000 hectares (1 300 km^2), bordering the Mackenzie River for more than 80 km. Vegetation loss was almost complete. In an adjacent unburned area, vegetation cover was observed to consist of a tree canopy, (primarily black spruce), open shrub and dwarf shrub layers (primarily willow and Labrador tea), and a closed ground cover of loose feather moss with lichen clumps.

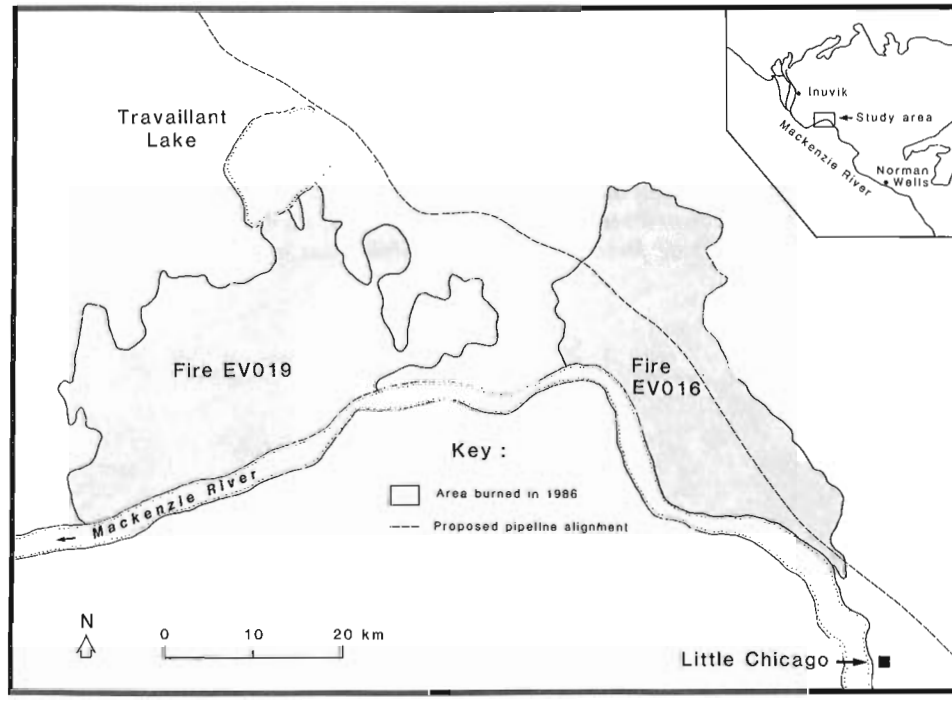

Figure 1. Limits of 1986 forest fires in the Little Chicago-Travaillant Lake area.

TERRAIN RESPONSE TO FIRE DISTURBANCE

Three main stages may be distinguished in the response of permafrost terrain in this area to fire disturbance. First, seasonal thaw depths have increased as a result of disturbance or destruction of vegetation and surficial organic material. Second, thaw of near-surface permafrost has resulted in the development of skin flows on sloping ground. Third, in some cases removal of active layer materials has exposed underlying ice-rich permafrost, triggering the growth of retrogressive thaw slumps.

Ground surface and active layer conditions

Preliminary observations of ground conditions were made at one locality adjacent to the Mackenzie River, within the area affected by fire EV016. This site shows evidence of intense burning, resulting in nearly complete loss of vegetation cover including most of the surficial organic mat (Fig. 2). Surface microrelief consists of earth hummocks, 20-30 cm in height, covered with a charred organic veneer overlying mineral soil. Depth to the frost table, measured by steel probe, was from 75-90 cm beneath hummock tops and from 51-63 cm beneath intervening hollows. Within an adjacent unburned area, thaw depths of 41-68 cm were measured beneath hummock tops and 21-25 cm beneath hollows. These observations suggest that, one year following the fire event, thaw depths within the burned area are 50-150 % greater than in adjacent unburned areas. Previous studies suggest that maximum active layer thickness occurs five years following the fire event, but that pre-burn seasonal thaw conditions may not be re-established for 20-25 years (Viereck, 1982, p. 134).

Skin flows (active layer detachment failures)

Skin flows, also termed active layer glides (Mackay and Matthews, 1973), are initiated by the detachment of a thin veneer of vegetation and active layer materials and their subsequent movement along the inclined surface of the permafrost table (McRoberts and Morgenstern, 1973). They frequently occur as long ribbon-like debris flows, which may coalesce to form broad sheets of unstable terrain. Within the area affected by fire EV016, skin flows appear to have been initiated on slope angles greater than 20 degrees, although the coalescent run-out zone may be more gently inclined. On some slopes, at least 50 % of the ground surface has been affected by skin flow development (Fig. 3). Skin flows have also occurred at numerous locations along the Thunder River valley (Fig. 4).

Figure 2. Ground conditions within area affected by EV016. Note soil auger (1.5 m) for scale.

Figure 3. Skin flows on hillside within limits of EV016.

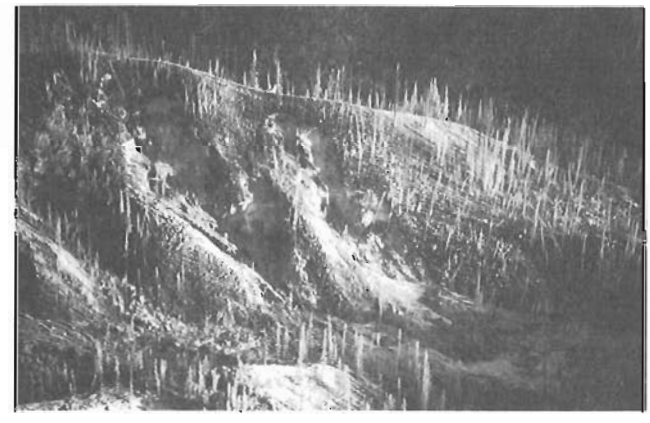

Figure 4. Skin flows on south side of Thunder River valley.

Figure 5. Retrogressive thaw slump showing characteristic bimodal morphology.

Figure 6. Debris flows extend across Mackenzie River beach at 30-50 m intervals for more than 50 km within fire limits.

Figure 7. Retrogressive thaw slump headwall, exposing ice-rich silt overlain by sand.

Retrogressive thaw slumps (ground ice slumps)

Retrogressive thaw slumps are a form of bimodal flow, characteristic of permafrost regions (McRoberts and Morgenstern, 1973). They consist of a steep headwall, formed by the ablation of massive ice or ice-rich permafrost, and a low-angle tongue of thaw-mobilized debris (Fig. 5). In many cases, headscarp development is initiated when active layer materials are removed by skin flows. Within the areas affected by fires EV016 and EV019, ground ice slumps are particularly prevalent along the banks of the Mackenzie River. Debris tongues extend across the river beach at intervals of approximately 30-50 m (Fig. 6). Many of the thaw slumps observed in September 1987, possessed actively ablating headwalls (Fig. 7). The probable existence of massive ice and icy beds beneath terrain upslope of these features suggests that they may continue to grow for some time.

CONCLUSION

Catastrophic permafrost terrain degradation has been triggered in the Little Chicago-Travaillant Lake area by the effects of forest fire on ground thermal regime. Active layer thickness is likely to increase for several years, possibly resulting in further terrain instability. Variable amounts of differential than settlement may be anticipated at interfaces between burned and unburned terrain units. Further research is required to quantify terrain response to fire disturbance in this area. Fire-initiated terrain instability represents a significant hazard to existing and planned development projects within the Mackenzie Valley transportation corridor. This case history also underlines the sensitivity of ice-rich permafrost to other forms of thermal and physical disturbance, including the construction and operation of linear facilities.

REFERENCES

Heginbottom, J.A.
1978: Some effects of surface disturbance on the permafrost active layer at Inuvik, N.W.T., Canada; *in* Permafrost, North American Contribution to the Second International Conference (Yakutsk, USSR), National Academy of Sciences, Publication 2115, p. 649-657.

Hughes, O.L., Veillette, J.J., Pilon, J., Hanley, P.T. and van Everdingen, R.O.
1972: Surficial geology and geomorphology of 106J, K, O, District of Mackenzie, N.W.T., and Yukon Territory; Geological Survey of Canada, Open File 108.
1973: Terrain evaluation with respect to pipeline construction, Mackenzie Transportation Corridor, Central Part; Environmental-Social Committee Northern Pipelines, Task Force on Northern Oil Development, Report No. 73-37, 74 p.

Johnson, L. and Viereck, L.
1983: Recovery and active layer changes following a tundra fire in northwestern Alaska; *in* Proceedings, Fourth International Conference, Fairbanks, Alaska, vol. 1, National Academy Press, Washington, D.C., p. 543-547.

Mackay, J.R.
1970: Disturbances to the tundra and forest tundra environment of the western Arctic; Canadian Geotechnical Journal, v. 7, p. 420-432.
1977: Changes in the active layer from 1968 to 1976 as a result of the Inuvik fire; *in* Report of Activities, Part B, Geological Survey of Canada, Paper 77-1B, p. 273-275.

Mackay, J.R. and Mathews, W.H.
1973: Geomorphology and Quaternary history of the Mackenzie River Valley near Fort Good Hope, N.W.T., Canada; Canadian Journal of Earth Sciences, v. 10, p. 26-41.

McRoberts, E.C. and Morgenstern, N.R.
1974: The stability of thawing slopes; Canadian Geotechnical Journal, v. 11, p. 447-469.

Polar Gas
1984: Geotechnical assessment (volume 5): Documentation submitted in suport of applications to National Energy Board and Indian and Northern Affairs Canada.

Viereck, L.
1982: Effects of fire and firelines on active layer thickness and soil temperatures in interior Alaska; *in* The R.J.E. Brown Memorial Volume, Proceedings, Fourth Canadian Permafrost Conference, Edmonton, Canada, National Research Council of Canada, p. 123-135.

The Rapid Fault Array: a foldbelt in Arctic Yukon.[1]

L.S. Lane
Institute of Sedimentary and Petroleum Geology, Calgary

Lane, L.S., The Rapid Fault Array: a foldbelt in Arctic Yukon; in Current Research, Part D, Geological Survey of Canada, Paper 88-1D, p. 95-98, 1988.

Abstract

The Rapid Fault Array, in the vicinity of Blow River, Yukon, contains no regionally important strike-slip or normal faults and is best characterized as a fold and thrust belt. Albian shale, sandstone and conglomerate are folded into north trending, upright, chevron style structures. Owing to competence contrast between the coarse and fine grained clastic units, local thrust faults are required to accommodate the shortening. Shallow fold plunges, together with subvertical east striking extension fractures, indicate components of vertical and north-south extension.

Comparison with structures on the Yukon coastal plain and on the continental shelf suggest that the Rapid Fault Array is part of an extensive arcuate belt of folds that developed in Paleocene-Eocene time, indicating a correlation with Laramide Cordilleran structures.

The regional geometry of the foldbelt suggests that right-lateral strike-slip displacement on the Porcupine — Sharp Mountain zone was transformed into shortening across the fold belt. Such a correlation has important implications for the magnitude and significance of strike-slip displacement.

Résumé

Le réseau de failles de Rapid, à proximité de la rivière Blow au Yukon, ne contient aucune faille à décrochement horizontal ou aucune faille normale qui soient régionalement importantes, et se laisse au mieux définir comme une zone de plissements et chevauchements. Les schistes argileux, grès et conglomérats de l'Albien sont plissés en structures verticales à orientation nord, disposées en accordéon. En raison des différences de compétence entre les unités clastiques grossièrement et finement grenues, des failles chevauchantes locales doivent compenser le rétrécissement. Le plongement peu prononcé des plis, conjugué à l'existence de fractures d'extension subverticales de direction est, témoignent de la présence de composantes d'extension à direction verticale et nord-sud.

La comparaison des structures observées avec celles de la plaine côtière du Yukon et de la plateforme continentale, permet d'avancer que le réseau de failles de Rapid fait partie d'une vaste zone arquée de plis dont la formation date du Paléocène et de l'Éocène, phénomène à partir duquel on peut déduire une corrélation avec les structures de la cordillère Laramienne.

La géométrie régionale de la zone de plissements semble indiquer qu'un décrochement horizontal dextre survenu dans la zone de Porcupine et de Sharp Mountain a été transformé en un rétrécissement de la zone de plissements. Cette corrélation présente d'importantes conséquences en ce qui a trait à l'évaluation de l'ampleur et de l'importance de la faille de décrochement.

[1] Contribution to Frontier Geoscience Project

INTRODUCTION

Five weeks of fieldwork were devoted to 1:50,000-scale mapping in the Blow River area (Anker Creek map area, NTS 117 A/10), Arctic Yukon (Fig. 1). This work forms part of a long term project to study the structural and tectonic evolution of the Beaufort-Mackenzie continental margin, funded through the Frontier Geoscience Program (FGP). Reconnaissance mapping (Norris 1981) had identified a series of north striking faults (Blow, Kaltag, Skull, Buckland and several unnamed structures) that separated folded panels of Cretaceous to lower Tertiary shale, sandstone and conglomerate. The purpose of detailed mapping was to define more precisely the situation, age and kinematics of the major structures crossing the map area.

Access to the area was by helicopter from a base camp near the Shingle Point DEW Line site on the Beaufort Sea coast. Terrain is generally undulating, with gently sloping sandstone and conglomerate ridges producing local relief up to 2500 feet (760 m). Exposure is typically poor; the ridges consist principally of felsenmeer, and flatter areas are covered by a veneer of Pleistocene deposits and tundra. However, very good exposures in stream-cut banks allow reliable mapping of structures both along and across strike.

STRATIGRAPHY

Three fossil localities in the map area and five others near by constrain the age of the strata to the Cretaceous Period, and most of the rocks are mapped as early Albian map unit Kbr (Norris 1981).

Rock types are mainly pyritic black shale with interbedded discontinuous sandstone or sandstone-conglomerate units. In the northwest corner of the map area, a grey shale succession may belong to the Late Cretaceous Boundary Creek Formation. Due to poor exposure in that area, the location and nature of the contact with underlying Albian strata is uncertain. Where the coarse clastics make up more than about 30 percent of the section, these units tend to form ridges that can be mapped in areas of poor exposure. In general, however, resistant units cannot be traced with certainty for more than a few kilometres. Sandstone beds rarely exceed 2 m in thickness, but most are less than 50 cm thick, and are interbedded with shale. Sedimentary structures are common and consist of parallel laminations, ripple crosslaminations, massive beds, channel scours, and flute and load casts. Conglomerates are massive or crudely bedded and occur as local layers 2 to 3 m thick, or as lenses or channels that cut into underlying beds. Locally they consist of pebble-rich layers in a sandstone or shale matrix. The conglomerate beds are almost always associated with sandstones. Pebble and cobble clast sizes are most common; boulders are locally abundant. Clasts are generally well rounded. Black, grey and green chert dominate the clast compositions. Lesser amounts of vein quartz, quartzite, locally dominant black shale, and minor conglomerate, limestone, gneiss and granodiorite also occur.

The Albian sandstone-shale sequence appears to be an essentially continuous stratigraphic succession over the area mapped, although contraction faulting causes local disruption, particularly in fold hinges where more competent sandstones tend to fault through rather than fold with the shales. Although only local disruption by faulting can be documented, the possibility of large-scale repetition by thrust faulting cannot yet be ruled out. If faulting is of only local importance, the entire map area, with the exception of the northwest corner, may be underlain by Albian rocks in the order of 5 to 10 km thick. Microfossil samples may resolve the question of the scale of thrust repetition.

STRUCTURE

The structural geometry of the shales consists of chevron style folds on steeply dipping, north striking axial surfaces. The sandstone-conglomerate units define more rounded hinge zones (Fig. 2). Overall plunges are northward, with local reversals (Fig. 3). This corroborates a general northward-younging evident from published microfossil assemblages (Norris 1981). Contraction faults are common but, due in part to a lack of stratigraphic markers and to discontinuous exposures, cannot be convincingly traced for many kilometres

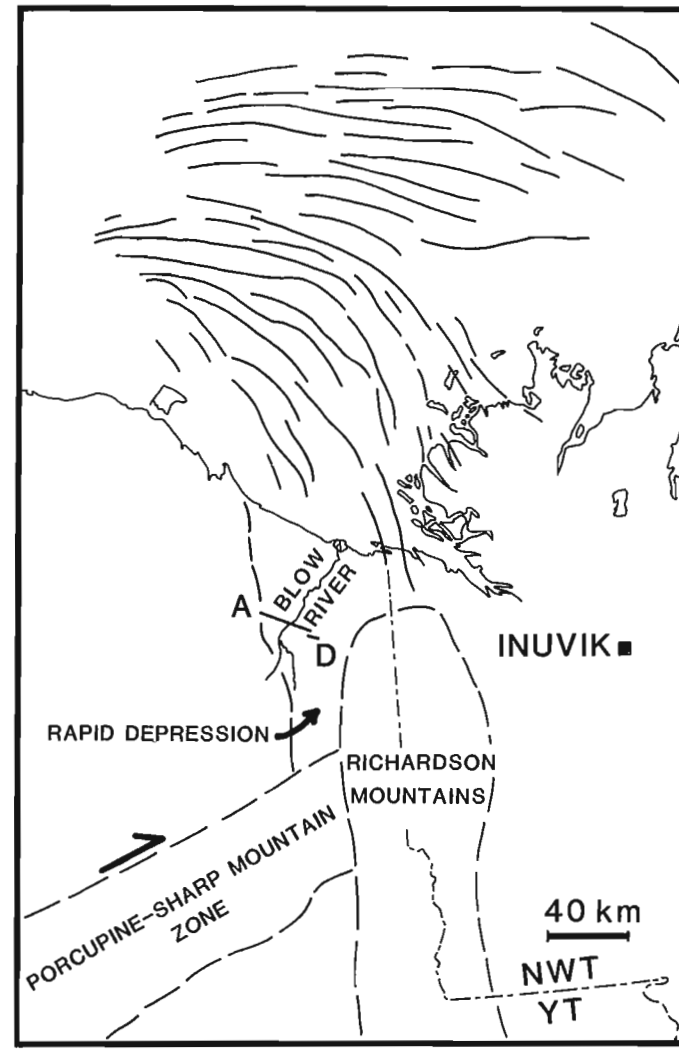

Figure 1. Selected structural elements of the northern Yukon and adjacent District of Mackenzie, with location of cross-section AD (Fig. 2). Axial surface traces of pre-Late Eocene anticlines define an arcuate belt on the Beaufort continental shelf (from J.R. Dietrich, unpublished compilation).

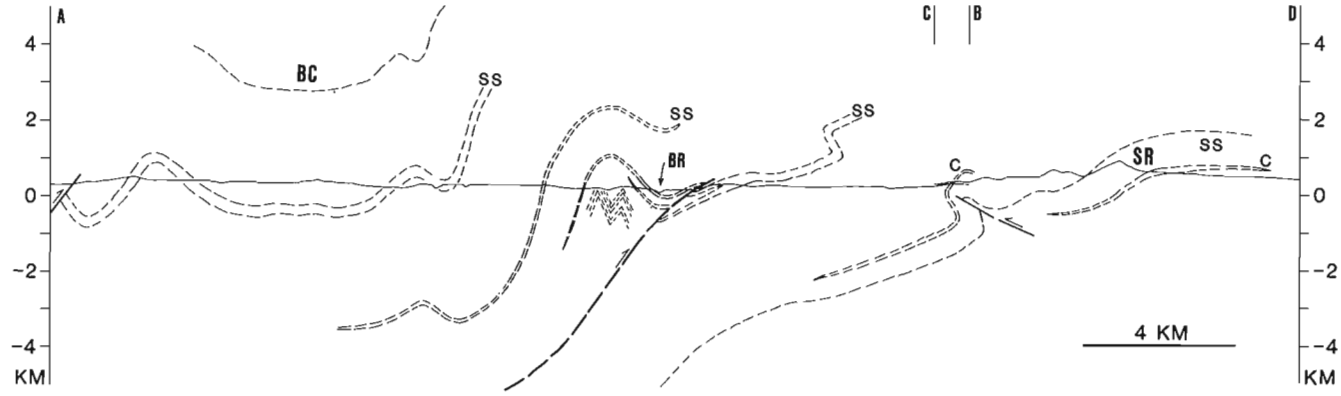

Figure 2. Preliminary cross-section through the Blow River area. Structures are outlined by discontinuous sandstone-rich (SS) and conglomerate (C) units. An estimate of 10 km of Albian sediments assumes that thrust repetitions are insignificant. A minimum estimate of 4-5 km is suggested by the continuous succession westward from Blow River. BC, Boundary Creek Formation; BR, Blow River; SR, Skull Ridge sandstone-conglomerate unit.

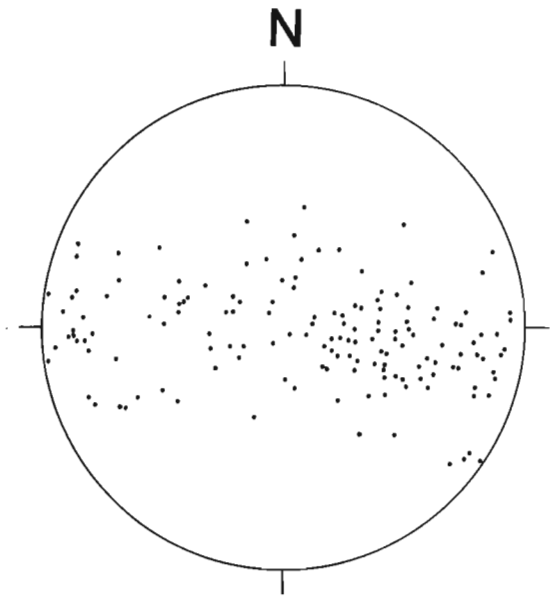

Figure 3. Lower hemisphere equal-area projection of 152 poles to bedding from 50 stations near the line of section in Figure 2.

along strike. They may be local features that accommodate competence contrast between sandstone-conglomerate layers and the shale matrix. Several larger faults have an important component of east-west shortening, indicating a kinematic regime consistent with the chevron folds. Most of the faults are oblique-slip, and some have two or more discrete sets of striations. Usually, one set is oblique or dip-slip, the other is strike-slip; however, too few multiple sets have been observed to distinguish a time sequence with confidence. Analysis of the fracture and striation patterns is in progress.

Quartz-filled extension fractures are ubiquitous in sandstone layers. Most frequently they strike east and dip steeply southward, consistent with a subhorizontal north-south extension direction, and essentially normal to the fold axes. The extension fractures and the fold geometry together (considering both as due to a single event) indicate a bulk flattening strain with east-west shortening and components of extension on shallow north-south and subvertical axes.

DISCUSSION

The recognition that folding is the dominant deformation mechanism suggests that the stratigraphy can be represented by a simple succession rather than a series of separate, fault-bounded panels as indicated by reconnaissance mapping (Norris 1981). Future mapping to the north and south will constrain more closely the upper and lower boundaries of the Albian succession.

Well defined Bouma cycles in the sandstone-conglomerate units identify off-shelf deposition. The well rounded clasts, together with local conglomerate clasts and the presence in the area of Paleozoic conglomerates indicate a multicyclic history for the coarse sediments. The abundance of black, grey and green chert suggests a source area in the lower Paleozoic succession like that presently exposed near by in the Barn Mountains to the southwest. Chert clasts, as well as conglomerate and limestone, have probable sources in the adjacent upper Paleozoic rocks. Although no systematic survey of flute cast orientations was conducted, their orientations were rather uniform and indicate a north-directed current flow.

The structural geometry is a result of east-west shortening by folding in shales, complicated locally by thrusting of more competent sandy members. The timing is constrained by the age of the shales as younger than early Albian. If the grey shale exposed in the northwest corner of the map area belongs to the Late Cretaceous Boundary Creek Formation, then the folding postdates Late Cretaceous as well. The regional reconnaissance map (Norris 1981) also identified north-south folds affecting lower Tertiary rocks of the Deep Creek Syncline. Comparison with the regional structural patterns on the Beaufort continental shelf (Fig. 1; see Dixon et al. 1985, Part A, Figs. 44, 47) indicates that the folds in the Rapid Depression may correlate with a large arcuate belt of folds affecting much of the western Beaufort continental shelf. These structures are well defined by marine seismic control to be pre-Late Eocene in age (Dixon et al. 1985, Part A, Figs. 30b, 52b, c).

Preliminary tectonic implications

Mapping in the Blow River area together with reconnaissance coverage of adjacent areas during 1987 have produced much new data. The following discussion is a reflection of how the new data help to elucidate aspects of the regional tectonics.

If the Blow River structures and the arcuate continental shelf fold belt represent one deformation, the age of these structures is early Tertiary. Well controlled seismic reflection data indicate that the east-west compression postdated deposition of the lower Reindeer Sequence, of Paleocene age, but was largely complete by Late Eocene (Dixon et al. 1985, Part A, Fig. 52c). This age is also consistent with deformation of Upper Cretaceous and lower Tertiary strata on the Yukon coastal plain (Norris 1981). A Paleocene-Eocene age for the development of these structures implies a link to Laramide deformation in the Cordillera.

Offshore, the Eocene folds describe a broad arc that curves toward the northwesterly and westerly structural trends in the western Beaufort. The mechanism by which this geometry was developed is not clear, but the orientation of thrust faults north of the Barn Mountains (Norris 1981), together with strike-slip structures in the area of the Porcupine — Sharp Mountain zone (Fig. 1) suggest an overall northeast shortening direction. (The Porcupine — Sharp Mountain zone coincides with the combined Keele Block and Dave Lord Uplift of Norris (1983) and consists of an array of faults and folds with northeast trends, bounded by the Kaltag and Sharp Mountain faults). The local north-south trend of structures in the Blow River area suggests that the orientation of older basement structures, possibly relating to the Early Cretaceous or older basin into which the Albian sediments were deposited, controlled the orientation of later compressional structures. At the other end of the arc, east trending structures may reflect a component of lateral escape of soft Cretaceous-Tertiary sediment toward a free face — the Eocene continental margin.

If there are no regionally significant strike-slip structures in the Rapid Depression, then tectonic models invoking major post-Albian strike-slip through the Blow River area are invalid. Reconnaissance mapping indicates that structures in the northern Richardson Mountains (Fig. 1) are not offset by strike-slip faults (Norris 1984). Where then, is the right-lateral strike-slip on structures in the Porcupine — Sharp Mountain zone accommodated? The geometric and kinematic constraints are met if right-lateral strike-slip in the Porcupine — Sharp Mountain zone is accommodated by northeastward to eastward shortening across the Blow River area (Fig. 1). Based on this model, an estimate of the magnitude of right-lateral strike-slip across the Porcupine — Sharp Mountain zone may be obtained from the magnitude of shortening across the fold belt north of it. Also, the displacement magnitude across the Porcupine — Sharp Mountain zone would be predicted to decrease eastward, to zero at the northern Richardson Mountains.

SUMMARY

In the Blow River area, the structural geometry consists of chevron folds on steeply dipping, north striking axial planes and gently north plunging axes. Contraction faulting is closely associated with hinge areas of folds, and fold hinges involving sandstone and conglomerate units. Faulting can be linked to local accommodations as strain intensity increased (interlimb angles decreased), or to competence contrast between the shale and coarser units.

Apparent structural and stratigraphic continuity across the map area appears to rule out the existence, in the Blow River area, of regionally significant strike-slip faults, including the Blow, Kaltag and Skull (Yukon) faults, which had previously been interpreted as projecting into the area.

The foregoing is consistent with a tectonic history that includes an Early Cretaceous (as young as early Albian) basin in the Rapid Depression, collapsing and inverting in Eocene time, accommodating right-lateral displacement on faults in the Porcupine — Sharp Mountain zone. Future mapping across the area to determine the extent of the east-west shortening may then reflect the magnitude of right-lateral displacement in the strike-slip system.

REFERENCES

Dixon, J., Dietrich, J.R., McNeil, D.H., McIntyre, D.J., Snowdon, L.R., and Brooks, P.

1985: Geology, biostratigraphy and organic geochemistry of Jurassic to Pleistocene strata, Beaufort-Mackenzie area, northwest Canada; Course Notes, Canadian Society of Petroleum Geology, Calgary, Alberta, 65 p.

Norris, D.K.

1981: Geology, Blow River and Davidson mountains, Yukon Territory — District of Mackenzie; Geological Survey of Canada, Map 1516 A (1:250,000).

1983: Geotectonic correlation chart 1532 A — Operation Porcupine Project Area; Geological Survey of Canada.

1984: Geology of the Northern Yukon and Northwestern District of Mackenzie; Geological Survey of Canada, Map 1581 A (1:500,000).

Corridor traverse through Barn Mountains, northernmost Yukon

M.P. Cecile
Institute of Sedimentary and Petroleum Geology, Calgary

Cecile, M.P., Corridor traverse through Barn Mountains, northernmost Yukon; in Current Research, Part D, Geological Survey of Canada, Paper 88-1D, p. 99-103, 1988.

Abstract

The Barn Uplift is a small, ovoid, structural culmination of probable Laramide age that exposes a succession of highly deformed Cambrian to Devonian strata. These rocks are unconformably overlain by moderate to gently dipping Lower Carboniferous conglomerates of the Kekiktuk Formation. Three major stratigraphic units are recognized in the pre-Kekiktuk succession: Cambrian argillite, Ordovician chert, and Silurian shale. The Cambrian unit can be subdivided on the basis of colour, and contains a mappable limestone member. The Ordovician unit contains a mappable limestone member near its base in the western half of the area. The core of the uplift (pre- Kekiktuk Formation) can be divided into two structural domains: a western succession of steeply dipping imbricate thrusts, with strata in a single thrust panel younging westward; and an eastern zone of tight, upright folds. On the east side of the uplift is a thrust fault that places Cambrian argillite against an upper Paleozoic and/or Mesozoic succession of shale, siltstone and conglomerate. Small outcrops of Ordovician chert more than one kilometre east of this thrust are thought to be klippen.

Résumé

Le soulèvement de Barn est une petite culmination structurale de forme ovoïde et probablement d'âge laramien, qui expose une succession de strates cambriennes à dévoniennes fortement déformées. Ces roches reposent en discordance sous des conglomérats moyennement à légèrement inclinés de la formation de Kekiktuk, datant du Carbonifère inférieur. On a identifié trois grandes unités stratigraphiques dans la succession antérieure à la formation de Kekiktuk: une argilite cambrienne, un chert ordovicien, et une schiste argileux silurien. On peut subdiviser l'unité cambrienne selon ses couleurs; cette unité contient un membre calcaire que l'on peut cartographier. L'unité ordovicienne contient un membre calcaire qui peut être cartographié, près de sa base, dans la moitié ouest de la région. Le noyau du soulèvement (antérieur à la formation de Kekiktuk) se laisse subdiviser en deux domaines structuraux: une succession ouest de chevauchements fortement inclinés dont les strates contenues dans un unique lambeau de charriage deviennent progressivement plus récentes en direction de l'ouest; et une zone est de plis verticaux étroits. Du côté est du soulèvement, on rencontre une faille chevauchante qui place l'argilite cambrienne contre une succession de schiste argileux, de microgrès et de conglomérat datant du Paléozoïque supérieur ou du Mésozoïque, ou les deux. De petits affleurements de chert ordovicien situés à plus d'un kilomètre à l'est de ce chevauchement pourraient être des klippes.

INTRODUCTION

The Barn Uplift is one of several small uplifts that expose lower Paleozoic strata on either side of the Yukon-Kaltag fault system in the northernmost Yukon. This uplift is also the best exposure of post-Silurian, pre-Carboniferous ("Ellesmerian") deformation in the northernmost Yukon (Norris and Dyke, 1987; Norris and Yorath, 1981; Dyke, 1974).

In June of 1987, an east-west corridor was traversed through the central Barn Mountains as part of a reconnaissance study prior to major detailed mapping of northernmost Yukon uplifts, planned for 1988 and 1989.

Geological setting

The Barn Uplift is a 15 km wide (east-west), 25 km long, doubly plunging, structural high, which exposes north trending lower Paleozoic cherts, shales, argillites, and minor quartzite and limestone in its core (Norris, 1972; Norris and Yorath, 1981). The steeply dipping core strata are a striking aspect of the Barn Uplift; they are abruptly cut off by more gently dipping Carboniferous units. The youngest age reported from the core strata is Late Silurian (Ludlovian; Lenz and Perry, 1972), and the oldest age of the gently dipping succession is Early Carboniferous (Viséan; Bamber and Waterhouse, 1971). Dyke (1974) hypothesized a probable Late Devonian age for deformation in the core of the complex, but noted that the uplift itself was likely a "Laramide" feature. Dyke (1974) and Norris and Yorath (1981) concluded that "Ellesmerian" deformation consisted of reverse movement on three to four steeply dipping faults. Dyke (1974) estimated the thickness of core strata at approximately 3 km ("10 000 ft.") and more likely to be 6 km ("20 000 ft.").

1987 OBSERVATIONS

The structural fabric of the Barn Uplift core can be divided into east and west domains (Fig. 1). The western domain is characterized by a number of thin imbricate thrusts, and the eastern domain consists of tight, closely-spaced folds (Fig. 1). Based on the style of repetition of stratigraphic units

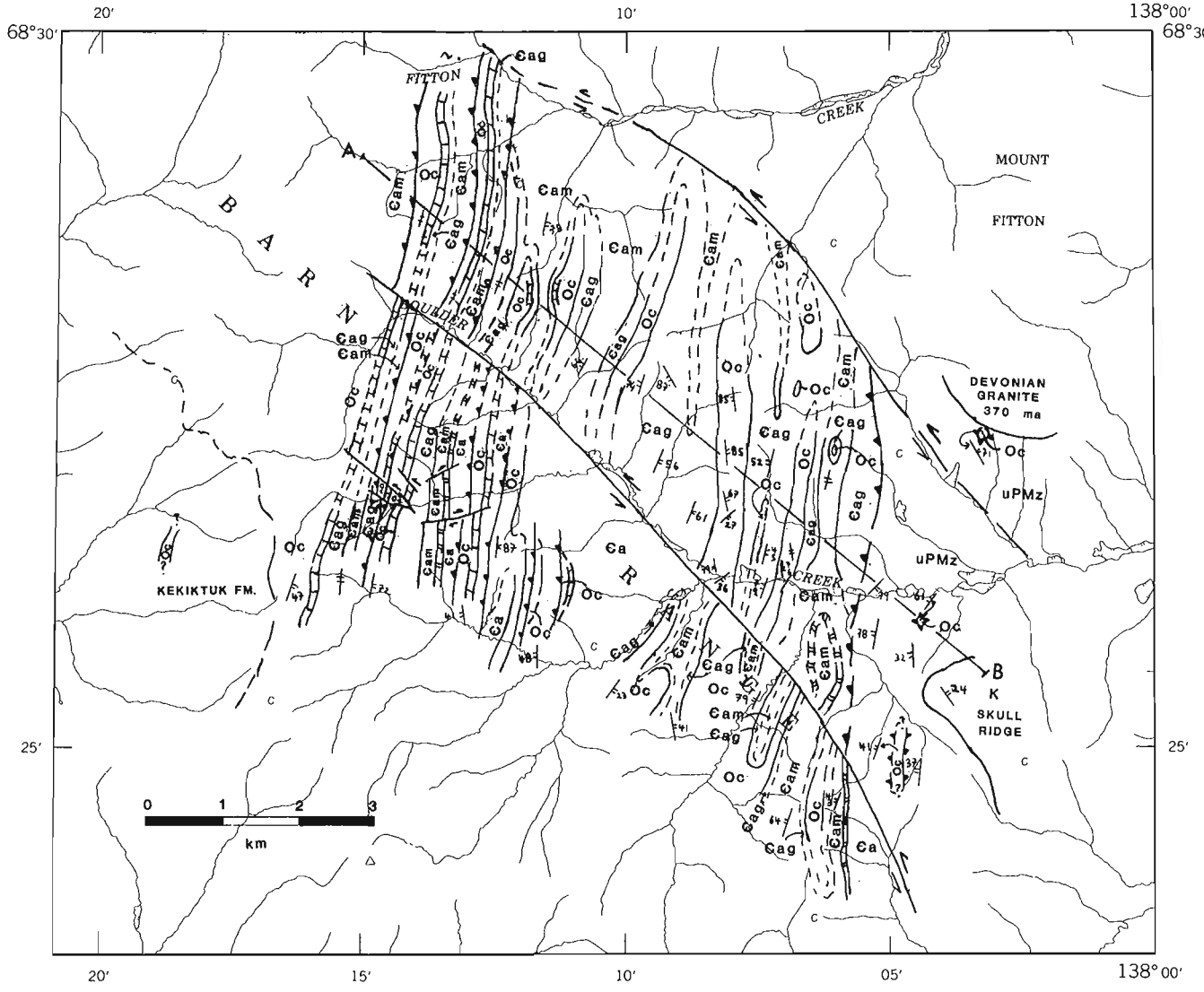

Figure 1. Geological map of Boulder Creek area, Barn Mountains, Yukon Territory, and geological cross-section AB.

in folds and thrusts, and on published data from other parts of the uplift, a stratigraphic succession can be established for the core of the Barn Uplift (Fig. 1).

Stratigraphy of core units

The entire stratigraphic succession within the core of the uplift consists of 500 to 800 m of Lower Cambrian to Silurian shale, which can be divided into three major units: Cambrian argillite, Ordovician chert and Silurian shale. The major units commonly contain one or more additional mappable units.

The oldest stratigraphic unit, the "Cambrian argillite" ($\mathcal{C}_a$), consists of 200 to 500 m of drab green or maroon and green argillites (both containing thick units of quartzite), and minor limestone. In the study area, the Cambrian argillite may be divided into a lower succession of maroon and green argillite and an upper succession of drab green argillite. There is a large range in the apparent thickness of the units (Fig. 1), which is likely the result of both facies colour changes and structural repetition. A mappable succession of limestone was also found within the maroon and green unit. Strata beneath the limestone were not well exposed and their typical colour is not known. Cambrian argillites commonly preserve trace

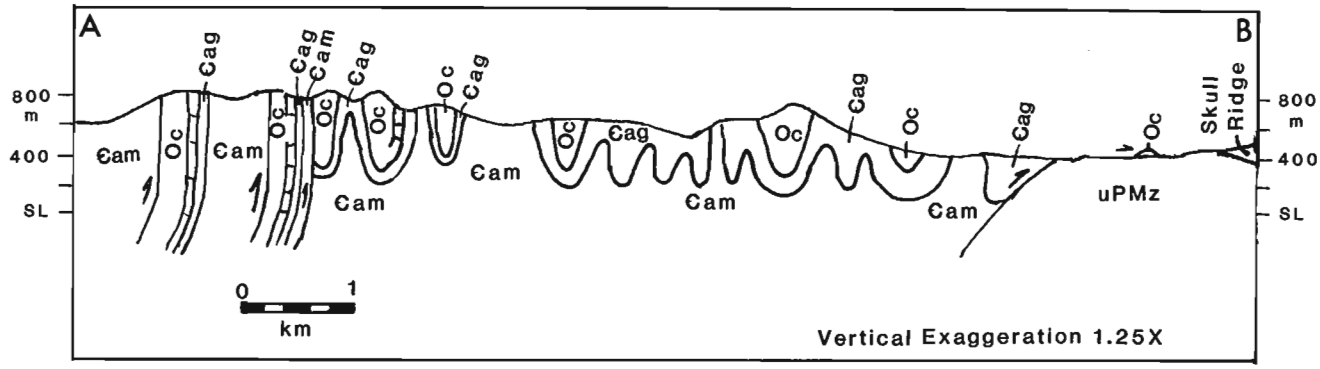

LEGEND - Figure 1

uPMz — Upper Paleozoic to Lower Cretaceous, black weathering shale, siltstone; minor sandstone, chert pebble conglomerate.

K — Kekiktuk Formation – Lower Carboniferous (Viséan) chert pebble conglomerate.

Oc — Ordovician chert: in the lower part, thin bedded, argillaceous chert; in the upper part, blocky, massive, dark-grey, white and commonly malachite green.

Ordovician chert, limestone "member": thin bedded grey to buff limestone.

Ca — Cambrian argillite: green (Cag) and, maroon with green (Cam) argillite, with minor units of quartzite and limestone.

Cambrian argillite, limestone "member": Buff weathering thin bedded limestone.

thrust fault; known, assumed . . . .

strike-slip fault; known, assumed . . . . . .

geological contact; known, assumed . . . . . .

bedding, tops unknown (although stratigraphic succession is known, internal folding makes unequivocal determination of individual facing directions difficult) 79

fossils and are bioturbated. One common trace fossil resembles Planolites sp., and specimens of the trace fossil Oldhamia sp. have been collected from this unit elsewhere in core strata of the Barn Uplift (A.W. Norris, pers. comm., 1981). The occurrence of these fossils indicates that this unit is probably of Early Cambrian age (Hofmann and Cecile, 1981).

The Cambrian argillite unit is overlain by the "Ordovician chert" (Oc), an approximately 200 m thick, ridge-forming succession of siliceous argillite and chert. The lower half of this succession consists dominantly of thinly bedded siliceous argillite or argillaceous chert, and the upper half of massive chert containing thick, extensively bioturbated beds. The upper half commonly displays a prominent, malachite-green weathering colour that is visible only in hand specimen. In the western half of the Barn Uplift, the lowermost beds of the Oc unit contain a mappable succession of 50 to 100 m of white to buff weathering, thin bedded, ripple crosslaminated limestone — the "Ordovician chert, limestone member". There are typically a few metres of chert below this limestone that are included with the limestone unit to facilitate mapping (Fig. 1). Graptolites found in this succession along the study corridor were all of Ordovician age. In a measured traverse to the north of cross-section AB (Fig. 1), Lenz and Perry (1972) found Lower and lower Middle Ordovician (lower, middle and upper Arenigian, and Llanvirnian) graptolites in shales associated with this unit.

Core strata in the area of the cross-section include no rocks younger than the Oc unit. However, Silurian graptolites have been collected from black shales to the north of this area (Lenz and Perry, 1972) and to the south (Norris, 1981), and therefore the youngest stratigraphic unit within the core of the uplift is inferred to be a succession of Silurian black shale.

It is interesting to note that the stratigraphic succession, overall thickness of units, facies assemblages, and, to a lesser degree, structural styles of the core units of the Barn Uplift are very similar to strata found in the outer parts of the Selwyn Basin. In the Niddery Lake map area, equivalent rocks, in ascending order, consist of: 50 to 100 m of Cambrian maroon argillites containing the trace fossils Planolites sp., Oldhamia radiata, Oldhamia? sp. and Gordia? sp.; 400 m of Cambrian, buff weathering, green argillite with minor quartzite, carbonate, chert and volcanic strata; 80 to 130 m of Lower to Middle Ordovician chert with the upper part bioturbated and locally coloured malachite green, and also locally containing a lower member of limestone; and finally, a 15 to 25 m thick succession of green Silurian argillite with black shale (Hofmann and Cecile, 1981; Cecile 1986a). Like the core strata of the Barn Uplift, equivalent rocks in the Niddery Lake map area are tightly folded and/or stacked in imbricate thrusts, although the Niddery strata appear to be considerably more foreshortened (to less than a third of their original extent; Cecile, 1986b). The similarity between the strata of the Selwyn Basin and those of the Barn uplift is attributed to their having had a similar facies position (distal part of the Cordilleran miogeocline) at the time of deposition, and similar mechanical properties during deformation.

Stratigraphy of flanking units

On the west side of the uplift, ridges of Oc unit are truncated by chert-pebble conglomerates of the Lower Carboniferous Kekiktuk Formation. The configuration of the two units, coarseness of the conglomerate, and presence of a regolith in Ordovician chert near the contact, suggest that it is close to an exhumed pre-Kekiktuk erosional surface.

On the east side of the uplift, Cambrian argillites are in fault contact with a succession of steeply dipping black siliceous shale and siltstone with chert-granule sandstone and chert-pebble conglomerate. Norris (1981) mapped a unit in this position that he describes as the Lower Cretaceous Blow River Formation. However, the overall appearance and internal stratigraphy of this unit are atypical of the Lower Cretaceous Blow River Formation. Farther to the east this unit is overlain by moderately east dipping Lower Cretaceous Skull Ridge conglomerates. Because no units similar to this are known from the core of the uplift, the conglomerates are therefore likely to be late Paleozoic or Early Cretaceous in age.

Structure

The Barn Uplift has been subjected to at least two phases of deformation. The abrupt truncation of steeply dipping core strata by late Paleozoic strata indicates a post- Late Silurian and pre-Early Carboniferous deformation ("Ellesmerian"). Evidence for an "Ellesmerian" deformation are widespread in the northern Yukon (Norris and Dyke, 1987; Norris and Yorath, 1981). The presence of post-Early Cretaceous age thrusts, with north-northwest and northwest trends, in younger units to the west of the uplift, show that a second phase of deformation occurred, which may have produced the actual uplift itself (Dyke, 1974). The presence of a large thrust fault that placed Cambrian argillites on the west against upper Paleozoic — Lower Cretaceous strata on the east (Fig. 1) supports that hypothesis. The presence of what are apparently Ordovician klippen more than one kilometre east of this thrust shows some degree of overthrusting on a shallowly dipping fault surface. The degree to which core strata of the Barn uplift were deformed by the "Ellesmerian" as opposed to younger deformation(s) is yet to be determined.

Considering the small scale of folds and thrusts, the master detachment unit for all core structures is likely the Cambrian argillite sequence (Fig. 1). The western domain consists of more than four imbricate thrusts. Each thrust sheet is between 200 and 1000 m thick and, within the thrust, strata young to the west. Fault planes are vertical or steeply east or west dipping. The eastern domain consists of as many as seven, tight, upright to slightly east or west verging folds. The horizontal distance between syncline axes varies between 500 and 1500 m.

The youngest structures in the area are a set of northwest striking, left-lateral faults with offsets of less than one kilometre. These faults cut all pre-existing structures.

REFERENCES

Bamber, E.W. and Waterhouse, J.B.
1971: Carboniferous and Permian stratigraphy and paleontology, northern Yukon Territory; Bulletin of Canadian Petroleum Geology, v. 19, no. 1, p. 29-250.

Cecile, M.P.
1986a: Niddery Thrust Sheet — a Selwyn Basin structural feature (Abs.); Geological Association of Canada, Program with Abstracts, v. 11, p. 54.
1986b: Geology of east and northeast Niddery Lake map area, Yukon and N.W.T. (N.T.S. 105O/7N1/2, 8N1/2, 9, 10, 15, 16); Geological Survey of Canada, Open File Report 1326.

Dyke, L.D.
1974: Structural investigations in Barn Mountains, northern Yukon Territory; *in* Report of Activities, Part A, Geological Survey of Canada, Paper 74-1A, p. 525-532.

Hofmann, H.J. and Cecile, M.P.
1981: Occurrence of Oldhamia and other trace fossils in Lower Cambrian (?) argillites, Niddery Lake (105O) map area, Selwyn Mountains, Yukon Territory; *in* Current Research, Part A, Geological Survey of Canada, Paper 81-1A, p. 281-290.

Lenz, A.C. and Perry, D.G.
1972: The Neruokpuk Formation of the Barn Mountains and Driftwood Hills, northern Yukon; its age and graptolite fauna; Canadian Journal of Earth Sciences, v. 9, p. 1129-1138.

Norris, D.K.
1972: Structural and stratigraphic studies in the tectonic complex of northern Yukon Territory, north of Porcupine River; *in* Report of Activites, Part B, Geological Survey of Canada, Paper 72-1B, p. 91-99.
1981: Geology of Blow River and Davidson Mountains; Geological Survey of Canada, Map 1516 A (1:250 000).

Norris, D.K. and Dyke, L.D.
1987: The Ellesmerian orogeny in northern mainland Canada (Abs.); Canadian Society of Petroleum Geologists, Second International Symposium on the Devonian System, Program and Abstracts, p. 178.

Norris, D.K. and Yorath, C.J.
1981: The North American plate from the Arctic Archipelago to the Romanzof Mountains; *in* The ocean basins and margins, Arctic Ocean, v. 5, chap. 3, The Arctic Ocean, E.M. Nairn, M. Churkin, Jr., and F.G. Stehli (eds.); Plenum Press, p. 37-103.

Stratigraphy and structure of the late Proterozoic Miette Group, northern Selwyn Range, Rocky Mountains, British Columbia

Michael R. McDonough[1] and Philip S. Simony[1]
Institute of Sedimentary and Petroleum Geology, Calgary

McDonough, M.R. and Simony, P.S., Stratigraphy and structure of the late Proterozoic Miette Group, northern Selwyn Range, Rocky Mountains, British Columbia; in Current Research, Part D, Geological Survey of Canada, Paper 88-1D, p. 105-113, 1988.

Abstract

Three informal map units are recognized within the upper Proterozoic Miette Group of the northernmost part of the Selwyn Range of the Rocky Mountains. A pelite and quartzite succession of previously unknown affinity is assigned lower Miette status. This unit underlies a thick sequence of conglomeratic sandstones and green pelite belonging to the middle Miette. The upper Miette, consisting of a sequence of dark calcareous pelites and black limestone, with minor sandstone, lies conformably over the middle Miette. The middle Miette is markedly thinner on the west side of the study area. Thinning is attributed to a topography that restricted deposition. A continuous and widespread marker unit, comprising green pelite, carbonate, and black pelite is found near the middle of the middle Miette.

The structure of the northernmost Selwyn Range is dominated by a series of large, upright F_2 folds that form an anticlinorium in the hanging wall of the Moose Lake Thrust, which truncates the west limb of the Mount Robson Synclinorium. Pelites of the lower and upper Miette are thickened primarily by folding and foliation development. Middle Miette strata are thickened both by folding and thrust faulting. Pre-F_2, east verging, bedding-parallel thrusts that thicken the middle Miette are recognized for the first time.

Résumé

On a identifié trois unités cartographiques non formellement reconnues dans le groupe de Miette du Protérozoïque supérieur, qui occupe la partie la plus septentrionale du chaînon Selwyn dans les montagnes Rocheuses. Une succession pélitique et quartzitique d'affinité jusque-là inconnue a été placée dans la partie inférieure du groupe de Miette. Cette unité repose sous une épaisse séquence de grès conglomératiques et de pélites vertes appartenant à la partie intermédiaire du groupe de Miette. La partie supérieure de ce groupe, qui se compose d'une séquence de pélites calcaires sombres et de calcaires noirs, ainsi que d'une petite quantité de grès, repose en concordance sur la partie intermédiaire du groupe de Miette. Cette partie intermédiaire est nettement plus mince du côté ouest de la région à l'étude. On attribue l'amincissement à une topographie qui limitait la sédimentation. Une unité repère continue et étendue, qui se compose de pélites vertes, de roches carbonatées, et de pélites noires, se manifeste près du milieu du niveau intermédiaire de Miette.

La structure de la partie la plus septentrionale du chaînon Selwyn est dominée par une série de grands plis verticaux F_2 qui forment un anticlinorium au toit du chevauchement de Moose Lake, lequel tronque le flanc ouest du synclinorium de Mount Robson. L'épaississement des pélites de la partie inférieure et de la partie supérieure de Miette est dû principalement à la formation de plis et à la foliation. Les strates de la partie intermédiaire de Miette sont épaissies à la fois par des plissements et des failles chevauchantes. Les chevauchements parallèles au litage, antérieurs à F_2 et inclinés vers l'est, responsables de l'épaississement du niveau intermédiaire de Miette, ont été identifiés pour la première fois.

[1] Department of Geology and Geophysics, University of Calgary, Calgary, Alberta T2N 1N4.

INTRODUCTION AND PREVIOUS WORK

The study area comprises approximately 300 km^2 between Moose Lake and Tête JauneCache, lying east and northeast of Valemount, British Columbia, and forms the northernmost part of the Selwyn Range of the Rocky Mountain Main Ranges subprovince (Fig. 1). Mapping was conducted at 1:24 000 scale as part of a project designed to elucidate the structure, stratigraphy and strain hisotry of Miette Group rocks.

Campbell (1968) assigned the strata of the Selwyn Range to the Miette Group of the Windermere Supergroup. To the northwest, a similar succession of Miette Group rocks in the McBride map area was divided informally into lower, middle, and upper units by Campbell et al. (1973). In 1986, McDonough and Simony tentatively divided Miette strata of the northern Selwyn Range into informal 'lower' and middle units. At that time it was not known if 'lower' Miette pelites and quartzites were conformably overlain by middle Miette sandstones and conglomerates, or if an early thrust fault separated the two, placing middle Miette onto a pelitic succession of possible upper Miette affinity. Alternatively, it was thought that the conglomeratic sandstones could be basal lower Miette that had been thrust onto a pelitic succession belonging to the 'lower' Miette.

Units of 'lower' and middle Miette have been mapped northwestward and are found to underly a pelite and carbonate succession that is typical of the upper Miette. Thus, the Miette Group in the northern Selwyn Range is characterized by having distinct lower, middle, and upper units. A continuous and widespread marker within the middle Miette shows that the middle Miette is considerably thinner on the west side of the area (Figs. 2, 3). The boundary between lower and middle Miette reported by McDonough and Simony (1986) has been revised.

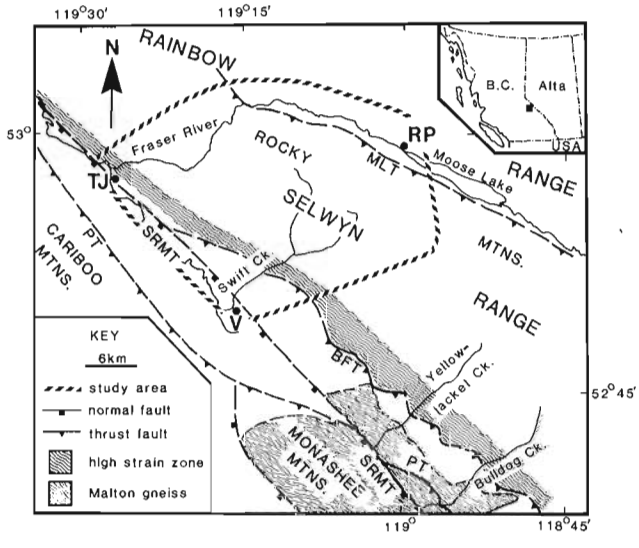

Figure 1. Location map and generalized geological map of the northern Selwyn Range and adjacent ranges. Data are from Campbell (1968), Mountjoy (1980), McDonough (1984), and McDonough and Simony (1986); V, Valemount; TJ, Tête Jaune Cache; RP, Red Pass; MLT, Moose Lake Thrust; BFT, Bear Foot Thrust; PT, Purcell Thrust; SRMT, Southern Rocky Mountain Trench.

STRATIGRAPHY

A maximum thickness of 4 km of Miette strata are exposed in the northern Selwyn Range (Fig. 2). These strata constitute three informal lithological units called lower, middle, and upper Miette, which essentially are continuous with the divisions of the Miette Group in the McBride and Mount Robson map area.

There is a minimum of 850 m of structurally thickened lower Miette exposed in the study area (Fig. 2), and a maximum of 3 km is estimated from cross-sections. Thickening of these strata was accomplished primarily by two phases of folding, F_1 and F_2, and development of S_1 and S_2 foliations. The lower Miette is composed mostly of recessive, dark grey to black, chloritoid-bearing phyllites and phyllitic schists with lesser bands of fine to medium grained, light brown to white quartzites, and rare, thin beds of black, silty limestone. Numerous mappable bands of quartzite are present in the lower Miette; the most notable one occurs 300 m below the base of the middle Miette (Fig. 2). This quartzite unit outlines Terry Fox Anticlinorium (McDonough and Simony, 1986) and Swift Anticline to the east.

The lower Miette is conformably overlain by a 2300 to 2600 m thick sequence that is dominated by thick bands of sandstone and conglomerate containing bands of green pelite and subordinate bands of black pelite (Fig. 2) that closely resembles middle Miette elsewhere in the Main Ranges (Charlesworth et al., 1967; Carey and Simony, 1985; Mountjoy and Forest, 1986; McDonough and Simony, 1986). The middle Miette can be divided into three distinct units. Two thick sequences dominated by coarse clastics are separated by a marker unit of green pelite and carbonate of possible regional significance (Figs. 2, 3). Individual middle Miette conglomeratic sandstone units are generally continuous, and can be "walked out".

We have revised the lower-middle Miette contact to the base of the lowest thick bedded conglomeratic sandstone band (cf. McDonough and Simony, 1986), above which the pelite map units are green or grey-green. Below this unit the pelites are no longer green, but are dark grey, and the clastic bands are fine grained quartzites. At the base of the middle Miette near the head of the Swift Creek watershed, there is a cliff- forming unit of thick bedded sandstone and granule-to-small-pebble conglomerate that is in sharp contact with the recessive dark grey phyllitic schists below it. The basal sandstone band thins and becomes finer grained toward the west before it pinches out under Terry Fox Anticlinorium (Figs. 2, 3, 5). Thus, the middle Miette thins westward, and the base of the middle Miette in the western part of the area is higher up in the succession than the base in the east (Fig. 2).

On the east side of the area, overlying the basal conglomeratic sandstone band of the middle Miette, is a thick green phyllite unit (Fig. 2). It contains numerous thin and unmappable sandstone beds, and a few mappable lenses of sandstone in its upper part, forming a gradational contact with the second conglomeratic sandstone band in some sections. This is the gradational contact we described previously as the base of the middle Miette in Swift Syncline (McDonough and Simony, 1986).

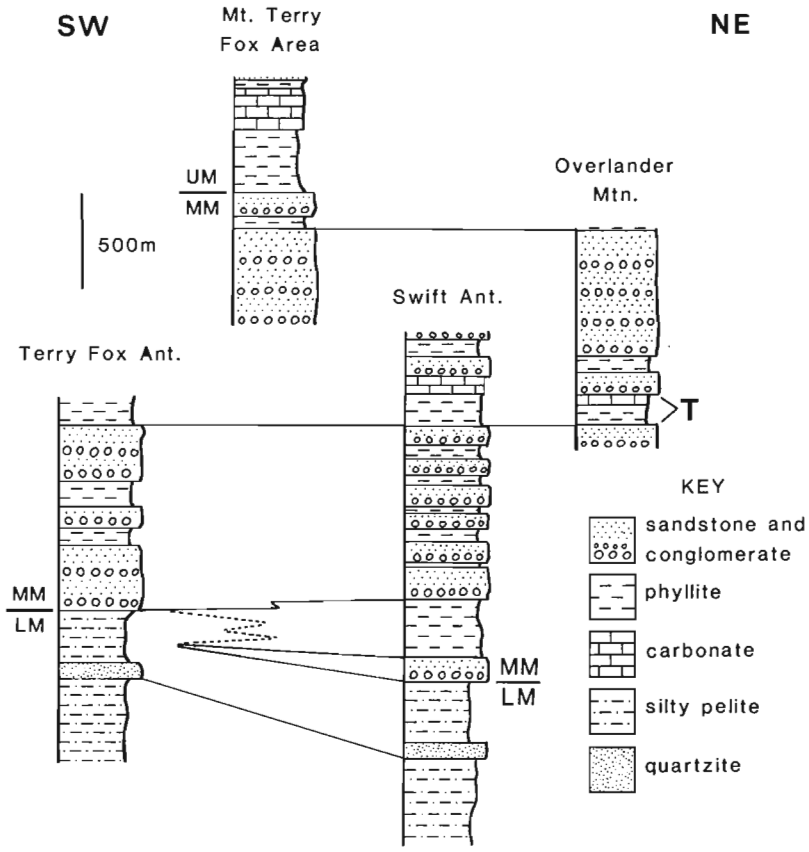

Figure 2. Stratigraphic columns for the Miette Group of the northern Selwyn Range; LM, lower Miette; MM, middle Miette; UM, upper Miette; T, triad marker. Locations are given in Figure 3.

Figure 3. Geological map of the northernmost Selwyn Range and adjacent parts of the Rainbow Range. Red Pass Thrust and lower Cambrian-upper Miette contact from Mountjoy (1980); TJ, Tête Jaune Cache; RP, Red Pass; MTF, Mount Terry Fox; OM, Overlander Mountain.

A widespread marker that occurs near the middle of the middle Miette comprises a triad of green phyllite carbonate, and black phyllite (Figs. 2, 3). It is composed of a 120 to 200 m thick basal green phyllite member that is overlain by a 20 to 100 m thick carbonate member, which is capped by a thin, 0 to 12 m thick black phyllite member.

The basal green phyllite member of the triad contains thin interbeds of siltstone and argillaceous green sandstone. Its distinct green colour is due to a high chlorite content. The basal unit is thickest (200 m) west of Overlander Mountain (Fig. 3), where the overlying carbonate member is thinnest and most argillaceous. There, the contact between green pelite and carbonate is gradational; 2 to 5 m thick beds of silty green phyllite are intercalcated with 1 to 4 m thick beds of silty, orange weathering limestone.

The carbonate member of the marker is composed of three laterally equivalent facies, informally designated A, B, and C, in a general east to west distribution. Facies A is found in the eastern part of the area, and is up to 100 m thick. It is composed of rhythmically bedded, argillaceous, calcareous and dolomitic siltstones. Facies A has 5 to 10 cm thick beds displaying sharp bases of reddish orange dolomitic siltstone with 1 mm thick intercalations of fine grained, white sand lenses. Red siltstones fine upward into argillaceous, calcareous, light brown siltstone with intercalated white siltstone laminae. Upward fining rhythmic beds are suggestive of a turbiditic depositional regime for facies A of the carbonate member.

Facies B is 20 m thick, and is exposed west of Overlander Mountain (Fig. 3). It is composed of thin (2-5 cm) interbeds of silty brownish orange limestone and green phyllite, and is transitional between facies A and C.

Facies C occurs throughout the western part of the area. It consists of 30 to 40 m of orange weathering, slightly silty, white limestone with abundant millimetre scale plane laminae and lesser small-scale trough crossbedding. White limestone beds 5 to 8 cm thick are interbedded with 1 to 3 cm thick beds of light brown, dolomitic siltstone. Some plane laminae in white limestone are composed almost entirely of fine grained calcite with a minor argillaceous content, and possibly are cryptalgal in origin.

The black pelite cap that overlies the carbonate member is a thinly bedded, slightly silty, carbonaceous black phyllite. It is missing in Swift Synclinorium between Swift Creek and its southern tributary (Fig. 3). There, the presence of carbonate rip-up clasts in the overlying sandstone band is suggestive of syndepositional erosion of limestone, as well as of the black phyllite member.

Overlying the marker in the middle Miette is a thick sequence of sandstones and conglomeratic sandstones that contains relatively few mappable pelite units (Fig. 2). The amount of interbedded pelite within the sandstone bands is greater than that of the bottom part of the middle Miette, however.

A minimum of 600 m of upper Miette strata conformably overlie the middle Miette in the northern Selwyn Range (Fig. 2). In a manner analgous to that used in defining the lower-middle Miette contact, we place the middle-upper Miette contact at the top of the highest thick bedded, mappable conglomeratic sandstone band. Below this contact the pelite units of the middle Miette are predominantly green. The upper Miette succession above this contact is dominated by dark grey to dark brown, calcareous phyllites with minor thin sandstone beds in the basal part. The basal phyllite unit comprises 330 m of dark silty phyllite with thin interbeds of limestone in its upper part (Fig. 2). Within this phyllite unit, a 1.5 m thick, calcite cemented, limestone and quartz-pebble conglomerate bed is found approximately 300 m above the base of the upper Miette.

Overlying the basal pelite of the upper Miette is a 200 m thick, cliff-forming, silty to sandy, black limestone unit, which locally contains beef calcite. The black limestone unit is overlain by 70 m of brown phyllites with minor thin interbeds of coarse grained sandstone and granule conglomerate (Fig. 2).

The upper Miette succession of brown pelite, calcareous pelite, black limestone, and minor coarse grained sandstone contrasts with the dark grey pelite and fine to medium grained quartzite succession of the lower Miette.

STRATIGRAPHIC CORRELATION AND INTERPRETATION

The basal conglomeratic sandstone band of the middle Miette in the eastern side of the study area (Fig. 2) can be correlated with Mountjoy and Forest's (1986) unit G2 of their lower Miette in the southern Selwyn Range, on the basis of lithological similarity, thickness, and position within the stratigraphic column (Fig. 4). The second conglomeratic sandstone band of the middle Miette may then be correlated with Mountjoy and Forest's (1986) basal middle Miette unit, and the quartzite marker in the lower Miette of the northern Selwyn Range can be correlated with their lower Miette unit G1 in the southern Selwyn Range (Fig. 4).

The green pelite-carbonate marker unit within the middle Miette is a distinctive marker than can be "walked-out" throughout the northern Selwyn Range (Fig. 3). It can be traced around the hinge of Terry Fox Anticlinorium, and is the same marker as that within the conglomeratic sandstone succession on the west limb of Terry Fox Anticlinorium on the ridges southeast of Swift Creek (Figs. 1, 2). Thus, the conglomeratic sandstones on the west limb of Terry Fox Anticlinorium are indeed middle Miette, as proposed by McDonough and Simony (1986). The marker triad (green pelite- carbonate-black) bears a lithological resemblance to a marker reported by Pell and Simony (1987) in the southern Cariboo Mountains (Fig. 4), and one observed by Ross and Murphy (in press) in the Cariboo Mountains west of the McBride, British Columbia. Both of these markers in the Cariboos occur at the top of the middle Kaza Group, below a thick sequence of conglomeratic sandstones of the upper Kaza. On the basis of the presence of the marker, and its overall thickness, and lithological similarity, the middle Miette can be correlated with the middle and upper Kaza as originally proposed by Young (1969) and Campbell et al. (1973).

The marker of the Selwyn Range also is very similar in lithology and thickness to the Meadow Creek section of

the Old Fort Point Formation of the Jasper, Alberta area (Charlesworth et al., 1967). The triad units in the Selwyn Range can be correlated practically one for one with Charlesworth et al.'s unit 2 of member B (green slate and siltstone), unit 3 of member B (limestone and interbedded slate), and unit 1 of member C (blue grey slate), of the Old Fort Point Formaton (Fig. 4).

If Aitken's (1969) correlation of the Old Fort Point Formation with the red and green slates of the Hector Formation near Lake Louise, Alberta (Fig. 4) is correct, then the upper part of the middle Miette in the northern Selwyn Range (e.g. Overlander Mtn. section in Fig. 2) is equivalent to the Hector Formation. The lower half of the middle Miette would then be equivalent to the Corral Creek Formation, which Aitken correlated with the Meadow Creek Formation (Fig. 4). An implication of this interpretation is that the Old Fort Point Formation is sandwiched between two intervals of coarse clastic deposition, and was not deposited directly on basement, as suggested by Mountjoy and Price (1985).

Upper Miette strata of the northern Selwyn Range can be correlated with the Isaac Formation of the Cariboos (Campbell et al., 1973; Pell and Simony, 1987) on the basis of lithological similarity and stratigraphic position (Fig. 4). Both sections overlie a thick sequence of coarse clastics (middle Miette in the Rockies and upper Kaza in the Cariboos), and contain a succession of dark pelites with thin sandstone beds near the base. In each section this lower unit grades upward into calcareous pelite with siltstone, before passing into a black silty carbonate unit.

The apparent thinning of the middle Miette toward the west might possibly be explained by a major, early, west verging thrust fault that cuts upsection through the bottom part of the middle Miette, similar to the Pleasant Valley Thrust of Struik (1986). However, the presence of a gradational contact between a thick sand- and conglomerate-bearing pelite unit and the second cliff-forming conglomeratic sandstone interval of the middle Miette suggests that an early, flat-lying thrust fault is not present at this level in the middle Miette. Except for the basal sand and conglomerate unit of the middle Miette, which becomes finer grained and pinches out on the west limb of Swift Syncline (Figs. 2, 3), individual map units of the middle Miette are continuous and do not exhibit west verging cutoffs or early folds that would corroborate an early, west verging thrust fault.

Alternatively, a thin deposit of middle Miette on the west side of the area may be related to a Late Proterozoic structural high. The carbonate marker, as well as individual sandstone and conglomerate units in the middle Miette, thin westward, which is suggestive of syndepositional topography. Westward thinning of the middle Miette, and the presence of conformable relationships at the bases of the lowest two conglomeratic sandstones, suggest that the middle Miette is "glued" to the lower Miette. The westward thinning deposits are on strike with the thin Upper Proterozoic and lower Cambrian deposits of the McBride Arch (Young, 1979), and nearly on strike with the thin lower Miette strata on the basement rocks to the southeast (Fig. 1; McDonough, 1984).

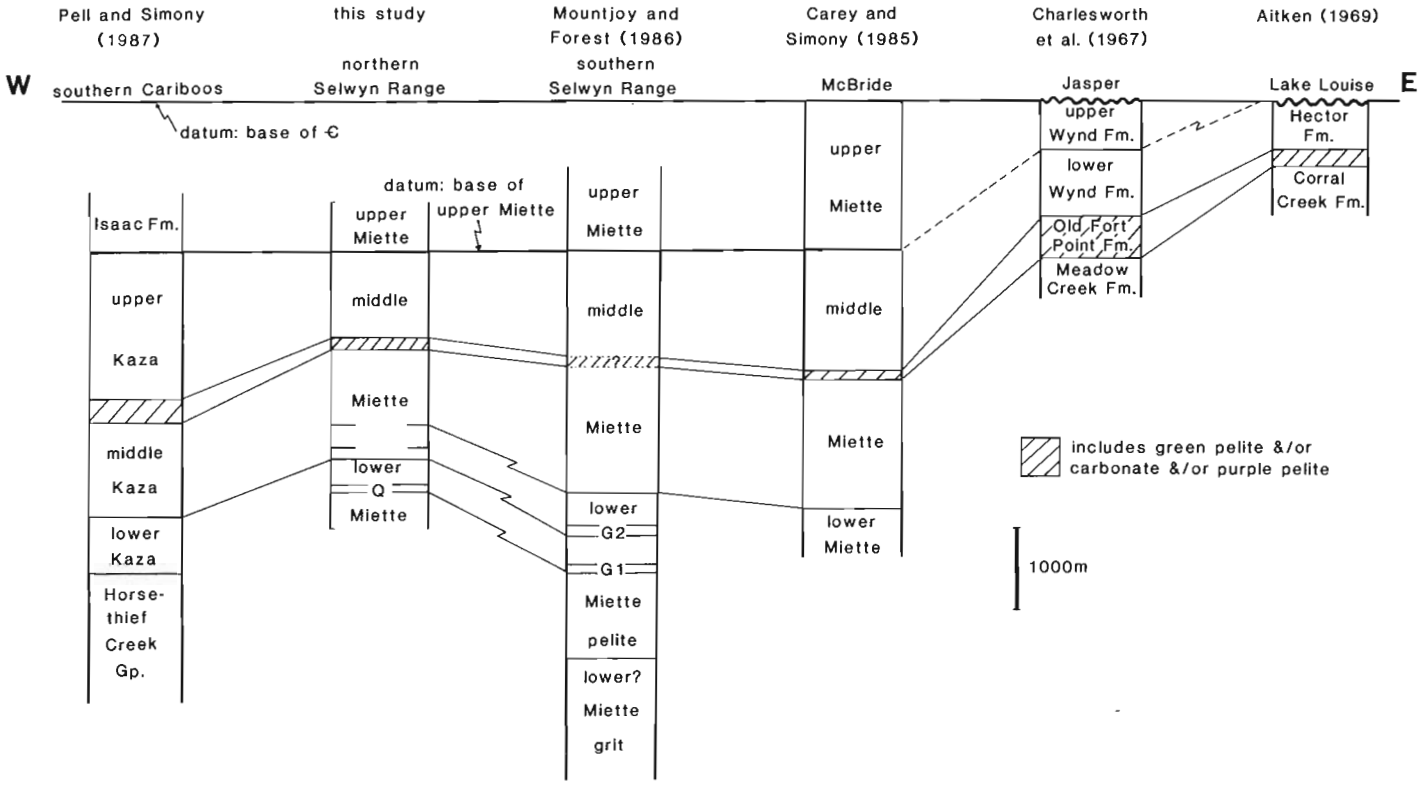

Figure 4. Stratigraphic correlation chart for Miette Group.

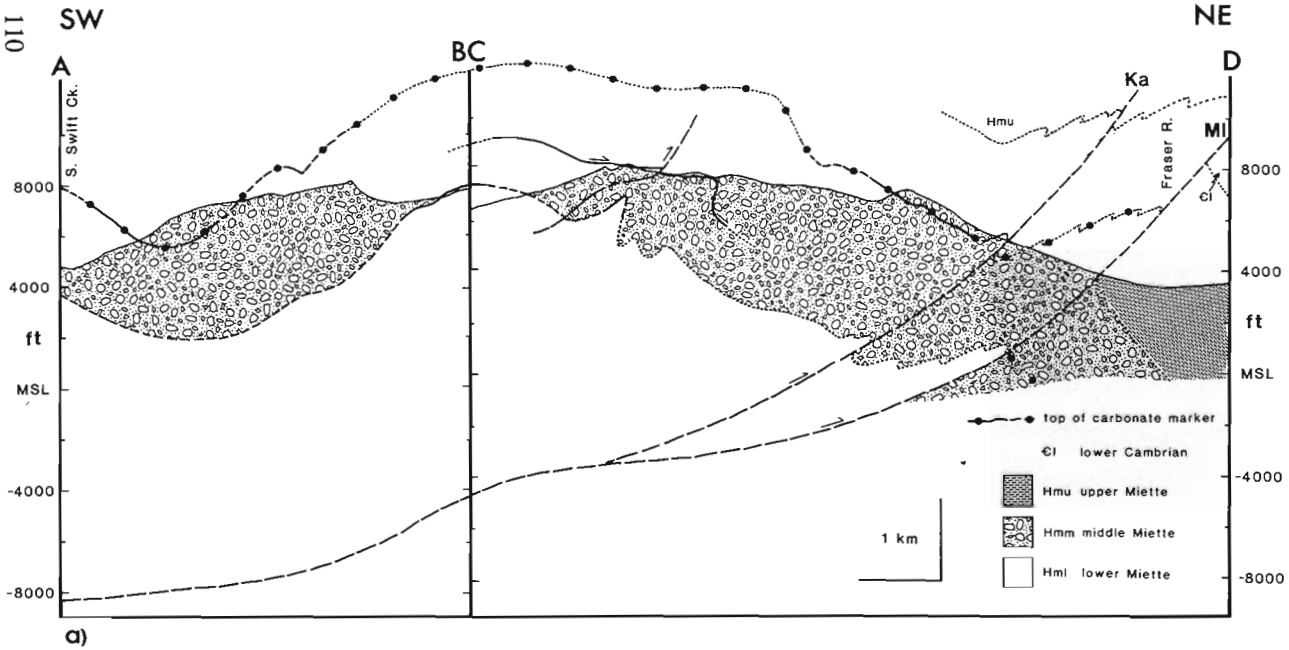

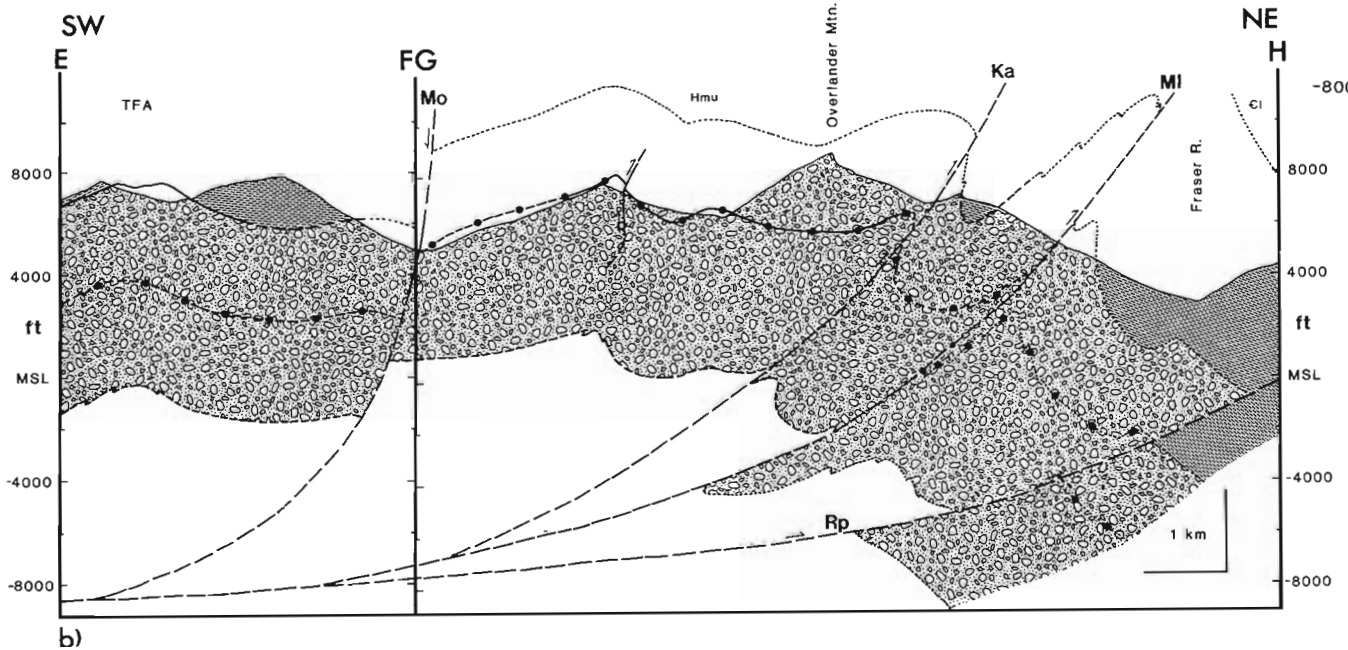

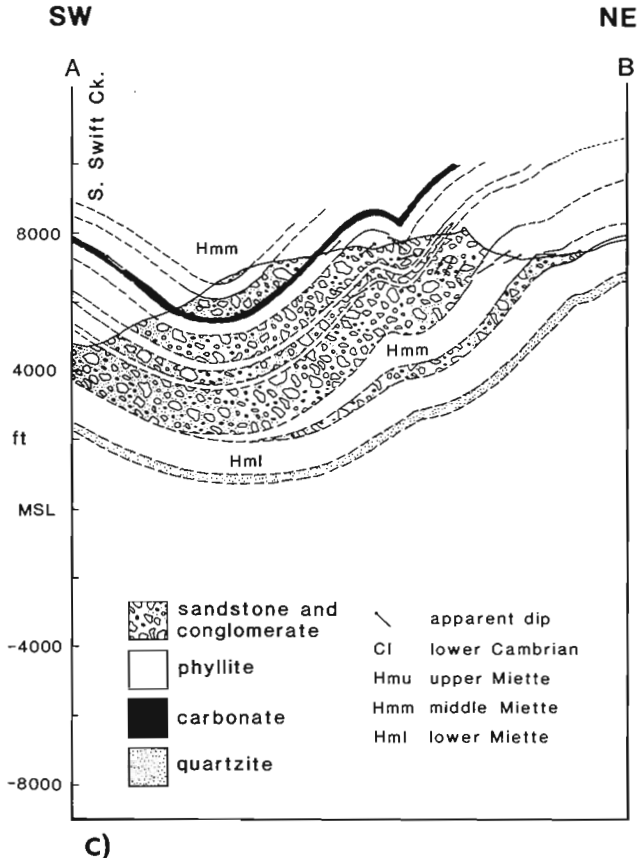

Figure 5. Cross-sections (1:1) along section lines A-B-C-D and E-F-G-H. The Red Pass Thrust Sheet shown in b) forms part of the west limb of the Robson Synclinorium. The section in c) shows in detail the structure of the western part of a). Ml, Moose Lake Thrust; Rp, Red Pass Thrust; Ka, Klapperhorn Thrust; Mo, Morey Fault; TFA, Terry Fox Anticlinorium. Lines of section are given in Figure 3.

STRUCTURAL GEOLOGY

The structure of the northernmost Selwyn Range is dominated by six, major F_2 folds that form a composite anticlinorium in the hanging wall of the Moose Lake Thrust (Figs. 3, 5). The east limb of this anticlinorium is cut by the Moose Lake and Red Pass thrusts, but the stratigraphy is essentially continuous with that of the Mount Robson Synclinorium to the east. No major regional thrust faults exist between Moose Lake Thrust and Bear Foot Thrust (Fig. 3). Thus, most of the rocks of the area form part of the Moose Lake Thrust Sheet.

Two phases of folding (F_1 and F_2) and foliation (S_1 and S_2) development that are contemporaneous with thrust motion can be observed in the Moose Lake Thrust Sheet. Superimposed on these structures developed during a minor phase of thrusting that occurred during the latter part of the second phase, and a later phase of west-side down normal faulting. A minor phase of dextral oblique-slip faulting that postdates F_2 also was observed.

The relationship of bedding to S_1 and S_2 has been described elsewhere (McDonough and Simony, 1986). Two S_2 crenulation cleavages in pelite, one dipping northeast and one dipping southwest, show mutually contradictory cross-cutting relationships, which suggests synchronous development of a conjugate S_2 set. They transect Terry Fox Anticlinorium (TFA) and Swift Synclinorium such that the axial planes of these large F_2 folds nearly bisect the acute angle between the two cleavages.

An early bedding-parallel thrust fault near the base of the middle Miette places middle Miette onto middle Miette, and lies within the second lowest conglomeratic sandstone band of the middle Miette (Figs. 3, 5, 6). The fault is folded by F_2, and probably formed during F_1 time. It is visible as a brown weathering, soil-like horizon with very low-angle footwall cutoffs that indicate northeast vergence, and adds a minimum of 60 m of structural thickness to the middle Miette (Fig. 6). Displacement is on the order of 1 to 2 km, and is distributed eastward along the bedding planes of the faulted unit. Shortening on the fault locally balances the F_1 shortening in the lower part of the middle Miette in its footwall (Fig. 5). Younger, small displacement thrusts either die out into or root into this earlier detachment (Fig. 6).

Near Red Pass, British Columbia (Fig. 3), the Moose Lake Thrust (MLT) places middle Miette onto upper Miette strata (Fig. 5). The thrust loses stratigraphic throw to the

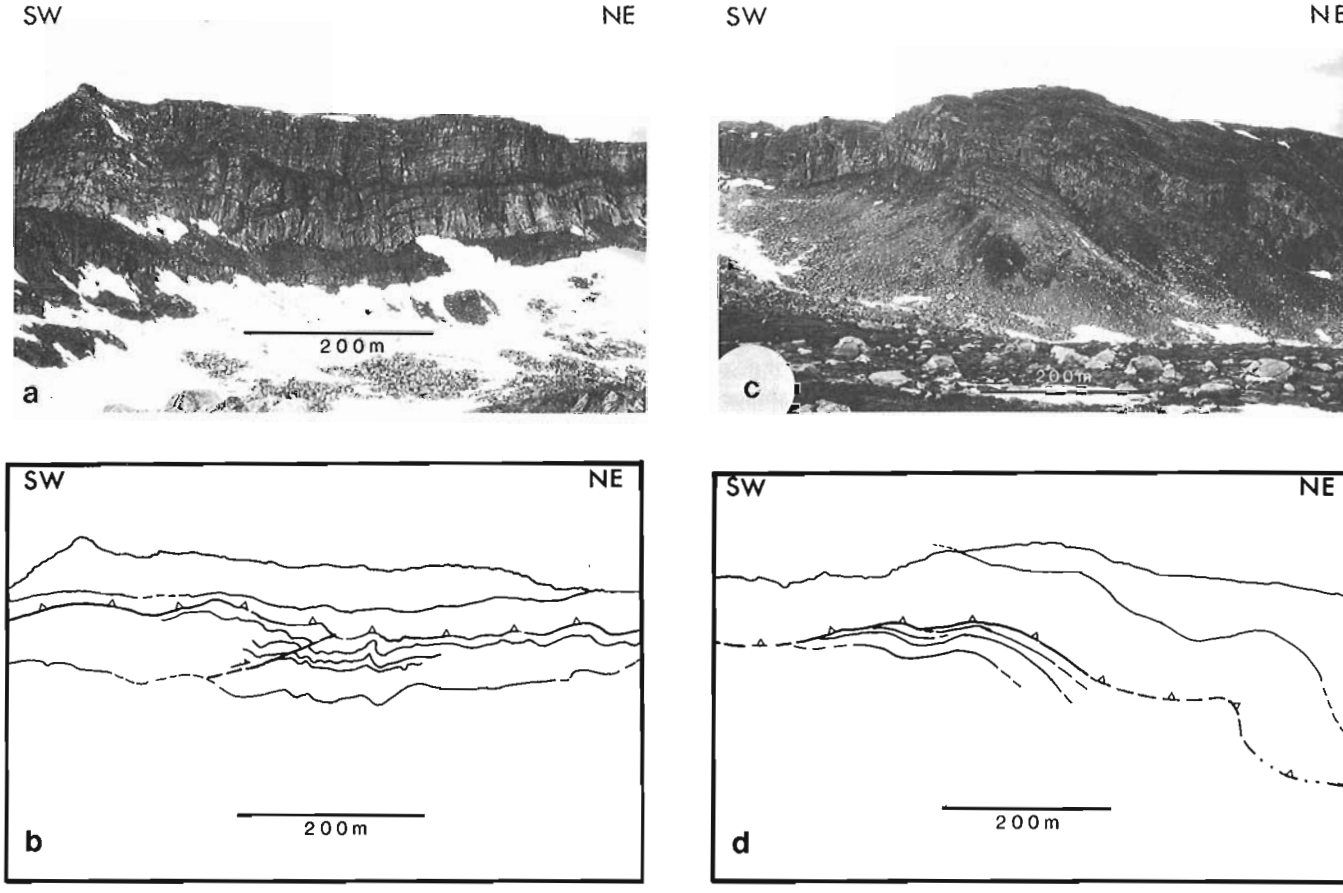

Figure 6. Field photographs and corresponding line diagrams looking northwest at an early thrust fault near the base of the second conglomeratic sandstone unit of the middle Miette. Footwall cutoffs in c) and d) suggest a northeast sense of vergence. The fault balances shortening in its footwall, and adds a minimum of 60 m of structural duplication to the middle Miette.

northwest, and it places middle Miette on middle Miette where the fault crosses the Fraser River valley. Maximum displacement estimates for the Moose Lake Thrust and its imbricates are on the order of 3 to 5 km. The Moose Lake Thrust could be the same fault as the Chatter Creek Thrust (E.W. Mountjoy, pers. comm., 1986), which places middle Miette onto Gog Group near the head of the Fraser River (Mountjoy and Forest, 1986).

First phase folds are important locally, particularly near the Moose Lake Thrust. The existence of recumbent first phase folds at the deepest exposed levels, moderately inclined F_1 at intermediate levels, and upright F_2 at higher structural levels in the hanging wall of the Moose Lake Thrust suggest that motion of the thrust sheet was synchronous with F_1 and F_2. This scenario of increasing axial plane dip with higher structural level suggests that the Sanderson (1982) model of increasing shear strain with depth is applicable to the Moose Lake Thrust (cf. McDonough and Simony, 1986). A step in the fault is postulated to account for the large anticlinorium shown in Figure 5.

The thrust faults near the head of Swift Creek (Fig. 1), shown by Campbell (1968), exist only in part and are not regional in extent. They are reverse faults of less than 100 m displacement that formed late during F_2 in response to room problems in the folds (Figs. 3, 5). One of these small faults exhibits S-C fabric with a downdip stretching lineation of small pebbles that represents the transport direction. Shear is accommodated on C-planes oriented at approximately 130°/45°SW. Associated with C-planes is sigmoidal S_1, which yields a top to the northeast shear couple. The X-direction of the strain ellipsoid plunges 35° to 50° toward 190 to 200°, yielding a transport direction of 010° to 020°. Thus, late F_2 reverse faults are essentially dip-slip, but have a slight dextral component.

A small strike-slip fault that truncates S_2 offsets a 1 m thick sandstone bed on the south side of the Fraser River valley, approximately 5 km east of Tête Jaune Cache (Fig. 3). The attitude of the fault is 107°/70°SW, having a net slip vector that pitches 20°SE. Offset is limited to 1.5 m of dextral strike-slip motion, and 30 cm of dip-slip thrust displacement. This fault is suggestive of an oblique slip regime during the latter part of the deformation, but larger scale dextral structures have yet to be identified.

A normal fault with approximately 1 km of west-side down dip-slip displacement (Fig. 5a) exists in the creek valley that intersects the CN rail line at Morey Siding (Fig. 3). Previously, a major thrust fault was thought to exist in this valley (Fig. 1; Campbell, 1968). The Morey normal fault downdrops the Terry Fox Anticlinorium in its hanging wall, allowing preservation of the upper Miette strata found there. Morey Fault also downdrops the middle-upper Miette contact on the west limb of Robson Synclinorium north of the Fraser River valley (Fig. 3). The fault is hinged to the south where it dies out near the northern termination of Swift Synclinorium (Fig. 3), suggesting that it does not cut Moose Lake Thrust, but is contained within the upper plate of the thrust (Fig. 5b).

A narrow zone of high strain that is oblique to the Rocky Mountain Trench is found on the west limb and core of Terry Fox Anticlinorium (Fig. 1). This zone is 2 to 3 km wide and extends along strike for more than 90 km from Bulldog Creek northwestward to Small River, 30 km northwest of Tête Jaune Cache (Fig. 1). Severely stretched pebbles in coarse grained facies form a b-lineation parallel to axes of northeast verging F_1 and F_2 folds. Pebbles are flattened by S_1 associated with inclined F_1 in the immediate footwall of Bear Foot Thrust to the south of Yellowjacket Creek (Fig. 1), and are deformed by S_2 in the northern part of the zone, where upright and overturned F_2 predominate (McDonough and Simony, 1986; McDonough, 1987). The b-axis lineation that is parallel to F_2 axes on the west limb of Terry Fox Anticlinorium is in marked contrast to the a-axis lineation developed on F_2 thrusts on the east side of the area.

Van Den Driessche and Maluski (1986) observed stretched pebbles at Tête Jaune Cache, and proposed a transpression model with a large, through-going, dextral strike-slip fault in the southern Rocky Mountain Trench. Such faults have yet to be identified, however. Faults in the Rocky Mountain Trench southeast of Valemount are Tertiary brittle normal faults. The small dextral strike-slip fault discussed above truncates S_2, and therefore postdates F_2 stretched pebble lineations. Middle Miette stratigraphy can be mapped continuously from the eastern part of the Selwyn Range up to the Bear Foot Thrust, indicating that the strain is footwall strain related to oblique motion on the Bear Foot Thrust (McDonough, 1987; McDonough and Simony, work in progress). The presence of the same pelite and quartzite facies of the lower Miette in both the footwall and hanging wall of the Bear Foot Thrust suggests a minimal amount of dextral motion on the fault.

Van De Driessche and Maluski (op. cit.) also proposed a Tête Jaune Cache Series, which they envisioned as highly allochthonous relative to the Main Ranges Upper Proterozoic stratigraphy. Our detailed mapping shows that stretched-pebble conglomerates at Tête Jaune Cache are an integral part of the middle Miette, and are not in fault contact with Miette strata to the east. We therefore recommend that the proposed Tête Jaune Cache Series be discarded.

METAMORPHISM

Most of the rocks in the map area belong to the chlorite zone of the greenschist facies. Chloritoid is common in aluminous pelites of the lower Miette, but occurs spordically in middle and upper Miette pelites.

A biotite isograd was mapped on the west limb of Terry Fox Anticlinorium in middle Miette pelites (Fig. 3). Biotite occurs as porphyroblastic clusters within oblate patches of dark green, porphyroblastic chlorite and siderite. The host rock usually is light green phyllite with abundant fine grained chlorite and white mica.

SUMMARY

Three distinct lithological units are found within a structurally thickened 4 km thick sequence of Miette Group rocks in the northern Selwyn Range. A minimum of 600 m of upper Miette strata conformably overly a maximum of 2600 m of middle Miette sandstones, conglomerates and pelites. This sequence is resting conformably on a minimum of 850 m of lower Miette pelites and quartzites.

The Miette succession is considerably thinner on the west limb of Terry Fox Anticlinorium. The westward thinning of individual units within the middle Miette, and their continuous nature, suggest that the thin western succession is related to a Late Proterozoic structural high.

We define the middle Miette as a sequence of thick conglomeratic sandstone units interspersed with pelite units that are green, and, to a lesser extent, black (graphitic). The thickness of middle Miette shown in Figure 2 may be more than the true thickness due to structural thickening by unrecognized bedding-parallel thrust faults.

The structure of the area is dominated by large, upright F_2 folds. The stratigraphic sequence can be mapped around these structures, and passes in a continuous manner into a zone of high strain on the west side of the area. The high strains recorded in pebble conglomerates in this zone are related to motion on the Bear Foot Thrust. The area is underlain by the Moose Lake Thrust, which has a relatively small displacement. Thus, the entire Moose Lake Thrust Sheet lies above the master detachment surface of the western part of the Main Ranges.

ACKNOWLEDGMENTS

This work would not have been possible without the assistance of Dr. M.E. McMechan of the I.S.P.G. The logistical support of Yellowhead Helicopters and Brian Hannis of Valemount, British Columbia is gratefully acknowledged. D. Umbsaar, G. Addison, and J. Cody provided able assistance in the field.

REFERENCES

Aitken, J.D.
1969: Documentation of the sub-Cambrian unconformity, Rocky Mountain Main Ranges, Alberta; Canadian Journal of Earth Sciences, v. 6, p. 193-200.

Campbell, R.B.
1968: Canoe River (83D), British Columbia; Geological Survey of Canada, Map 15-1967.

Campbell, R.B., Mountjoy, E.W., and Young, F.G.
1973: Geology of the McBride map area, British Columbia; Geological Survey of Canada, Paper 72-35, 104 p.

Carey, J.A. and Simony, P.S.
1985: Stratigraphy, sedimentology, and structure of late Proterozoic Miette Group, Cushing Creek area, British Columbia; Bulletin of Canadian Petroleum Geology, v. 33, p. 184-203.

Charlesworth, H.A.K., Weiner, J.L., Akehurst, A.J., Bielenstein, H.U., Evans, C.R., Griffiths, R.E., Remington, D.B., Stauffer, M.R., and Steiner, J.
1967: Precambrian geology of the Jasper region, Alberta; Research Council of Alberta, Bulletin 23, 74 p.

McDonough, M.R.
1984: Structural evolution and metamorphism of basement gneisses and Hadrynian cover, Bulldog Creek area, British Columbia; unpublished M.Sc. thesis, University of Calgary, Calgary, Alberta, 163 p.
1987: Tectonic significance of the high strain zone on the west edge of the Rocky Mountains near Valemount, British Columbia; Geological Society of America, Abstracts with Programs, v. 19, p. 430.

McDonough, M.R. and Simony, P.S.
1986: Geology of the northern Selwyn Range, western Main Ranges, Rocky Mountains, British Columbia: preliminary report; *in* Current Research, Part A, Geological Survey of Canada, Paper 86-1A, p. 619-626.

Mountjoy, E.W.
1980: Mount Robson (83E), Alberta-British Columbia; Geological Survey of Canada, Map 1499, (1:250,000).

Mountjoy, E.W. and Forest, R.
1986: Revised structural interpretation, Selwyn Range between Ptarmigan and Hugh Allan creeks, British Columbia – an antiformal stack of thrusts; *in* Current Research, Part A, Geological Survey of Canada, Paper 86-1A, p. 177-183.

Mountjoy, E.W. and Price, R.A.
1985: Jasper, Alberta (83D/16); Geological Survey of Canada, Map 1611A, (1:50,000).

Pell, J. and Simony, P.S.
1987: New correlation of Hadrynian strata, south-central British Columbia; Canadian Journal of Earth Science, V. 24, p. 302-313.

Ross, G.M. and Murphy, D.C.
— Transgressive stratigraphy, anoxia and regional correlations within the late Precambrian Windermere grit of the southern Canadian Cordillera; Geology (in press).

Sanderson, D.J.
1982: Models of strain variations in nappes and thrust sheets: a review; Tectonophysics, v. 88, p. 201-233.

Struik, L.C.
1986: Imbricated terranes of the Cariboo gold belt with correlations and implications for tectonics in southeastern British Columbia; Canadian Journal of Earth Sciences, v. 23, p. 1047-1061.

Van Den Driessche, J. and Maluski, H.
1986: Mise en évidence d'un cisaillement ductile dextre d'âge crétacé moyen dans la région de Tête Jaune Cache (nord-est du complexe metamorphique Shuswap, Columbie-Britannique); Canadian Journal of Earth Sciences, v. 23, p. 1331-1342.

Young, F.G.
1969: Sedimentary cycles and facies in the correlation and interpretation of Lower Cambrian rocks, east-central British Columbia; unpublished Ph.D. thesis, McGill University, Montreal, 189 p.
1979: The lowermost Paleozoic McNaughton Formation and equivalent Cariboo Group of eastern British Columbia: piedmont and tidal complex; Geological Survey of Canada, Bulletin 288, 60 p.

A reconnaissance study of the marine geology of the Lougheed-King Christian — Cameron islands region, northwest Arctic Island channels[1]

G.V Sonnichsen and B. MacLean
Atlantic Geoscience Centre, Dartmouth

Sonnichsen, G.V. and MacLean, B., A reconnaissance study of the marine geology of the Lougheed-King Christian — Cameron islands region, northwest Arctic Island channels; in Current Research, Part D, Geological Survey of Canada, Paper 88-1D, p. 115-120, 1988.

Abstract

A marine geophysical and geological survey was conducted in July and August, 1987, in the Arctic Island channels east of Lougheed Island and south of King Christian Island. This helicopter-supported program used inflatable boats operated in open-water leads that form in the near-perennial ice cover during the summer thaw. Sixteen leads and over 280 km of seafloor were surveyed with single-channel sparker and 12 kHz profiling systems. Subbottom penetrations as deep as 80 m show gently dipping strata of sedimentary bedrock, overlain by unconsolidated sediments ranging from less than 5 m to at least 45 m. Sediments interpreted to be glacial drift are the thickest and the most widespread. These are overlain by up to 5 m of draped and sometimes ponded, acoustically transparent sediments, which are interpreted to be postglacial marine muds. Sediment samples and bottom photographs were collected at three locations along the leads.

Résumé

Un levé géophysique et géologique marin a été réalisé en juillet et août 1987 dans les chenaux des îles arctiques, à l'est de l'île Lougheed et au sud de l'île King Christian. Pour réaliser ce programme assisté par des hélicoptères, on a utilisé des bateaux gonflables dans des chenaux d'eau libre qui se forment dans la glace quasi pérenne durant le dégel d'été. On a effectué des levés dans 16 chenaux sur plus de 240 km de fond océanique au moyen des enregistreurs de profils 12-kHz à étinceleur monocanal. Les ondes qui ont pénétré le fond à une profondeur de plus de 80 m indiquent la présence de couches de roches sédimentaires faiblement inclinées, sur lesquelles reposent des sédiments non consolidés dont l'épaisseur varie de moins de 5 m à au moins 45 m. Ces sédiments qui auraient été transportés par les glaciers sont les plus épais et les plus étendus. Ils sont surmontés par plus de 5 m de sédiments acoustiquement transparents, drapés et parfois inondés, qui pourraient être des boues marines post-glaciaires. On a recueilli des échantillons de sédiments et des photographies du fond océanique à trois endroits le long des chenaux.

[1] Contribution to Northern Oil and Gas Action Program.

INTRODUCTION

Interest in geology of the Arctic Island channels has increased in recent years with the number of oil and gas discoveries in the northwestern Canadian Arctic Islands. Since 1984, the Atlantic Geoscience Centre (AGC) of the Geological Survey of Canada has undertaken a series of investigations of the Quaternary sediments of the Arctic Island Channels (MacLean and Vilks, 1986; Sonnichsen and Vilks, 1987; MacLean et al., in prep.) as part of the Northern Oil and Gas Action Program (NOGAP). Objectives are to determine the geological and geotechnical properties, regional character and history of the unconsolidated sediments, and to identify geological constraints to the development of subsea engineering and production facilities in the inter-island channels. This information plays a role in both regulatory and developmental planning for hydrocarbon exploration, production and transportation. These studies also provide data on the glacial and postglacial history of the Arctic Archipelago as well as on the structure of the underlying, near-surface bedrock.

The most serious factor constraining research in the channels is the almost perennial sea ice cover. While the southern channels can be surveyed using conventional shipborne techniques in favourable ice years (MacLean et al., 1987), the northwestern channels are largely inaccessible to ships. This has led to the development of alternate methods of data collection for these areas.

In 1986, the permanently ice covered channels surrounding Lougheed Island (Fig. 1) were investigated by AGC using an experimental technique (see Sonnichsen and Vilks, 1987) that utilized small boats which were transported by helicopter to open water cracks (or leads) to collect continuous seismic reflection profiles. Previous knowledge of the Quaternary sediments in the region was confined to that available from scattered samples of the upper metre of the seabottom (MacLean and Vilks, 1986, Marlowe, 1968). The 1986 program obtained reconnaissance information in the channels south and west of Lougheed Island, despite unusually harsh ice and weather conditions.

This report concerns the second AGC leads program, conducted from July 2 to August 10, 1987 which focused on the region between Lougheed and King Christian islands (Fig. 1). The resulting geophysical coverage is sufficient to provide a preliminary assessment of the types, thicknesses, and extent of the unconsolidated sediments in these channels.

METHODS

Survey procedures in 1987 were the same as those developed the previous year (Sonnichsen and Vilks, 1987), with minor improvements to the efficiency and ease of assembly and operation of the equipment in the boat (Fig. 2, 3). The project was carried out from the same base camp site on southern Lougheed Island used in 1986 (Fig. 1), with logistical and helicopter support coordinated through the Polar Continental Shelf Project. A JetRanger 206-L helicopter was used to transport the inflated Zodiac boat, seismic equipment, and personnel from lead to lead. The principal seismic system was a single channel Ferranti ORE Geopulse 350 joule sparker subbottom profiling system which provided up to 100 milliseconds penetration of the unconsolidated sediments and the underlying bedrock. Additional acoustic information on

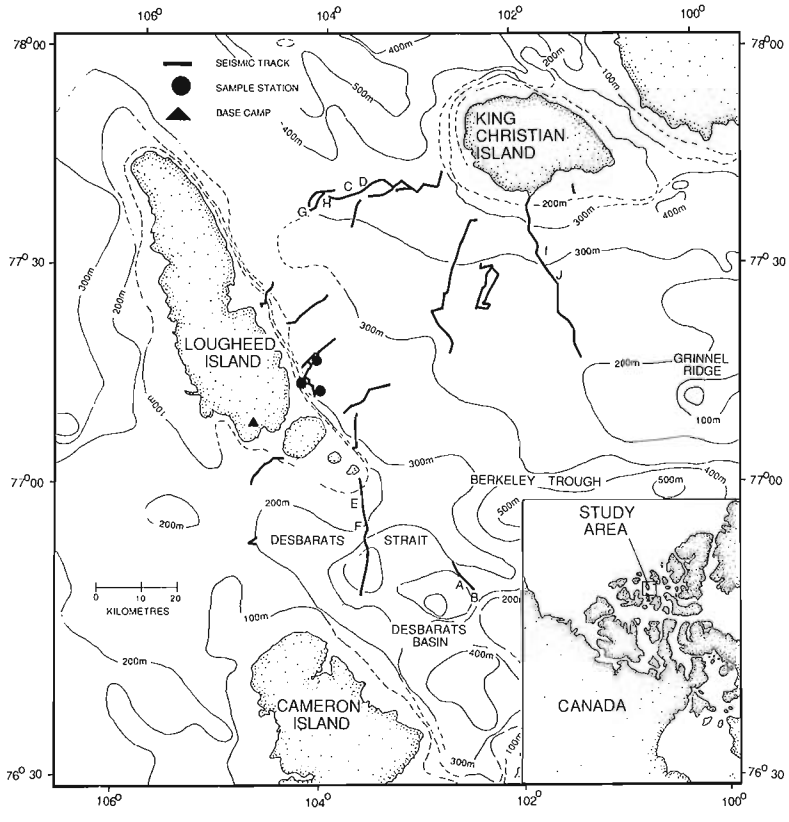

Figure 1. Index map of the 1987 survey area, showing locations of seismic tracks, sediment sample or bottom photograph stations, and base camp location. Isobths from CHS Hydrographic Chart 7951.

the presence and thickness of fine-grained surficial sediments was provided by a 12-kHz transducer linked to a Raytheon PTR transceiver. Sparker and 12-kHz data were collected on separate traverses of each lead. In addition to the acoustic data, sediment grab samples, shallow gravity cores, and bottom photographs were collected from the lead edge (Fig. 4) at three locations.

Positioning for seismic profiles and sediment samples was obtained from the Transit Satellite System using a Magnavox MX 5102 satellite receiver, operated from the boat. Sixteen leads with a combined length of 280 km were surveyed in 1987. The longest was 44 km, while widths varied from 2 to 25 m. Leads encountered in 1987 were generally longer, more continous and freer of broken ice than those surveyed in 1986. This was attributed to the existence of areas of first-year ice, which favoured lead development in the 1987 study area. Some profiles were collected in areas where the sea ice had broken into drifting floes, but this was terminated as open water areas became too transient and unsafe.

RESULTS

The acoustic records show variable thicknesses of unconsolidated sediments overlying gently dipping to near-horizontal strata of sedimentary bedrock (Fig. 5 to 9). The contact between the bedrock surface and the overlying sediments varies from a distinct angular unconformity surface (Fig. 5, 6), to a less distinct horizon where the strata are more horizontal. The apparent dips of strata on seismic profiles are to some extent dependent on the orientation of the profile; however the records indicate some very gentle folding south of Lougheed Island and south and west of King Christian Island.

Unconsolidated sediment thicknesses range from less than 5 m to at least 45 m (based on sound velocity in water). These deposits are thickest in the deep-water depressions along the east side of Lougheed Island and the south side of King Christian Island. Sediments thin considerably to the southeast on the flanks of Grinnel Ridge and in Desbarats Basin (Fig. 5).

Sediments are tentatively divided into two stratigraphic units on the basis of their acoustic character. The lowermost, which is both the most widespread and the thickest, rests directly on the underlying bedrock. This unit consists of unstratified sediments of variable thickness, with a typically hummocky and incised surface (Fig. 7). This unit is interpreted to be of glacial origin on the basis of its constructional character and similarity to marine sediments interpreted as glacial drift elsewhere (King and Fader, 1986; Josenhans et al., 1986; Praeg et al., 1986). The seismic data suggest that more than one drift unit may be present locally.

Figure 2. Five-metre Zodiac inflatable boat equipped for sparker seismic profiling in one of sixteen leads surveyed in 1987. The majority of the boat equipment was left attached during transfer between survey leads by helicopter, to prevent major disassembly of the system and navigation electronics.

Figure 3. Two AGC technicians carrying out sparker seismic survey of a lead. One technician deployed the sparker source and hydrophone array and steered the boat, while the other operated the receiver and satellite navigation.

In some areas the lower unit has smoother surface relief and a more transparent acoustic character (Fig. 8, 9). Sediments with similar character in Austin Channel have been interpreted as glacial drift on the basis of sample data (MacLean et al., in prep.). These variations in character may reflect changes in the sediment sources or depositional processes, e.g. ice loading, associated with the drift.

The 12 kHz acoustic profiles show that in places the lower unit is overlain by an upper acoustically unstratified, transparent unit with a smooth surface which is ponded in bathymetric depressions or draped over the underlying sediments. Thicknesses range from less than 1 m up to 5 m. Gravity cores collected in 1987 penetrated up to 1.4 m of mud in areas where the upper unit was observed. Despite only localized appearance of the unit on the acoustic profiles, sediments which are considered analogous have been identified in over 75 gravity cores, collected in water depths between 35 and 495 m, from the channels surrounding Lougheed Island (MacLean and Vilks, 1986; Marlowe, 1968). This disparity suggests the upper unit forms an extensive veneer which is thinner than the resolving capability of the acoustic systems. These sediments are interpreted to represent Holocene postglacial muds because of their stratigraphic position, and because of acoustic and textural similarities to muds identified in Jones Sound, which contain shells dated between 2610 ± 110 and 8410 ± 200 years BP (G. Vilks, 1986, pers. comm.), and to Holocene muds in other Canadian Arctic areas (Praeg et al., 1986). Sediment samples and bottom photographs from the study region (MacLean and Vilks, 1986; Sonnichsen and Vilks, 1987) show no evident signs of current acitivity, e.g. coarse grained sediments or bedforms. Marlowe (1968) noted a lack of fine-grained sediments north of Cameron Island and on Grinnel Ridge which he attributed to current winnowing. This suggests that modification of the sediment by bottom currents is occurring locally. Seismic profiles from some areas show an incised seabed relief at the top of the lower unit (Fig. 7). These irregularities are interpreted to be relict iceberg scours.

DISCUSSIONS

The apparent dips of bedrock strata recognized on seismic reflection profiles from the leads between Lougheed, King Christian, and Cameron islands are of a similar magnitude to the dips (2 to 8 degrees for Lougheed and Cameron, 5 to 19 degrees for King Christian Island) of the Mesozoic-Cenozoic sedimentary bedrock exposed on the surrounding

Figure 4. Photograph showing collection of a Benthos gravity core. The portable winch, powered by a Honda 3000 watt generator, is attached to the cantilevered tripod. Ice thicknesses at the lead edge were typically one to two metres.

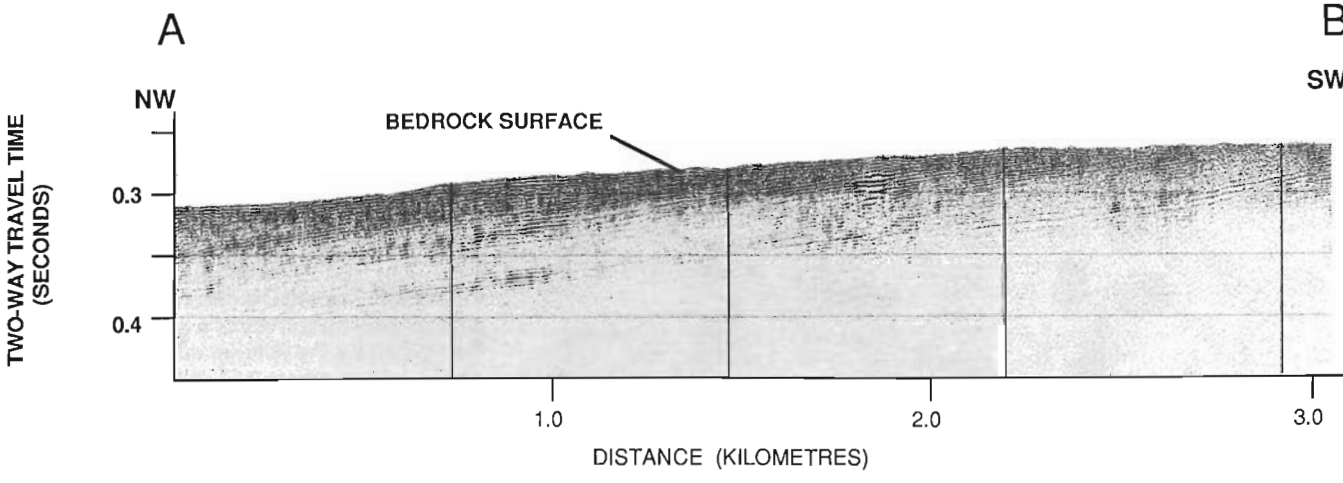

Figure 5. Geopulse sparker seismic reflection profile (A-B) showing gently dipping strata of sedimentary bedrock that are truncated at or near the seafloor. Unconsolidated sediments, if present, are too thin to be resolved by the Geopulse system (see Fig. 1 for location).

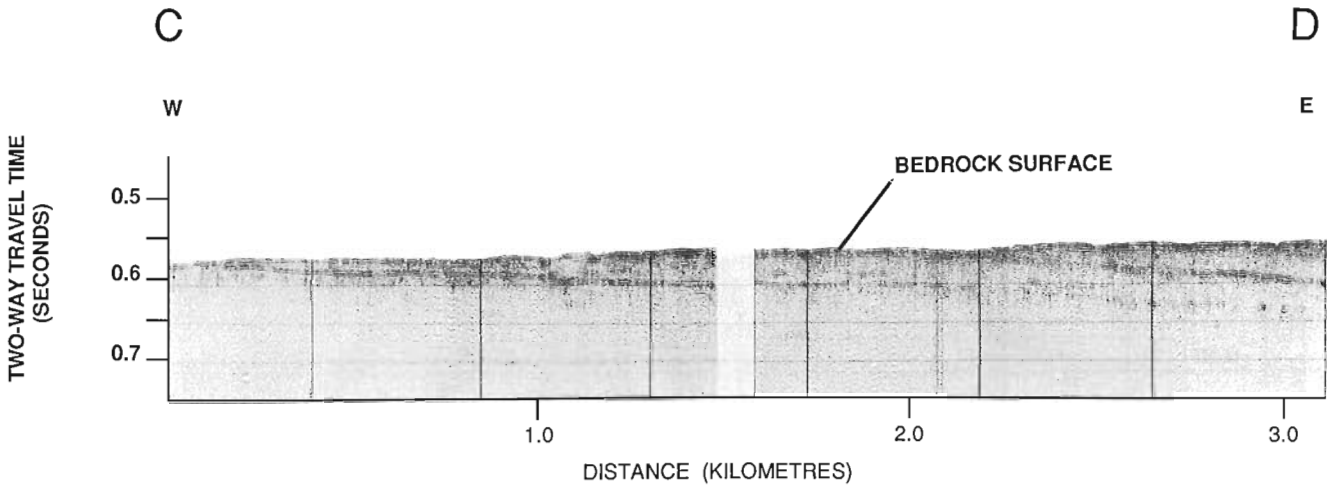

Figure 6. Geopulse sparker seismic reflection profile (C-D) showing gently dipping strata with little or no cover of unconsolidated sediments. The acoustic character of the bedrock differs from Figure 5, with fewer and more broadly spaced reflectors (See Fig. 1 for location).

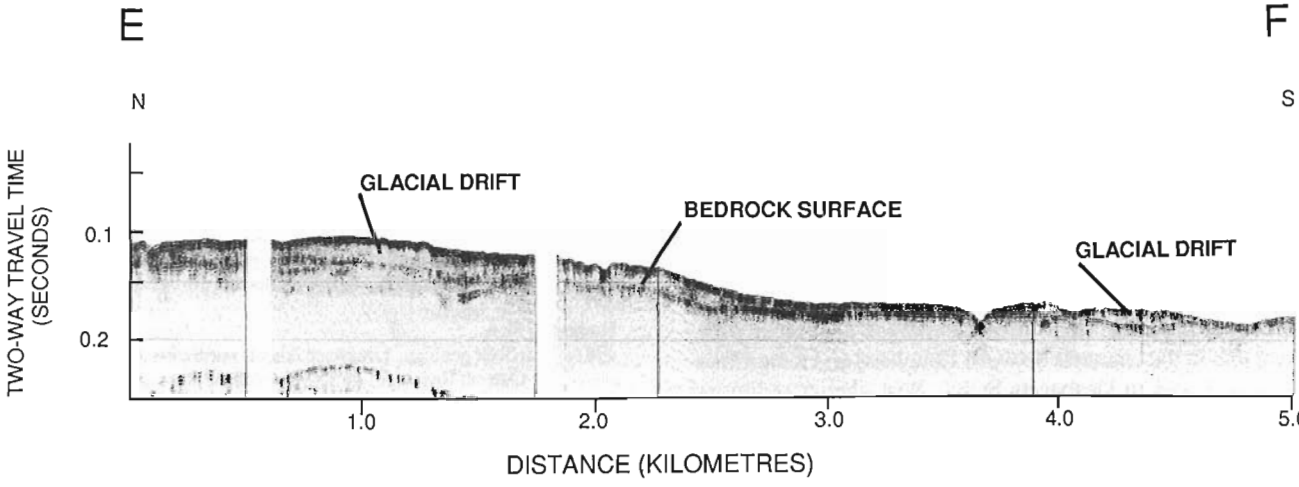

Figure 7. Geopulse sparker seismic reflection profile (E-F) showing up to 15 metres of unstratified sediment interpreted to be glacial drift, overlying an irregular bedrock surface. Note the seabed depressions at 0.1 , 2.1, and 3.8 km. These are interpreted to be relict iceberg scour features. (see Fig. 1 for location)

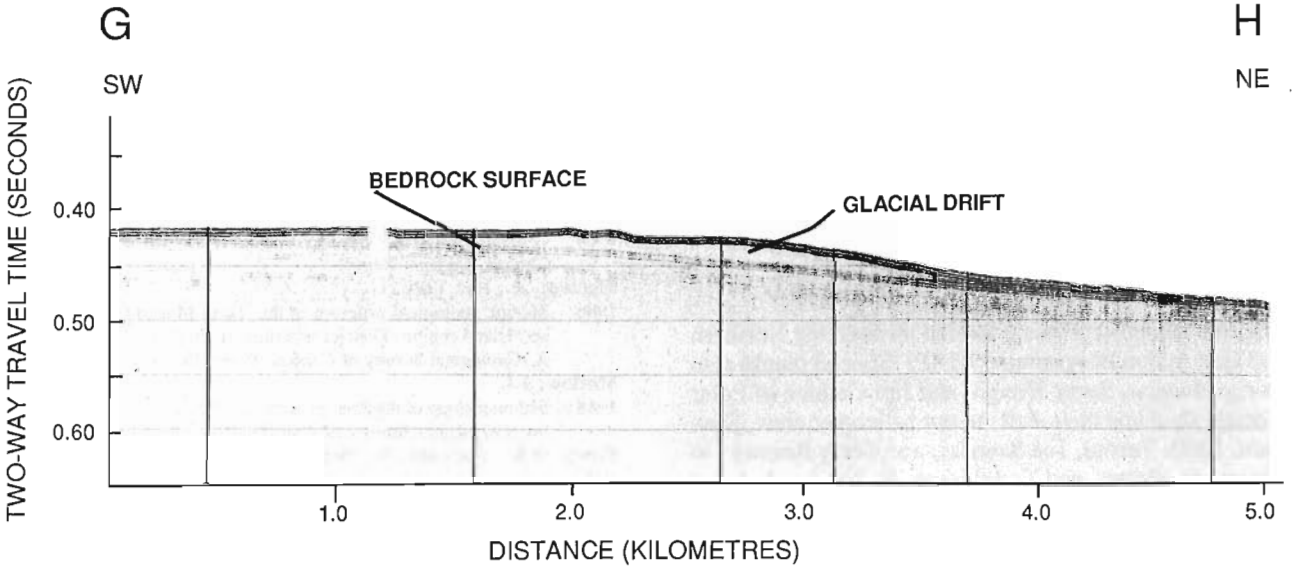

Figure 8. Geopulse sparker seismic reflection profile (G-H) showing up to 16 metres of unstratified and transparent sediments, interpreted as glacial drift, overlying gently dipping strata of sedimentary bedrock. (see Fig. 1 for location)

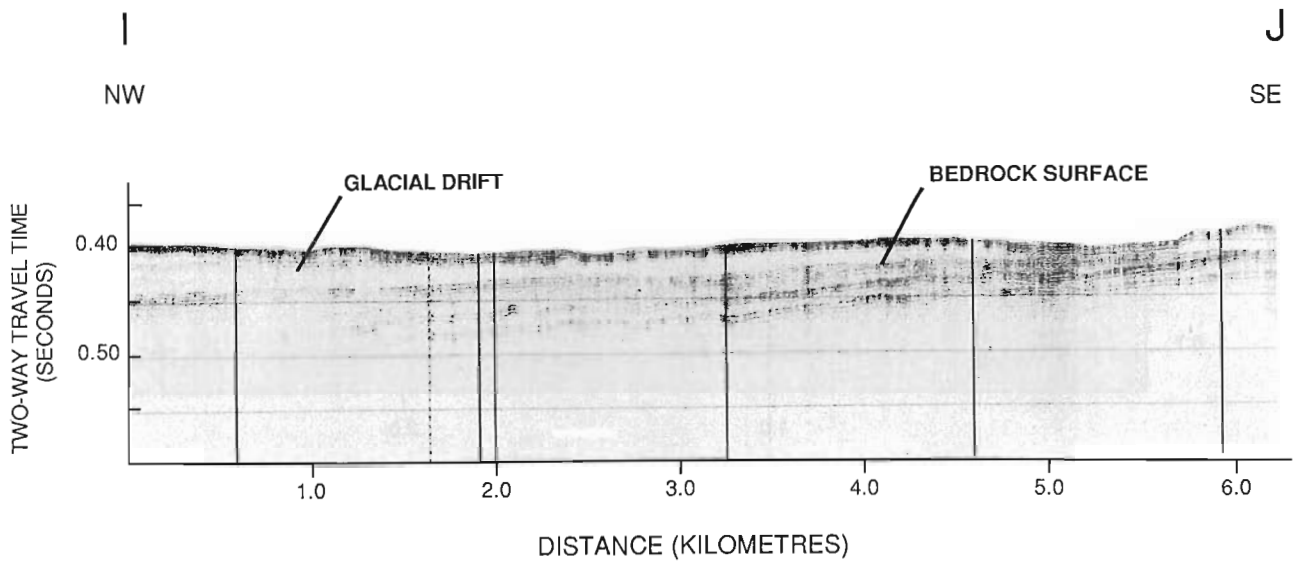

Figure 9. Geopulse sparker seismic reflection profile (I-J) showing up to 33 m of acoustically unstratified and transparent sediment interpreted as glacial drift overlying gently dipping strata of sedimentary bedrock. 12 kHz profiles across this section show that the drift is overlain by from 1 to 5 m (at 2.0 km) of transparent sediment which is interpreted to be postglacial mud. (see Fig. 1 for location)

islands (Balkwill et al., 1982; Balkwill and Roy, 1977; Kerr, 1974). While no direct correlation can be made, the bedrock strata offshore are presumed to represent extensions from the bedrock sequences of the adjacent islands.

Unconsolidated sediments in the interisland channels suggest the presence of at least one episode of grounded glacial ice followed by postglacial marine deposition. Sediments interpreted as glacial drift form the thickest and most widespread unit in the channels between Lougheed and King Christian islands and in Desbarats Strait. Post glacial sediments in the study region are thin and appear to have been deposited under generally quiet marine conditions. This stratigraphic sequence is similar to that identified from research in adjacent channels (MacLean et al., in prep.).

Although, up to 120 m of regional uplift over the last 10 000 years has been tentatively attributed to isostatic rebound from a large ice sheet (Hodgson, 1981; Hodgson and Vincent, 1984), only sparse indication for this ice has been found on land (Hodgson, 1981; Hodgson, 1982). However, the inter-island channels may have been more active depositional sites, and may provide a more complete record of the Quaternary glacial and postglacial history which has been preserved below the erosive effects of fluctuating sea levels.

ACKNOWLEDGMENTS

Funding for this project was provided through the Northern Oil and Gas Action Program (NOGAP). Special thanks also to George Hobson, Barry Hough, and Jim Godden of Polar Continental shelf and their staff; to our helicopter crew, Ross Bertram, Keith Veroni, Joe Sawicki, and Terry Rooney; to technicians E. Wolter, and T. Atkinson, F. Jodrey, A. Law, and Kevin Robinson of the Atlantic Geoscience Centre for their field support. Thanks as well to D.L Forbes and D.B. Praeg for critically reading this paper.

REFERENCES

Balkwill, H.R., and Roy, K.J.
1977: Geology of King Christian Island, District of Franklin (part of 69C); Geological Survey of Canada, Memoir 386.

Balkwill, H.R., Hopkins, W.S.,Jr., and Wall, J.H.
1982: Geology of Lougheed Island and nearby small islands, District of Franklin (part of 69C, 79D); Geological Survey of Canada, Memoir 395.

Hodgson, D.A.
1981: Surficial geology, Lougheed Island, northwest Arctic archipelago; *in* Current Research, Part C, Geological Survey of Canada, Paper 81-1C, p. 27-34.
1982: Surficial materials and geomorphological processes, western Sverdrup and adjacent islands, District of Franklin; Geological Survey of Canada, Paper 81-9, 34 p.

Hodgson, D.A., and Vincent, J.S.
1984: A 10 000 year B.P. extensive ice shelf over Viscount Melville Sound, Arctic Canada; Quaternary Research 22, p. 18-30.

Josenhans, H.W., Zevenhuizen, J., and Klassen, R.A.
1986: The Quaternary geology of the Labrador shelf; Canadian Journal of Earth Sciences, v. 23, no. 8, p. 1190-1213.

Kerr, J. Wm.
1974: Geology of Bathurst Island Group and Byam Martin Island, Arctic Canada (Operation Bathurst Island); Geological Survey of Canada, Memoir 378.

King, L.H., and Fader, G.B.J.
1986: Wisconsinan glaciation of the Atlantic continental shelf of southeast Canada; Geological Survey of Canada, Bulletin 363, 72 p.

MacLean, B.
1986: Cruise report; CSS Hudson cruise 86-027; Geological Survey of Canada, Internal Report.

Maclean, B., and Vilks, G.
1986: Marine geological program in the Byam Martin Channel, Lougheed Island region, District of Franklin; *in* Current Research, Part A, Geological Survey of Canada, Paper 86-1A, p. 769-774, 1986.

Marlow, J.I.
1968: Sedimentology of the Prince Gustaf Adolf Sea area, District of Franklin; Geological Survey of Canada, Paper 66-29, 53 p.

Praeg, D.B., MacLean, B., Hardy, I.A., and Mudie, P.J.
1986: Quaternary geology of the southeast Baffin Island continental shelf; Geological Survey of Canada, Paper 85-14.

Sonnichsen, G.V. and Vilks, G.
1987: A small boat seismic reflection survey of the Lougheed Island Basin — Cameron Island Rise — Desbarats Strait region of the Arctic Island channels using open water leads; *in* Current Research, Part A, Geological Survey of Canada, Paper 87 -1A, p. 877-882.

Stratigraphic framework and depositional setting, Judy Creek coalfield, northern Alberta

Li Baofang[1] and F.M. Dawson
Institute of Sedimentary and Petroleum Geology, Calgary

Baofang, Li and Dawson, F.M., Stratigraphic framework and depositional setting, Judy Creek coalfield, northern Alberta; in Current Research, Part D, Geological Survey of Canada, Paper 88-1D, p. 121-128, 1988.

Abstract

Upper Cretaceous/Tertiary strata of the Scollard Formation have been recognized in the Judy Creek coalfield of northern Alberta. The Ardley coal zone, which contains potentially economic coal resources, was examined using exploration borehole samples and data, resulting in the development of a stratigraphic framework and depositional model for the rock succession. Similarities in stratigraphic and depositional setting between the Judy Creek coalfield and other Cretaceous/Tertiary coal deposits within the Ardley basin suggest that regional geological events controlled the development of coal precursors for the Ardley coal zone. Proposals are made concerning local depositional environments and these are examined in the context of the regional paleogeography of the Ardley basin.

Résumé

Des strates du Crétacé supérieur/Tertiaire de la formation de Scollard ont été identifiées dans le bassin houiller du nord de l'Alberta. La zone charbonnière d'Ardley, qui possède un potentiel économique en charbons, a été étudiée par des prélèvements de carottes et aussi à partir de données antécédentes; ces études ont apporté une meilleure connaissance du milieu stratigraphique et la réalisation d'un modèle de sédimentation pour les séquences rocheuses. Des similitudes de la stratigraphie et de la sédimentation entre le bassin houiller de Judy Creek et d'autres gisements de charbons du Crétacé/Tertiaire à l'intérieur du bassin d'Ardley indiquent que ces évènements géologiques régionaux ont eu une influence sur la phase pré-houillère de la zone d'Ardley. Des suggestions sont faites au sujet des milieux locaux de sédimentation en se référant au contexte paléogéographique régional du bassin d'Ardley.

[1] Beijing Graduate School of Geology, Peoples Republic of China

INTRODUCTION

The Judy Creek coalfield is situated on the northeastern periphery of what is called the Ardley Coal Basin (Fig. 1). Situated approximately 150 km northwest of Edmonton, the study area, which totals approximately 320 square km, is contained within Townships 63 and 64, Ranges 9 and 10, west of the 5th meridian.

This study was undertaken to establish the sedimentological framework of the commercially significant coal beds within the Judy Creek coalfield of northern Alberta. The presence of the Cretaceous — Tertiary boundary near the base of the major coal-bearing sequence indicates that the strata in this study are of Late Maastrichtian to Paleocene age, and in this respect similar to other Cretaceous-Tertiary coal deposits in Alberta. The Judy Creek study represents the initial phase of a major project that will examine the Ardley coal basin within Alberta. More than 8000 exploration boreholes in the province have penetrated rocks of the Ardley basin.

Data utilized for this initial study were derived from 238 coal exploration boreholes. Of these, 19 boreholes were cored from surface (Fig. 1). All holes were geophysically logged, and detailed lithological interpretations were made using gamma ray, density, resistance and caliper log responses. Drillcore was examined and sampled to aid in the interpretation of depositional environments, and to confirm the lithology calibration of the geophysical logs.

This paper presents the preliminary results of the investigation by outlining the lithostratigraphy and stratigraphic framework of the coal-bearing succession in the Judy Creek area, and briefly describes the depositional setting for the rock sucession penetrated in the exploration boreholes.

STRATIGRAPHIC NOMENCLATURE AND CORRELATION

Late Maastrichtian to Paleocene strata were derived from a source area to the west. Palynological sample analyses from several coreholes indicate that the Upper Cretaceous —

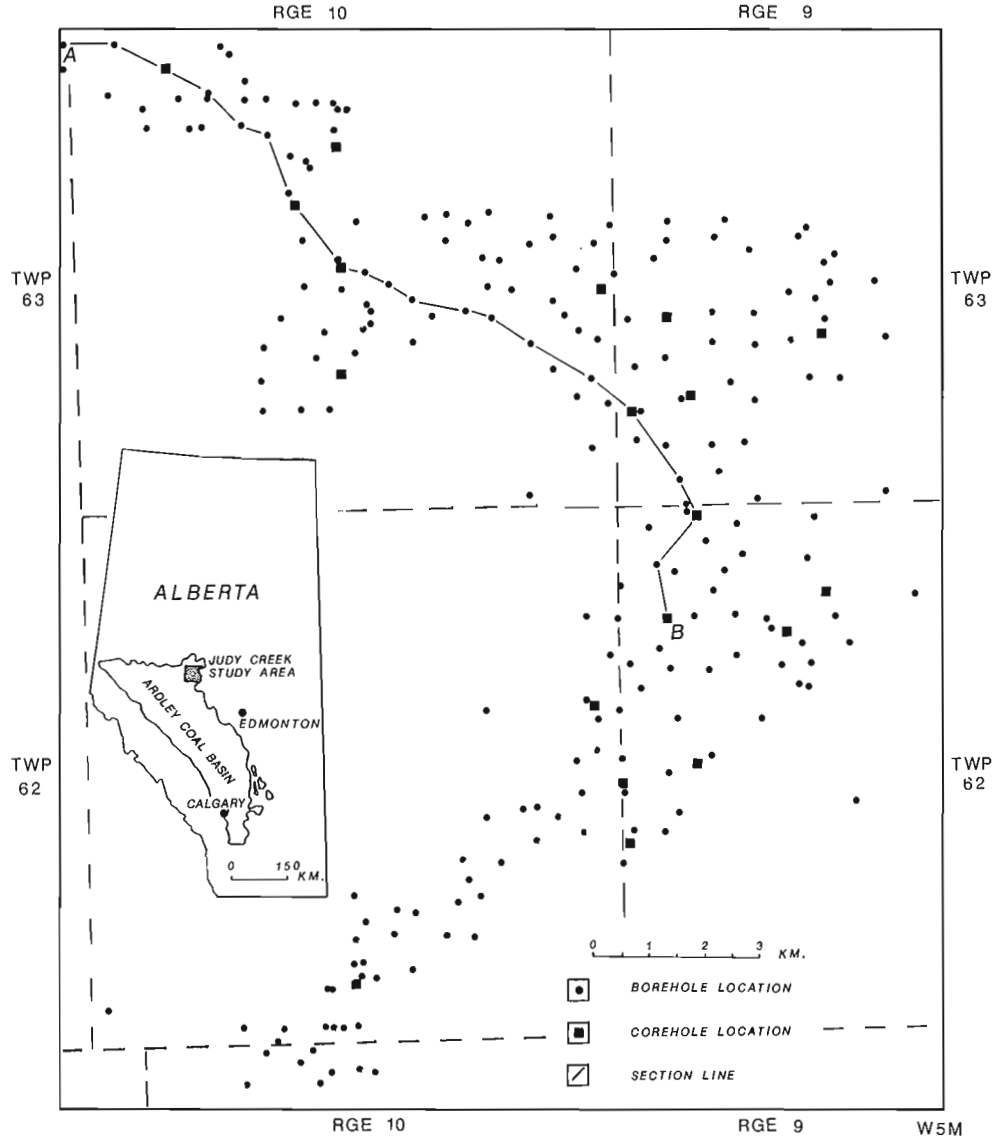

Figure 1. Borehole location map of the Judy Creek study area.

Tertiary boundary (K-T) lies at the base of the major coal-bearing unit within the stratigraphic section (pers. comm., A.R. Sweet, 1987). The K-T boundary, as defined by Lerbekmo (1985), lies at the base of the Ardley coal zone in the Red Deer River valley of central Alberta. The principal coal zone within the Judy Creek coalfield is considered to be correlative with the Ardley coal zone of the Red Deer River area (Fig. 2).

The application of the Upper Cretaceous — Tertiary stratigraphic nomenclature used in the Red Deer River valley of southern Alberta (Gibson, 1977), poses several problems within the Judy Creek coalfield. The Battle and

Kramers and Mellon 1972		Gibson 1977		Li and Dawson (this paper)
PASKAPOO FORMATION		PASKAPOO FORMATION		PASKAPOO FORMATION
WAPITI GROUP	Ardley coal zone	EDMONTON GP.	SCOLLARD FORMATION	SCOLLARD FORMATION
	Upper			
	Kneehills		BATTLE FM.	
			WHITEMUD FM.	
	Middle		Thompson / HORSESHOE CANYON FM.	Thompson / WAPITI GROUP
			BEARPAW FM.	
	Lower		JUDITH RIVER FM.	

Figure 2. Table of Upper Creataceous — Tertiary formations and coal zones in northern Alberta.

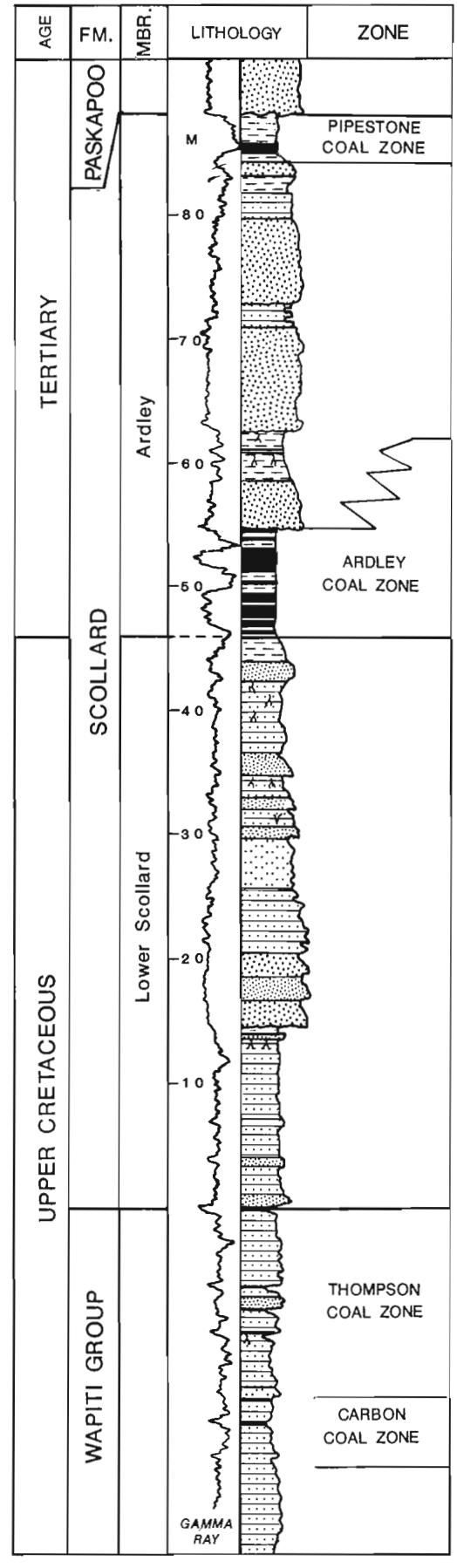

Figure 3. Composite type section, Judy Creek project area.

LEGEND

- COARSE GRAINED SANDSTONE
- MEDIUM GRAINED SANDSTONE
- FINE GRAINED SANDSTONE
- SILTSTONE
- MUDSTONE
- COAL

Whitemud formations in the Red Deer River valley area lie below the Scollard Formation. They have not been recognized in either geophysical log responses or drillcore in the Judy Creek coalfield. Coal seams that are believed to be correlative with both the Thompson and Carbon coal zones of central Alberta have been recognized approximately 25 to 30 m below the Ardley coal zone. This stratigraphic separation is approximately equal to that observed in the Red Deer River valley if the Battle and Whitemud formations were missing (Gibson, 1977).

The utilization of the northern Alberta stratigraphic nomenclature for the Upper Cretaceous — Tertiary strata tends to be confusing. The term Wapiti Group was first applied by Dawson in 1883 to the sequence of rocks between the marine Smoky Group and the Paskapoo Formation. Kramers and Mellon (1972) continued the usage of this name, and subdivided the succession into five informal members. The Ardley coal zone represents the uppermost unit. An upper member underlain by either the Kneehills member, or

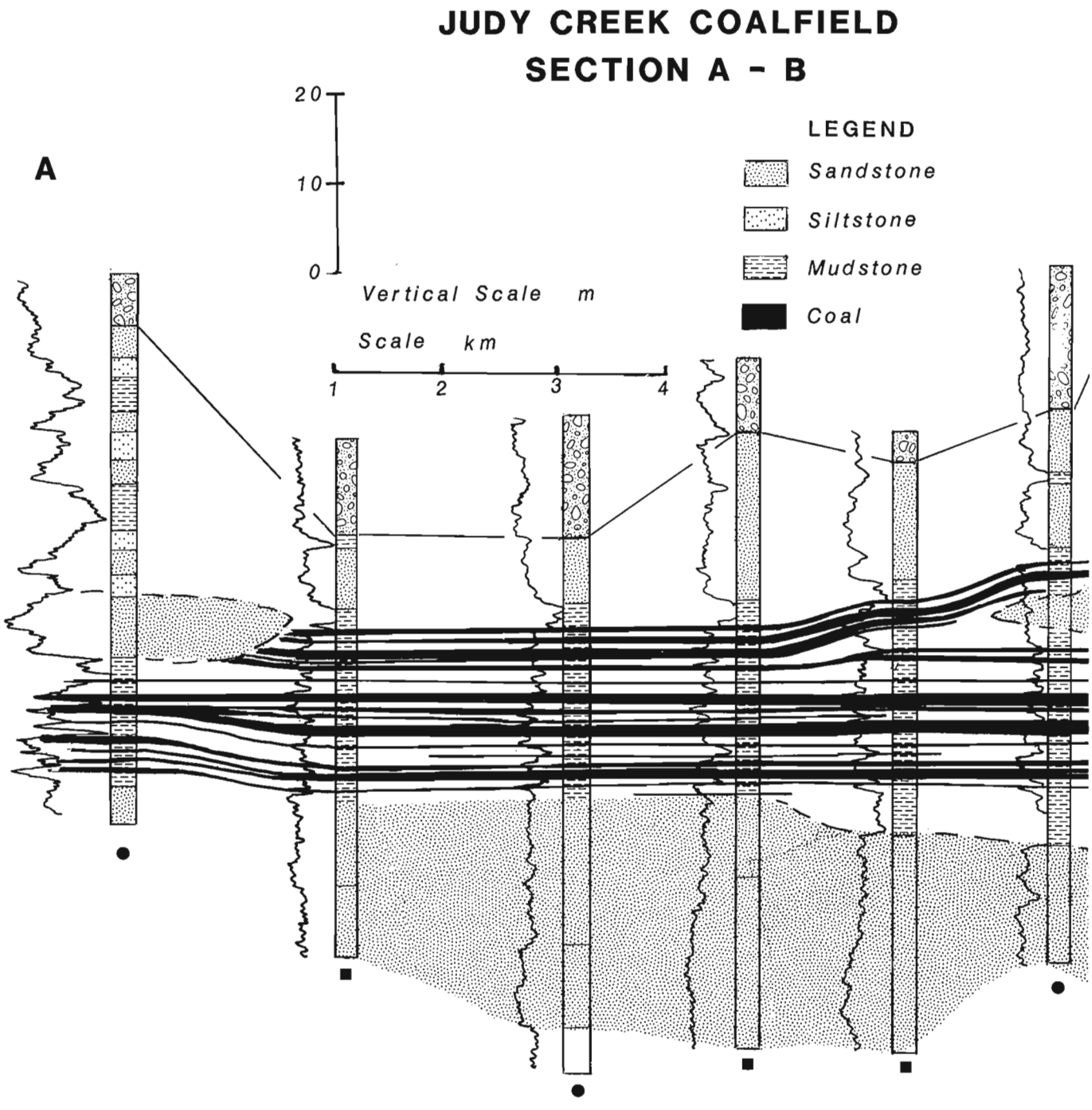

Figure 4. Cross-section illustrating relationships between coal seams and Scollard Formation channel sandstone units.

Battle and Whitemud formations equivalent, lies immediately below (Fig. 2). Neither formation status nor member status have been formally applied to the units of the Wapiti Group.

In the Judy Creek coalfield area, the rock succession appears to be very similar to the strata observed in south central Alberta, apart from the absence of the Battle and Whitemud formations. In this paper, stratigraphic nomenclature of the Red Deer River valley area will be applied, with the base of the Scollard Formation lowered to lie immediately above the Thompson equivalent coal zone (Fig. 3).

STRATIGRAPHIC FRAMEWORK

Two lithologically different stratigraphic units can be distinguished within the Scollard Formation in the Judy Creek coalfield. A predominantly non-coal-bearing sequence lying at the base is defined as the "lower Scollard member". The overlying sequence, which contains both economic coal seams and thick arenaceous sequences, is referred to as the "Ard-

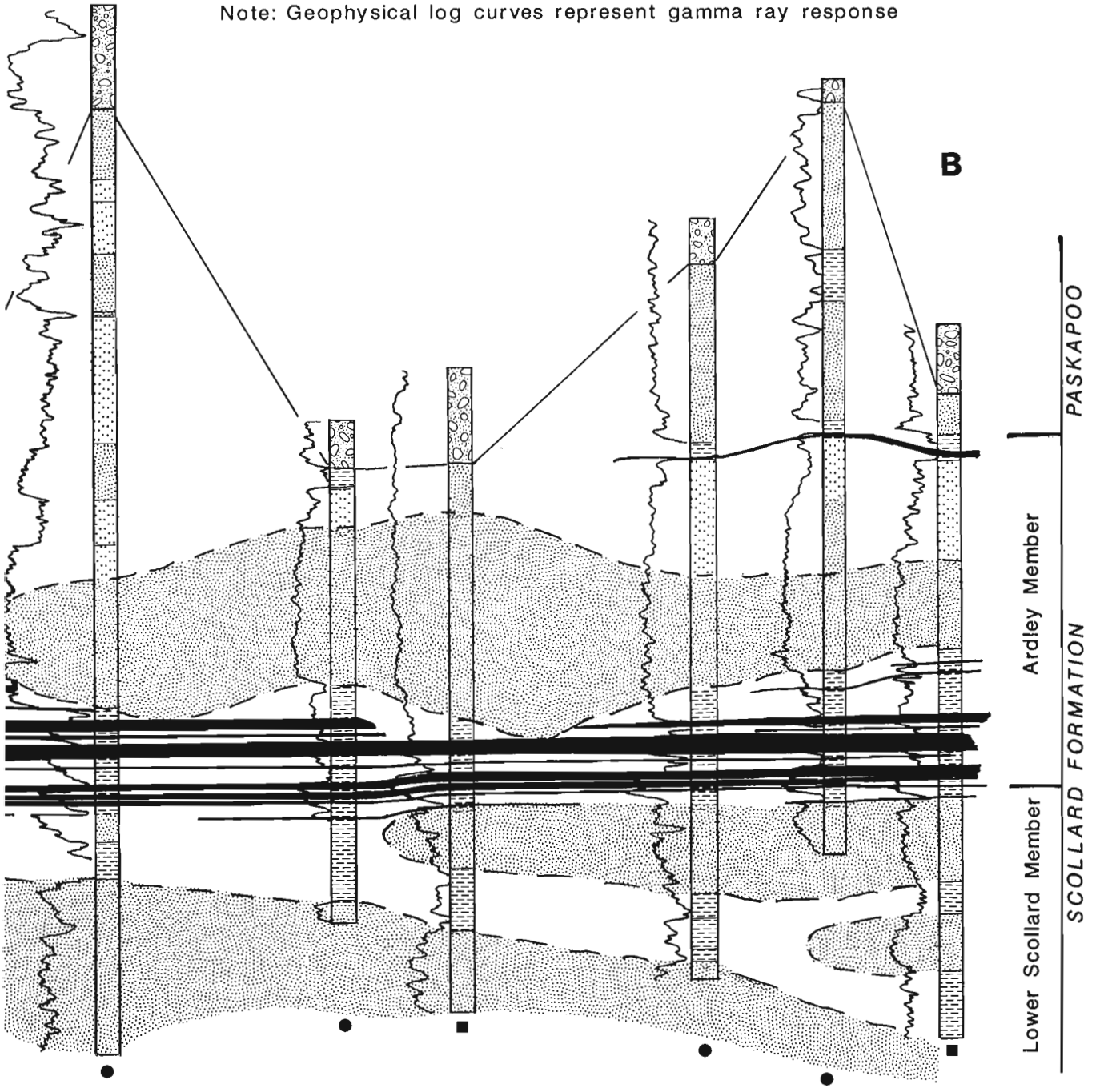

ley member'' (Fig. 3). A new formal stratigraphic nomenclature for this sequence of rocks within the Ardley basin is currently in preparation by Dawson, Demchuk and Strobl.

The ''lower Scollard member'' consists of interbedded sandstone, siltstone, and mudstone, with little or no coal. Thick sandstone units have been recognized and are generally characterized by a fining-upward response on the gamma ray geophysical logs. The base of these sandstone units is usually erosional, commonly.containing channel lag pebbles. The thick sandstones grade laterally into fine grained deposits of mudstone and siltstone. In many localities, ''the lower Scollard member'' lies immediately above the Thompson coal zone of the Wapiti Group (Fig. 3). In some cores, a dark grey mudstone with tuffaceous lenses is found near the base of the ''lower Scollard member''; it may represent the equivalent of the Battle Formation. The ''lower Scollard member'' ranges in thickness from 25 to 45 m, depending on whether the thick sandstone units are present. The top of the member is generally represented by a coarsening-upward sequence of fine grained sandstone or siltstone with numerous carbonaceous fragments and rootlets.

The ''Ardley member'' lies above the ''lower Scollard member'', and contains the only significant economic coal horizons within the Judy Creek study region. The member varies in thickness from 30 to 40 m and is abruptly overlain by the coarse to medium grained sediments of the Paskapoo Formation. The Ardley coal zone lies at the base of the Ardley member and ranges in thickness form 10 to 25 m. Up to 13 coal seams have been correlated from borehole to borehole. Individual seams range in thickness between 0.1 and 2.0 m. Seam partings consist of mudstone or carbonaceous claystone. Both coal seams and partings are very uniform in thickness and laterally continuous, particularily the lower 8 seams in the coal zone (Fig. 4). Similar thickness and distribution patterns to those of the Ardley coal zone can be recognized in many other Tertiary coal deposits within the Ardley basin. The upper coal seams within the Ardley coal zone are more laterally discontinous and tend to be intercalated with the sandstone units that erosionally overlie the lower coal seams (Fig. 4). A carbonaceous, fine grained sequence referred to as the Pipestone horizon lies at the top of the ''Ardley member''. This zone ranges from 0.2 to 5 m thick. In other coalfields to the south, seams up to 3 m thick have been reported in this interval. The contact with the overlying Paskapoo Formation is abrupt and may represent an unconformity. Very little detailed information is available for the upper part of the ''Ardley member''.

DATA ANALYSIS

Results of core examination and sample analyses, combined with the geophysical log interpretation of the lithologies in the boreholes within the study area, have enabled the authors to arrive at the following conclusions pertinent to the establishment of a sedimentological model for the Judy Creek coalfield.

1. Palynological analyses demonstrate that the major coal zone present in the Judy Creek coalfield is of Paleocene age and correlative with the Ardley coal zone of central Alberta. The sequence of seams and rock partings in the Judy Creek coalfield is similar to that of other Tertiary coal deposits in the Ardley basin.

2. The ''lower Scollard member'' is essentially barren of coal or carbonaceous beds and is characterized by a sequence of thick, medium grained sandstone units and associated fine grained strata, which are interpreted as representing floodplain deposits. This member may include the lateral equivalents of the Battle and Whitemud formations of southern Alberta; however, it has not been possible to recognize these two horizons within the area.

3. The thick sandstone beds of the ''lower Scollard member'' appear similar to those in the upper part of the ''Ardley member'' and the overlying Paskapoo Formation. Both facies are medium to coarse grained, and contain similar mineralogical components. The source of sediment supply was probably the areas uplifted to the west as a result of the Laramide Orogeny.

4. Coal seams of the lower sequence of the ''Ardley member'' are laterally continuous throughout the coalfield. Partings consist of mudstone and claystone and are very uniform in thickness.

5. The upper coal seams of the ''Ardley member'' are laterally discontinuous and of poor quality. Where they are discontinuous, the interval is occupied by fine grained mudstone and siltstone units, or medium grained sandstone beds. In places, these sandstone sequences cut down into the coal seams of the lower Ardley zone (Fig. 4).

6. The base of the ''Ardley member'' is generally represented by a coarsening-upward sequence of fine grained sandstone and siltstone with abundant plant material.

7. The upper succession of the ''Ardley member'' consists of thick medium to coarse grained sandstone units capped by a fine grained, carbonaceous sequence referred to as the Pipestone coal zone (Fig. 4).

8. The major thick sandstone units of the ''Ardley member'' are situated stratigraphically above the area of thick mudstone development within the ''lower Scollard member''. Conversely, the thickest coals are situated above coarse grained sandstone beds of the ''lower Scollard member''. Localized, uninterrupted peat growth and subsequent channel migration appears to have been controlled by differential compaction of the underlying stratigraphic sequence (Fig. 4).

9. The thick, buff coloured sandstone units of the Paskapoo Formation abruptly overlie the Pipestone zone of the ''Ardley member''. This distinctive break in stratigraphy, although poorly preserved in the Judy Creek coalfield, can be recognized throughout much of the Ardley basin, and represents a significant change in depositional setting during the Paleocene.

DEPOSITIONAL HISTORY

The results of the Judy Creek coalfeld study have been used to produce a new stratigraphic framework and depositional model for the Scollard Formation within the area. However, the relationship of this stratigraphic framework and depositional model to similar stratigraphic successions in other areas

of the Ardley basin in Alberta remains speculative. Additional work must be undertaken in the intervening areas.

The two stratigraphic members of the Scollard Formation appear to be distinctive, and have formed under different geological conditions or within different depositional environments.

Core and geophysical log responses indicate a variable sequence of interbedded sandstone, siltstone and mudstone rocks for the "lower Scollard member" sequence. Deposition probably occurred on an alluvial plain, characterized in the Judy Creek area by large, freshwater lakes, which probably contributed a significant lacustrine component during deposition of this rock sequence. Several coarsening-upward sequences capped by thick sandstone beds suggest that small, lacustrine deltaic sequences may have formed along the margins of the lakes. However, freshwater fossils have not been observed, nor are there any laterally thick mudrock successions to indicate a regionally extensive lacustrine component. The lack of coal development during "lower Scollard" time was probably due to the high sediment input into the depositional basin. This barren zone, typical of the "lower Scollard member", is overlain by the laterally persistent Ardley coal zone. Similar stratigraphic relationships can be recognized in many coalfields throughout the Ardley basin. It appears that the regional tectonic history associated with the Laramide uplift to the west (Douglas et al., 1972) played a major role in the deposition of coal-bearing sediments during the late Maastrichtian to Paleocene time period.

Immediately prior to the deposition of the Ardley coal zone strata, sediment input into the Judy Creek area decreased. The area appears to have undergone subsidence, accompanied by the development of regionally extensive swamps or marshes. Alternatively, sediment input may have been diverted away from the Judy Creek area by an avulsion event; however, the regional continuity of the Ardley coal zone with respect to the K-T boundary suggests that the depositional controls were more regional. Widespread peat growth throughout the Ardley basin led to laterally continuous, thick coal development over large areas. In places, channels separated these large peat swamps and provided the sediment input for the fine grained partings that separate the individual coal seams. These partings tend to be very uniform in thickness. Similar depositional patterns can be recognized from the Judy Creek coalfield south to Dry Island Buffalo Jump Provincial Park, a distance of approximately 300 km. The widespread similarity in depositional pattern in conjunction with the occurrence of the K-T boundary at the base of the coal zone implies that this area of quiescence in which the Ardley coal zone formed was widespread along the orogenic front.

Following the deposition of the Ardley peats, the region was again subjected to fluvial activity as is reflected by the thick sandstone units of the middle to upper part of the "Ardley member". These thick sandstone beds probably represent channels. This increased fluvial activity was in response to renewed orogenic activity to the west. The resultant increased sediment deposition in the basin effectively led to the termination of peat growth with only areas of higher elevation in the peat swamps being protected from suffocation by overbank sedimentation. These areas of continued peat growth are represented by the upper coal seams of the "Ardley member". As noted previously, these seams generally lie above the thick sandstones of the "lower Scollard member". Differential compaction of the sedimentary sequence produced areas of higher relief during late "Ardley member" deposition, leading to uninterrupted peat growth in some regions. Channel sedimentation was concentrated in areas of low elevation, leading to erosional downcutting into the lower Ardley coal seams above the region of mudstone sedimentation which lies immediately below the Ardley coal zone.

The increased orogenic activity resulted in the deposition of coarse grained sediments in the Ardley basin. Isolated peat swamps associated with an alluvial plain setting are represented by the discontinuous carbonaceous beds of the Pipestone zone at the top of the "Ardley member". Following this period, peat growth was effectively suffocated by rapid sedimentation into the basin. The depositional environment changed to one characterized by numerous fluvial channels and widespread channel migration. The thick, massive, buff coloured sandstones of the Paskapoo Formation that abruptly overlie the "Ardley member" reflect this change of environment.

CONCLUSIONS

Commercially significant coal intervals have been defined within the Judy Creek coalfield. Comparison of exploration data with palynological analyses indicate that these coals are of early Paleocene age and are correlative with the Ardley coal zone of central Alberta. A stratigraphic framework based upon nomenclature from the Red Deer River valley region of central Alberta has been applied to the strata of the Judy Creek area. Strata of the "lower Scollard member" were probably deposited in an alluvial plain environment, characterized locally by large lakes and lacustrine deltas. Strata of the lower "Ardley member" were deposited in a large, subsiding basin characterized by regionally extensive swamp/marsh environments. Strata of the upper "Ardley member" are similar to those of the "lower Scollard member" and were deposited in an alluvial plain environment, which was, at times, characterized locally by local swamps and marshes. Further work will be required to refine these depositional interpretations and their relationships to correlative facies in other areas of the Ardley basin. Expansion of the size of the project area will allow a more regional paleogeographic model to be developed.

REFERENCES

Dawson, G.M.
1883: Preliminary Report on the geology of the Bow and Belly River region, North West Territory with Special Reference to the Coal Deposits; Geological Survey of Canada, Report of Progress, Part B.

Douglas, R.J.W., Gabrielse, H., Wheeler, J.O., Stott, D.F., and Belyea, H.R.
1972: Geology of Western Canada, Chapter VIII; *in* Geology and Economic Minerals of Canada, Geological Survey of Canada and Department of Energy and Mines and Resources, Canada, Economic Geology Report No. 1.

Gibson, D.W.
1977: Upper Cretaceous and Tertiary coal-bearing strata in the Drumheller-Ardley region, Red Deer River Valley, Alberta; Geological Survey of Canada, Paper 76-35

Kramers, J.W. and Mellon, G.B.
1972: Upper Cretaceous — Paleocene coal-bearing strata, Northwest-Central Alberta Plains; Research Council of Alberta, Information Series No. 60

Lerbekmo, J.F.
1985: Magnetostratigraphic and biostatigraphic correlation of Maastrichtian to early Paleocene strata between south-central Alberta and southwestern Saskatchewan; Bulletin of Canadian Petroleum Geology, v. 33, p. 213-226

Ground probing radar investigations of gravel roadbed failures, Rae Access road, N.W.T.

P.T. LaFleche, A.S. Judge, B.J. Moorman, B. Cassidy[1], and R. Bedard[1]
Terrain Sciences Division

LaFleche, P.T., Judge, A.S., Moorman, B.J., Cassidy, B., and Bedard, R., Ground probing radar investigations of gravel roadbed failures, Rae Access road, N.W.T.; in Current Research, Part D, Geological Survey of Canada, Paper 88-1D, p. 129-135, 1988.

Abstract

Ground probing radar surveys were undertaken, in early April 1987, along sections of the Rae Access road, near Fort Rae, N.W.T., to detect and delineate massive ground ice bodies. Such ground ice bodies were thought to be the cause of thaw degradation of the road embankment. Two sites were surveyed and an ice body was mapped at one of them. The ice was found to protrude almost to the bottom of the roadfill, indicating that further problems could be encountered at this site. Subsequent cracking and a collapse in the roadbed in September 1987 near this survey site, confirmed the survey results. A thicker clay layer at the second site limited the useful penetration of the radar system and prevented the detection of any possible ground ice.

Résumé

Des levés radar ont été effectués dans le sol au début d'avril 1987, le long de tronçons de la route Rae Access, près de Fort Rae (T.N.-O.) dans le but de détecter et délimiter d'épaisses masses de glace dans le sol. La présence de ces masses de glace semblait être la cause de la détérioration par le dégel des remblais routiers. Les résultats des levés effectués à deux emplacements ont permis d'identifier et de porter sur carte une masse de glace se manifestant à l'un de ces emplacements. La glace pénétrait presque jusqu'à la base du remblai indiquant que d'autres problèmes pourraient ultérieurement survenir à cet endroit. La fissuration et un effondrement de l'assiette qui se sont produits par la suite en septembre 1987 près de l'endroit observé ont confirmé les résultats du levé. La présence d'une couche d'argile plus épaisse au second emplacement a limité le degré de pénétration utile du système radar et a empêché la détection de toute glace dans le sol.

[1] Transportation Engineering, Northwest Territories Public Works and Highways, Yellowknife, N.W.T. X1A 2L9

INTRODUCTION

During April of 1987 two ground probing radar (GPR) surveys were undertaken along sections of the Rae Access road, near Fort Rae, N.W.T.. These sections of the roadbed had shown evidence of thaw degradation, including surface undulation, cracking and general settling, during the previous summer seasons. The settling was assumed to be due to the melting out of large ground ice bodies. The Rae Access road is a 13-km long gravel road which branches off the Yellowknife Highway, approximately 100 km northwest of Yellowknife (Fig. 1). It is the only all-weather route into the settlement of Fort Rae on the shore of Great Slave Lake. Little information on permafrost distribution and ground temperatures is available for the Rae area. The site is in the zone of discontinuous permafrost. Permafrost thickness in the area can exceed 50 m, however, where overburden cover is extensive. This is especially true in peat-covered areas (Bateman, 1949).

The purpose of the surveys was to establish if a high resolution geophysical technique, such as ground probing radar, could identify and delineate the areas of ground ice, the thawing of which was assumed to be the cause of the roadbed failures. The performance of road embankments in areas of ice-rich permafrost and their general construction techniques are reviewed by Esch (1983) and Johnston (1981).

GROUND PROBING RADAR

Ground probing radar is a fairly new geophysical tool, the first models being commercially available in the mid 1970s. GPR is similar in principle to the reflection seismic method in that a pulse of energy is directed into the ground and the arrival times of reflections from subsurface interfaces are recorded. Seismic and ground radar records are very similiar, the most visible difference being in the magnitudes of the vertical time scales. The main difference between the techniques is that radar uses an electromagnetic as opposed to an acoustic energy source. Radar possesses a much more limited depth of penetration than seismic, typically of the order of 50 m or less, but provides a significant increase in resolution. Subsurface resolution is dependent upon the pulse length and, as such, can be as low as 0.5 m. This high spatial resolution can be important in the solution of complex, near-surface problems. Ground probing radar has been found to be most useful in engineering geophysical applications such as the delineation of overburden thickness, permafrost extent and depth (Annan and Davis, 1976; LaFleche and Judge, 1987), water table depth and ice thickness (Annan and Davis, 1977) or for locating buried cables, pipes (Morey, 1974), fractures (Olhoeft, 1978), voids (Owen and Suhler, 1980), gravels (Davis et al., 1984) and tunnels (Dolphin et al., 1978).

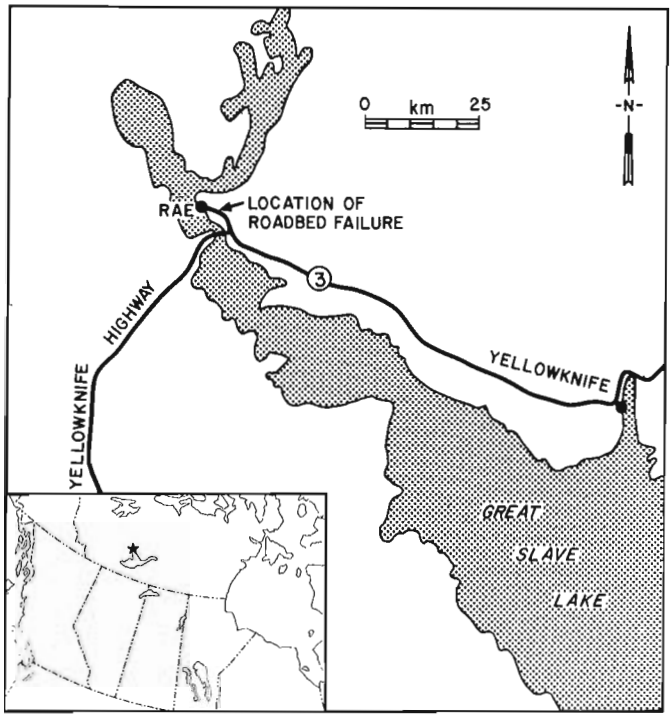

Figure 1. Location map for the Rae Access road area.

Radar reflections are produced by interfaces between materials of contrasting electrical properties, specifically the dielectric permittivity or electrical conductivity. Common causes of subsurface reflections are material interfaces (overburden-rock, gravel-sand), top of the water table, boundaries between frozen and unfrozen soil, voids, fractures and ice lenses. Within the radio frequency band, a large dielectric and conductivity contrast exists between water and most natural geological materials (Morey, 1974). The ability of a material to retain water within its pore spaces is an important factor for determining its bulk electrical properties. As such, the presence or absence of water and its chemistry, controls to a large degree the subsurface propagation characteristics of the radar pulse. Distinct variations in grain size or rock porosity, and the associated changes in the volume percentage of retained water, will produce radar reflections.

The depth to shich a radar pulse will effectively "penetrate" is dependent upon the electromagnetic absorption characteristics of the ground and the amount of energy lost due to reflection, refraction and diffraction effects. The electromagnetic absorption is controlled by the dielectric permittivity and the conductivity of geological materials. In a general sense, the depth of penetration will decrease with increasing water content. Dry, homogenous or frozen materials will offer the greatest potential depth penetration. Pulsed radar, for example, has been found to be extremely useful in underground mapping of salt and coal mines of the United States and Europe (Stewart and Unterberger, 1976; Nickel et al., 1980; Fowler, 1981). Penetration distances of over 1 km in salt (Unterberger, 1978), 15 m in coal (Coon et al., 1981), 50 m in granite (Johansson, 1986) and 30 m in dolomite (Dolphin et al., 1974) have been reported.

The depths to specific reflectors are calculated from a knowledge of the subsurface radar velocity distribution. In air, the radar pulse, typically in the MHz or GHz frequency range, travels with the speed of light (0.3 m/ns). In the ground the pulse travels with a velocity which is dependent upon the electrical properties of the material traversed. This velocity will be some appreciable fraction of the speed of light, usually between 10% and 50%. The radar velocity distribution in the ground can be determined, as in the case of seismic surveys, by a common depth point sounding (CDP)

(Annan and Davis, 1976). Subsurface velocities to different interfaces are calculated from a plot of antenna separation versus travel time. The depth scale of a radar profile over a layered geological medium will depend on the radar velocity in each layer encountered and the thickness of that layer.

Ground probing radar has been used previously in areas underlain by permafrost or containing ground ice (Annan and Davis, 1976, Kovacs and Morey, 1985). The low conductivity and low dielectric losses of very high frequency (VHF) electromagnetic waves in permafrost allows considerable depth penetration. The location of taliks can be mapped as the sharp contrasts in conductivity and permittivity between frozen and unfrozen zones result in strong reflections from these boundaries. Similarly the low relative permittivity value (approximately 4) of ice and its good propagation characteristics permit its identification within frozen fine-grained soils.

SURVEY SITES

The Rae Access road is a gravel highway constructed with a thickness of about 1 m of well-graded gravel or sand and gravel mixture. The roadway consists of a raised embankment rising approximately 1 m above the surrounding terrain. Drainage ditches are located on either side of the road where feasible. Several boreholes were drilled at various locations along the entire length of the road in order to determine soil stratigraphy and investigate specific locations where thaw degradation had been evident. One thermistor cable was placed at station 7+780 to record ground temperatures throughout the year. The road embankment is underlain by approximately 1 m of silty or clayey sands in some cases. Local overburden consists of inorganic clays which contain a variable low to high ice content. This is in the form of individual inclusions or ice formations. Solid or massive ice, up to several metres thick, is found at various depths within the drillholes. Table 1 shows the borehole log for the thermistor hole at station 7+780. The hole was drilled in the fall of 1986. One half metre of freezeback is observable in the drill log. The thaw zone extends down to 3.7 m. Ground temperatures for April 1987, are also listed. They remain below 0°C down to the bottom of the thermister cable, varying from −5.0°C at 0.5 m depth to −0.7° C at 6 m depth. The thaw zone detected at the time of the initial drilling of the hole was below 0°C at the time of the radar survey, indicating that full freezeback had occurred over the winter of 1986/87. Thaw penetration, as indicated by the ground temperatures, was 4 m in September 1987.

Two short sections of the Rae access road were investigated with the ground probing radar. Both of these section had shown evidence of extensive thaw degradation over several years.

Site 1

Site 1, located approximately 10 km from the Yellowknife Highway turnoff, developed a severe vertical drop in the highway alignment in the fall of 1986 for no obvious reason. Water ponded on both sides of the road embankment. Settlement of the road surface has been constant over the last few years. Several 15-20 cm dips in the surface are evident over a 100-m stretch. Cracks up to 15 cm wide are also visible on the embankment sides. The soil stratigraphy, as determined from the nearest borehole at station 9+650 consists of 1 m of well-graded sand fill underlain by 1.5 m of clay overburden. Massive ice with minor clay inclusions extends from 2.5 m to the bedrock at 6 m depth.

Site 2

Site 2, located approximately 8 km from the Yellowknife Highway turnoff, has exhibited cracking over the past several years at the tops of the side slopes of the road embankment. Longitudinal cracks generally opened up from 10 to 15 cm over a section about 150 m in length from stations 7+700 to 7+850. The west side of the highway was rebuilt between stations 7+600 and 7+700 in the fall of 1984. Longitudinal cracks up to 4 cm wide opened up along the west shoulder in 1986 and 1987. Gradual settlement of the roadbed has occurred over the past six years. In an attempt to retain the overburden underlying the road embankment in a frozen state year round peat moss has been placed on the side slopes in the past to provide insulation. This has served to slow down the cracking for about three years, but cracking has become progressively worse in the past two years. Slumping has occurred on the east slope of the embankment at station 8+100. Total failure of the roadbed, evidenced by a slump of approximately 1 m and logitudinal cracking, occurred in September of 1987 at station 8+500 (Fig. 2).

The soil stratigraphy compiled from boreholes at stations 7+600, 7+780 and 8+100 is varied along the affected section. All three holes indicate the existence of ground ice at 4 to 5 m depth below the road surface. At the thermistor borehole location (Fig. 7) the overburden immediately below the road fill is a reddish clayey sand down to 4.5 m depth. This is underlain by a greyish brown clay from 4.5 to 5 m

Figure 2. Longitudinal cracking in the road surface at Site 2, during September, 1987.

depth. Ice lensing (5 to 15 mm) is evident in the latter layer. Massive ice with up to 25 % included clay soil extends from 5 m depth to the end of the borehole at 6 m. There is no indication of bedrock in any of the boreholes.

GROUND PROBING RADAR RESULTS

The radar equipment used was the A-Cubed Inc. Pulse EKKO III Ground Probing Radar system. The operational frequency employed was 100 MHz. Transmitter-receiver antenna separation was 2 m. Readings were taken every metre along profile. A common depth point sounding was performed at the location of the thermistor cable (station 7+780). The results and interpretations are shown in Figures 3 and 4 respectively. The results indicate a propagation velocity of about 0.12 m/ns in the sand and gravel road fill. This velocity is consistent for similar frozen materials encountered in previous surveys. No velocity measurement is available for the clay because of the location of the CDP sounding.

Table 1. Drill core log (Fall, 1986) and downhole temperatures (April, 1987) for the borehole at location 7+780, section 8 km, Rae Access road. Air temperature is −10°C.

DEPTH (m)	SOIL DESCRIPTION SOIL STRENGTH, DENSITY COMPRESSIBILITY, COLOUR COMPOSITION, STRUCTURE	ICE DESCRIPTION	CLAY %	SILT %	SAND %	GRAVEL %	GROUND TEMP 0°C (APRIL, 1987)
0	SURFACE GRAVEL 19 mm (−)	FROST	15	—	20	65	−5.0
1	REDDISH BROWN SAND		25	—	60	15	−5.3
2	REDDISH CLAYEY SANDS, TRACE OF GRAVEL MEDIUM PLASTICITY	THAW ZONE	50	—	40	10	−4.5 −3.8 −3.3 −2.7
3							
4	GRAYISH BROWN CLAYS.	ICE LENSING 5 TO 15 mm IN THICKNESS 30 TO 40% ICE CONTENT	85	—	15	0	−1.3
5		75 TO 100% ICE CRYSTALS SOME SOIL.					−0.7
6							−0.7

Site 1

The radar profile at Site 1 (Fig. 5) indicated that depth penetration of the ground radar system was extremely limited in this area. The nearest drillhole at station 9+650 shows that there is at least 1.5 m of clay underlain by massive ice below the gravelly-sand roadbed fill. In this case, the radar is either not getting through the clay or just penetrating to the top of the massive ice. The near horizontal layering in the radar records most likely represents layer boundaries within the clay, but without ground truthing from a drillhole this remains speculation. A small delay in arrivals is noticeable between 40 m and 55 m. This could indicate a slightly finer grained or partly unfrozen fill. A disturbance within the clay layer is also observed between 35 m and 50 m. Figure 6 shows the interpreted reflectors on the radar profile.

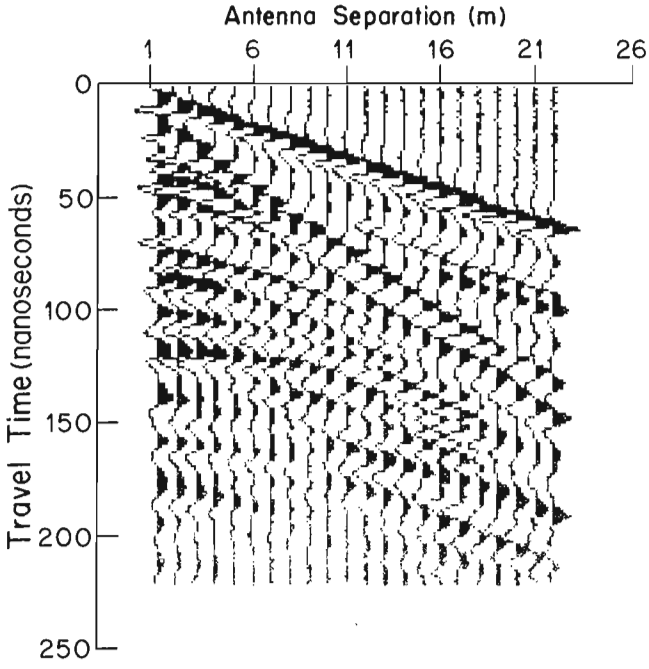

Figure 3. A 100 MHz common depth point sounding at the thermistor cable at station 7+780.

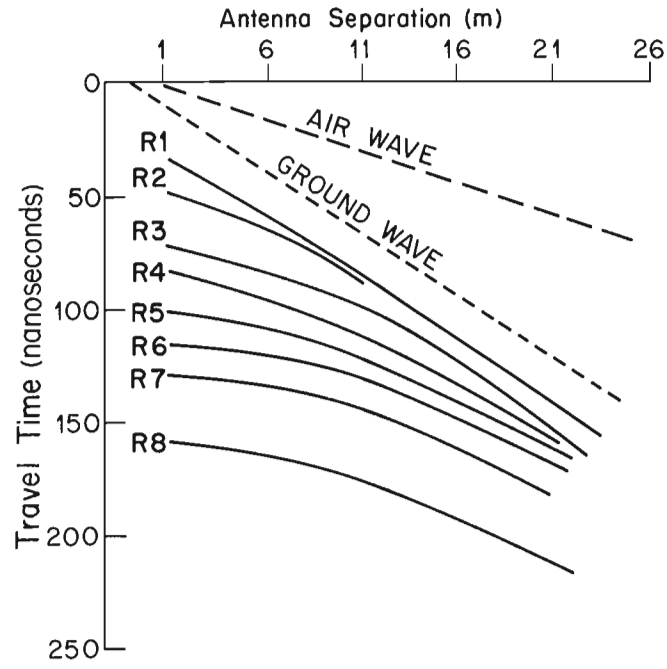

Figure 4. Interpreted arrivals for the sounding shown in Figure 3.

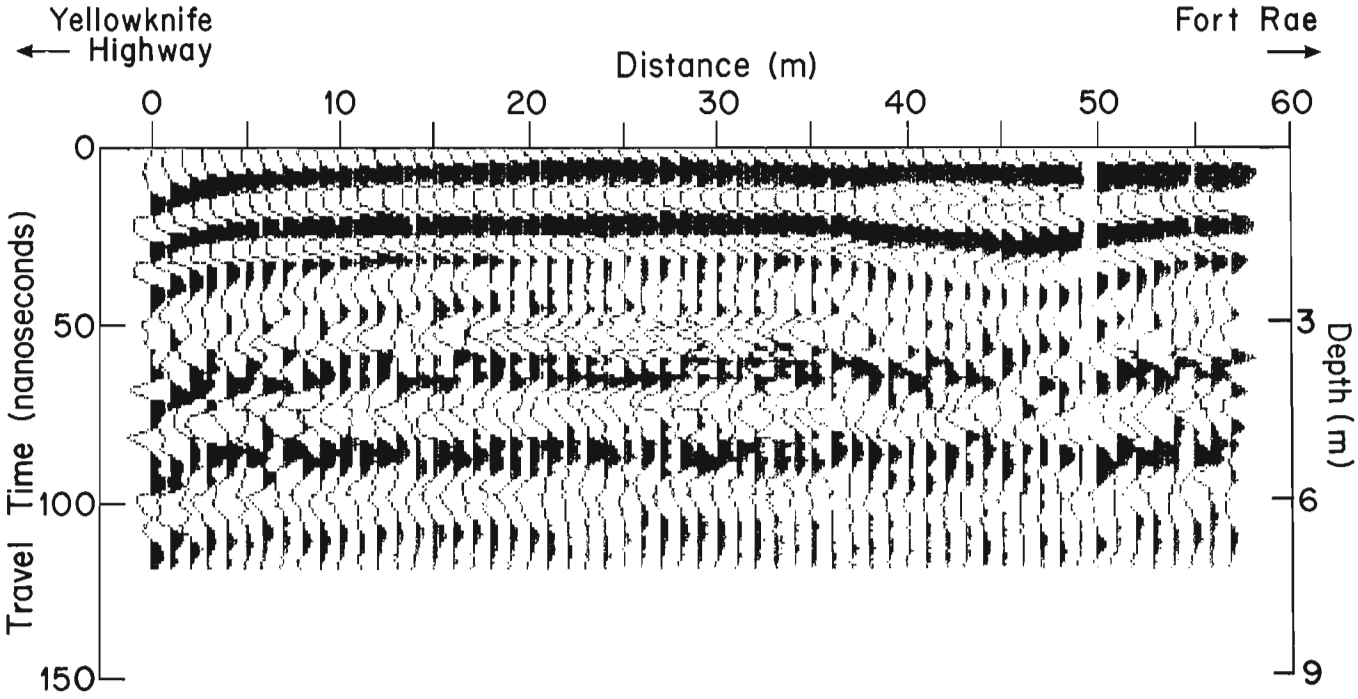

Figure 5. A 100 MHz radar survey at Site 1 (km 10) of the Rae Access road.

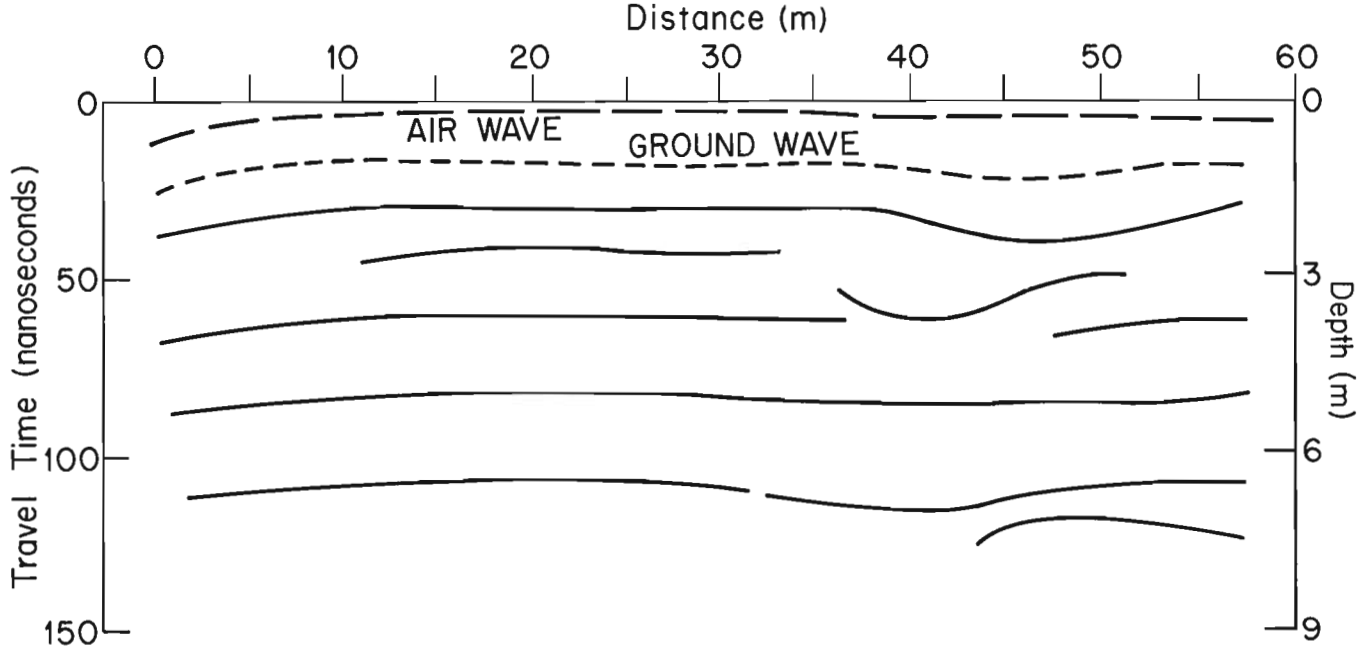

Figure 6. Interpreted section, with major reflectors indicated, for the ground radar profile shown in Figure 3. The depth scale is based upon the ground wave velocity for the sand and gravel fill.

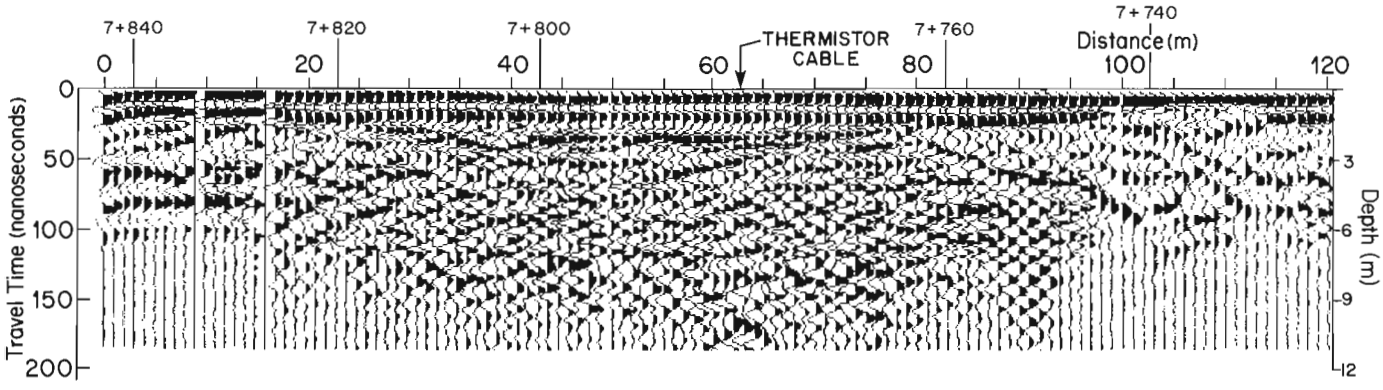

Figure 7. A 100 MHz radar survey along Site 2 (km 8) of the Rae Access road.

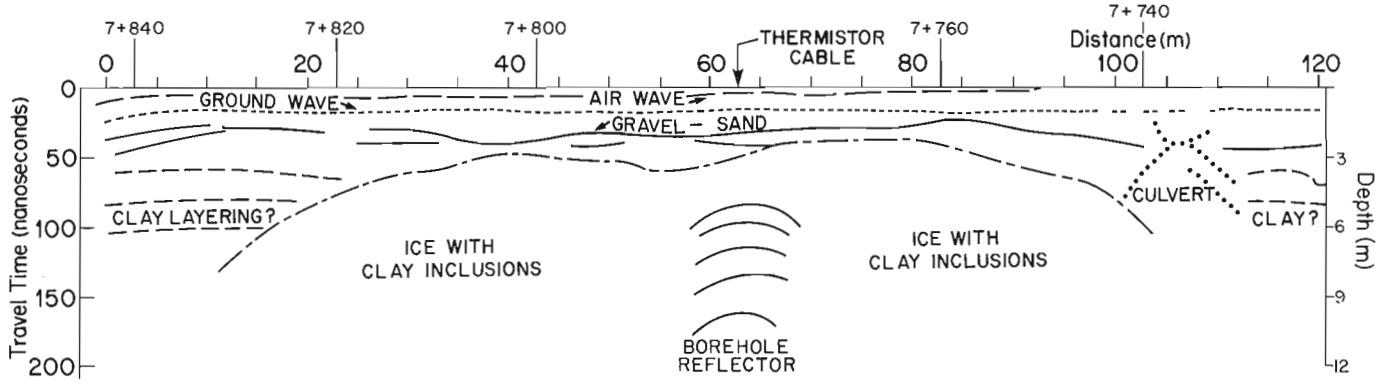

Figure 8. Interpreted section for the ground radar profile shown in Figure 7. The depth scale is based upon the ground wave velocity for the sand and gravel fill.

Site 2

The clay layer pattern seen at Site 1 is evident at the extremes of the Site 2 radar profile (Fig. 7). This pattern is broken by a broad, dome-shaped feature between 15 m and 100 m along the profile. The interpreted section for the radar profile is shown in Figure 8. The central feature corresponds with the massive ice located in the thermistor borehole. Thin clay layering within the ice causes several internal reflections, indicating that the ice body could consist of segregated ice. The radar profile indicates that the ice approaches within 3 m of the road surface at its highest point near the thermister borehole. This is determined from the CDP ground wave velocity estimate for propagation in the sand and gravel fill. The point reflector locates the response of this borehole. A buried culvert is visible at 107 m along the profile. The radar was able to locate the ice body in this case as the overlying clay layer was thin, less than 0.5 m at the thermister borehole, and the top of the ice protruded almost to the base of the road fill.

CONCLUSION

The ground probing radar was able to locate and delineate the extent of a buried massive ice body under the Rae Access road at Site 2. The proximity of the ground ice detected to the bottom of the road bed indicates that further problems may occur. Subsequent cracking and slumping, during September and October of 1987, at stations 7+700, 8+100 and 8+500 confirm this interpretation. The thicker clay unit at Site 1 limited the radar's ground penetration and prevented any definite location of an ice body. As the surveys were performed in early April, when ground thaw was minimal, deeper penetration would not be expected at any other time of year. Lowering the operational frequency of the system by employing 50 MHz antennas could offer more penetration coupled with a loss of resolution. Since the goal is to map the extent of the ice zones a tradeoff between resolution and depth penetration is acceptable.

This short survey, which was intended as a test of the suitability of the radar technique for detecting roadbed problems in permafrost areas, will be followed up in November 1987 by a more extensive survey using the 50 MHz operational frequency and taking more frequent CDP soundings.

AKNOWLEDGMENTS

The authors wish to express their gratitude to John Bowen of the Northwest Territories Public Works and Highways Department for originally suggesting this project.

REFERENCES

Annan, A.P., and Davis, J.L.
1976: Impulse radar sounding in permafrost; Radio Science, v. 11, p. 383-394.
1977: Impulse radar applied to ice thickness measurements and fresh water bathymetry; *in* Current Research, Part B, Geological Survey of Canada Paper 77-1B, p. 63-65.

Bateman, J.D.
1949: Permafrost at Giant Yellowknife; Transactions of the Royal Society of Canada, v. 43, p. 7-11.

Coon, J.B., Fowler, J.C., and Schafers, C.J.
1981: Experimental uses of short pulse radar in coal seams; Geophysics, v. 46, p. 1163-1168.

Davis, J.L., Annan, A.P., and Vaughan, C.
1984: Placer exploration using radar and seismic methods: Expanded abstracts of the 54th Annual International S.E.G. Meeting.

Dolphin, L.T., Beaty, W.B., and Tanzi, J.D.
1978: Radar probing of Vitorio Peak, New Mexico; Geophysics, v. 43, p. 1441-1448.

Dolphin, L.T., Bollen, R.L., and Oetzel, G.N.
1974: An underground electromagnetic sounder experiment; Geophysics, v. 39, p. 49-55.

Esch, D.C.
1983: Evaluation of experimental design features for roadway construction over permafrost; ;Proceedings of the Fourth International Conference on Permafrost, p. 283-288.

Fowler, J.C.
1981: Subsurface reflection profiling using ground probing radar; Mining Engineering, v. 33, p. 1266-1270.

Johansson, B.E., Sveriges Geologiska AB, Sweden
1986: Personal communication.

Johnston, G.H.
1981: Permafrost Engineering design and construction, Associate Committee on Geotechnical research, National Research Council of Canada, John Wiley and Sons.

Kovacs, A., and Morey, R.M.
1985: Impulse radar sounding of frozen ground. US Army Corps of Engineers Cold Regions Research and Engineering Laboratory, Special Report 85-5, p. 28-40.

LeFleche, P.T., Judge, A.S., and Pilon, J.A.
1987: Ground probing radar investigation of the competency of frozen tailings pond dams: *in* Current Research, Part A, Geological Survey of Canada, Paper 87-1A, p. 191-197.

Morey, R.M.
1974: Continuous subsurface profiling by impulse radar: Proceedings of the Engineering Foundation Conference on Subsurface Exploration for Underground Excavation and Heavy Construction, American Society of Civil Engineers.

Nickel, N., Sender, F., Thierback, R., and Weichart, H.
1980: High frequency electromagnetic tools for the prospection of salt-dome structures from boreholes; Expanded abstracts of the 50th Annual International S.E.G. Meeting.

Olhoeft, G.R.
1978: Surficial mapping and in situ electrical measurements by impulse radar; American Geophysical Union, Transactions, v. 59, p. 1055.

Owen, T.E., and Suhler, S.A.
1980: Subsurface void detection using surface resistivity and borehole electromagnetic techniques: Expanded abstracts of the 50th Annual International S.E.G. Meeting.

Pilon, J.A., LaFleche, P.T., and Judge, A.S.
1987: Applications of ground probing radar in permafrost regions to granular deposits, pipeline right of way and frozen core dams: Expanded abstracts of the 57th Annual S.E.G. Meeting.

Stewart, R.D., and Unterberger, R.R.
1976: Seeing through rock-salt with radar; Geophysics; v. 41, p. 123-132.

Unterberger, R.R.
1978: Radar propagation in rock salt; Geophysical Prospecting; v. 26, p. 312-328.

Waite, A.H., Jr.
1966: International experiments in glacier sounding, 1963 and 1964; Canadian Journal of Earth Sciences, v. 3, p. 887-92.

Reconstruction of marine transgression history from an offshore ground temperature profile, Esso Angasak L-03 wellsite, Beaufort Sea

Alan Taylor and Alan Judge
Terrain Sciences Division

Taylor, A. and Judge, A., Reconstruction of marine transgression history from an offshore ground temperature profile, Esso Angasak L-03 wellsite, Beaufort Sea; in Current Research, Part D, Geological Survey of Canada, Paper 88-1D, p. 137-142, 1988.

Abstract

Marine transgression in arctic regions represents a major thermal event, as sea water near its freezing point encroaches on a permafrost landscape. The history of recent transgression is preserved in precise temperatures measured to 48 m below the seabed in a geotechnical borehole at the Esso Angasak L-03 wellsite, offshore Cape Dalhousie, Beaufort Sea. Simple geothermal modelling suggests that the thermal event accompanying marine transgression at this site occurred at least 300 years ago. This implies an average (maximum) rate of coastal retreat of 6 to 7 m/year over the past three centuries. Due to limitations in the models, the actual time of transgression was probably somewhat earlier, with lower rates of retreat. The models suggest that mean surface temperatures prior to marine transgression were 2 to 3 K lower than today, possibly reflecting the nature of the Little Ice Age in the region.

Résumé

La transgression marine dans les régions arctiques constitue un phénomène thermique important étant donné que l'eau de mer près de son point de congélation a empiété sur un terrain pergélisolé. La transgression récente a laissé des traces à des températures spécifiques mesurées à 48 m sous le fond océanique dans un trou de sondage géotechnique au site du puits Angasak L-03 d'Esso, au large de Cap Dalhousie dans la mer de Beaufort (Canada). Une simple modélisation géothermique permet de supposer que ce phénomène thermique causé par la transgression à ce site particulier a eu lieu il y a au moins 300 ans. Par conséquent, le littoral aurait reculé à la vitesse moyenne (maximale) de 6 à 7 m par année pendant les trois derniers siècles. Compte tenu des limites des modèles, la transgression a probablement eu lieu quelque peu de temps avant, à des vitesses de retrait inférieures. D'après les modèles, les températures de surface moyennes avant la transgression étaient de 2 à 3 K inférieures par rapport à aujourd'hui, reflétant peut-être les effets du Petit âge glaciaire dans cette région.

INTRODUCTION

Most of the shelf of the Beaufort Sea is underlain by ice-bonded permafrost that is a relic from periods during the late Pleistocene when the seabed was exposed to subaerial arctic conditions by lower sea levels. Offshore permafrost is presently degrading in response to the recent marine transgression and the resulting thermal disequilibrium may be apparent in temperature profiles beneath the seabed (Mackay, 1972). Marine transgression represents a major thermal event, as seawater near its freezing point encroaches on a permafrost landscape whose surface temperatures are of the order of −10°C.

In February, 1987, a 56 m geotechnical borehole was drilled from the sea ice at the Esso Angasak L-03 wellsite, about 2 km offshore from Cape Dalhousie in the eastern Beaufort Sea (Fig. 1a); water depth is 6.7 m (Fig. 1b). A 100 m multithermistor cable was placed in the hole at the end of drilling; the surplus length was to allow for some ice movement. An automatic data logger was attached and a time series of precise temperatures were recovered until early April, when the cable broke, apparently due to ice motion.

Temperature data from the installation are presented here. Simple geothermal models have been undertaken to estimate in an objective way the latest time of marine transgression across this site, and to predict the nature of the deeper thermal regime within the degrading permafrost.

Acknowledgments

The geotechnical hole was drilled by the Atlantic Geoscience Centre, EMR Canada, with the co-operation of Esso Resources. The cable was manufactured and installed by Golder Associates; we thank Ken Been for his assistance. The Polar Continental Shelf Project, EMR Canada provided logistic assistance. Funding for the program of temperature measurement was provided by the Office of Energy Research and Development, EMR Canada. S. Blasco of AGC provided some unpublished geotechnical data; we thank him also for useful discussions.

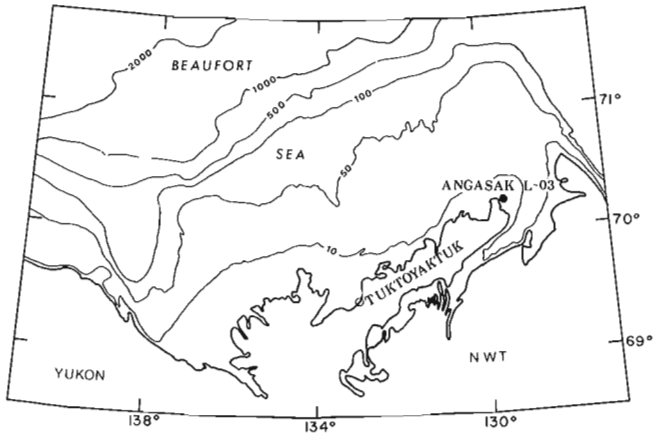

Figure 1a. Location of the Esso Angasak L-03 well within the Mackenzie Delta-Beaufort Sea region. Bathymetry is in metres.

INSTALLATION OF THE TEMPERATURE CABLE

Following the drilling of the geotechnical borehole, 3.8 cm diameter ABS-type plastic pipe was lowered inside the 10 cm drill casing and filled with glycol. The temperature cable was lowered into the plastic pipe and the 10 cm casing withdrawn around it. A Seadata model 1250 data logger, set at a 2 hour reading interval, was attached to the cable and left on site until mid-April, when the logger was removed prior to ice break-up.

The temperature cable consists of 12 YSI-type 44033 thermistors at a 5 m spacing. These sensors have a nominal resistance of 7400 ohms at 0°C and a manufacturer-specified interchangeability of 0.1°K; they were not calibrated further, and a relative imprecision in temperature values of ± 0.05°K is assumed.

TEMPERATURE DATA

Temperature profiles show cooling of the hole following the thermal disturbance due to drilling (Fig. 2). The rate of cooling at each sensor depth is a function of the disturbance at that depth, and the actual formation properties such as thermal conductivity, porosity and ice content. For several weeks prior to the last log on April 3, no changes in temperature were measured and this log may be considered a measure of the undisturbed formation temperatures. It is apparent from Figure 2 that bottom water temperatures decreased between February and April.

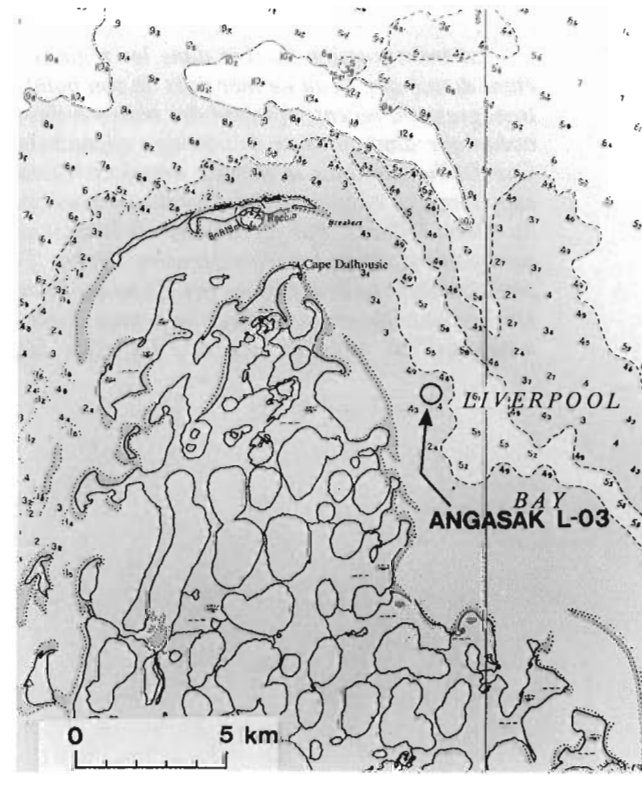

Figure 1b. Location of the study well offshore from Cape Dalhousie. Bathymetry is in metres. Part of Canadian Hydrographic Service chart 7605.

The shape of the overall temperature profile is similar to a number of seabed temperature profiles measured in the western Beaufort Sea (Osterkamp and Harrison, 1982). In general, temperatures increase to a depth of 8 m below the seabed and then decrease to the bottom of the cable. The upper, positive gradient reflects the response of the upper few metres of sediment to the seasonal cooling of the seabed due to lower bottom water temperatures over the winter; similar shallow seabed temperature perturbations have been modelled in terms of variations in water temperatures elsewhere on the Beaufort Shelf (Taylor and Allen, 1987). Qualitatively, the deeper, negative gradient is similar to that predicted near the upper surface of thick relict permafrost degrading in response to marine transgression (Mackay, 1972). It is the negative gradient that is modelled here.

Ice-bonded permafrost has been interpreted from geophysical well logs in deep petroleum exploration wells to extend 400 to 600 m below the seabed offshore from Cape Dalhousie; the actual depth of ice-bonding may be interpreted from the geophysical logs taken at the Angasak L-03 well, when they become available. The depth of the 0°C isotherm may be somewhat deeper (Judge and Taylor, 1985).

The shallow geotechnical borehole at Angasak penetrates an unfrozen zone to 30 m, partial ice-bonding from 30 to 40 m and ice-bonded permafrost below 40 m (Fig. 2). In the upper 40 m, salt and moisture transport may play a role in the melting of the ice-bonded permafrost (Harrison and Osterkamp, 1978). Despite this complex environment and although the profile represents only 10% of the permafrost section, an attempt is made here to apply simple models to determine what information may be gained on the history of marine transgression in the area and on the nature of the deeper permafrost.

GEOTHERMAL MODELS

Two analytic models have been undertaken. The first is a one-dimensional model that predicts the transient variation in subsurface temperatures in offshore permafrost following marine transgression (Lachenbruch et al., 1982). The second is a two-dimensional model that predicts subsurface temperature-depth gradient anomalies near shorelines following marine transgression or regression. This latter model was used to assess the degree to which the proximity of the present shoreline may effect the shallow, subsurface thermal regime. Both models assume that the transgression occurred in a short period at some time in the past and that it was accompanied by a sudden increase in surface temperature.

Model parameters

These models require an estimate of the subsurface temperatures prior to inundation. The thermal regime is controlled

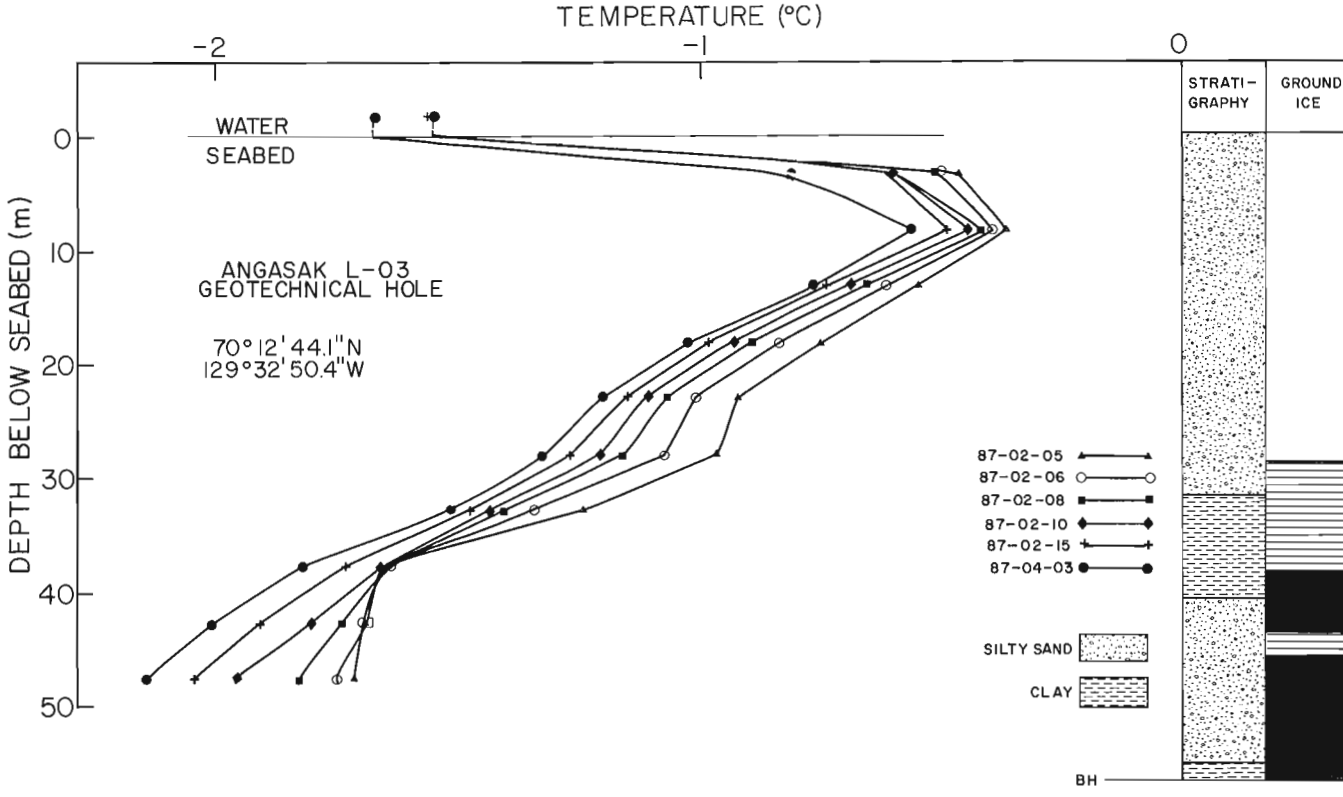

Figure 2. Temperature-depth profiles measured by the automatic data acquisition system, selected at several times following completion of drilling. The top thermistor is in water, about 2 m above the bottom. Probable relative imprecision in temperature measurements is ±0.05°C. Stratigraphy and observed ground ice are from an unpublished report by Golder Associates; partial ice-bonding was observed between 30 and 39 m and generally ice-bonded permafrost below.

by the terrestrial heat flow originating deeper within the earth, the thermal properties of the rock and sediments, and the temperature of the land surface. None of these parameters are known for the Angasak area, but some reasonable estimates may be made. Based on a knowledge of the geology of the region, Judge (1973) estimated the terrestrial heat flow to lie between 63 and 84 mWm^{-2}; a value of 70 mWm^{-2} was taken. A thermal conductivity of 4 $Wm^{-1}K^{-1}$ and a thermal diffusivity of 1.4×10^{-6} $m^{-2}s^{-1}$ were taken as representative of frozen, unconsolidated sands. For a surface temperature of −10°C, equilibrium permafrost thicknesses of 570 m are predicted by these parameters; 680 m would be in equilibrium with −12°C. The similarity of these surface temperatures and permafrost thicknesses to those of the Tuktoyaktuk Peninsula today suggests that these parameters are reasonable in defining the initial thermal environment.

Model A

The subsurface temperature field T(z,t) at times t following inundation of a site due to marine transgression may be described by (Lachenbruch et al., 1982, eq. 24, 27)

$$T(z,t) = T_s + (T_o - T_s)\frac{2}{\pi}\sum_{n=1}^{\infty}\frac{1}{n}\exp\left(\frac{-n^2\pi^2 t}{4\lambda}\right)\sin\left(n\pi\frac{z}{Z}\right)$$

where z is the depth below the seabed, T_o the initial land surface temperature before inundation, T_s the seabed temperature after inundation, Z the thickness of ice-bonded permafrost in equilibrium with the surface temperature T_o and λ the thermal time constant, defined as (Lachenbruch et al., 1982, eq. 28a)

$$\lambda = \frac{Z^2}{4\alpha}$$

for a thermal diffusivity α. For permafrost thickness of 400 to 600 m, this time constant is of the order of 900 to 2000 years. Latent heat of melting at the base of the permafrost horizon is not considered; at times much smaller than λ, the "signal" of the new surface state has not penetrated to the base of the permafrost and little melting occurs (Lachenbruch et al., 1982, eq. 32-33). The more complex processes at the upper boundary, as discussed above, are not considered.

Using equation 1, subsurface temperatures were calculated for a range of pre-transgression surface temperatures T_o (−20 to −6°C, 1° steps), for several post-transgression seabed temperatures T_s (−1° to 0°C) and for a range of times t of inundation (100 to 1500 years ago, 100 to 250 year steps). Calculated temperatures were compared to the measured data, and the best model selected in a least squares sense (Fig. 3). The model best fitting the measured data suggests that surface temperatures were −12°C prior to inundation and seabed temperatures −0.3°C after; the former value requires an equilibrium permafrost thickness of 680 m, perhaps somewhat greater than the actual thickness. The best fitting model requires transgression to have occurred about 300 years ago.

Temperatures calculated from the best model at greater depths (Fig. 4) illustrates the relatively limited picture provided by the shallow data of the transient thermal regime resulting from marine transgression. Variations in thermal conductivity with depth would modify the detail of the profiles but, as the predicted equilibrium permafrost thickness is similar to that thought to exist in the area, some confidence is gained in the generalized thermal regime depicted in Figure 4. The general shape of the predicted profile is similar to that measured in thick degradational permafrost further offshore (Weaver and Stewart, 1982).

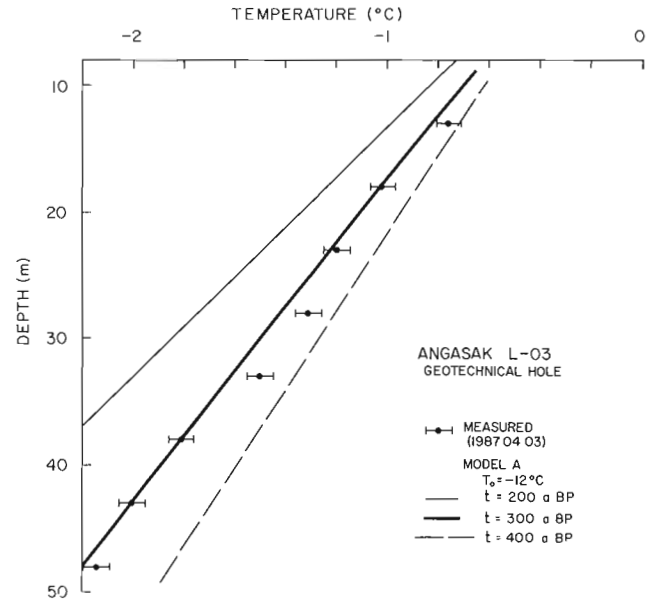

Figure 3. Temperature profiles predicted by model A for transgressions occurring 200, 300 and 400 years ago, for a surface temperature of −12°C prior to inundation and a seabed temperature of −0.3°C after. Best fit to the measured data occurs at 300 years.

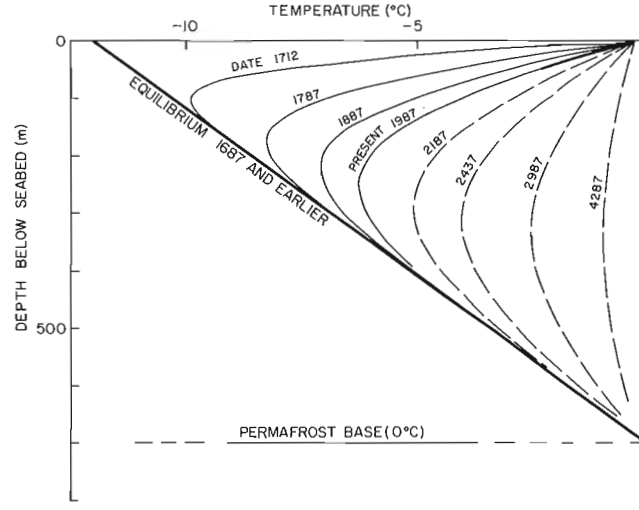

Figure 4. The temperatures predicted by model A at various dates following marine transgression 300 years ago. The thermal regime predicted for today is labelled '1987', and the portion of the curve fitted to the measured data is heavier. Future subsurface temperatures are predicted by the model to follow the dashed curves.

Model B

This two-dimensional model determines the changes in the subsurface thermal regime due to a shoreline that has shifted at some time in the past. It differs from model A in that model B includes the thermal effect of the proximity of the site to the new shoreline. The model calculates the transient and steady-state change expected in the temperature-depth gradient as a function of offshore distance x, depth z and time t since inundation (Lachenbruch, 1957, eq. 14):

$$\frac{dT}{dz} = -A \left[\frac{x}{\pi(z^2 + x^2)} \exp - \left(\frac{z^2 + x^2}{4 \propto t}\right) + \frac{1}{2\sqrt{\pi \propto t}} \exp - \left(\frac{z^2}{4 \propto t}\right) \left[1 + \operatorname{erf} \frac{\propto}{2\sqrt{\propto t}} \right] \right\}$$

In this model, A is the step increase in temperature experienced by the land surface upon inundation (equivalent to T_s-T_o of model A) and erf is the error function.

Figure 5 shows the temperature gradient anomalies predicted by equation 3 for A = +12°C and x = 2000 m. Note that the largest anomalies are predicted for more recent transgressions. The actual gradient anomaly is estimated as follows. The measured gradient below 18 m is about -40 mKm^{-1} (Fig. 2); the expected gradient before inundation in equilibrium with the lower surface temperature is about $+20$ mKm^{-1}. The gradient anomaly over the upper few tens of metres is, then, -60 mKm^{-1}. From Figure 5, this value is consistent with the marine inundation occurring 280 years ago. For x = 2000 m and z < 50 m, the gradient anomaly arises from the time term in equation 3; the effect of the nearby shoreline at these depths becomes appreciable only at distances x < 100 m.

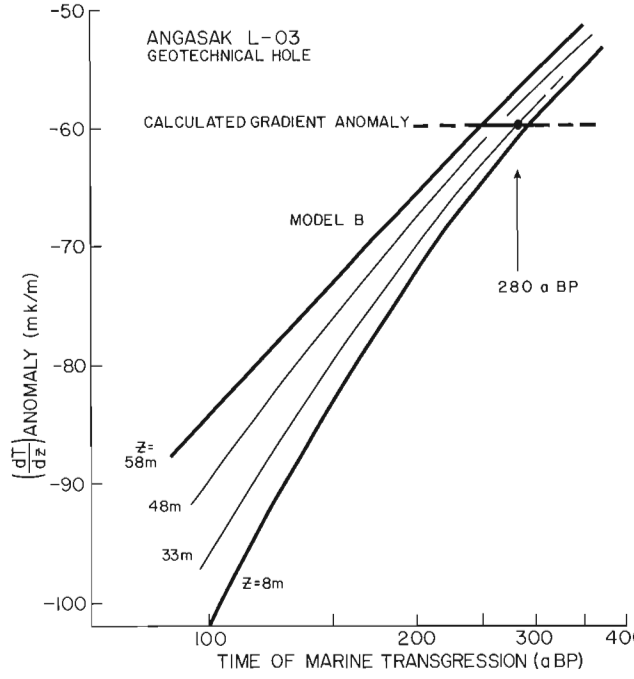

Figure 5. Model B, showing the temperature-depth gradient anomalies versus time of marine transgression. The model incorporates the effect of the distance of the site from the present shore. The upper and lower curves represent the anomaly expected at 58 and 8 m depth, respectively. The horizontal line at dT/dz = -60 mWm^{-1} is the estimated gradient anomaly calculated from the measured data; this suggests an inundation time of about 280 years ago.

DISCUSSION

The time of marine transgression predicted by these models is a minimum. Two factors contribute independently and cumulatively to an under-estimate of the time since inundation.

First, neither model considers the effects of latent heat in melting the top 30-40 m of the inundated seabed; these ice-rich sediments (Fig. 2) would result in a slower evolution of the transient temperature profiles than predicted in Figures 3 and 4. In this respect, the formalism developed by Harrison and Osterkamp (1978) or the numerical model including latent heat of phase change developed by Outcalt (1985), may give improved estimates when more information on the porosities and salinities are available.

Second, the time calculated by the models refers to the time of the main thermal event accompanying transgression, i.e. the sudden increase in mean surface temperature. This time is probably later than the transgression event as observed from geomorphic evidence. For some time after the sea actually overran the site, water might be shallow, sea ice could be grounded at the site for much of the winter and hence, the apparent mean annual surface temperature would be, perhaps, little changed from its previous subaerial value. Only when water depths at the site exceeded, perhaps, 1.2 m would the inundated surface experience year-round the higher mean temperatures assumed in the models. The marine transgression event, in the thermal sense, would thus occur somewhat later than the geomorphic event. This ambiguity would have to be addressed even in more sophisticated models.

IMPLICATIONS TO RATE OF SHORELINE RETREAT

The Anagasak site at present lies 2 km offshore from a coast described as low tundra with an inundated section (Harper et al., 1985, Appendix 2, Map 91); such zones might experience a moderate to higher rate of retreat in the face of a transgressing sea. Considering the limited bathymetric data, the site appears to lie near a local high in the seabed, with deeper water being reported to landward and to the north and to the southeast (Fig. 1b). Had the site prior to transgression been under a large, old lake, the encroachment of the sea would represent a minor thermal event and the large negative gradient in the shallow seabed temperatures would not be observed today.

The thermal modelling undertaken above suggests that 2 km of shoreline retreat has occurred in the Cape Dalhousie area in a (minimum) period of 300 years. This suggests an average (maximum) rate of erosion of 6 to 7 m/year over the past three centuries.

In a recent study, Harper et al. (1985, Table 5.3, Fig. 5.19) measured contemporary rates of coastal retreat from geomorphic evidence along this coast; values are as high as 1.5 m/year, although the average is 0.5 m/year. Mackay (1963, section 60) wrote that "at Cape Dalhousie, an island 20 feet high and several hundred feet across is reported to have been washed away in the past 20 years"; this may be suggestive of the higher rates that may be observed locally in the area. While the 6 to 7 m/year retreat rate calculated here is large, and for reasons discussed above actually may be somewhat lower, rates of 6 to 9 m/year have been measured from a series of airphotos spanning a period of 32 years for a coastal exposure of ground ice west of Tuktoyaktuk (Rampton and Mackay, 1971, p. 14).

Hill et al. (1985) have suggested that a fairly constant rate of sea level rise, 0.55 cm/year, has been occurring in the past 27 000 years across the Beaufort Shelf. Considering the water depth at the site, transgression might have occurred 1200 years ago, or the thermal event about 1000 years ago.

IMPLICATIONS TO THE PALEOCLIMATE

Extrapolating temperatures in the upper 50 m at four petroleum exploratory wells in the Tuktoyaktuk Peninsula yields mean surface temperatures today of -9 to -10°C (Taylor and Judge, 1977). The mean surface temperature predicted here prior to transgression, -12°C, is several degrees lower; this is consistent with lower temperatures expected during the Little Ice Age.

CONCLUSIONS

The Esso Angasak L-03 wellsite lies in 6.7 m of water about 2 km offshore from Cape Dalhousie, in the Beaufort Sea. The thickness of ice-bonded permafrost is probably between 400 and 600 m in the area. A geotechnical borehole to 56 m depth encountered ice-bonded permafrost at 40 m. A time series of precise ground temperatures to 48 m depth below the seabed have been obtained from an automatic data logger attached to a cable left in the hole. Temperatures decrease with increasing depth between 8 and 48 m, with an average gradient of -40 mKm^{-1}. This profile shape is compatible with the thermal signature resulting from encroachment of the sea upon the site as relative sea levels rose.

Simple geothermal modelling of these data suggests that marine transgression occurred at the site at least 300 years ago. This implies an average (maximum) rate of coastal retreat of 6 to 7 m/year over the past three centuries. Limitations inherent in the models suggest that actual rates were probably less. In addition, the geomorphic event associated with marine transgression probably precedes the major thermal event, due to sea ice being grounded for much of the winter until water depths exceed maximum ice thickness.

The value in a geothermal approach lies in its ability to estimate the time of marine transgression from data independent of geomorphic evidence, and to determine rates of coastal retreat over much longer periods than is possible from other evidence. More advanced numerical models might overcome some of the limitations noted in the analytic formulation used here.

REFERENCES

Harper, J.R., Reimer, P.D., and Collins, A.D.
1985: Canadian Beaufort Sea physical shore-zone analysis; *in* report by Dobrocky Seatech Ltd. to Geological Survey of Canada. 105 p + 3 appendices. (Unpublished).

Harrison, W.D. and Osterkamp, T.E.
1978: Heat and mass transport processes in subsea permafrost. 1. An analysis of molecular diffusion and its consequences; Journal of Geophysical Research, v. 83, p. 4707-4712.

Hill, P.R., Mudie, P.J., Moran, K., and Blasco, S.M.
1985: A sea-level curve for the Canadian Beaufort Shelf; Canadian Journal of Earth Sciences v. 22, p. 1383-1393.

Judge, A.S.
1973: The prediction of permafrost thickness; Canadian Geotechnical Journal, v. 10, p. 1-11.

Judge, A.S. and Taylor, A.E.
1985: Permafrost distribution in northern Canada: interpretation of well logs; *in* Workshop on Permafrost Geophysics, ed. J. Brown, M.C. Metz, and P. Hoekstra, Golden, Colo., October 1984. p. 19-25.

Lachenbruch, A.H.
1957: Thermal effects of the ocean on permafrost; Geological Society of America, Bulletin, v. 68, p. 1515-1530.

Lachenbruch, A.H., Sass, J.H., Marshall, B.V., and Moses, T.H., Jr.
1982: Permafrost, heat flow, and the geothermal regime at Prudhoe Bay, Alaska; Journal of Geophysical Research, v. 87, p. 9301-9316.

Mackay, J.
1963: The Mackenzie Delta area, N.W.T.; Geographical Branch Memoir 8, reprinted 1974, as Geological Survey of Canada, Miscellaneous Report 23, 202 p.
1972: Offshore permafrost and ground ice, southern Beaufort Sea, Canada; Canadian Journal of Earth Sciences, v. 9, p. 1550-1561.

Osterkamp, T.E. and Harrison, W.D.
1982: Temperature measurements in subsea permafrost off the coast of Alaska; *in* Proceedings of the Fourth Canadian Permafrost Conference, ed. H.M. French; Calgary, March, 1981. p. 238-248.

Outcalt, S.
1985: A numerical model of subsea permafrost; *in* Freezing and Thawing of Soil-water Systems, ed. D.M. Anderson and P.J. Williams; American Society of Civil Engineers, New York. p. 58-65.

Rampton, V.N. and Mackay, J.R.
1971: Massive ice and icy sediments throughout the Tuktoyaktuk Peninsula, Richards Island, and nearby areas, District of Mackenzie; Geological Survey of Canada, Paper 71-21, 16 p.

Taylor, A.E. and Judge, A.S.
1977: Canadian geothermal data collection- northern wells 1976-77; Geothermal Series of the Earth Physics Branch, EMR Canada. 194 p.

Taylor, A.E. and Allen, V.S.
1987: Shallow sediment perturbations and sediment thermal conductivities, Canadian Beaufort Shelf; Canadian Journal of Earth Sciences, v. 24.

Weaver, J.S. and Stewart, J.M.
1982: *In-situ* hydrates under the Beaufort Sea shelf; *in* Proceedings of the Fourth Canadian Permafrost Conference, ed. H.M. French; Calgary, p. 320-328.

The Eureka Sound Group: alternative interpretations of the stratigraphy and paleogeographic evolution-Discussion

A.D. Miall[1]

Miall, A.D., The Eureka Sound Group: alternative interpretations of the stratigraphy and paleogeographic evolution-Discussion; in Current Research, Part D, Geological Survey of Canada, Paper 88-1D, p. 143-147.

INTRODUCTION

Independent research by two workers, myself and B.D. Ricketts, has led to alternative stratigraphic schemes for the rocks formerly classified as the Eureka Sound Formation. These notes are offered as an attempt to defend some of my views, to reconcile some of the differing interpretations, and to focus on some of the remaining problems that future research may resolve.

The pertinent papers are listed at the end of this discussion (Miall, 1981, 1984, 1985, 1986a; Ricketts, 1984, 1985, 1986; Ricketts and McIntyre, 1986), and the two stratigraphic scheme (Miall's and Ricketts') are illustrated in Figure 1.

FORMATIONS AS FACIES

Several workers have formally (e.g. Ricketts, 1986, p. 364) or informally criticized my stratigraphic scheme in the mistaken understanding that the formations are based on genetic criteria, such as interpreted depositional systems. According to the rules of stratigraphic nomenclature, a formation is a lithologically distinctive, mappable unit. The fact that lithologies are described in term of facies does not change the fact that rocks are described in objective detail. The facies assemblages first erected in my 1981 paper are based strictly on observational detail, they can readily be recognized in the field and mapped. They are given noninterpretative names, such as "facies assemblage B", and interpretative names, such as "prodeltaic assemblage", which may be revised upon further work without changing the overall assemblage designation, or its designation as "assemblage B". The facies assemblages are therefore an ideal basis on which to erect formations. The observational, descriptive detail has now been considerably expanded, and illustrated, in my major stratigraphic paper (Miall, 1986a). In their type areas in the eastern Arctic, the formations erected and described in this paper have valid descriptions, with documented type sections and age relations, and they have been mapped. In their type areas they are therefore as valid as any that have been proposed for the Arctic.

As carefully explained in an introductory section in one of my recent papers (Miall, 1986a, p. 245-246) there is not necessarily a one-for-one correspondence between facies assemblages and formations, mainly because the conventions of stratigraphic nomenclature and mapping require a somewhat simplified approach to lithological subdivisions.

There is certainly some room for differences of opinion on the advisability of applying formation names to distant areas, outside their type areas, on the basis of lithological (facies assemblage) similarity. If the units were probably never physically connected it may be questioned whether they should be given the same name. To imply such a connection requires an interpretation of the regional tectonics and paleogeography, thus introducing an interpretative element into formation designation. This may not be considered advisable, because formation designation is required to be strictly based on description. In fact, both Ricketts and myself have proposed cross- Arctic correlations which, apart from name, do not differ substantially.

The best approach to the naming of now physically separated outliers is that of convenience. If the nomenclature works, makes sense, is convenient and can readily be understood, then it should be retained.

BLANKETS OR WEDGES?

I have long made the suggestion that the Eureka Sound Group was deposited in a series of isolated or semi-isolated basins separated by intrabasin upwarps. This view is in contrast with the tectonic setting of most older units in the Arctic, which are typically Arctic-wide in their extent. The implication of this interpretation is that many, if not all, of the units within the Eureka Sound are laterally restricted, and were derived from relatively local source areas. They would therefore be expected to show wedge or lens shaped geometries, and sharp lateral facies changes.

The contrasting view (that of Ricketts) is that some, and possibly all of the Eureka Sound units are much broader in areal extent, perhaps representing regional changes in base level in response to regional tectonics or eustatic sea level change. The best supporting evidence for this view is Ricketts' Strand Bay Formation which, he maintains, can be traced from Strand Fiord to Strathcona Fiord, and can be correlated with rocks of similar lithology and partially overlapping age-range in other parts of the Arctic Islands (Ricketts, 1986,

[1] Geology Department; University of Toronto, Toronto, Ontario M5S 1A1.

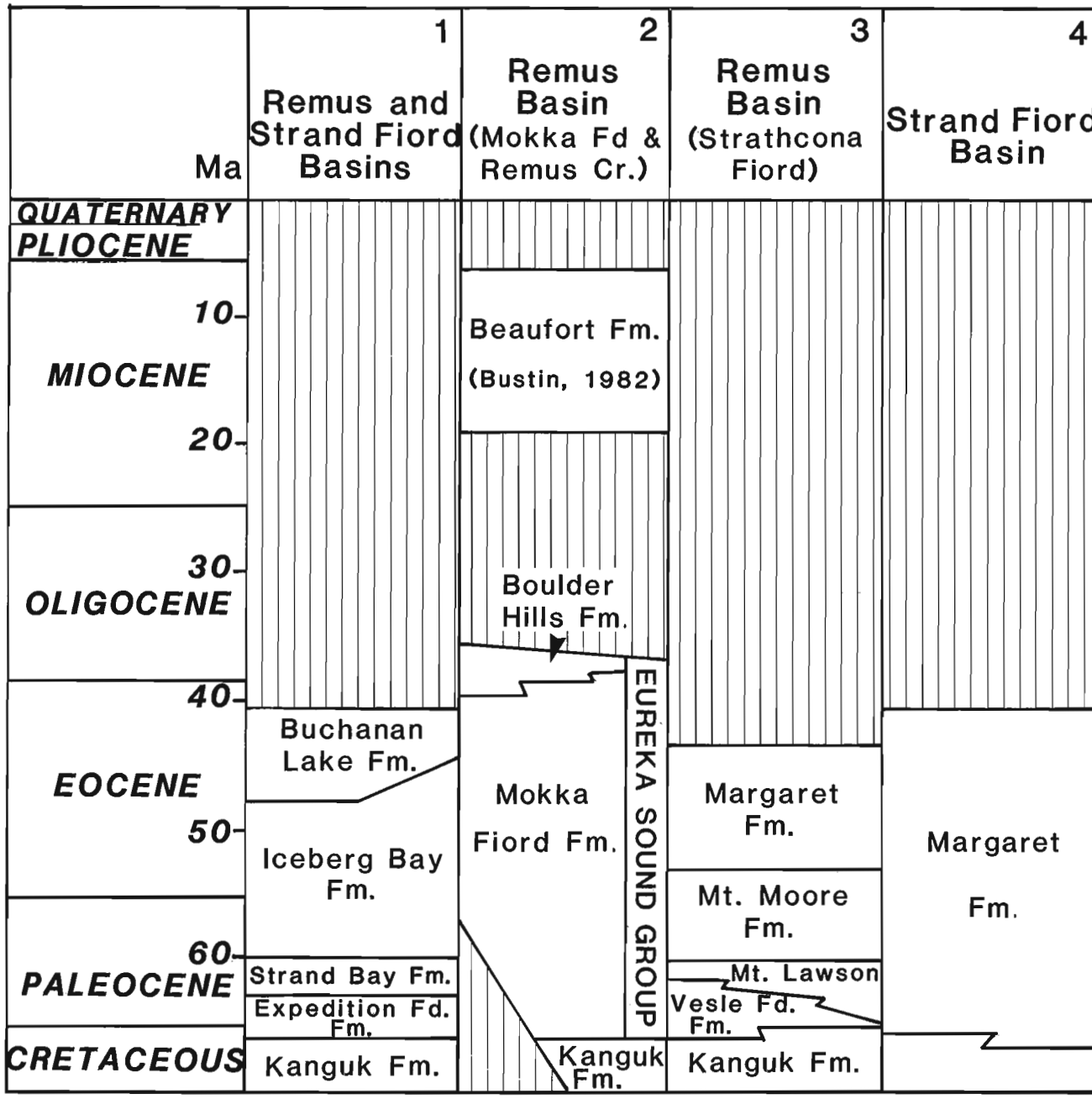

Figure 1. Alternative stratigraphic schemes for the Eureka Sound Group. Column 1 from Ricketts (1986); columns 2 to 4 from Miall (1986a).

Table 39.2). He interprets this fine grained unit as the product of a regional marine transgression.

This is a reasonable interpretation, but is not, in my view, conclusive proof for the "blanket" interpretation of the entire Eureka Sound Group. The Strand Bay represents only one formation, and Ricketts himself documents or refers to many other lateral facies changes elsewhere in the Eureka Sound Group that indicate locally complex paleogeographies. It remains an open question whether the occurrence of an Arctic-wide transgression can be proven for the Strand Bay interval, and, even if it did occur, it may have had little bearing on events during the remainder of the Cenozoic.

To accept Ricketts' "blanket" interpretation is to lend credence to the use of locally defined formation names for Arctic-wide correlation purposes. So interpretation enters again into the definition of formations.

What evidence is there in support of my view, that the Sverdrup Basin was broken up by intrabasin tectonic activity in the Late Cretaceous, and that this radically changed the paleogeographic and stratigraphic patterns? Balkwill (1978) was the first to document the three stages of the Eurekan Orogeny, and he specifically referred to basin and arch formation beginning in the Late Cretaceous. Nobody denies that

basins and arches now exist. The question is, were they there, and did they influence sedimentation during the early Cenozoic, as I have maintained? There seems to be no disagreement between Ricketts and myself that Eureka Sound sedimentation was terminated by active tectonism and the progradation of alluvial fan wedges sometime between the mid-Eocene and the Early Oligocene. The main area of disagreement relates to the time from the initiation of the Eureka Sound sedimentation (Campanian or Maastrichtian) until the mid-Eocene.

Generally the best way to tackle this kind of problem is to turn to paleocurrent data, detrital petrology, lateral facies changes and general stratigraphic relationships. Unfortunately, petrology is of little help in this case, because most of the Eureka Sound clastics are very mature, having been derived mainly from recycled, already mature Mesozoic and Paleozoic detritus. However, the other lines of evidence offer much food for thought:

1. The Sverdrup Basin Rim is known to have affected Sverdrup Basin sedimentation since the late Paleozoic (Meneley et al., 1975). Cretaceous and, probably, Cenozoic sediments onlap it under the Arctic Coastal Plain. In northern Banks Basin there are some facies and paleocurrent data that indicate that the rim was an active uplift area and at least a minor sediment source during the early Cenozoic (Miall, 1979a).

2. Balkwill (1983) documented an intra-Eureka Sound Group unconformity on Cornwall Island, overlying the Cornwall Arch, and estimated that 3.6 km of erosion took place between the latest Cretaceous and the Paleocene.

3. In Eclipse Trough there is some facies and paleocurrent evidence that fluvial-deltaic dispersal paralleled the basin axis from Late Paleocene to mid-Eocene, suggesting a tectonic control, and there is some suggestion of a marginal conglomerate facies bordering the trough to the northeast, indicating active faulting (Miall et al., 1980).

4. In Judge Daly Basin the conglomerates containing Paleocene plants are clearly of syntectonic origin (Mayr and DeVries, 1982; Miall, 1982).

5. The evidence for intrabasin tectonism from Strand Fiord and Remus basins is somewhat more equivocal. I have suggested that the Princess Margaret Arch functioned as a sediment source throughout most of the time of Eureka Sound sedimentation. The unconformable contact of the Eureka Sound Group with Upper Jurassic strata at Flat Sound on eastern Axel Heiberg Island (Balkwill et al., 1975) indicates at least some early Cenozoic uplift in that area. Paleocurrent evidence (Miall, 1985) is consistent with this interpretation, suggesting the possibility of sediment being shed to both the east and west sides of the uplift prior to the major mid- to Late Eocene rejuvenation. But the stratigraphic evidence is not conclusive. The major wedge of fluvial sediment northwest of Vesle Fiord Thrust is interpreted by me as an alluvial plain at the head of the "gulf" formed by Remus Basin. But it could be the remnant of a larger alluvial plain, of which the Strand Fiord deltaic sediments are the distal equivalent, with the intervening fluvial-deltaic transition (under what is now Princess Margaret Arch) lost as a result of subsequent uplift and erosion. The latter interpretation is presumably what Ricketts would prefer. Only more detailed work in the future will resolve this problem.

The importance of these five points is that they do demonstrate at least some intra-Sverdrup Basin tectonism. It would therefore seem to me essential to allow for the possibility of major lateral facies and thickness changes within the Eureka Sound. Such changes cannot be regarded as stratigraphically insignificant on the basis of a preferred "blanket" approach to the stratigraphy.

The question has been raised as to whether these "small" intrabasins uplifts were capable of yielding all the sediment that I have ascribed to them. I suggest that the proven depth of erosion over some of them, particularly 3.6 km of erosion over the Cornwall Arch, indicates that they were. The Eureka Sound basin or basins should not be thought of as comparable to the major foreland basins, such as the Alberta or Indo- Gangetic basins. A better analogy would be to the Laramide Rocky Mountain basins (e.g. Wind River, Green River, Uinta, Hoback, etc.), which are about 50 to 200 km across (comparable in scale to the Eureka Sound basins), contain numerous, narrow, uplifted intrabasin source areas, and display significant syntectonic sedimentation. The underlying tectonic control may be similar too: a series of deep-seated ramp faults partially controlled by earlier lines of weakness. I have suggested elsewhere that in the Arctic some of the latter may be Caledonian in origin (Miall, 1986b).

DETAILED CRITIQUE OF RICKETTS (1986) AND RICKETTS AND McINTYRE (1986)

It should be emphasized that I do not question any of the facts presented in these two papers, only the interpretations put upon some of them. There is no doubt that the detailed mapping work carried out by Ricketts is invaluable, and he has contributed many original factual observations on the sedimentology of these rocks. My purpose in offering the following notes is only to point out that there may be other ways of interpreting these facts, and to suggest some clarifications.

1. The main basis for Ricketts' approach to the stratigraphy seems to be the widespread recognition of a "shale" marker bed, which he has named the Strand Bay Formation. From this unit he extrapolates to a "blanket" approach to the stratigraphy (despite the lithological heterogeneity in other units, as pointed out above). The Strand Bay Formation appears in my stratigraphic sections (Miall, 1986a, Figure 3) but is assessed by me as having a different importance in different parts of the eastern Arctic. In Strand Fiord Basin this fine grained sequence may be simply a thick interdeltaic unit. It appears at slightly different stratigraphic levels in my Sections 80-1 and 80-2. In Remus Basin the shale virtually corresponds to the Mount Lawson Formation of Miall (1986a), and is interpreted by me as the product of a marine transgression. So here, at least, we agree. I do not believe that there is good evidence for the occurrence of this unit in the Hot Weather Creek-Remus Creek area. This part of the section is very poorly exposed there.

2. Under "Previous terminology" Ricketts (1986) indicates that his approach introduces "a simple nomenclatural scheme

based on the general lithological homogeneity of rock units and their mappability'' (emphasis added). But it should be pointed out that his Iceberg Formation contains at least four major facies assemblages (his Figure 39.5) with major lateral facies changes between them. This unit is NOT lithologically homogeneous. These facies changes were recognized by Miall (1986a) and used as a basis for defining four separate formations (Mokka Fiord, Margaret, Vesle Fiord and Mount Moore). It seems that the Iceberg Bay Formation of Ricketts (1986) is distinguished mainly on the basis that it overlies the apparently more homogeneous Strand Bay Formation. Can Ricketts really be sure that his ''blanket'' approach is suitable?

3. The Expedition Formation was described thus by Ricketts (1986): ''the proportion of major lithotypes varies considerably across the Eureka Sound Basin''. Is this a good basis for an objectively described, mappable unit? I agree with Ricketts' facies descriptions but not with the interpretations made from them. In Strand Fiord Basin the rocks at this stratigraphic level are mainly coarsening-upward cycles of probable deltaic origin, with a transitional basal contact with the Kanguk. In Remus Basin the equivalent interval is somewhat thinner, the cyclicity is much more difficult to interpret, and I tentatively concluded that the rocks were fluvial. Here they commonly rest unconformably on Paleozoic strata, and may form the initial infill of erosional hollows. I recognized these differences by erecting two formations (Margaret and Mount Bell), which seems to me a more refined approach to the stratigraphy. Again, is the ''blanket'' approach really suitable?

4. I agree that the definition of the Kanguk-Eureka Sound contact is a very difficult one, because of its gradational nature. Differences of opinion are not surprising here.

5. The stratigraphic subdivisions recognized by Ricketts (1984, 1986) in the Strand Fiord Basin of Western Axel Heiberg Island are superior to the thick, un-subdivided Margaret Formation of Miall (1986a). These subdivisions should clearly be retained, either by using Ricketts' new formational nomenclature, or by classifying the units as members of the Margaret Formation.

6. I have not seen any unconformable contact between the rocks termed Iceberg Bay and Buchanan Lake formations by Ricketts (1986), and interpret this contact as a gradational facies change caused by increasing tectonism.

7. Buchanan Lake Formation: Identical to the Boulder Hills Formation of Miall (1986a), which was named on the basis of descriptions of the type section published by me earlier (Miall, 1979b). However, the assignment of the conglomerates on the east coast of Ellesmere Island (my Cape Lawrence Formation) to the Buchanan Lake Formation is questionable if the Paleocene age of the plants in the Cape Lawrence Formation is upheld. The conglomerate wedges cannot have ever formed one continuous unit if they are tens of millions of years different in age.

8. The reassignment by Ricketts and McIntyre (1986) of Bustin's (1982) Beaufort Formation exposures in the Geodetic Hills area to the Buchanan Lake Formation is interesting, and perhaps reasonable. However, some of the suggested reasons for rejecting Bustin's original designation may themselves be questioned. Thus the differences in induration, cementation, wood compression and lignite maturity almost certainly relate, at least in part, to the tectonism the rocks have undergone along the Stolz Fault Zone (during either phase 2 or 3 of the Eurekan Orogeny), and not to the differences in age between these rocks and the Beaufort Formation of the western Arctic (which is tectonically undisturbed).

9. The palynostratigraphic data reported by Ricketts and McIntyre (1986) for the Buchanan Lake (Boulder Hills) Formation certainly seem to support a Middle Eocene age for the rocks sampled. However, I do not think that their data rule out a Late Eocene to Early Oligocene age, as suggested by Miall (1984, 1985, 1986a), for the thick conglomerates that cap the formation at Mokka Fiord and Lake Hazen.

10. Ricketts and McIntyre (1986) imply that their mid-Eocene age for the Boulder Hills/Buchanan Lake formation are the first data that pin down the timing of the major episode of Eurekan diastrophism: ''In previous investigations, the age of Eurekan deformation has been bracketed between Middle Eocene (the date of the youngest typical Eureka Sound Group), and Early Miocene (an age based primarily on the oldest Beaufort Formation that unconformably overlies Eureka Sound rocks)''. Such an interpretation dates back to syntheses of Balkwill (1978, and earlier papers) and ignores the specific interpretations made by me as early as 1979 (tentatively, in Miall, 1979, p. 22, 23; more explicitly in Miall, 1984), that the age of the conglomerates could be used to date the main episode of Eurekan diastrophism. In my 1984 paper I interpreted this as Late Eocene and/or Early Oligocene.

REFERENCES

Balkwill, H.R.
1978: Evolution of Sverdrup Basin, Arctic Canada; American Association of Petroleum Geologists, Bulletin, v. 62, p. 1004-1028.
1983: Geology of Amund Ringnes, Cornwall and Haig Thomas islands, District of Franklin; Geological Survey of Canada, Memoir 390, 76 p.

Balkwill, H.R., Bustin, R.M, and Hopkins, W.S., Jr.
1975: Eureka Sound Formation at Flat Sound, Axel Heiberg Island, and chronology of the Eurekan Orogeny; *in* Report of Activities, Part B, Geological Survey of Canada, Paper 75-1B, p. 205-207.

Bustin, R.M.
1962: Beaufort Formation, eastern Axel Heiberg Island, Canadian Arctic Archipelago; Bulletin of Canadian Petroleum Geology, v. 30, p. 140-149.

Mayr, U. and de Vries, C.D.S.
1982: Reconnaissance of Tertiary structures along Nares Strait, Ellesmere Island, Canadian Arctic Archipelago; *in* Nares Strait and the drift of Greenland: a conflict in plate tectonics, P.R. Dawes and J.W. Kerr (eds.); Meddelelser om Gr/onland 8, Special Issue, p. 167-175.

Meneley, R.A., Henao, D., and Merritt, R.K.
1975: The northwest margin of the Sverdrup Basin; *in* Canada's continental margins and offshore petroleum exploration, C.J. Yorath, E.R. Parker and D.J. Glass (eds.); Canadian Society of Petroleum Geologists, Memoir 4, p. 531-544.

Miall, A.D.
1979a: Mesozoic and Tertiary geology of Banks Island, Arctic Canada: the history of an unstable craton margin; Geological Survey of Canada, Memoir 387, 235 p.
1979b: Tertiary fluvial sediments in the Lake Hazen intermontane basin, Arctic Canada; Geological Survey of Canada, Paper 79-9, 25 p.
1981: Late Cretaceous and Paleogene sedimentation and tectonics in the Canadian Arctic Islands; *in* Sedimentation and tectonics in alluvial basins, A.D. Miall (ed.); Geological Association of Canada, Special Paper 23, p. 221-272.
1982: Tertiary sedimentation and tectonics in the Judge Daly Basin, northeast Ellesmere Island, Arctic Canada; Geological Survey of Canada, Paper 80-30, 15 p.
1984: Sedimentation and tectonics of a diffuse plate boundary: the Canadian Arctic Islands from 80 Ma B.P. to the present; Tectonophysics, v. 107, p. 261-277.

Miall, A.D.
1985: Stratigraphic and structural predictions from a plate-tectonic model of an oblique orogen: the Eureka Sound Formation (Campanian-Oligocene), northeast Canadian Arctic Islands; *in* Strike-slip deformation, basin formation, and sedimentation, K.T. Biddle and N. Christie-Blick (eds.); Society of Economic Paleontologists and Mineralogists, Special Publication 37, p. 361-374.
1986a: The Eureka Sound Group (Upper Cretaceous-Oligocene), Canadian Arctic Islands; Bulletin of Canadian Petroleum Geology, v. 34, p. 240-270.
1986b: Effects of Caledonian tectonism in Arctic Canada; Geology, v. 14, p. 904-907.

Miall, A.D., Balkwill, H.R., and Hopkins, W.S., Jr.
1980: The Cretaceous-Tertiary sediments of Eclipse Trough, Bylot Island area, Arctic Canada, and their regional setting; Geological Survey of Canada, Paper 79-23, 20 p.

Ricketts, B.D.
1984: Geological Survey of Canada, Open File Map 1147.
1985: Geological Survey of Canada, Open File Map 1182.
1986: New formations in the Eureka Sound Group, Canadian Arctic Islands; *in* Current Research, Part B, Geological Survey of Canada, Paper 86-1B, p. 363-374.

Ricketts, B.D. and McIntyre, D.J.
1986: The Eureka Sound Group of eastern Axel Heiberg Island; new data on the Eurekan Orogeny; *in* Current Research, Part B, Geological Survey of Canada, Paper 86-1B, p. 405-410.

The Eureka Sound Group: alternative interpretations of the stratigraphy and paleogeographic evolution — Reply

B.D. Ricketts
Institute of Sedimentary and Petroleum Geology, Calgary

Ricketts, B.D., The Eureka Sound Group: alternative interpretations of the stratigraphy and paleogeographic evolution - Reply; in Current Research, Part D, Geological Survey of Canada, Paper 88-1D, p. 149-152, 1988.

INTRODUCTION

The different nomenclatural schemes introduced for the Eureka Sound Group by A.D. Miall (1986) and myself (1986) reflect different perceptions of Late Cretaceous- Tertiary basin evolution in the Arctic Archipelago. The discussion-reply papers presented here provide an opportunity to air some of these differences. In addition to the specific comments made by Miall on papers by Ricketts (1986) and Ricketts and McIntyre (1986), the discussion is centered on two fundamental problems: the permissible level of interpretation in designating formal lithostratigraphic units; and the validity of the hypothesis of multiple basins during Eureka Sound Group deposition. The alternative schemes are summarized in Figure 1.

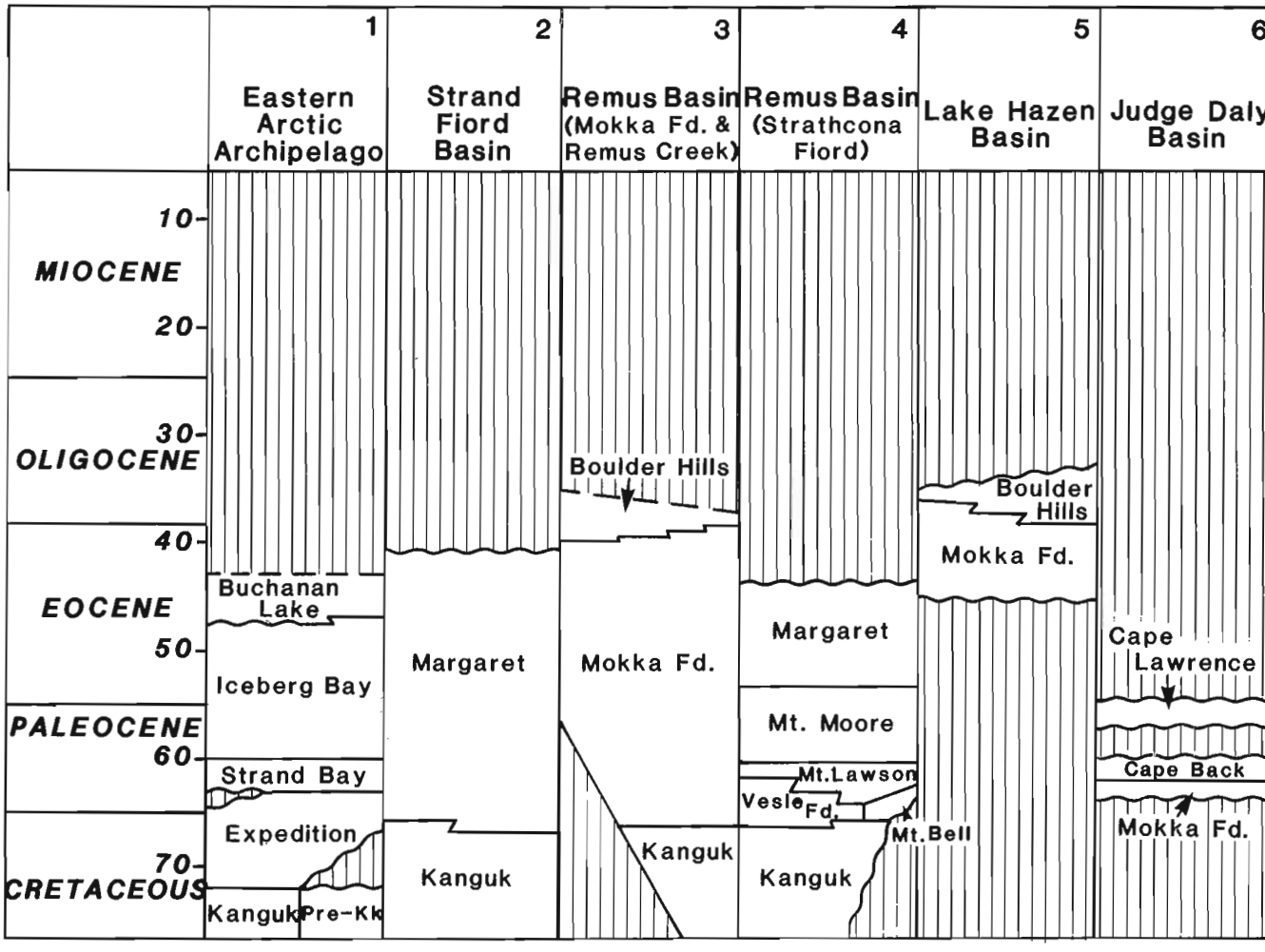

Figure 1. Comparison of stratigraphic schemes for the Eureka Sound Group. Column 1 from Ricketts (1986); columns 2-6 from Miall (1986a).

FACIES OR FORMATIONS: DIFFERENT LEVELS OF INTERPRETATION

In Miall's nomenclatural scheme for the Eureka Sound Group, a facies assemblage is made up of two or more lithofacies, the latter being defined on the basis of textural characteristics and sedimentary structures (Miall, 1986, Table 1). Each lithofacies, for example, Gm or Sp, has a specific or limited set of hydrodynamic and paleoenvironmental interpretations. Thus interpretation enters even the smallest defined component of a facies assemblage. Each of Miall's formations consists of one or more facies assemblages.

It is questionable whether Miall's formations are defined on a strictly objective basis. For example in Miall (1981) equal emphasis is given to interpretation as in "Assemblage A, Estuarine". There is no doubt that there exists a descriptive element in the definition of all these assemblages, as in reasonably objective parameters such as grain size and internal organization; but I submit that there is an inextricable link between these descriptive elements and interpretation. I do not single Miall out with respect to this problem; it is a problem facing any geologist (scientist) who attempts to reconcile empirical data and inference. Some degree of interpretation enters all levels of observation. The word "facies" contains strong connotations of genesis whether we like it or not. Miall has suggested that the same observational data can be used for defining formal lithostratigraphic units in an objective manner, and subsequently used for interpreting their origin (Miall, 1986, p. 246). I dispute this to the extent that both the process of observation and at least some level of interpretation occur almost simultaneously, despite the fact that in geological manuscripts the data and interpretations are usually listed separately.

The problem here is to try and minimize the level of interpretation used when designating formations. The more traditional method of employing the criteria of mappability and lithological homogeneity without direct reference to facies is at present our best approach, despite the pitfalls of defining such qualities as homogeneity. I do not doubt that some level of interpretation enters even this approach, but it seems less prone to interpretive input. The definition of facies assemblages, on the other hand, possesses strong connotations of genesis, despite the good intentions of Miall. Simply labelling such assemblages A, B, and C does not provide automatic legitimacy to the notion of objective definition.

The concept of lithological homogeneity requires further comment. A body of rock that contains mostly sandstone can be regarded, for the purpose of mapping, as homogeneous, despite the fact that it may also contain some coal and mudstone. Similarly, a rock unit made up of alternating rock types may also be considered homogeneous for the purpose of mapping, if it is distinguishable from superjacent and subjacent rock units that consist of different lithological associations. The critical point here is that, whatever the composition of a body of rock, it should be confined within mappable boundaries.

There are several other problems of a practical nature that need to be addressed:

1. Miall contends that a change in the paleoenvironmental interpretation of a facies assemblage does not necessitate a change in the overall assemblage designation. This implies that the newly interpreted setting be represented by the same assemblage of facies — an assumption that may not always be justified.

2. The problems inherent in reinterpreting facies assemblages are illustrated in the following example. At Strand Fiord, Miall defines a single formation over 3000 m thick, the Margaret Formation, consisting almost entirely of Facies Assemblage E (proximal delta front – delta plain) with minor fluvial components of Assemblages F and G. I have interpreted this sequence as representing two different delta environments: basal, wave-dominated (Expedition Formation), and upper, fluvial-dominated (Iceberg Bay Formation), separated by a thick, laterally extensive marine shale (Strand Bay Formation). In comparison at Strathcona Fiord, Miall divides a sequence of about 2000 m thickness into five formations, each represented by a single facies assemblage. At Remus Creek, again according to Miall, a succession of at least 2500 m consists of a single formation (Mokka Fiord Formation) comprising three fluvial facies assemblages. My work indicates that the basal 200 to 300 m at Remus Creek is of shallow marine, possibly barrier island-lagoon origin. An additional shallow marine sandstone-shale facies occurs higher in the sequence and is probably a nearshore equivalent of the Strand Bay Formation. The problem immediately apparent here is that reinterpretation of Miall's facies assemblages and assemblage boundaries can indeed necessitate revision of formation status.

3. Individual facies assemblages or sets of assemblages may recur throughout a stratigraphic sequence. Therefore, the possibility exists for one of Miall's formations to be repeated. However, the sequence of repetition in one area may not correspond to the sequence in another. Miall circumvents this problem by applying different names to the repeated assemblages. Thus, the Margaret Formation at Strand Fiord, consisting of Facies Assemblage E, is compared with the Vesle Fiord, Mount Lawson, Mount Moore and Margaret formations at Strathcona Fiord, which are represented by Assemblages E, D, A, and E, respectively. Miall indicates that the nomenclature of the sequence at Strand Fiord could be revised, given the greater degree of (stratigraphic) resolution presented in my scheme. However, problems arise in redefining the Strand Fiord succession; for example, should the upper fluvial-dominated assemblage (my Iceberg Bay Formation) be assigned to Miall's Margaret or Vesle Fiord formations, or should a new formation be erected (in this case redefinition of the type section would also be necessary)? Miall's suggestion that such units could be redefined as members of the Margaret Formation would mean that both members and formations would comprise the same facies assemblages.

In summary, it appears that Miall has conflated the traditional concept of lithostratigraphic nomenclature with the more subjective system of facies assemblages. As such, the potential for considerable confusion exists in his scheme. This is indeed unfortunate, because the concept of facies assemblages is particularly valuable in basin analysis. It is not clear why Miall finds it necessary to apply formation names to these assemblages. Why not simply refer to them as facies?

BASIN GEOMETRY AND BASIN FILL

The second part of Miall's discussion is based on the hypothesis of the existence of multiple depositional basins during the period from Late Cretaceous to Paleogene, and the resulting geometry of lithostratigraphic units. I do not deny the existence of at least some sub-basins, but I do question the timing and paleogeographic extent as propounded by Miall (1981, and subsequent papers). There is no doubt that arches exist at present; for example, the Cornwall and Princess Margaret arches (Balkwill, 1978); the main problem is determining when they formed. I have argued in a recent paper (Ricketts, in press), that Princess Margaret Arch developed during the climactic phase of Eurekan deformation that began in the Middle Eocene; there is no evidence to indicate that Remus and Strand Fiord basins were ever separated prior to the Eurekan event. The sub-Eureka Sound Group unconformities on eastern Axel Heiberg Island are a product of erosion localized around salt diapirs.

It appears to me that the hypothesis of multiple basins, at least in the eastern Arctic, is based more on the present location of major uplifts or arches, rather than on well established stratigraphic evidence. Most of these uplifts possess an important structural component associated with Eurekan folding and faulting. To establish whether they were present as topographic highs during sedimentation requires good stratigraphic evidence, such as demonstrable thinning of sedimentary units, and knowledge of facies trends (including paleocurrent interpretations). In the cases cited by Miall, much of the existing evidence is certainly equivocal and can legitimately be interpreted in different ways. For example, the variability in crossbed azimuths in the Lake Hazen and Judge Daly Peninsula areas (Miall, 1979, 1982) could be attributed to highly variable fluvial and alluvial plain facies, rather than to small, isolated sedimentary basins (Lake Hazen and Judge Daly basins, respectively). The real test as to whether these basins were separate entities will be provided by more precise age determinations and palinspastic reconstructions, from which the effects of Eurekan deformation (superimposed on Ellesmerian structures) can be unravelled.

Miall has misconstrued the word "blanket" in referring to the stratigraphic units in my scheme. He assumes that even if several separate basins did exist, broadly similar sedimentary sequences identified within them, cannot in principle be correlated. On the contrary, if, for example, an Arctic-wide transgression did take place during the Early Paleocene, it is quite conceivable that the event would be recorded in each of the basins. The point is, that even if the multiple-basin hypothesis is correct, this in itself does not justify the argument that major transgressive and regressive events, and their resulting sedimentary sequences, cannot be identified and correlated. As well, the fact that my formations can be correlated over a wide area does not preclude the possibility of multiple basins. Furthermore, the apparent "blanket" configuration of my formations does not preclude the existence of wedge-shaped facies (or assemblages of facies; in particular note Figure 39.5 in Ricketts, 1986).

REPLY TO SPECIFIC CRITICISMS

The points listed below refer to those in Miall (this volume) under "Detailed critique, etc.".

Point 1. The Strand Bay Formation can be traced with confidence in the Fosheim Anticline area, where sandstone beds comprise coarsening-upward sequences, and associated mudstones contain a few arenaceous foraminifera (J.H. Wall, pers. comm., 1986). These lithological features, together with the suite of sedimentary structures, are in marked contrast to those in the immediately underlying and overlying strata, which consist primarily of fining-upward sequences. Correlation of this unit with strata in the nearby Remus Creek area is tentative, and is hampered by structural complications. The higher sandstone content of the Strand Bay Formation in these areas is interpreted as reflecting nearshore conditions, equivalent to the deeper water shales.

Point 2. The basis for defining the Iceberg Bay Formation is that it contains mostly sandstone and has mappable contacts. That it also contains several different facies (having wedge, deltoid and tabular geometries) is not relevant with respect to this definition. Because Miall's formations are based primarily on facies content, it is not surprising that some conflict will arise. If necessary, these facies can be assigned member status, if they are mappable units.

Point 3. The Expedition Formation is diachronous; at Strand Fiord the basal strata are middle to upper Campanian, whereas in the Ca non Fiord-Vesle Fiord area basal strata that overlie eroded Franklinian bedrock are probably Lower Paleocene, or at most upper Maastrichtian. That a variety of facies also occurs in the Expedition Formation is not surprising. Each facies consists predominantly of sandstone; the formation as a whole has easily mappable contacts. However, the fact that all of the facies are included in a single formation implies nothing about the configuration of the basin(s). Basin configuration is determined by the relationships amongst facies types, facies geometries and structural-palinspastic considerations.

Points 4 and 5. No comment required.

Point 6. A disconformity between the Iceberg Bay Formation and Buchanan Lake Formation can be inferred at Mokka Fiord, although the duration of the hiatus cannot presently be resolved paleontologically. The following criteria apply:

1. Strata of the Iceberg Bay Formation consist of supermature quartz sandstone, shale, and coal seams; although thin pebble lags are common, they rarely contain diabase pebbles. On the other hand, Buchanan Lake sandstones and conglomerates are characterized by abundant diabase detritus, and a distinct paucity of quartz sand.

2. The mapped contact between the two lithotypes along the southwest margin of Mokka Fiord is abrupt.

3. Style of bedding and bedforms are fundamentally different in the two formations: tabular, laterally extensive beds in the Iceberg Bay Formation, and pronounced lateral discontinuity in the Buchanan Lake units.

4. The Iceberg Bay coals and shales contain an insignificant amount of reworked palynomorphs compared with the high degree of reworking found in the Buchanan Lake deposits, including late Paleozoic, early Mesozoic and Maastrichtian floras. The transition in degree of reworking across the contact is abrupt.

Point 7. I have included conglomerates on the east coast of Ellesmere Island in the Buchanan Lake Formation on the basis of their unique lithological characteristics. Like their counterparts at Mokka Fiord and Lake Hazen, the conglomerate facies (and associated finer grained lithologies) occur in the footwall of a major thrust (or zone of thrusts), and were in fact derived from major uplifts, including thrust sheets (Balkwill, 1978; Miall, 1979, 1982, 1985; Ricketts and McIntyre, 1986). It is possible that the timing of conglomerate deposition is not coincident in each of these areas and that deformation and associated syntectonic sedimentation was diachronous throughout the eastern Arctic Archipelago from Paleocene to Eocene and even Early Oligocene; there is as yet no unequivocal stratigraphic evidence for this. Nowhere in my papers have I excluded this possibility. The other point to be stressed here is that applying the same name to these deposits (Buchanan Lake Formation) in no way implies a "blanket" distribution. In fact, separate orogenic foredeeps were hypothesized by Ricketts and McIntyre (1986) for the eastern Axel Heiberg and eastern Ellesmere Island sequences.

Point 8. The critical factors in reassigning strata at Geodetic Hills and surrounding areas from the Beaufort Formation to the Buchanan Lake Formation are: the Middle Eocene age determined from a well preserved palynoflora; and the position of the strata in the footwall of a thrust in the Stolz Fault Zone (Ricketts and McIntyre, 1986).

Points 9 and 10. The debate over whether Eureka Sound Group deposits as young as Early Oligocene occur is important, because an upper age limit is required to bracket the timing of major folding and faulting during the Eurekan Orogeny.

In Miall's early work at Lake Hazen, the Boulder Hills Formation was considered to be Eocene to (?)Oligocene in age. In the original (GSC) paleontology reports it was stressed that the Early Oligocene designation was questionable; the evidence cited was the presence of some species that ranged in age from Eocene to Pliocene. Later, Sepulveda and Norris (1982) described species that ranged from Early Paleogene to Oligocene. However, Miall's later publications on regional synthesis and lithostratigraphy (Miall, 1984, 1985), all state, with greater confidence, an upper age limit of Early Oligocene for these deposits of the Eureka Sound Group. Yet the database has not changed. The Oligocene age designation is based solely on the fact that some floral species range into the Oligocene or younger time periods. The contention in our 1986 paper is therefore reiterated; no definitive evidence for an Oligocene age exists at present. Our search continues for more compelling evidence to resolve this issue.

ACKNOWLEDGMENTS

I would like to thank R.L. Christie, J. Dixon, A.F. Embry, R. Thorsteinsson, and H.P. Trettin (all of the I.S.P.G) for useful criticisms and comments.

REFERENCES

Balkwill, H.R.
1978: Evolution of Sverdrup Basin, Arctic Canada; American Association of Petroleum Geologists, Bulletin, v. 62, p. 1004-1028.

Miall, A.D.
1979: Tertiary fluvial sediments in the Lake Hazen intermontane basin, Ellesmere Island, Arctic Canada; Geological Survey of Canada, Paper 79-9.
1981: Late Cretaceous and Paleogene sedimentation and tectonics in the Canadian Arctic Islands; *in* Sedimentation and tectonics in alluvial basins, A.D. Miall (ed.); Geological Association of Canada, Special Paper 23, p. 221-272.
1982: Tertiary sedimentation and tectonics in the Judge Daly Basin, northeast Ellesmere Island, Arctic Canada; Geological Survey of Canada, Paper 80-30, 15 p.
1984: Sedimentation and tectonics of a diffuse plate boundary: The Canadian Arctic Islands from 80 Ma B.P. to the present; Tectonophysics, v. 107, p. 261-277.
1985: Stratigraphic and structural predictions from a plate-tectonic model of an oblique orogen: the Eureka Sound Formation (Campanian-Oligocene), northeast Canadian Arctic Islands; *in* Strike-slip deformation, basin formation, and sedimentation, K.T. Biddle and N. Christie-Blick (eds.); Society of Economic Paleontologists and Mineralogists, Special Publication 37, p. 361-374.
1986: The Eureka Sound Group (Upper Cretaceous-Oligocene), Canadian Arctic Islands; Bulletin of Canadian Petroleum Geology, v. 34, p. 240-270.

Ricketts, B.D.
1986: New formations in the Eureka Sound Group, Canadian Arctic Islands; *in* Current Research, Part B, Geological Survey of Canada, Paper 86-1B, p. 363-374.
in press: Princess Margaret Arch: re-evalution of an element of the Eurekan Orogen, Axel Heiberg Island, Arctic Archipelago; Canadian Journal of Earth Sciences.

Ricketts, B.D. and McIntyre, D.J.
1986: The Eureka Sound Group of eastern Axel Heiberg Island; new data on the Eurekan Orogeny; *in* Current Research, Part B, Geological Survey of Canada, Paper 86-1B, p. 405-410.

Sepulveda, E.G. and Norris, G.
1982: A comparison of Paleogene fungal spores from northern Canada and Patagonia, Argentina; Armeghiniana, v. 19, p. 319-334.

CURRENT RESEARCH PART B
EASTERN AND ATLANTIC CANADA

RECHERCHES EN COURS PARTIE B
EST ET RÉGION ATLANTIQUE DU CANADA

CONTENTS

CURRENT RESEARCH PART C
CANADIAN SHIELD

RECHERCHES EN COURS PARTIE C
BOUCLIER CANADIAN

CONTENTS

CURRENT RESEARCH PART E
CORDILLERA AND PACIFIC MARGIN

RECHERCHES EN COURS PARTIE E
CORDILLÈRE ET MARGE DU PACIFIQUE

CONTENTS

CURRENT RESEARCH PART F
NATIONAL AND GENERAL PROGRAMS

RECHERCHES EN COURS PARTIE F
PROGRAMMES NATIONAUX ET GÉNÉRAUX

CONTENTS

NOTE TO CONTRIBUTORS

Submissions to the Discussion section of Current Research volumes are welcome from both the staff of the Geological Survey and from the public. Discussions are limited to 6 double-spaced typewritten pages (about 1500 words) and are subject to review by the Chief Scientific Editor. Discussions are restricted to the scientific content of Geological Survey reports. General discussions concerning branch or government policy will not be accepted. Illustrations will be accepted only if, in the opinion of the editor, they are considered essential. In any case no redrafting will be undertaken and reproducible copy must accompany the original submissions. Discussion is limited to recent reports (not more than 2 years old) and may be in either English or French. Every effort is made to include both Discussion and Reply in the same issue. Submissions should be sent to the Chief Scientific Editor, Geological Survey of Canada, 601 Booth Street, Ottawa, Canada, K1A 0E8.

AVIS AUX AUTEURS D'ARTICLES

Nous encourageons tant le personnel de la Commission géologique que le grand public à nous faire parvenir des articles destinés à la section discussion de la publication Recherches en cours. Le texte doit comprendre au plus six pages dactylographiées à double interligne (environ 1500 mots), texte qui peut faire l'objet d'un réexamen par le rédacteur en chef scientifique. Les discussions doivent se limiter au contenu scientifique des rapports de la Commission géologique. Les discussions générales sur la Direction ou les politiques gouvernementales ne seront pas acceptées. Les illustrations ne seront acceptées que dans la mesure où, selon l'opinion du rédacteur, elles seront considérées comme essentielles. Aucune retouche ne sera faite aux textes et dans tous les cas, une copie qui puisse être reproduite doit accompagner les textes originaux. Les discussions en français ou en anglais doivent se limiter aux rapports récents (au plus de 2 ans). On s'efforcera de faire coïncider les articles destinés aux rubriques discussions et réponses dans le même numéro. Les articles doivent être renvoyés au rédacteur en chef scientifique: Commission géologique du Canada, 601, rue Booth, Ottawa, Canada, K1A 0E8.

Energy, Mines and Resources Canada

Énergie, Mines et Ressources Canada